Some Investigations on the Optimal Allocation of Distributed Generation Resources in Distribution Systems

A Thesis Submitted to
Delhi Technological University
For the Award of Doctor of Philosophy
In
Electrical Engineering

Submitted By

IMRAN AHMAD QUADRI
(2K14/PhD/EE/02)

Under the Supervision of

Dr. Suman Bhowmick
Professor, EED, DTU

Dr. Dheeraj Joshi
Professor, EED, DTU

DEPARTMENT OF ELECTRICAL ENGINEERING
DELHI TECHNOLOGICAL UNIVERSITY
(Formerly Delhi College of Engineering)
DELHI-110042, INDIA
2019

DECLARATION

This thesis titled "**Some Investigations on the Optimal Allocation of Distributed Generation Resources in Distribution Systems"** is my original work and contains no material previously published or written by another person except where due reference has been made in the text. I have clearly stated the contribution of others to my thesis as a whole, including statistical assistance, data analysis, significant technical procedures and any other original research work(s) used or reported in my thesis. The contents of my thesis is the result of the work that I have carried out since the commencement of my candidature as a doctoral research scholar and does not include any work that has been submitted to qualify for the award of any other degree or diploma in any university or other institute.

I acknowledge that an electronic copy of my thesis will be submitted to the university library and immediately made available for research and study in accordance with the copy right act of Delhi Technological University.

Place : New Delhi

Date : 13.05.2019 Imran Ahmad Quadri

DEPARTMENT OF ELECTRICAL ENGINEERING

DELHI TECHNOLOGICAL UNIVERSITY

(Formerly Delhi College of Engineering)

CERTIFICATE

This is to certify that the thesis titled "**Some Investigations on the Optimal Allocation of Distributed Generation Resources in Distribution Systems",** submitted b**y Mr. Imran Ahmad Quadri,** Roll No. 2K14/PhD/EE/02, a student of Doctor of Philosophy in the Department of Electrical Engineering at Delhi Technological University (Formerly Delhi College of Engineering), is a work carried out by him under my guidance during 2014-2019 towards the partial fulfillment of the requirement of the award of degree of Doctor of Philosophy and is an original contribution with existing knowledge and faithful record of research work carried out by him under my guidance and supervision.

To the best of my knowledge this work has not been submitted in part or full for any degree or diploma to this university or eslwhere.

Dr. Suman Bhowmick
Professor, EED, DTU
(Supervisor)

Dr. Dheeraj Joshi
Professor, EED, DTU
(Co-Supervisor)

ACKNOWLEDGEMENT

First and foremost, I thank to the Almighty for everything, who command the successes and failures of life.

Next, I express my profound sense of gratitude to my supervisor and motivator Prof. Suman Bhowmick, Electrical Engineering Department, Delhi Technological University, not only for his continued morale-boosting efforts and support towards the completion of my research work but also for his fatherly attitude towards me throughout my association with him along with co-operation and help in providing necessary facilities and resources during the entire period of this research work and Co-supervisor Prof. Dheeraj Joshi, Electrical Engineering Department, Delhi Technological University, Delhi, for his invaluable suggestions and motivation during the entire period of this research work.

In the same vein, I also acknowledge Prof. Madhusudan Singh, Head, and all the faculty members of the Electrical Engineering Department, Delhi Technological University, who enlightened me during my research, especially Dr. M. Rizwan, Associate Professor, for always standing beside me throughout my research work, personally and professionally.

Also worthy of appreciation is my friend Dr. Shagufta Khan, because of her support I started my research journey with my supervisor.

And, of course, every bit of me would always remain indebted to my loving parents Late Afgana Khatoon and Janab Mustaque Ahmad Quadri, whose blessings have been and will always be an inseparable part of every stride I take towards progress and insight in life.

I would like to extent my distinctive thanks to Dr. Afroz Alam, Assistant Professor, AMU, Aligarh, who has given me valuable advice for my research work.

I extend my personal thanks to my friends and colleagues specially, Md. Tausif Ahmad, Sarwar Alam, Shahzad Ahsan, Astitva Kumar, Varsha Agarwal, Priyanka Chaudhary, Sami Ahmad, Arbaz Ahmad along with my family members as well as relatives and my well-wisher Nesar Ahmad Siddiqui, Afzal Ahmad Farooqui and Mehnaz Farooqui for their valuable support and reminding me to complete my work at the earliest.

The assistance of the valuable staffs of Sr. Machine Lab of Delhi Technological University is gratefully acknowledged. I am especially thankful to Mr. TPS Rana and Mr. Vickey Kumar Prasad for their substantial assistance.

This acknowledgement would not be complete without mentioning my wife, Farha Naaz and son, Arhaan Ahmad Quadri. They are my core support system and words cannot articulate my admiration for them. Both gave their unconditional support and continue to be a source of inspiration during my research.

Place : New Delhi

Date : Imran Ahmad Quadri

ABSTRACT

Competitive electricity markets, rapid growth of electricity demand, reliability issues of electric power supply, technological advancement in power generation resources, utility supporting devices and increased assimilation of telecommunication and information technology in distribution networks (smart grid) completely transform their behavior and operation. Further, integration of dispatchable or non-dispatachable distributed energy resources near the load centres results in enhancement of distribution network performance. The foremost concept behind the smart grid is allocating and operating Distributed Generation (DG) resources in distribution networks tactically by considering various technical, economic and environmental issues. Therefore, the aim of the research work in this thesis is to develop methodologies for the strategic planning and operation of DGs considering various objectives.

The primary contribution of the thesis is to address the development and application of meta-heuristic optimization techniques used for optimal allocation of several types of distributed energy resources and / or network reconfiguration under various loading conditions to reduce the power losses, improve network voltage profile, enhance operational cost savings and improve the loadability of the distribution networks.

At the outset, a comprehensive teaching-learning based optimization (CTLBO) algorithm has been developed which is almost parameter independent and has the capability to handle mixed integer variables with fast convergence characteristics. Its implementation in standard mathematical benchmark functions demonstrate its

superiority over many existing optimization algorithms. Thereafter, CTLBO is used for optimal allocation of DGs in different radial distribution networks, considering single as well as multi-objective formulations (based on weighted sum and ε-constraints approach). The results again demonstrate the superiority of CTLBO over teaching-learning based optimization (TLBO) and quasi-oppositional teaching-learning based optimization (QOTLBO) algorithms.

Subsequently, a Hybrid teaching-learning based optimization (HTLBO) algorithm is developed, which can handle a large number of variables. This algorithm is again validated using single as well as multi-objective mathematical benchmark functions. It is observed that the HTLBO algorithm has either equivalent or better performance than many existing algorithms such as TLBO and QOTLBO. Further, this algorithm is used to optimally allocate several DGs for multi-objective problems in several distribution networks. It is found that the ε-constraints based approach gives better solution than weighted sum approach for multi-objective problems and results in significant reduction in losses, improvement in voltage profile and voltage stability index over TLBO and QOTLBO algorithms.

Subsequently, an analytical approach based on power loss sensitivity has been developed in this thesis to allocate multiple reactive power compensation devices in different radial distribution networks to reduce power losses and emission, along with improvement in cost savings and various network performance indices. The proposed approach takes very less computational time as compared to immune algorithm (IA), bat algorithm(BA) and bacteria foraging optimization algorithm (BFOA). Subsequently, the CTLBO algorithm is used for optimal allocation of distribution static compensators (DSTATCOMs) and / or network reconfiguration to get multiple operating points (Pareto solution) of the distribution networks. This

Pareto solution enables the distributed network operators (DNOs) to maneuver the distribution networks to achieve maximum benefits under different operating conditions.

Finally, in this thesis, the CTLBO technique is used to enhance the loadability of distribution networks by adopting a multi-objective approach to address the growing load demand without additional expenditure on the existing networks. Results demonstrate that simultaneous allocation of DGs with varing power factors and network reconfiguration yields the highest loadability enhancement in distribution networks.

Table of contents

List of figures

List of tables

List of symbols and abbreviations

ABC	Artificial Bee Colony
ACO	Ant Colony Optimization
APL	Active Power Loss
APLR	Active Power Loss Reduction
AR	Asset Rate of Return
ASR	Auto Selection Rate
BA	Bat Algorithm
BCBV	Branch Current to Bus Voltage
BFOA	Bacteria Foraging Optimization Algorithm
BIBC	Bus Injection to Branch Current
BR	Branch
BW	Bandwidth
Conj	Conjugate
CPF	Continuous Power Flow
CSOA	Cuckoo Search Optimization Algorithm
CT	Computational Time
CTLBO	Comprehensive Teaching-Learning Based Optimization
DABC	Discrete Artificial Bee Colony
DG	Distributed Generation
DN	Distribution Network
DSTATCOM	Distribution Static Compensator
EL	Energy Loss
ER	Emission Rate
ES	Emission Saving
GA	Genetic Algorithm
HFACO	Hybrid Fuzzy-Ant Colony Optimization
HMCR	Harmony Memory Consideration Rate
HPSO	Hybrid Particle Swarm Optimization
HSA	Harmony Search Algorithm
HTLBO	Hybrid Teaching-Learning Based Optimization

IA	Immune Algorithm
ICA	Imperialist Competitive Algorithm
IEEE	Institute of Electrical and Electronics Engineers
KMML	kVA Margin to Maximum Loadabilty
LF	Loading Factor
MLI	Maximum Loadability Index
MOF	Multi-Objective Function
NO_2	Nitrogen di-Oxide
NOx	Nitrogen-Oxide
PAR	Pitch Adjustment Rate
PSO	Particle Swarm Optimization
PV	Photovoltaic
QLI	Qualified Load Index
QOTLBO	Quasi Oppositional Teaching-Learning Based Optimization
RDN	Radial Distribution Network
RES	Renewable Energy Source
RPC	Reactive Power Consumption
RPCR	Reactive Power Consumption Reduction
SD	Standard Deviation
SOF	Single Objective Function
SV	Solution Vector
SVM	Solution Vector Matrix
TAC	Total Annual Cost
TACS	Total Annual Cost Saving
TBVVB	Total Bus Voltage Violation Boundary
TLBO	Teaching-Learning Based Optimization
VD	Voltage Deviation
VDI	Voltage Deviation Index
VP	Voltage Profile
VPI	Voltage Profile Index

Parameters/variables

a_i	Weight coefficient

a	Teaching factor rate
A	Incidence matrix of the distribution network
APL_b/RPC_b	Active power loss/Reactive power consumption without DG and reconfiguration in network, respectively
APL_{DG}/RPC_{DG}	Active power loss/Reactive power consumption with only DGs in network, respectively
BR_{nb}	Branch current flowing through the branch 'nb' of network
BW_{min}/BW_{max}	Minimum/maximum value of BW
$Cost_{nDG}$	Cost of nDG^{th} DG of the network
$Cost_{nDG,year}$	Annual cost of nDG^{th} DG of the network in particular year
Dcost	Total cost of DSTATCOM in the network, $
DGL_{nDG}^{SVS}	nDG^{th} DG location of SVS^{th} solution vector
DGS_{nDG}^{SVS}	nDG^{th} DG size of SVS^{th} solution vector
DST_{nTS}^{SVS}	nTS^{th} open tie or sectional switch location of SVS^{th} solution vector
E/E^{DG}	Annual emission of air pollution without/with DG and/ or reconfiguration, tons
F_i	i^{th} single objective function
$F(X_{old}^{SVS})$	Fitness of old SVS^{th} solution vector in SVM
$F\mu(X)$ / $F_m(X)$	Fitness of main /constraint objective function corresponding to solution vector (X)
g_p/h_q	Inequality/equality constraint
$HMCR_{min}/HMCR_{max}$	Minimum/maximum value of HMCR
$HMCR^{ci}$	HMCR value of current iteration
I_j^{max}	Magnitude of maximum loading in branch 'j' of the network
I_{k+1}^{i}	Current injected or absorbed at $(k+1)^{th}$ bus at i^{th} iteration
I_{nb}	Current injected or absorbed at nb^{th} bus
J	Maximum allowable DGs penetration in network
K_{ci}	Time duration proportion
K_e	Energy cost factor of loss
$LF_{P\text{-}II}$	Load factor of II^{nd} curve at point 'p'
M	Total number of buses beyond branch 'j' of the network

M	Total number of constraint objective functions
M_i	Mean of i^{th} solution variable of solution vector
n , nb	Total number of buses and branches in network, respectively
N	Total number of variables in each solution vector
n_{DG}	Total year of operation of DG in the network
nDG	Total number of DGs in the network
NI	Number of improvisation
np/nq	The active / reactive load voltage exponents
Ob	Total number of single objective functions
PAR_{min}/PAR_{max}	Minimum/maximum value of PAR
$P_{DG,k}/Q_{DG,k}$	Real/ Reactive power generated at bus 'k'
P_{loss}/Q_{con}	Total network active power loss /reactive power consumption before network reconfiguration and DG allocation, kW/kVAr
$P_{loss,i}$	Network active power loss without DG at i^{th} hour, kW
$P_{loss,j}$	Active power loss in branch 'j' of network, kW
$P_{loss}^{DG}/Q_{con}^{DG}$	Total active power loss/reactive power consumption in the network after DGs placement
$P_{loss,i}^{DG}$	Network active power loss at i^{th} hour with DG, kW
P_{loss}^{t}	Active power loss of the network at t^{th} hr of the day, kW
$P_{L,k}(t)/Q_{L,k}(t)$	Active and Reactive load demand of network at t^{th} time, respectively kW/kVAr
P_{k+1}/Q_{k+1}	Active power/ Reactive power injected or absorbed at bus 'k+1'
P_{sub}/Q_{sub}	Active/Reactive power supplied by substation to the network, kW/kVAr
$Q_{DG,k}^{min}/Q_{DG,k}^{max}$	Minimum/maximum allowable reactive power supplied by the DG in the network at bus 'k'
Q_k	Optimal reactive power calculated at bus 'k'

R_j /X_j	Resistance/ Reactance of the line section 'j' between buses 'i' and 'k'
rand	Uniformly distributed random number between '0' and '1'
S_{DG}	Total apparent power injected by DGs in the network, kVA
$S_{DG,k}$	Apparent power injected or absorbed by DG at bus 'k' in the network, kVA
S_{load}	Total apparent load in the network, kVA
$S_{L,k}$	Apparent load power at the k^{th} bus in the network, kVA
S_{k+1}	Apparent power injected or absorbed at bus 'k+1'
SVS	Total number of solution vectors in the SVM
T_i	Hours per year
T_F	Teaching Factor
Δt	Time duration, hour
TAC^{DG}	Total annual operational cost after DG Allocation,$
V^i	Voltage of bus at i^{th} iteration during load flow
ΔV^{i+1}	Change in voltage of k^{th} bus between two consecutive iterations in load flow
ΔV	Voltage difference between two buses of the network
V_k	Voltage magnitude of bus 'k'
V_{rated}	Bus voltage of network at nominal load
$\|V\|_{k,limit}$	Voltage magnitude limit of k^{th} bus
VSI_{k+1}	Voltage stability index at the 'k+1' bus
X^{SVS}	SVS^{th} solution vector in the SVM
X_i^{SVS}	i^{th} variable of SVS^{th} solution vector in SVM
$X_{min,i}/X_{max,i}$	Minimum/maximum value of i^{th} variable of solution vector in the SVM
$X_{old}^{SVS}/X_{new}^{SVS}$	SVS^{th} old/new generated solution vector
$X_{old,i}^{SVS}/X_{new,i}^{SVS}$	i^{th} variable of SVS^{th} old/new generated solution vector in the SVM
$X_{teacher}$	Solution vector having maximum fitness in SVM in each iteration
$X_{teacher,i}$	i^{th} variable of solution vector having maximum fitness in SVM in each iteration

X_{worst}	Solution vector having worst fitness in the SVM
$X_{worst,i}$	i^{th} element of solution vector having worst fitness in the SVM
Z_{ij}	Line impedance between bus ' i' and bus ' j' of the network
ε_m	The upper bound value of $F_m(X)$
λ	Loading factor
λ_{max}	Maximum loading factor

CHAPTER 1

INTRODUCTION

1.1 BACKGROUND

In 1878, for the first time, Thomas Alva Edison locally generated and distributed direct current electricity [1], which was sold commercially. Subsequently, centralized power generation evolved where electricity was transmitted through transmission and distribution networks to meet the demand of geographically distributed load. However, the technical, financial and environmental challenges associated with centralized power generation paved the way for alternate resources of electricity generation. Hence, to mitigate the challenges of centralized power generation and to utilize the distributed energy resources, power began to be generated near the load to meet the demand locally. Such power generation is known as distributed generation (DG) which can be based on renewable as well as non-renewable energy resources. The international energy agency (IEA) [2] has cited five major concerns that contribute to the use of DG resources. These are (i) the development of DG technology (ii) limitations on the erection of new transmission lines (iii) requirement of highly reliable electricity from customer (iv) liberalization of the electricity market (v) environmental issues.

DG is defined in various ways [3]. The IEEE defines DG [4] as "the generation of electricity by facilities that are sufficiently smaller than central generating plants so as to allow interconnection at nearly any point in a power system, a subset of distributed resources". IEEE 1547 series standards [5] was introduced in 2003 for interconnection

---

This Chapter is partially based on the following published paper

I.A. Quadri, S. Bhowmick and D. Joshi, "Potential of distributed generation resources in India," *2016 IEEE 1st International Conference on Power Electronics, Intelligent Control and Energy Systems (ICPEICES)*, Delhi, pp. 1-6, 2016.

Table 1.1: Worldwide potential of renewable energy

	Technical potential of electric power (ExaJoule /year)						
				Wind			
	Solar CSP	Solar PV	Hydro power	On shore	Off-shore	Ocean	Geothermal
North America	21	72	5	156	2	68	5
OECD Europe	0.5	13	7	16	5	20	2
Non-OECD Europe and FSU	25	120	5	67	4	27	6
Africa and Middle East	679	683	8	33	1	19	5
Asia	22	254	14	10	3	103	12
Latin America	59	131	10	40	5	32	11
Oceania	187	239	1	57	3	51	4
WORLD	992	1693	50	379	22	329	45

of DG to electricity networks where network reliability and safety is considered. IEC-62109, IEC-62477 and ENTSO-E [6] comprise a separate set of standards specifying the grid code for integration of DGs. There is enormous potential for DG worldwide, which includes both conventional and non-conventional resources as shown in Table 1.1. Approximately 80% of the world's energy demand is expected to be accomplished by renewable energy resources (RES) by the middle of this century, if supported by adequate policies. During 2008-09, almost 300 Gigawatts (GW) of new capacity was added globally, where the share of renewable energy was 140 GW [7]. Despite a global financial crisis, there was improvement in addition of renewable energy capacity. The world [8] produced approximately 16,893.54 TWh (Terra Watt hour) of renewable energy in 2016. Its breakup is shown in Fig. 1.1. It comprises 4036.074 TWh of hydropower, 959.53 TWh of wind power, 333.05 TWh of solar power, 561.66 TWh of geothermal and biofuel production and 11003.22 TWh of traditional biofuels. The world has witnessed huge investment in renewable power from 47 billion USD in 2004 to 286 billion USD in2016. Investment has grown across all regions as shown in Fig. 1.2. China

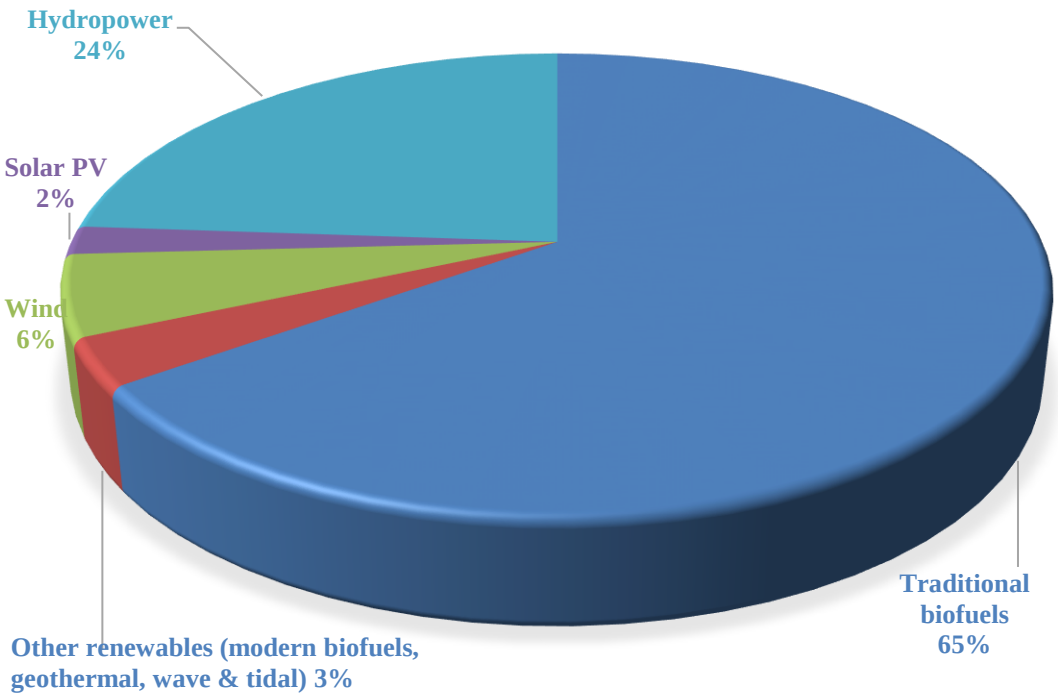

Fig. 1.1: Global renewable energy consumption

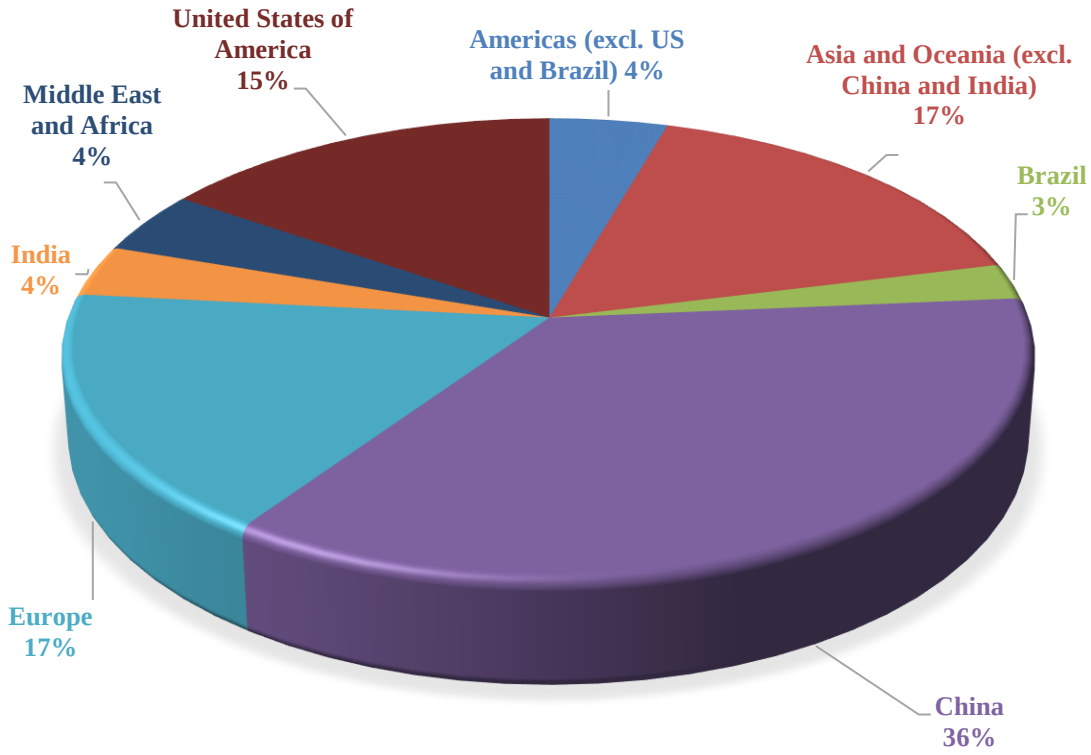

Fig. 1.2: Investment in renewables by regions

Table 1.2: Distributed generators with available sizes

S. No.	Technology	Type	Power module size
1	Fuel cell	PAFC	200 kW -2 MW
2		MCFC	250 kW -2 MW
3		SOFC	250 kW-5 MW
4		PEMFC	1-250 kW
5	Hydro	Micro	Up to 100kW
6		Mini	100-1000kW
7		Small	1-25MW
8	IC engine	-	5 kW -10 MW
9	Biomass gasification	-	100 kW-20 MW
10	Geothermal	-	5-100 MW
11	Ocean energy	-	0.1-1 MW
12	Wind turbine	-	200 W - 3 MW
13	Solar	Central receiver	1-10MW
14		PV	20 W-100kW

Table 1.3: Voltage levels for grid connected DGs

Power	Grid connection	Voltage level (kV)
<10 kW	Low voltage (single phase)	254/127
		440/220
10-75 kW	Low voltage (three phase)	220/127
		380/220
76-150 kW	Low voltage (three phase) /Medium voltage	220/127
		380/220
		13.8/34.5
151-500 kW	Low voltage (three phase) /Medium voltage	220/127
		380/220
		13.8/34.5
501kW-10MW	Medium voltage/High voltage	13.8/35.5/69/138
11-33MW	Medium voltage/High voltage	13.8/35.5/69/138
>30 MW	High voltage	69/138

become a major investor in 2015 from 3 billion USD in 2004 to 103 billion USD by 2015 followed by Europe, Asia and Oceana (excluding China and India), USA, Middle East & Africa, India and Brazil. Intergovernmental panel on climate change (IPCC) also predicted that penetration of renewable energies could result in saving of greenhouse potential of renewable energy that could be utilized by DG [9].

1.2 DISTRIBUTED GENERATION TECHNOLOGY

DG technology can be based upon internal combustion engines, combustion gas/ wind-turbines, fuel cells or photovoltaic (PV) systems. DG can also be classified into renewable and non-renewable sources with different available sizes as shown in Table 1.2 [10]. Although DG is in practice almost throughout the world, there exists a lack of consensus on its standard definition. This is also the case with the voltage and power levels of DGs for integration to power systems as shown in Table 1.3 [11].

1.3 INTEGRATION OF DGS TO POWER SYSTEM

The integration of DGs to power systems is beneficial for customers as well as utilities. Some of the major advantages are as follows,

- It provides opportunities for the power sector reforms.
- It promotes clean energy and exploration of renewable sources of energy.
- Proper siting and sizing of DGs can help in reducing the power loss in the network.
- Allocation of DG near the load reduces transmission costs while smaller DG units reduce construction time and investment cost.
- DGs have high reliability and ensure better power quality particularly when they are combined with power quality technology and energy storage.

However, in spite of several benefits like improved voltage profile, reliability of power, Competition to provide quality power to customers, less environmental impact and reduced transmission and distribution losses, there are several issues that need to be focused while integrating DGs to power systems. These are as follows.

1.3.1 Mode of operation and control mechanism

Active power injected by a DG in an existing power network depends upon the variation of the customer-end load. Experiences with integrating hydro and wind based DGs in Norway [12] reveal major voltage profile and stability issues that can be resolved by change in the regulator setting of a DG from constant power factor mode to the constant voltage mode. Also, hybrid DGs (e.g. solar + diesel or diesel + wind) prove to be more promising than single source based DGs and improves the network static and dynamic stabilities as well as the voltage and frequency variations by proper implementation of power flow controllers [13]. Although increased DG penetration causes control and stability issues, studies show that when DG penetration levels increase, the power losses also increase [14] Also, DG integration in ring type distribution systems proves to be better than in radial distribution networks [15].

1.3.2 Optimal sizing and siting (location) of DG

Appropriate sizing and location of DGs improves the quality of power to the consumers and also reduces the distribution losses. The capacity and the operating power factor of a DG also play important roles in reducing the distribution losses. Optimal DG placement (ODGP) plays a crucial role in the planning of DG integration. There are several research works available in the literature to analyze the impact of DG location and sizing on the distribution system performance, based on single or multi objective based ODGP that use various analytical, numerical and heuristic methods [16]. Since any ODGP study is based on the current load and power requirement, it needs to be modified time to time as per the power system configuration and the operating condition.

1.3.3 Issues of protection

Integration of DGs in distribution systems cause alterations in the power flow direction (s) and the short circuit level(s). Hence existing protection strategies have to be modified. Depending upon the size and the location of DG and the fault location, the fault current profile will change which may cause mal-operation of protective devices in the network. The relay setting may become invalid due to unpredictable dynamic output power characteristics of DG sources, which may lead to false tripping and reclosing problems. To overcome this problem, differential and WAP (wide area protection) scheme are implemented [17]. Global positioning system (GPS) based synchronized relays can also be employed for protection of connecting lines [18]. Coordination among the recloser-fuse can allow utilities to provide uninterrupted and reliable power for most of the portions of a feeder [19].

1.3.4 Short circuit capacity

DG installation results in an increase in the fault levels at the point of connection. This causes overall increased fault levels in the distribution equipment. PV based DGs have severe impact on power systems because they act as a power injector only [20]. Hence, the feeder which is connected to a PV system will inject more power at the short circuit, resulting in disastrous consequences.

1.3.5 Power quality

Due to intermittent availability of renewable energy sources like solar and wind, power electronic devices are required to maintain the reliability of power supply, which in turn, leads to power quality problems. Unified power quality conditioner (UPQC) is used for

the compensation of reactive power and harmonic reduction while maintaining grid voltage profile and minimization of load current disturbances [21]. Active network management (ANM) technique may be used to improve the power quality of DNs [22].

1.3.6 Stability

Radial distribution systems without any DG have proved to be mostly stable. However, with DG integration, it will have transient, dynamic and small signal stability issues that must be addressed properly [23] .

1.4 DISTRIBUTED GENERATION IN INDIA

With limited reserves of resources and environmental and health concerns, the Indian government has taken several technical and financial initiatives for power generation from renewable energy resources. Growth of energy from renewable sources has been reported to be over 20% in the last five years [24]. In the beginning of 2009, total installed capacity of renewable power was only 14,400 MW. By the end of 2014, it rose to 33,791 MW. Out of this, wind energy has a share of 66 % (22,465 MW) followed by SHP (3,991 MW), biomass (4,165 MW), solar power (3,063 MW) and urban & industrial waste (107.5 MW). By the end of 2018 [8], it rose to 75055.92 MW. Out of this, wind energy has a share of 47 % (35288.1 MW) followed by 6.03 % SHP (4528.05 MW), 12.09 % biomass (9075.5 MW), 34.68 % solar power (26025.97 MW) and 0.19 % urban & industrial waste (138.3 MW). Fig. 1.3 and Fig. 1.4 show the total installed renewable based power in India till December 2018.

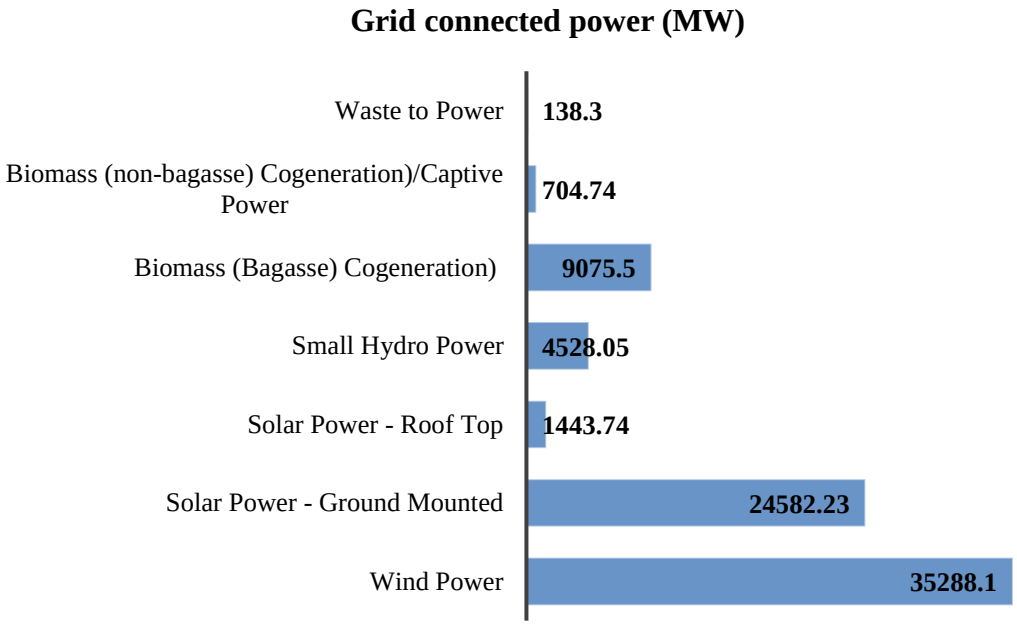

Fig. 1.3: DG capacity connected to grid in India

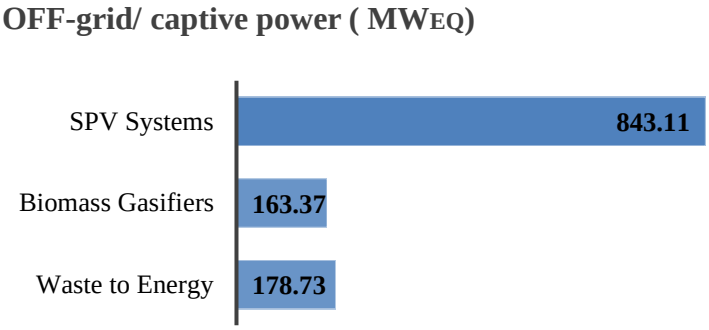

Fig. 1.4: Off-grid DG capacity in India

1.4.1 Wind energy

India currently occupies 5th position in wind power production in the world after China, USA, Germany, and Spain. The estimated potential of on-shore wind power is 49,130 MW at 50 m height. The extrapolated potential at 80 m height is 1, 02,788 MW. Till December 2018, 35,288.1 MW of wind generation has been installed in the country.

1.4.2 Biomass power and bagasse co-generation

The estimated potential of power from agro-industrial residues and agriculture is about 18,000 MW along with 7000 MW from sugar mills through bagasse cogeneration. Thus, the total potential estimated from biomass is about 25,000 MW. The total installed biomass power and co-generation is about 4528.05 MW till December 2018 for feeding the grid.

1.4.3 Small hydro power

The estimated potential of power from small / mini hydel (less than 25 MW) is 19,749 MW at 6474 sites in the country. Alternate hydro energy center (AHEC), IIT, Roorkee, provides facilities for survey, DPRs, project monitoring and training to promote hydro power in country. The ministry of non-renewable energy (MNRE) is promoting to set up power generation up to 100 kW under the remote village electrification scheme. The 12^{th} Plan has set up a target of 1600 MW for small hydro power (SHP) addition. The total installed SHP was about 4528.05 MW till December 2018 for feeding the grid.

1.4.4 Solar energy

India is having average solar radiation incident in the range of 4000-7000 Wh per day and with about 300 sunny days, the estimated energy potential is about 6,000 million GWh annually. Jawaharlal Nehru national solar mission (JNNSM) is a mile stone project by the government of India and administered by MNRE to explore solar potential in India. The JNNSM has set a agenda to have additional 20,000 MW grid connected solar power by 2022. This is to be achieved in three stages (first stage will completed by 2012-13, second stage by 2013 -17 and third stage by 2017- 22).

1.4.5 Geothermal energy

Geothermal potential in India is estimated at 10,000 MW. USA, Sweden, Germany, Switzerland, Canada, Japan and China are the leading countries using this technology. It is targeted to install 1000 MWth (MegaWatt thermal) till 2022. India is in Low geothermal potential region having low/medium heat enthalpy. Government is encouraging the demonstration projects to estimate the technical feasibility of the project before going to the commercial production.

1.4.6 Fuel cell technology

The fuel cell based DG is still in the research and development stage in India. The university of Calcutta, Kolkata and Advance study in science and technology, Guwahati is working on different fuel cells to improve their efficiency.

1.5 CONVENTIONAL POWER SECTOR AND ITS IMPACT

India is currently occupying the 5^{th} position in the world in electricity production, where thermal power production has a share of 66%, hydro 19% and the remaining 15% includes other sources like natural gas, nuclear energy and renewables. As per Central Electricity Authority (CEA), in 2010-11, India was the 4^{th} largest consumer of electricity in the world. It has an electricity demand of 122 GW against availability of 110 GW. Emission standards of India are lagging far behind that of Australia, China, USA and the EU. In 2011-12, the total power generation of 111 coal fired power plants was 121 GW, which consumed 503 million tons of coal. The estimated pollution per year, of particulates is shown in Fig. 1.5. These emissions cause premature deaths ranging from 80,000 to 115,000. In 2011-2012, more than 20.0 million asthma cases

were seen, and the government expenditure was estimated to be ranging from 16,000 to 23,000 crores of Rupees [25]. Hence, we need alternative sources of power to meet our power requirement. Centralized power generation has various issues like transmission and distribution losses, limited reserves of conventional fuel, land acquisition issues, non-economical remote village electrification etc. which necessitate the use of DG resources. Although DGs have the advantages of improved power reliabilty, availabilty of power at remote areas at cheaper rate and reduced environmental issues, integration of DGs to the network is a challange and needs several technological advancement and mitigation techniques to resolve these issues. DGs have a distinctive character compared to the traditional centralized power generation model and energy delivery to the loads in the power distribution network (DN). However, DGs are not essentially advantageous for all stake holders in the electricity infrastructure. Utilities may view on-site power generation as challenging because they have diverse consumption patterns than that of average customers. Fuel ingestion, noise pollution, carbon and other pollutant emissions, can increase or decrease depending on the operating technology of the DG system. Inherent in this, there is a need to analyse DG costs and benefits and the influence of public policy on DG adoption and operation. While DG may itself become a dominant force in the provision of energy, its capability to be used in

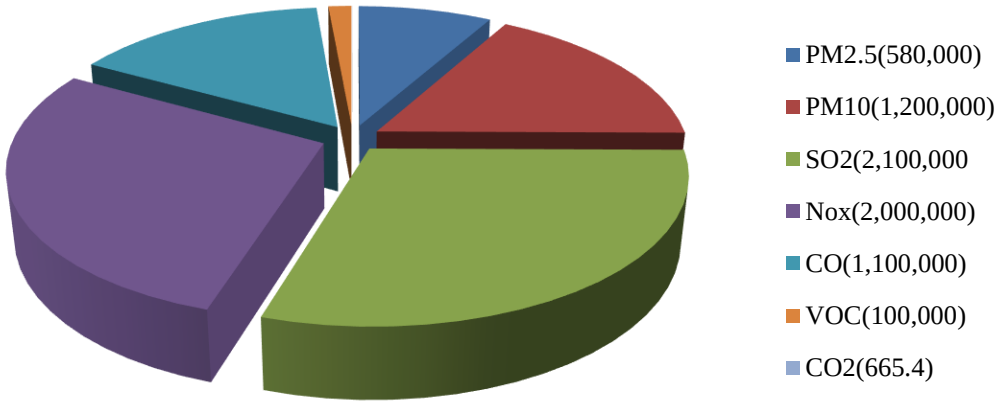

Fig. 1.5: Pollution caused by coal power plants annually

numerous locations and being integrated into the grid is its greatest value. Ultimately, there has to be a clear, consistent and long-term market framework. Modern scientific developments in communications, energy storage and automation has made this possible. Recent developments in the regulatory arrangements and incentives to connect, particularly renewable technologies, to transmission and distribution networks have meant that the traditional pattern of network usage has altered and this situation is likely to continue. One of the principal challenges has been the increase in the volume of DGs connected to the network.

1.6 SCOPE OF THE WORK

Many technical, commercial and environmental challenges are associated with the integration of DGs in a distribution network. Both the industry and the academia have been attempting to minimize these challenges. The work in this thesis addresses the issue of optimal siting and sizing of DGs in distribution networks to improve the network performance vis-a-vis technical, economic and environmental aspects. The technical aspects include power loss minimization, voltage profile improvement and enhancement of voltage stability index of the distribution networks with DG integration. The economic aspects address the improvement in the savings in operational costs and annual energy with DGs. The environmental aspects investigate the improvement in emission and associated savings in costs with DGs. In all the cases, meta-heuristic algorithms have been developed for optimal allocation of DGs in the distribution networks considering both single and multi-objective formulations. The thesis also includes the development of a multi-objective approach to maximize the loadability of distribution networks by simultaneous reconfiguration and optimal allocation of DGs, using the meta-heuristic algorithms.

1.7 OUTLINE OF THE THESIS

Chapter 1: This chapter presents a detailed description of distributed generation resources (DER) and their type and the impact of their integration with distribution networks. The technical issues involved with DG installation, the benefits of DGs and the challenges of DG integration in power systems vis-à-vis the detrimental effects of conventional and centralized power generation have also been discussed.

Chapter 2: This chapter presents the literature review. It reveals the chronological description of the different types of DG resources used for mitigating the operational challenges of distribution networks. Detailed literature survey has been conducted to explore the contributions of past researchers in developing different analytical, heuristic and meta-heuristic approaches for the optimal allocation of different types of DGs. Based on the comprehensive literature survey, research gaps are identified.

Chapter 3: This chapter presents the mathematical modelling of a typical radial distribution system and the different types of loads. Power flow technique using the bus injection to branch current (BIBC) and branch current to bus voltage (BCBV) matrices has been discussed. Several network performance indices like voltage stability index, maximum line loadability index and bus voltage limit violation index have been elaborated. Network reconfiguration technique based on a graphical approach has also been illustrated in detail.

Chapter 4: This chapter presents the development of the CTLBO algorithm for the optimal siting and sizing of Type–I DGs. The developed algorithm is first validated on several standard mathematical benchmark functions. Both single and multi-objective formulations are carried out and a comparative analysis vis-à-vis existing methods, is

presented. The developed algorithm is subsequently implemented for optimal allocation of DGs in several RDS.

Chapter 5: This chapter presents a hybrid meta-heuristic (HTLBO) algorithm for the allocation and sizing of Type–I DGs. The proposed method first discusses the validation of the proposed algorithm on standard mathematical benchmark functions. Subsequently, HTLBO is implemented for the optimal allocation of DGs in several RDS, considering different network loading conditions.

Chapter 6: This chapter addresses the reactive power management in distribution networks using DSTATCOMs, based on analytical as well as meta-heuristic approaches. The optimal allocation of DSTATCOMs has been implemented based on both single and multi-objective formulations. Pareto solutions of the multi-objective formulations have been carried out to enable the distribution networks to be operated in several operational modes. This chapter also analyses the technical, commercial and environmental benefits possible with the optimal allocation of DSTATCOMs in different RDS.

Chapter 7: This chapter addresses the network loadability enhancement of radial distribution networks without any additionaln infrastructural investment which is possible with network reconfiguration and optimal DG allocation. A multi-objective approach is used. A comparative analysis vis-à-vis existing methods is also presented in this chapter.

Chapter 8: Finally, Chapter 8 presents the conclusions of the work reported in the thesis and makes some suggestions for further work in the area covered by the thesis.

CHAPTER 2

LITERATURE REVIEW

2.1 INTRODUCTION

This chapter provides an overview of the research works carried out to enhance the technical, commercial and environmental performances of distribution networks by integration of DG resources. Optimal distributed generation placement (ODGP) plays a crucial role on the distribution network performance and hence, in DG integration planning. There are several research works available in the literature to analyze the impact of DG location and sizing on distribution network performance, based on single or multi objective based optimal DG allocation that use various analytical, numerical and heuristic methods. This chapter systematically presents an inclusive literature review on the optimization techniques used for siting and sizing of different types of distributed energy resources in distribution networks and their impact on the network performance vis-à-vis power losses, voltage profile, voltage stability, savings in operational costs and environmental benefits. Finally, the major limitations and research gaps in these research works have been identified.

2.2 IMPACT OF DISTRIBUTED GENERATION

Currently, centralized power generation is unable to meet the continuously rising global energy demand. Around 16 % of the global population still live without electricity [26]. DG is a viable option where power is generated near the load centers. DG comprises both fossil fuel based conventional and non-conventional energy sources like solar power, hydro, biofuel, geothermal etc. ranging from few kilowatts to about 50 MW [27].

Competitive markets, environmental issues and reliability of power sources are some of the major criteria for the selection of energy sources. Depletion of fossil fuel sources and continuous improvement in the area of non-conventional ones have been the motivating factors for the utilities to go for DG. Although DGs have several environmental and economical benefits, they impose several operational issues in distribution systems. These may include but are not limited to relay co-ordination problems caused by reverse power flow, voltage rise issues, power quality and voltage stability issues etc. [28, 29]. Proper DG allocation has a marked effect on the power losses, voltage profile, line loadability, operational costs, reliability of power supply, pollution and stability issues in distribution systems. Therefore, optimal DG allocation has been a global challenge for both the academia and the industry.

2.3 REVIEW OF ANALYTICAL APPROACHES FOR ALLOCATION OF DGS IN DISTRIBUTION NETWORKS

Several research works have been reported on the optimal siting and sizing of DGs in distribution systems. In this context, some comprehensive research works for the placement of DGs using analytical methods to reduce network power losses and improvement of voltage profile including different loading conditions, have been reported in literature. [30] has suggested zero point analysis approach for the allocation of DG units, which is based on 2/3 rule for losses and voltage impact study. [31] has introduced an analytical approach which is applicable to different types of distributed loads. The effectiveness of this approach is demonstrated by placing a single DG unit in the 6-bus and 30-bus distribution networks. This methodology is not iterative and hence, no convergence issues are involved. Also, the computational time (CT) is very less. [32] has implemented the exact loss formula based analytical approach for DG

allocation in 30-bus, 33-bus and 69-bus radial distribution networks. This method is based on the Newton-Raphson based power flow algorithm. The results obtained using this approach demonstrate reduced power losses, improved voltage profiles and reduction in thermal capacity of main feeder. [33] has formulated an analytical approach having a loss sensitivity factor, based on the equivalent current injection at the bus. The suggested sensitivity factor is used for optimal allocation of DG units to minimize total power losses, without using the admittance matrix. Its effectiveness is tested on the 12-bus, 34-bus and 69-bus radial distribution networks. It is observed that the suggested method is better than the classical grid search algorithm. [34] has suggested an analytical approach based on linearized AC power flow and the optimal allocation of DG is based on active power loss sensitivity factor. This approach has been tested on 33-bus and 69-bus distribution networks where computational time for optimal allocation of DG units is found to be less in comparison to the exhaustive load flow approach. [35] has suggested analytical approach for allocation of different types of DG units, considering their power factors. The applicability of this approach has been tested on 16-bus, 33-bus and 69-bus radial distribution networks for DG unit allocation and is found better than the exhaustive load flow approach. [36] has suggested an analytical approach where optimal allocation is achieved using sensitivity analysis technique and the optimal DG unit capacity is calculated using a heuristic curve fitting technique. To validate the suitability of the proposed method, it has been applied to 12-bus and 33-bus test distribution systems for active power loss minimization. It is observed that a combination of DG units and capacitor allocation in distribution networks is found to be more suitable than DG units alone. [37] has suggested an analytical approach for DG unit allocation and sizing. This approach uses a novel power stability index (PSI), which identifies the most voltage sensitive bus and minimizes the

total power losses of the distribution network. The proposed algorithm has also been tested using three different radial distribution test systems and the results are found to be better than the golden section search algorithm. The computational time of the proposed approach for DG allocation reduces by 50–60% as compared to the golden section search algorithm. [38] has suggested an analytical approach based on the combined power loss sensitivity factor which is used to optimally allocate different types of DG units at optimal power factors. This approach is tested on 12-bus and 33-bus radial distribution networks. Many other approaches based on novel index vector and voltage sensitivity index methods for DG unit allocation have been compared. Although analytical methods for siting and sizing of DGs have fast convergence, with increase in the types and number of DGs, the computational complexity increases and may lead to non-optimal solutions. Further, complexities in the formulation of objective functions with multi-objective analysis affect the computational time with analytical methods.

2.4 REVIEW OF SOFT COMPUTING APPROACHES FOR DG ALLOCATION IN DISTRIBUTION NETWORKS

Advancements in soft computing techniques have led to the development of several evolutionary optimization algorithms for the optimal allocation of DGs in distribution systems. Some notable ones among these are genetic algorithms (GA), particle swarm optimization (PSO), artificial bee colony (ABC), ant colony optimization (ACO), bacterial foraging optimization algorithm (BFOA) etc. Some comprehensive research works on the use of GA for optimal allocation of DGs in distribution networks have been reported in [39-49]. In this respect, [47] has reported that GA requires increased computational time while suffering from premature convergence than analytical

approach.

PSO is another intelligent technique which has been widely used for DG placement in distribution networks. Some comprehensive research works on the use of PSO for optimal DG allocation in distribution systems are presented in [48] . In addition, several variants of PSO based optimization technique have also been used. Some notable ones include multi-objective evolutionary PSO (MEPSO) [49] and discrete PSO [50]. Although PSO possesses better search capability than GA, it may converge to strong local minima if optimization parameters are not properly tuned.

ABC has been used [51] for optimal placement of DGs to minimize overall investment cost. Apart from GA, PSO and ABC, researchers for optimal allocation of DGs have also proposed several other nature-inspired algorithms. These include the modified honey bee mating algorithm [52], cuckoo search optimization algorithm (CSOA) [53], bacterial foraging optimization algorithm (BFOA) [54], modified bacterial foraging optimization algorithm [55], firefly algorithm [56], Hereford Ranch algorithm [57], modified shuffled leaping algorithm [58], chaotic symbiotic organisms search (CSOS) algorithm [59], Kalman filter algorithm [60], harmony search algorithm (HSA) [61] and gravitational search algorithm [62]. Even if evolutionary methods are spontaneous, easy to realize and simple to implement as compared to analytical ones, the nature of the optimization variable (continuous, discrete or mixed) and inappropriate selection of algorithm parameters can lead to premature convergence in the event of strong local extrema. To avoid a non-optimal solution, these algorithms require proper parameter tuning.

In this perspective, teaching-learning based optimization (TLBO) reported in [63], is a parameter independent intelligent algorithm, which was developed and subsequently

used for the optimal placement of energy resources in distribution networks. Although TLBO is parameter independent and has a very fast convergence rate, it is prone to local maxima/minima trappings. It is observed that TLBO often converges to local minima when the numbers of DGs and/or operating constraints in the distribution network increase. In this context, a modified-TLBO algorithm [64] for DG placement has been suggested. However, it requires an additional mutation phase to find the global solution. Quasi-oppositional teaching-learning based optimization (QOTLBO) [65], which utilizes opposition–based learning to enhance the exploration of the search space, has also been implemented for DG placement in radial distribution systems. An improved TLBO, in which a cross over rate and a cross over parameter have to be specified, has been reported in [66]. However, this additional phase adds complexity to the TLBO and increases the computational time. Moreover, the parameters need to be tuned properly to achieve a satisfactory convergence while placing DGs in the distribution network.

Harmony search (HS) is another swarm intelligence algorithm which shows good exploration capability but poor exploitation capability for global solutions. Several HS variants have been suggested to solve complex optimization problems, such as SGHS (self-adaptive global harmony search algorithm) [67], IHS [68] , ITHS (intelligent tuned harmony search algorithm) [69], EHS (enhance harmony search) [70], NGHS (novel global harmony search) [71], DIHS [72], NDHS [73] and DSHS [74]. However, these improved versions of HS are also unable to handle complex optimization problems of high dimensionality and modality. IHS lacks in precise solution. It is observed that NGHS, SGHS and NDHS get easily trapped into strong local minima/maxima. Although solution provided by EHS and DSHS are satisfactorily but they require more convergence time for global solution with high-dimensional problems.

2.5 REVIEW OF REACTIVE POWER COMPENSATORY DEVICES ALLOCATION IN DISTRIBUTION NETWORKS

In recent years, integration and increased dissemination of DG resources in DNs have compelled the distribution network operators (DNOs) to take appropriate measures to enhance reliability, operational cost reduction and power quality. Some remedial steps by DNOs in this regard include fixed/switched capacitor [75], network reconfiguration [76] and load management [77]. Further, simultaneous network reconfiguration and distributed energy storage allocation [76] significantly improves the DG penetration in distribution networks. However, increased penetration of renewable based DGs and electric vehicles [78] often creates power quality challenges for the DNOs. Moreover, due to the predominantly resistive nature of distribution networks, uncertainties in load demands have a substantial repercussion on total harmonic distortion, voltage profile (VP), active power loss (APL), reactive power consumption (RPC) and stability [79]. Firefly algorithm has been implemented in [79] for the optimal placement of distribution static synchronous compensators (DSTATCOMs) for power quality enhancement and cost savings. These challenges aggravate with increased penetration of unbalanced load demands [80] and integration of intermittent energy resources [81]. To mitigate these operational challenges, fixed and switched shunt capacitors [82, 83, 84] placed in DNs used to be the earliest solution. Since the last two decades, advancement and operational flexibility in flexible alternating current transmission systems (FACTS) devices have led to better utilization of electric networks [85]. In a similar manner, custom power devices (CPD), identical to FACTS devices but with a different objective, are used to enhance the reliability of DNs and the quality of power [86]. Several custom power devices like static VAr compensators (SVCs) [87] and DSTATCOMs [88] have been widely used for reactive power compensation in distribution systems to alleviate the

operational challenges. DSTATCOM is a shunt device, which constitutes an energy storage device, an inverter, and a transformer. Their fast, dynamical response in respect of injection and absorption of reactive power makes their acceptability inevitable in distribution systems. DSTATCOM installations in DNs provide variable reactive power compensation [89] and improves the power factor [90], VP [91] voltage THD, while minimizing uncertainty of power generation due to renewable resources.

To ensure operational reliability and economic viability of distribution systems, DSTATCOM(s) of suitable capability must be sited at appropriate location(s) in the network [92, 93]. Although the literature on the use of FACTS devices in power transmission systems is extensive, that available on that of CPD is limited. Several comprehensive research works have been reported on the placement of DSTATCOMs in DNs in the perspective of sensitivity index, APL reduction [94, 95], energy and operational cost savings [96]. Optimal allocation of multiple DSTATCOMs in the IEEE 30-bus distribution system based on a hybrid of GA and ACO algorithm has been presented in [95]. In this perspective, Analytical methods based on VSI [97] and reactive stability index [98] has been suggested for the allocation of DSTATCOM for VP enhancement and APL reduction in the IEEE 33-bus radial distribution network (RDN). [99] has considered allocation of DSTATCOM in the 38-bus meshed DN based on VSI, fast VSI (FVSI), proposed stability index (PSI) and combined power loss sensitivity (CPLS) index. It is observed that CPLS and PSI yield better results than the rest. However, all these analyses are limited to the placement of a single DSTATCOM. Although analytical approaches require less computation time, intricacies in the framework of objective functions with multiple DSTATCOMs and multi-objective formulations have an impact on the accuracy and computational time.

Evolution of soft computing techniques contributed several evolutionary algorithms to allocate DSTATCOMs in distribution systems. Evolutionary algorithms are swarm intelligence-based optimization methodologies which are skilled in solving multi-objective, multimodal, continuous and discrete problems while satisfying various constraints. Some notable research works implementing evolutionary algorithms are detailed in [100]-[112]. In [100], Immune algorithm (IA) has been used to place DSTATCOM to decrease energy losses, operational costs, better network congestion management and VP improvement of 33-bus and 69-bus RDS. Although results illustrate the superiority of IA over GA in DSTATCOM placement, but analysis of optimal number of DSTATCOMs has not been considered to maximize the cost benefits. In [101], differential evolution (DE) algorithm is used for DSTATCOM allocation and network reconfiguration to improve APL and VP of the 69-bus and 83-bus DNs. Although DE algorithm is observed to be better than PSO for simultaneous reconfiguration and DSTATCOM allocation, actual loading of the DN is not considered. Optimal allocation of a DSTATCOM has been proposed employing binary gravitational search algorithm (BGSA) [102] in a 47-bus practical DN to enhance the reliability of the network by reducing load outage and momentary interruptions. However, the analysis is limited to the placement of a single DSTATCOM. Simultaneous network reconfiguration along with DG and DSTATCOM allocation has been presented in [103] based on improved cat swarm optimization (ICSO) for VP improvement and annual energy loss minimization in the 69-bus DN, with three different load levels. Although ICSO is reported to outperform both CSO and PSO, the analysis is again limited to the placement of a single DSTATCOM. The results show marked improvement in the total harmonic deviation (THD) and VP in the 16-bus distribution system over GA and PSO. In [104], HS algorithm is used to place a

DSTATCOM to improve annual energy savings in the IEEE 33-bus DN. Although results demonstrate marked improvement in the annual cost savings over the IA, only a single DSTATCOM and constant power load has been considered.

To further improve the performance and to prevent premature convergence of evolutionary algorithms, several hybrid algorithms have also been reported in the literature. In [105], the authors have implemented the hybrids of fuzzy logic and ant colony optimization (ACO), fuzzy and PSO as well as fuzzy and GA for network reconfiguration and allocation of PV arrays and a DSTATCOM in the IEEE 33-bus and the Taiwan power corporation networks. It has also considered the loadability of networks based on voltage stability margin. However, the analysis is again limited to the allocation of a single DG and DSTATCOM. [106] has reported DSTATCOM placement in the IEEE 30-bus RDS based on a hybrid of Nelder-Mead algorithms and imperialistic competition. This approach deals with a multi-objective formulation involving APL and VSI of the DN. However, comparative analysis with any other algorithm has not been carried out. It has been reported by many researchers that integration of distributed energy resources to DNs results in improved VP, line loadability enhancement [107, 108, 109], APL reduction [110, 111], greenhouse gas reduction [112] and VSI improvement [113].

2.6 REVIEW OF LOADABILITY ENHANCEMENT OF DN(s) USING DG(s)

Power distribution network operators have been facing major challenges because of several issues like uneven load growth, high penetration of DER and deficiency of investments in network infrastructure. This requires the operators to improve the performance of distribution networks. Researchers have reported several ways to reduce

power losses in distribution networks like network reconfiguration [114], load balancing [115] using transversality enforced Newton-Raphson algorithm for the loadability enhancement of several distribution networks , allocation of different types of DERs according to the load demand profile [116, 117] incentive based policy etc., which enhance the overall network efficiency. It is observed that the network loadability is restricted more by voltage limit constraints than by line thermal limit constraints [118] of the Brazilian distribution network. However, higher load growth rate poses serious network operational challenges like line thermal limit violations, voltage limit violations [119], voltage stability issues [120] and voltage collapse [121].

Researchers have reported loadability enhancement of RDN based on several indices. [122] has suggested a static approach based on VSI for real, reactive and apparent power loss minimization. A new loadability index 'Lp' ($0 \leq Lp \leq 1$) has been suggested by [123] where 'Lp' greater than unity indicates voltage collapse. However, this index is based on unidirectional power flow in the network. [124] has suggested an index 'MLI' (≥ 1) for the analysis of voltage stability along with line loading margins in RDN. However, MLI (Maximum loadablity index) is valid only when the load power factor angle is not equal to the line impedance angle. [125] has suggested a loadability index 'Ls' ($1 \leq Ls \leq 2$) to tackle the inherent problem posed by a new loadability index 'Lp'. It has used HPSO algorithm for the optimal allocation of multiple DGs in three different RDNs to improve the network loadability.

It is observed that optimal DER allocation, network reconfiguration [126] [127, 128] or both [129] significantly enhance the loading factor (LF) of RDN. [128] has used discrete artificial bee colony (DABC) to enhance the loadability in several cases which include simultaneous network reconfiguration and DG allocation in RDN. However, no

comparison with existing works has been reported. Simultaneous network reconfiguration and strategic allocation of multiple DGs in the RDS involve mixed integer variables (discrete variables for tie/DG locations and continuous variables for DG sizes). Analytical tool based tangent vector method and continuous power flow (CPF) approach for placement of Type-3 DER at the weakest bus has been suggested by [130] to enhance the 'λ' of the network. However, this approach is limited to the placement of a single DG. [131] has analysed the loadability improvement in distribution networks considering the allocation of various types of DGs and has reported that loadability improvement can be maximized by employing Type-4 DGs. However it has been reported [130, 131] that simultaneous network reconfiguration and DG allocation is the most effective way of enhancing the line loadability. [132] has observed that for the enhancement of network loadability, fuel cell based DGs are more effective than solar and wind based DGs. [133] has suggested a 'global sensitivity index' for loadability enhancement of the 33-bus RDN considering the uncertainty of renewable sources, loads and distribution feeder parameters. [134] has suggested several energy efficiency indices to enhance the loadability of the distribution network. Enhancement of the network loadability on the basis of voltage quality and voltage sensitivity index has been reported in [135]. [136] has reported loadability improvement of the network on an hourly basis.

2.7 ANALYSIS OF RESEARCH GAPS IN THE LITERATURE

This section summarizes the research gaps found in the literature survey discussed in the previous sections. It has already been discussed in previous sections of this chapter that in recent years, continuously increasing load demand and deficiency of capital resources vis-à-vis a competitive electricity market have forced transmission and

distribution utilities worldwide to maximize the efficiency and utilization of their existing infrastructure. The literature survey reveals that optimal allocation of distributed generation resources result in a marked improvement in the technical, commercial and environmental benefits of distribution networks. It has also been reported that optimal DG allocation and / or network reconfiguration enhance the distribution network loading capability significantly. The limitations of analytical as well as soft computing-based algorithms has also been reported in the literature review.

On the basis of these observations, the main objectives of the proposed research work are as follows:

- To improve the performance of the existing meta-heuristic algorithm(s) for the optimal siting and sizing of DG resources considering single as well as multi-objective criterion.
- To develop hybrid algorithm(s) for maximum exploitation and exploration of the solution search space to ensure global solution.
- Validation of the modified / hybrid algorithm(s) using several standard mathematical benchmark functions.
- Implementation of the modified / hybrid algorithm(s) for optimal DG allocation in several radial distribution networks (RDS). The analysis of distribution network performance is based on several indices for single as well as multi-objective functions, considering different types of DGs.
- Investigation on the improvement of distribution system performance vis-a-vis technical, economic and environmental aspects due to integration of DSTATCOMs.
- Development of a graphical approach-based network reconfiguration technique.
- Improvement in loadability of RDS by simultaneous reconfiguration and optimal

DG allocation.

The proposed research work has been carried out in the following manner.

(a) Performance enhancement of existing algorithm for allocation of DGs

Optimization algorithms play a crucial role in the allocation of DG resources in DNs for reducing active power losses, voltage profile improvements, economical operation and environmental benefits. The increase in the number and type of DGs, objective functions, network complexities and constraints often affect the convergence criteria of the optimization algorithms. The convergence characteristic of an algorithm is strongly dependent on the algorithm parameters. In this perspective, TLBO [63] algorithm, which is almost parameter independent, is considered in this work.

However, the existing TLBO algorithm is prone to local maxima/minima trappings when the number of solution variables increase. Hence, in this work, a modification in the "teaching factor" of the existing TLBO algorithm has been carried out to improve the exploitation capabilities while maintaining the convergence speed. This algorithm, known as CTLBO, yields better results over several existing meta-heuristic algorithms when implemented on several well-defined mathematical benchmark functions. The proposed algorithm is subsequently used for the optimal allocation of DGs in several RDS. Both single and multi-objective formulations have been implemented. The single objective functions involve criterion of power loss minimization, voltage profile improvement or voltage stability index. The multi-objective functions are implemented using the weighted sum approach and the ε-constraints method. From the results, it is observed that the performance of the proposed CTLBO algorithm is better as compared to several other existing algorithms.

(b) Development and validation of hybrid optimization algorithm for optimal DG allocation

From the literature survey, it is observed that while TLBO exhibits good exploitation capability of the solution search space, the HSA demonstrates good exploration capability. So, a proper integration of the merits of both TLBO and HS would result in a better optimization technique for high-dimensional and multimodality problems. To get a good balance of exploration and exploitation capability of the search space, a new optimization algorithm based on the hybridization of HS and TLBO (HTLBO) has been subsequently developed in this work. In this algorithm, at first the HS algorithm is utilized to explore the search space with a high probability of finding the global solution. Subsequently, the TLBO carries out exploitation of the search space for the global solution. To choose TLBO or HS, the proposed algorithm utilizes self adaptive selection probability.

In this work, at the outset, the performance of the proposed algorithm is tested on several standard mathematical benchmark functions for single as well as multi-objective formulations. Subsequently, the multi-objective problem of optimal DG allocation in the 33-bus [137], 69-bus [82] and 118-bus [138] RDN is solved by the Ɛ-constraint method using HTLBO. The proposed HTLBO is compared with existing TLBOs and QOTLBO. The results validate the proposed method.

(c) Reactive power management in DNs to enhance savings in energy, cost and emission

It is observed from the literature survey that reactive power management in distribution networks contribute significantly in reducing the APL, network operational costs and environmental pollutant emissions. So, in this work, two approaches have been used to

meet the desired objectives.

At first, an analytical approach has been developed for the allocation of single as well as multiple DSTATCOMs in several distribution networks for power loss minimization, based on the power loss sensitivity index [38]. The algorithm has a fast convergence rate and the results obtained are found to be better than several existing algorithms. However, increase in the number of objective functions, network complexities and constraints may yield non-optimal solutions. Subsequently, CTLBO has been used for the optimal allocation of DSTATCOMs for single as well as multi-objective formulations. The Pareto solution for DSTATCOM allocation has also been carried out, which offers the distributed network operators multiple options to operate the DN, as per their requirement.

(d) Development of a graphical approach for network reconfiguration

There are many network reconfiguration techniques available in the literature. It is observed that the available techniques are easy to implement for checking the radiality of the distribution networks. However, pictorial or graphical representation of the re-reconfigured network(s) is not possible. In this work, an approach has been developed to identify the network radiality and represent the closed tie/sectional switches graphically.

(e) Multi-objective approach to maximize the loadability of DNs by simultaneous reconfiguration and DG allocation

In recent years, transmission and distribution utilities worldwide have been engaged in maximizing the efficiency and utilization of their existing infrastructure. This thesis

presents a multi-objective approach to maximize the loadability of distribution networks by simultaneous reconfiguration and optimal allocation of DGs using the CTLBO algorithm. The proposed technique is based on the ε-constraints method. Loadability enhancement is validated on the 33-bus and 69-bus RDS. Several case studies are carried out to demonstrate the effectiveness of the proposed approach in reducing the network APL, improving the kVA loading margins and enhancing the voltage profiles while considering the voltage and thermal limit constraints. Results show that maximum loadability is obtained with simultaneous network reconfiguration and allocation of DGs with different power factors.

CHAPTER 3

POWER FLOW, LOAD MODELING AND TEST NETWORKS

3.1 INTRODUCTION

As described in chapter 2, power flow computational time for optimal allocation of DGs in different distribution networks by several optimization techniques plays a crucial role in the convergence characteristics. The load characteristics and integration of several types of DG to the distribution networks have significant impact on the network technical performance, economic operation and environmental benefits.

The power flow techniques like Gauss-Seidel [139], Newton–Raphson [140] and Fast Decoupled method [141] are best suited in transmission networks. They have convergence issues in distribution networks on account of their high R/X ratio, un-transposed lines, and unbalanced loading as well as different topographical structure and characteristics. Some of the modified classical power flow techniques such as Gauss implicit Z-matrix method [142] is a commonly used method but it is unable to converge for radial and weakly meshed network. Subsequently, compensation-based technique [143] is proposed where forward/backward sweep technique was adopted. However, this approach requires new data format and search procedure. In another technique [144], power flow is feeder lateral based model, which needs data format in accordance with the layer-lateral. [145] have suggested topographical based power flow technique where admittance and / or Jacobian matrix is no longer required as in the case of conventional power flow methods. Consequently, the suggested approach for power flow is found to be more robust and having less computational time. In this chapter, the topographical based power flow technique is first discussed, which is simpler and has

lesser computational time [145]. In [111] several voltage dependent and time-variant loads are modelled. For annual energy consumption, normalized average load has been presented. The different types of DGs used in this work are also detailed in this chapter. Finally, various test distribution networks used for implementing the proposed methods have been described.

3.2 POWER FLOW TECHNIQUE

A typical radial distribution network is shown in Fig. 3.1 by single line diagram, for demonstration of the power flow technique, which includes substations, buses, lines and loads. Fig. 3.2 represents the equivalent circuit of a section of the distribution network shown in Fig. 3.1.

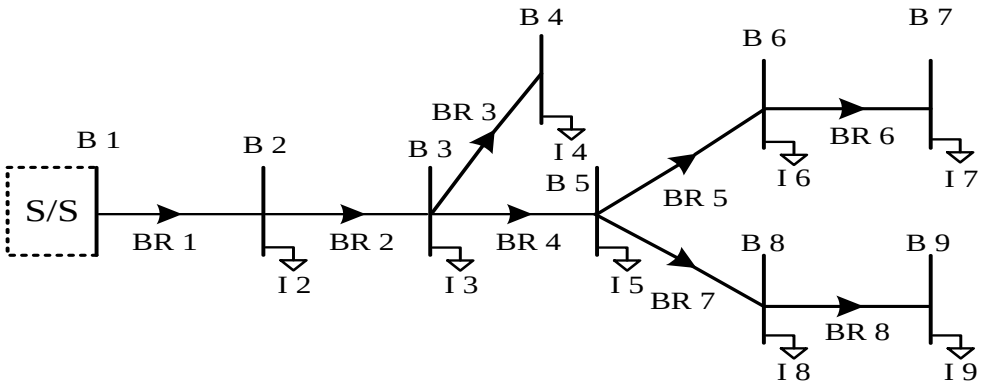

Fig. 3.1: Typical layout of a radial distribution network

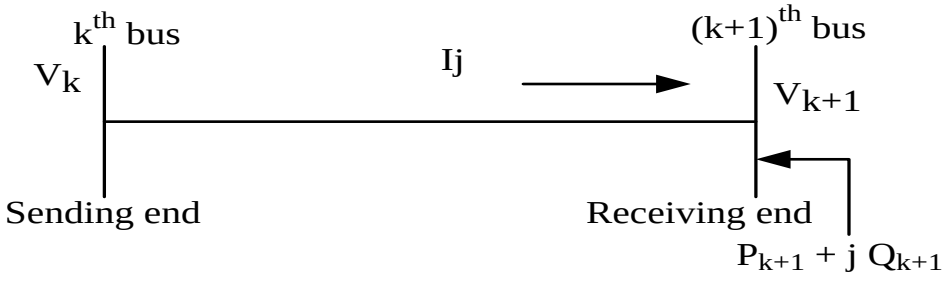

Fig. 3.2: Equivalent circuit of the j^{th} branch of the network between buses 'k' and '(k+1)'

The equivalent current-injection based model is found to be more realistic for distribution networks [145]. For bus $(k+1)^{th}$, the complex power injected is expressed as,

$$\mathbf{S_{k+1}} = (P_{k+1} + jQ_{k+1}) \quad k = 1,2 \dots n \tag{3.1}$$

At the i^{th} iteration, the equivalent current injected at the bus $(k+1)$ is shown as follows,

$$\mathbf{I_{k+1}^{i}} = re(\mathbf{I_{k+1}^{i}}) + j.\,im(\mathbf{I_{k+1}^{i}}) = conj\left(\frac{P_{k+1}+jQ_{k+1}}{\mathbf{V_{k+1}^{i}}}\right) \tag{3.2}$$

Where $\mathbf{V_{k+1}^{i}}$ and $\mathbf{I_{k+1}^{i}}$ are the bus voltage and equivalent current injection of bus $(k+1)$ at the i^{th} iteration, respectively. $re(\mathbf{I_{k+1}^{i}})$ and $im(\mathbf{I_{k+1}^{i}})$ are the real and imaginary parts of the equivalent current injection of bus $(k+1)$ at the i^{th} iteration, respectively. For the radial distribution network shown in Fig. 3.1, having 9 buses and 10 branches, the power injections at each bus can be converted into equivalent current-injections using Eqn. (3.2), and Kirchhoff's current law (KCL) is used to find the branch-currents by using equivalent current injected at each bus. As an example, four of the branch (BR) currents $\mathbf{BR_1}$, $\mathbf{BR_4}$, $\mathbf{BR_5}$ and $\mathbf{BR_6}$ can be written using equivalent injected current at the buses as,

$$\mathbf{BR_1} = \mathbf{I_2} + \mathbf{I_3} + \mathbf{I_4} + \mathbf{I_5} + \mathbf{I_6} + \mathbf{I_7} + \mathbf{I_8} + \mathbf{I_9} \tag{3.3a}$$

$$\mathbf{BR_4} = \mathbf{I_5} + \mathbf{I_6} + \mathbf{I_7} + \mathbf{I_8} + \mathbf{I_9} \tag{3.3b}$$

$$\mathbf{BR_5} = \mathbf{I_6} + \mathbf{I_7} \tag{3.3c}$$

$$\mathbf{BR_6} = \mathbf{I_7} \tag{3.3d}$$

Note: It may be noted that bold variables have been used to denote complex quantities and this has been adopted for the entire thesis.

In a similar manner, the rest of the branch currents can also be written. The relationship between the branch currents and the injected currents can be represented in matrix form as shown below,

$$\begin{bmatrix} \mathbf{BR_1} \\ \mathbf{BR_2} \\ \mathbf{BR_3} \\ \mathbf{BR_4} \\ \mathbf{BR_5} \\ \mathbf{BR_6} \\ \mathbf{BR_7} \\ \mathbf{BR_8} \end{bmatrix} = \begin{bmatrix} 1 & 1 & 1 & 1 & 1 & 1 & 1 & 1 \\ 1 & 1 & 1 & 1 & 1 & 1 & 1 & 1 \\ 0 & 0 & 1 & 0 & 0 & 0 & 0 & 0 \\ 0 & 0 & 0 & 1 & 1 & 1 & 1 & 1 \\ 0 & 0 & 0 & 0 & 1 & 1 & 0 & 0 \\ 0 & 0 & 0 & 0 & 0 & 1 & 0 & 0 \\ 0 & 0 & 0 & 0 & 0 & 0 & 1 & 1 \\ 0 & 0 & 0 & 0 & 0 & 0 & 0 & 1 \end{bmatrix} \begin{bmatrix} \mathbf{I_2} \\ \mathbf{I_3} \\ \mathbf{I_4} \\ \mathbf{I_5} \\ \mathbf{I_6} \\ \mathbf{I_7} \\ \mathbf{I_8} \\ \mathbf{I_9} \end{bmatrix} \tag{3.4}$$

The generalised expression of Eqn. (3.4) is shown below,

$$[\mathrm{BR_{nb}}] = [\mathrm{BIBC}][\mathrm{I_{nb}}] \tag{3.5}$$

Here, the constant matrix 'BIBC*'* is known as the bus injection to branch current matrix and it is an upper triangular matrix, contains values of '0' and '1' only.

The relationship between the branch currents and bus voltages for network as shown in Fig. 3.1, can be obtained by Kirchhoff's voltage law (KVL). For example, the voltages of buses 2, 4, and 5 are as follows,

$$\mathbf{V_2} = \mathbf{V_1} - \mathbf{BR_1 Z_{12}} \tag{3.6a}$$

$$\mathbf{V_4} = \mathbf{V_3} - \mathbf{BR_3 Z_{34}} \tag{3.6b}$$

$$\mathbf{V_5} = \mathbf{V_4} - \mathbf{BR_4 Z_{45}} \tag{3.6c}$$

Substituting Eqns. (3.6a) and (3.6b) into (3.6c), we get

$$\mathbf{V_5} = \mathbf{V_1} - \mathbf{BR_1 Z_{12}} - \mathbf{BR_2 Z_{23}} - \mathbf{BR_4 Z_{35}} \tag{3.7}$$

Similar to Eqn. (3.7), the rest of the bus voltages can also be expressed as a function of branch currents, line parameters, and the substation voltage. Accordingly, the relationship between the bus voltages and branch currents can be expressed in matrix form as shown below,

$$\begin{bmatrix} \mathbf{V_1} \\ \mathbf{V_1} \\ \mathbf{V_1} \\ \mathbf{V_1} \\ \mathbf{V_1} \\ \mathbf{V_1} \\ \mathbf{V_1} \\ \mathbf{V_1} \end{bmatrix} - \begin{bmatrix} \mathbf{V_2} \\ \mathbf{V_3} \\ \mathbf{V_4} \\ \mathbf{V_5} \\ \mathbf{V_6} \\ \mathbf{V_7} \\ \mathbf{V_8} \\ \mathbf{V_9} \end{bmatrix} = \begin{bmatrix} \mathbf{Z_{12}} & 0 & 0 & 0 & 0 & 0 & 0 & 0 \\ \mathbf{Z_{12}Z_{23}} & 0 & 0 & 0 & 0 & 0 & 0 & 0 \\ \mathbf{Z_{12}Z_{23}}Z_{34} & 0 & 0 & 0 & 0 & 0 & 0 & 0 \\ \mathbf{Z_{12}Z_{23}} & 0 & \mathbf{Z_{45}} & 0 & 0 & 0 & 0 & 0 \\ \mathbf{Z_{12}Z_{23}} & 0 & \mathbf{Z_{45}Z_{56}} & 0 & 0 & 0 & 0 & 0 \\ \mathbf{Z_{12}Z_{23}} & 0 & \mathbf{Z_{45}Z_{56}Z_{67}} & 0 & 0 & 0 & 0 & 0 \\ \mathbf{Z_{12}Z_{23}} & 0 & \mathbf{Z_{45}} & 0 & 0 & \mathbf{Z_{57}} & 0 & 0 \\ \mathbf{Z_{12}Z_{23}} & 0 & \mathbf{Z_{45}} & 0 & 0 & \mathbf{Z_{57}Z_{89}} & 0 & 0 \end{bmatrix} \begin{bmatrix} \mathbf{BR_1} \\ \mathbf{BR_2} \\ \mathbf{BR_3} \\ \mathbf{BR_4} \\ \mathbf{BR_5} \\ \mathbf{BR_6} \\ \mathbf{BR_7} \\ \mathbf{BR_8} \end{bmatrix} \tag{3.8}$$

The generalised expression of Eqn. (3.8) is shown below,

$$[\Delta V] = [\mathrm{BCBV}][\mathrm{BR_{nb}}] \tag{3.9}$$

Here constant matrix 'BCBV*'* is known as the branch current to bus voltage matrix and it is a lower triangular matrix, contains values of branch impedance. So, the 'BIBC' and 'BCBV' matrices are developed based on the topological structure of distribution networks as detailed above. The corresponding variations in branch currents, because of the variations in bus injected currents, can be calculated directly by using the 'BIBC' matrix. The corresponding variations at bus voltages, due to variations in branch currents, can be determined directly by using the 'BCBV' matrix. Combining Eqns. (3.5) and (3.9), the relationship between current injected at bus and change in bus voltages with respect to substation voltage can be expressed as,

$$[\Delta V] = [\mathrm{BCBV}][\mathrm{BIBC}][\mathrm{I}] \tag{3.10a}$$

$$[\Delta V] = [\mathrm{DLF}][\mathrm{I}] \tag{3.10b}$$

Where $[\mathrm{DLF}] = [\mathrm{BCBV}][\mathrm{BIBC}]$

The solution for distribution power flow can be obtained by using Eqn. (3.2) iteratively, as detailed in Eqn. (3.11a to 3.11c), till the bus voltage magnitude variation is less than a specified tolerance. This considerably reduces the amount of computation resources needed and makes the proposed method suitable for on-line operation. In this work, tolerance for $\Delta V^{i+1} \leq 10^{-6}$.

$$\mathbf{I_{k+1}^{i}} = \mathrm{re}(\mathbf{I}_{k+1}^{i}) + \mathrm{j}.\,\mathrm{im}(\mathbf{I}_{k+1}^{i}) = \mathrm{conj}\left(\frac{P_{k+1}+jQ_{k+1}}{\mathbf{V}_{k+1}^{i}}\right) \tag{3.11a}$$

$$\left[\Delta V^{i+1}\right] = [\mathrm{BCBV}][\mathrm{BIBC}]\left[I^{i}\right] \tag{3.11b}$$

$$\left[V^{i+1}\right] = \left[\Delta V^{i+1}\right] + \left[V^{i}\right] \tag{3.11c}$$

3.2.1 Steps for power flow

Following steps are taken to find branch current and bus voltages of the network,

Step 1. Initially the voltages of all buses (V^0) are assumed as 1 p.u.

Step 2. Calculate $\mathbf{I_{k+1}^{i}}$ using Eqn. (3.2) for all the buses.

Step 3. BIBC and BCBV matrices are formed using the topology of the distribution network as explained above.

Step 4. ΔV^{i+1} is calculated using Eqn. (3.11b).

Step 5. Updated voltages for all the buses using Eqn. (3.11c).

Step 6. Steps 2 to 5 are repeated till $\Delta V^{i+1} \leq 10^{-6}$ (tolerance).

Last updated bus voltages and calculated branch currents using Eqn. (3.5) are considered as the final bus voltages and branch currents of the distribution network.

3.3 POWER LOSS

The power loss in the distribution network is the summation of power losses in each branch of the distribution network. Many methods exist [35, 146] to calculate the power loss in the distribution network. Here, fundamental approach has been adopted to calculate APL and reactive power consumption, which is represented as follows,

$$\mathrm{APL} = \mathrm{P_{loss}} = \sum_{j=1}^{nb}(I_j^2 * R_j) \tag{3.12a}$$

$$\mathrm{RPC} = \mathrm{Q_{con}} = \sum_{j=1}^{nb}(I_j^{2*} X_j) \tag{3.12b}$$

$$\text{Where} \quad I_j = \mathrm{sqrt}\sum_{k=1}^{m}\left(P_{L,k}{}^2 + Q_{L,k}{}^2\right)/\left|V_k^2\right| \tag{3.12c}$$

When DG(s) is (are) allocated, the current magnitude in the branch changes along with the power loss in the branch, and can be expressed as.

$$I_j = \mathrm{sqrt}\sum_{k=1}^{m}\left(\left(P_{L,k} - P_{DG,k}\right)^2 + \left(Q_{L,k} - Q_{DG,k}\right)^2\right)/\left|V_k^2\right| \tag{3.12d}$$

3.4 ENERGY LOSS

The total annual energy loss (EL) (kWh) of the distribution network for time duration (Δt) of 1 h is mathematically represented as:

$$\mathrm{EL} = 365.\sum_{t=1}^{24} P_{loss}^t \,.\, \Delta t \tag{3.13}$$

3.5 DISTRIBUTION NETWORK PERFORMANCE INDICES

The performance of the distribution networks is monitored based on performance indices. Some of the performance indices used in this work is given as follows,

3.5.1 Loss reduction

The DG allocation and / or reconfiguration results in reduction in losses in the distribution networks. Therefore, the active power loss and reactive power consumption reduction is expressed as the ratio of changes in APL /RPC after DG allocation and /or network configuration, to the APL /RPC without any DG or network condition alteration. Mathematically this can be represented in percentage as follows,

3.5.1.1 Active power loss reduction (APLR)

$$\text{APLR}(\%) = \left(\frac{\text{APL}_b - \text{APL}_{DG}}{\text{APL}_b}\right) \text{X } 100 \ \ \% \tag{3.14}$$

3.5.1.2 Reactive power consumption reduction (RPCR)

$$\text{RPCR}(\%) = \left(\frac{\text{RPC}_b - \text{RPC}_{DG}}{\text{RPC}_b}\right) \text{X } 100 \ \% \tag{3.15}$$

3.5.2 DG penetration level

DG penetration level is defined as the ratio of the total DG power generation (S_{DG}) over the total network demand (S_{load}) as given by Eqn. (3.16) below.

$$\text{DG penetration level } (\%) = \frac{S_{DG}(\text{kVA})}{S_{load}(\text{kVA})} \times 100 \tag{3.16}$$

3.5.3 Voltage profile (VP)

DGs allocation near the loads and/or network reconfiguration changes the voltage profile of the network. The voltage profile of the buses in the distribution networks can be monitored using several mathematical formulations [65] and [129] as follows:

3.5.3.1 Voltage deviation (VD)

$$\mathrm{VD} = \sum_{k=1}^{n}(|V_k| - V_{rated})^2 \ (\mathrm{p.u.}) \tag{3.17}$$

3.5.3.2 Voltage profile index (VPI)

$$\mathrm{VPI} = \left(\sum_{k=1}^{n}(|V_k| - |V_{k,DG}|)^2\right)(\mathrm{p.u.}) \tag{3.18}$$

3.5.3.3 Voltage deviation index (VDI)

$$\mathrm{VDI} = \mathrm{sqrt}\left(\sum_{k=1}^{n}(|V_k| - |V_{k,limit}|)^2 / \mathrm{total\ bus}\right)\ (\mathrm{p.u.}) \tag{3.19}$$

3.5.4 Voltage stability index (VSI)

The voltage profile of a distribution network is characterized by its VSI [147], which should always be greater than zero. The VSI must be maximized to improve the voltage profile of the distribution network. Mathematically VSI of a radial distribution network can be given [121] as below,

$$\mathrm{VSI}_{k+1} = |V_k|^4 - 4\{P_{k+1}X_j - Q_{k+1}R_j\}^2 - 4\{P_{k+1}R_j + Q_{k+1}X_j\}|V_k|^2 \ (\mathrm{p.u.}) \tag{3.20}$$

3.5.5 Total bus voltage violation boundary

Load growth in distribution networks may cause voltage limit violations at buses. Total bus voltage violation boundary (TBVVB) indicate the number of buses in network violating the minimum or maximum permissible voltage magnitude limits. If no bus voltage violation occurs in the network, the TBVVB is '0' otherwise, TBVVB is calculated as follows,

$$TBVVB = 0$$

$$TBVVB = \sum_{k=1}^{n} TBVVB + 1 \qquad \text{if } |V_k| < V_{min} \text{ or } |V_k| > V_{max}$$

End (3.21)

3.5.6 Total annual cost saving (TACS)

Total annual cost (TAC) saving is the difference between the cost of the total energy losses in the network before installation of DG and the cost of the total energy losses after DG installation (and / or network reconfiguration) plus the annual cost of DG. It is calculated using Eqn. (3.22a) to (3.22d). The cost of investment can be extracted from the cost of the DG per year as shown below [109],

$$Cost_{nDG,year} = Cost_{nDG} \frac{(1+AR)^{n_{DG}} * AR}{(1+AR)^{n_{DG}} - 1} \quad (3.22a)$$

Total annual cost occurs due to power loss in the network without DG,

$$TAC = 365 * \left(K_e * \sum_{i=1}^{24} T_i * P_{loss,i}\right) \quad (3.22b)$$

Total annual cost occurs due to power loss in the network with DG,

$$TAC^{DG} = 365 * \left(K_e \sum_{i=1}^{24} T_i * P_{loss,i}^{DG} - \sum_{i=1}^{24} K_{ci} * Cost_{nDG,year}\right) \quad (3.22c)$$

So Total annual cost saving due to installation of DGs is calculated as below,

$$TACS = TAC - TAC^{DG} \quad (3.22d)$$

3.5.7 Emission saving (ES)

Air pollution is a global concern and remedial steps should be taken by the concerned agencies to improve the air quality. Gases like CO_2, NOx and SO_2 [148] are the major constituents of air pollution associated with fossil fuel based power generation. DG allocation and/or network reconfiguration in distribution networks plays a vital role in reducing these emissions. Emission data are given in Table A.5. Emission incurred while meeting the load demand and losses without DG is calculated as shown below,

$$E = \left(\sum_{k=1}^{n} P_{L,k} + P_{loss}\right). ER. 8760 \tag{3.23a}$$

Emission incurred while meeting the load demand and losses with DG is calculated as given in Eqn (3.23b),

$$E^{DG} = \left(\sum_{k=1}^{n} P_{L,k} + P_{loss}^{DG}\right). ER. 8760 \tag{3.23b}$$

Difference of Eqn. (3.23a) and (3.23b) gives annual emission savings as given below,

$$ES = E - E^{DG} \tag{3.23c}$$

3.5.8 kVA margin to maximum loadability (KMML)

KMML [124] is an important index, which shows the increment of the network loading from the nominal value to the maximum value, corresponding to a voltage collapse. KMML can be explained using the impact of LF on the minimum network voltage, as shown in Fig. 3.3. The range of LF from operating point A to point C (corresponding to $LF_{P\text{-}I}$ and $LF_{MAX\text{-}I}$ respectively) in Curve I represents the base KMML of the radial distribution network. Similarly, KMML enhancement by means of network reconfigu-

$$KMML = (LF_{max-I} - LF_{P-I}). \sum_{k=1}^{n} S_{L,k} \tag{3.24}$$

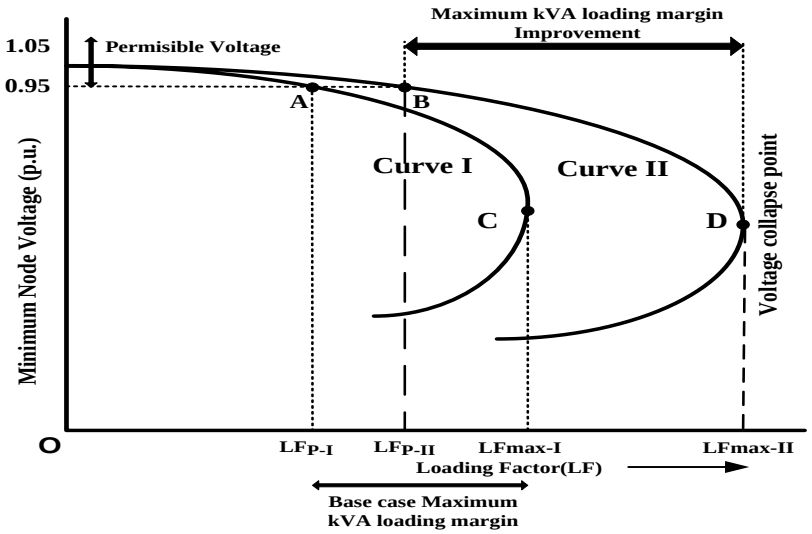

Fig. 3.3: Impact of loading factor on minimum network bus voltage

Table 3.1: Voltage exponents for various loads

Load type	np	nq
Constant	0	0
Industrial	0.18	6.00
Residential	0.92	4.04
Commercial	1.51	3.40

ration and/or DG allocation is presented in curve II from $LF_{P\text{-}II}$ to $LF_{MAX\text{-}II}$ corresponding to points B and D. So, KMML for curve I is obtained as per Eqn. (3.24) .Fig. 3.3 shows that curve II (with optimum reconfiguration and/or DG allocation) has higher loadability and voltage profile than curve I, at each loading point ($LF_{P\text{-}II} > LF_{P\text{-}I}$). The optimum network reconfiguration and/or DG allocation also increases the KMML significantly ($LF_{MAX\text{-}II} >> LF_{MAX\text{-}I}$).

3.5.9 Qualified load index (QLI)

Due to lack of reactive power support, it may not be possible to maintain all bus voltages at their desired values. So, it would be desirable to maintain as high amount of load as possible at the desired voltage level. The voltage index considers only the bus voltage

levels, but it cannot distinguish between heavily loaded and lightly loaded buses. Therefore, the proposed QLI [149] takes into account the voltage level and the power consumed by the load at each bus as a weighting factor as given below,

$$QLI = \sum_{k=1}^{n} |V_k| * P_{L,k} \text{ (p.u.)} \tag{3.25}$$

where $|V|_k$ and $P_{L,k}$ are the voltage magnitude and the active load at the k^{th} bus in per unit. The most important objective of this index is to maintain as high amount of loads as possible at higher voltages.

3.6 LOAD MODELLING

The voltage-dependent time-varying load model [150] can be mathematically expressed as follows:

$$P_{L,k}(t) = P_k(t) \times V_k^{np}(t) \tag{3.26a}$$

$$Q_{L,k}(t) = Q_k(t) \times V_k^{nq}(t) \tag{3.26b}$$

The load active and reactive power demand for particular load type at time duration 't' hours of the day at each bus 'k', can be calculated using Eqn. (3.26a) and 3.26b). The

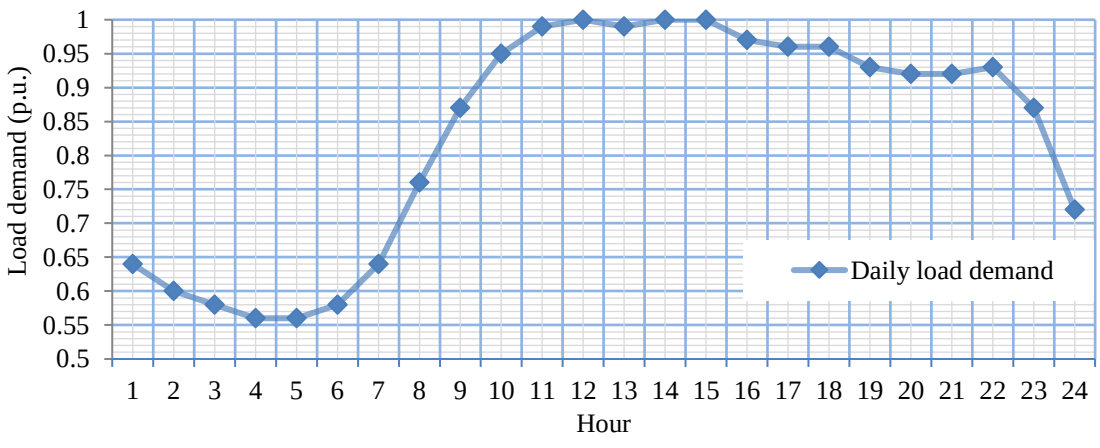

Fig. 3.4: Normalized average daily load demand curve

voltage exponents for the active and reactive load are detailed in Table 3.1 [106]. However, for actual annual energy loss calculation, a normalized daily load profile data reported in [111] has been used in the subsequent chapters 4, 5 and 6 after network reconfiguration and/or DG allocation in the distribution networks. The variation of the load for the 24-hour period is shown in Fig. 3.4.

3.7 GENERATION MODELLING

DG [151] is a better alternative to meet power demand near load centers than centralized power generation. DGs can be installed either at the remote location, to supplying the consumers' local demand or integrated into the grid. DG's can be classified as following,

Type I	Supplying only Active power to the distribution network. Ex. PV System
Type II	Supplying only reactive power to the distribution network. Ex. capacitor, DSTATCOMs, synchronous motor
Type III	Supplying both active and reactive power to the distribution network. Ex. synchronous generator
Type IV	Supplying active power and consuming reactive to the distribution network. Ex. induction generator

Type I DGs have been considered in chapters 4 and 5, Type-II DGs are considered in chapter 6 and Type-III DGs are considered in chapter 7 in this thesis. Based on energy delivery capabilities, DGs can be further categorized as dispatchable and non-dispatchable generation. If the output power of a DG unit is automatically controlled to a fixed value by varying the fuel inputs, the DG unit is considered as a dispatchable

source. Such as SHP plants and biomass-based gas turbines is considered as dispatchable sources of power. On the contrary, if the output power of a DG unit is weather dependent (e.g., wind speed and solar irradiance), it is considered as a non-dispatchable source. Examples of such power generation are solar and wind powers. The reactive power of a DG unit ($Q_{DG,k}$) can be expressed in terms of power factor ($pf_{DG,k}$) and active power of a DG unit ($P_{DG,k}$) [35] as shown in eqn. (3.27),

$$Q_{DG,k} = x\, P_{DG,k} \tag{3.27}$$

Where,$x = \pm\tan\left(\cos^{-1}\left(pf_{DG,k}\right)\right)$, 'x' is positive for a DG unit injecting reactive power and negative for the one consuming reactive power.

3.8 NETWORK RECONFIGURATION

Network reconfiguration is the process of closing or opening of tie/sectional switches to change the topology of the network in such, a way that no node left isolated. In this thesis only radial distribution network are considered. So, after reconfiguration, the radiality of the distribution network must be ensured by opening/closing the tie/sectional switches. Following two approach has been used to check radiality of distribution network,

3.8.1 Incidence matrix approach

The incidence matrix (A) is formed on the basis of graph theory for the reconfigured network and subsequently its determinant ensures the radiality as shown below,

$$\det(A) = +1 \text{ or } -1 \text{ (radial network)}$$

or $\det(A) = 0$ (not radial network) (3.28)

Although this approach requires less computation time but not able to depict the topology of the network. In this thesis, chapter 6 is based on this approach.

3.8.2 Spanning tree approach

Network radiality is ensured using the spanning tree graphical approach. The radiality is tested using the MATLAB function '**graphisspantree (D)**' where the adjacency matrix (D) is the matrix of undirected graph. If 'D' is the matrix corresponding to the spanning tree, this command returns unity for the true condition. The elements of the 'D' matrix in the form of '1's and '0's show the section of the branches available or absent between two nodes of the network.

The following steps are taken to ensure the radiality and accordingly modification is carried out in 'BIBC' and 'BCBV' matrix:

Step 1. Generate the matrix 'D' (bus-by-bus) assuming all the tie/sectional switches are connected. Then modify 'D' by replacing the '1's by '0's for the set of open tie/sectional switches.

Step 2. Make the modified 'D' matrix as sparse matrix.

Step 3. Test the radiality of network using MATLAB function '**graphisspantree** (D)'. Spanning tree can be obtained using the MATLAB function 'biograph (G)' where 'G' is the lower triangular matrix of 'D'.

Step 4. Modify the network data as per the modified matrix 'D' and update the 'BIBC' and 'BCBV' matrices according to modified network data.

In this manner, the radiality of the network is ensured and modifications of the 'BIBC'

and ‘BCBV’ matrices are carried for each set of open tie/sectional switches before the power flow.

3.9 SOFTWARE TOOLS AND TEST NETWORKS

In this thesis, the developed methodologies and algorithms for DG integration in DN for several objective functions, power flow technique have been coded in MATLAB R2015a environment on an Intel i5-4570, 3.2 GHz processor, 4GB RAM, desktop PC. For implementation of the proposed techniques, several standard test networks like the 33-bus, 69-bus and 118-bus radial distribution networks have been employed in this thesis. A brief detail of each network is provided in this chapter while corresponding network data is given in appendix.

3.9.1 33-bus test network

Fig. 3.5, shows the single line diagram of the 12.66 kV, 33-bus test radial distribution network, whose detailed network data is given in [137]**.** It has 33 nodes, 3 laterals, 37 branches with 5 tie switches normally kept open. The nominal loading values are 3.72 MW and 2.3 MVAr, respectively. The base case APL and RPC are 210.998 kW and 143 kVAr, respectively. The base case VSI is 0.6672 (p.u.) [152]. The network base kVA is 1000 [137]. The base load is 4.3736 MVA. The complete load data is given in appendix Table A.1.

3.9.2 69-bus test network

Fig. 3.6 shows the single line diagram of the 12.66 kV, 69-bus test RDN, whose detailed network data is given in [82]. It has 69 nodes, 7 laterals, 73 branches with 5 tie switches

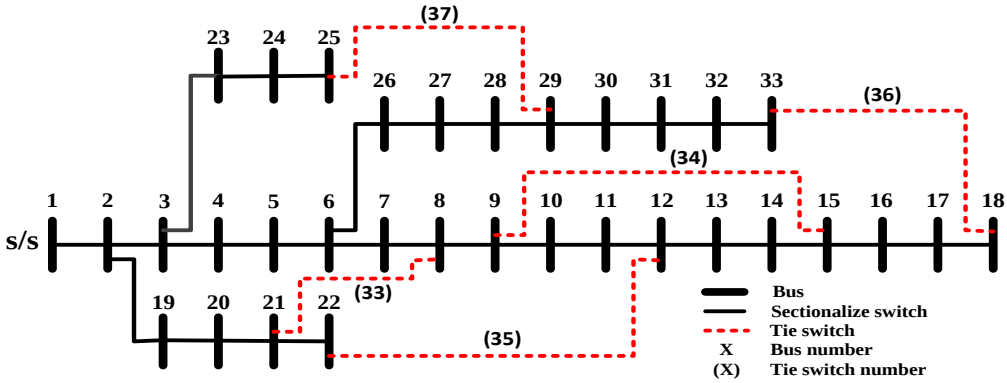

Fig. 3.5: Single line diagram of 33-bus radial distribution network

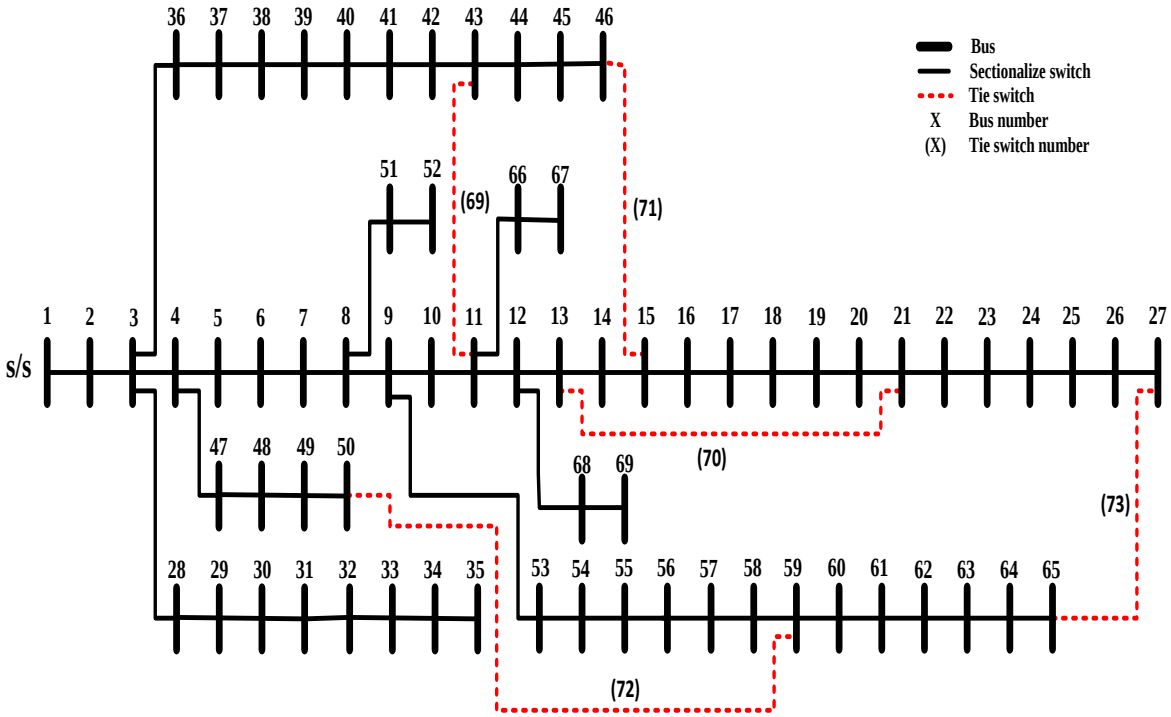

Fig. 3.6: Single line diagram of 69-bus radial distribution network

normally kept open. The nominal voltage rating is 12.66 kV. Nominal load demand on the RDN is 3.8 MW and 2.69 MVAr. The base case real and reactive power consumption are 224.9 kW and 102.13 kVAr, respectively. The base case VSI of this RDN is 0.6833 [152]. The network base kVA is 1000 [82]. The complete load data are given in appendix Table A.2.

3.9.3 118-bus test network

Fig. 1.1 shows the single line diagram of the 118-bus test RDN. The detailed network data is given in [138]. It has 118 nodes excluding substation node, 16 laterals, 132 branches with 15 tie switches normally kept open. The nominal voltage rating is 11 kV. Nominal load demand on the RDN is 22.709 MW and 17.041 MVAr. The base case APL and RPC are 1298.0916 kW and 978.736 kVAr, respectively. The base case VSI of this RDN is 0.5697 [152]. The network base is 100 MVA [138]. The load data is given in appendix Table A.3.

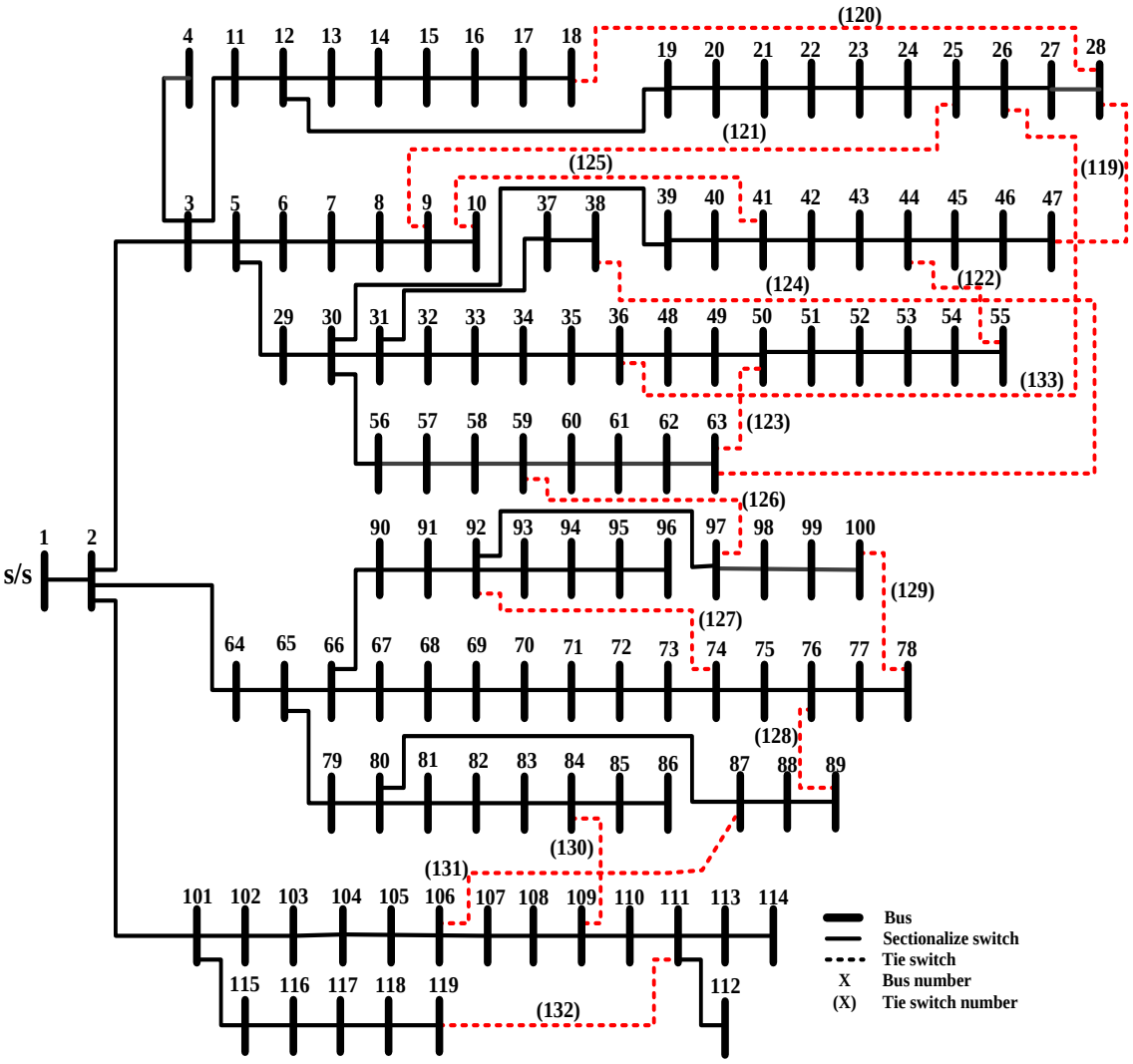

Fig. 3.7: Single line diagram of 118-bus radial distribution network

3.10 SOLUTION VECTOR FORMULATION AND IMPLEMENTATION OF OPTIMIZATION ALGORITHM

This section details the selection criterion for the number of variables in the solution vector for the optimization problem which is solved by meta-heuristic algorithms. Subsequently, this section illustrates the procedure adopted for the implementation of optimization algorithm for either single or multi-objective problems as follows:

3.10.1 Selection of number of variables in solution vector

For the placement of DGs (capable of injecting active and / or reactive power) without simultaneous network reconfiguration, the number of variables in the solution vector (SV) will be equal to twice the number of DGs i.e. one variable for its location and one variable for its size as represented below.

$$\mathrm{SV} = \left[\underbrace{\mathrm{DGL}_1^1 \quad \mathrm{DGL}_2^1}_{\text{DG Location}} \quad \underbrace{\mathrm{DGS}_1^1 \quad \mathrm{DGS}_2^1}_{\text{DG size}}\right] \tag{3.29a}$$

Where DGL_1^1, DGL_2^1 are the locations (discrete variables) of the DGs and DGS_1^1 , DGS_2^1 are the sizes (continuous variables) of DGs in MW/MVAr/MVA or kW/kVAr/kVA, respectively. But with simultaneous network reconfiguration and DG placement, the number of variables in the SV will be equal to the sum of the number of open switches plus twice the number of DGs i.e. one variable for its location and one variable for its size as represented below.

$$\mathrm{SV} = \left[\underbrace{\mathrm{DST}_1^1 \quad \mathrm{DST}_2^1}_{\text{Open tie/sectional Switches}} \quad \underbrace{\mathrm{DGL}_1^1 \quad \mathrm{DGL}_2^1}_{\text{DG Location}} \quad \underbrace{\mathrm{DGS}_1^1 \quad \mathrm{DGS}_2^1}_{\text{DG size}}\right] \tag{3.29b}$$

Where DST_1^1, DST_2^1 are the open sectionalizing/tie switches in the DN. It may be noted that closure of a tie-switch implies the opening of a sectionalizing one. Now for conve-

nience, variables used for locations or sizes will henceforth, be represented as X_i^{SVS} (where i = 1, 2, 3…N).

3.10.2 Optimization algorithm implementation procedure

The following sequence is adopted to optimize the network to meet the desired objective.

Step 1. Initialize the solution vector matrix and algorithm parameters.

In the beginning, a solution vector matrix (SVM) is formed, where each row represents a solution vector to meet the objective function defined for the optimization problem. Each variable of the SV (X_i^{SVS}) is computed using Eqn. (3.30) as shown below.

$$X_i^{SVS} = X_{min,i} + rand * (X_{max,i} - X_{min,i}) \tag{3.30}$$

A set of SV is generated using Eqn. (3.30) as shown in SVM matrix. Thus, after initialization, the SVM is represented as shown below,

$$SVM = \begin{bmatrix} X_1^1 & X_2^1 & X_3^1 & \dots & X_{N-1}^1 & X_N^1 \\ X_1^2 & X_2^2 & X_3^2 & & X_{N-1}^2 & X_N^2 \\ \vdots & \vdots & \vdots & \dots & \vdots & \vdots \\ X_1^{SVS-1} & X_2^{SVS-1} & X_3^{SVS-1} & \dots & X_{N-1}^{SVS-1} & X_N^{SVS-1} \\ X_1^{SVS} & X_2^{SVS} & X_3^{SVS} & & X_{N-1}^{SVS} & X_N^{SVS} \end{bmatrix} \tag{3.31}$$

The fitness is calculated for each SV (X_i^{SVS}) in the SVM.

Step 2. New SV generation

After initialization of the SVM, the new SV is generated using algorithms

equations while satisfying all the constraints.

Step 3. Updating the SVM

If fitness of the new SV 'F (X_{new}^{SVS})' is better than 'F(X_{old}^{SVS})' , X_{new}^{SVS} is accepted and SVM is updated otherwise it is discarded.

In each iteration, step 2 and 3 are repeated until the termination condition is satisfied. Finally, the SV corresponding to the best fitness in SVM is presented as a solution of the optimization problem.

3.11 SUMMARY

This chapter illustrates the topographical approach of power flow technique that has been used for optimal allocation of DGs in various distribution networks corresponding to various objective functions throughout the research work. This power flow technique is simple to implement and requires very less computation time. Subsequently, various network indices have been detailed that are used to monitor the condition of the network under various operating conditions. Further, there is a brief introduction of various time-varying voltage-dependent load models, different types of distributed generation and three radial test distribution networks that has been used in this research work. Finally, the procedure to implement the optimization algorithm(s) to improve the performance of the distribution network has been explained.

CHAPTER 4

COMPREHENSIVE TEACHING-LEARNING BASED OPTIMIZATION TECHNIQUE

4.1 INTRODUCTION

As discussed in Chapter 2, active power loss, voltage profile and voltage stability are the major issues that have to be contended at the DN level because of their major impact on utilities' expenses. A reduction in power loss in the network will decrease power flows in distribution feeders. Hence, the occupancy of system capacity is released which improves the network performance. From the utilities' perception, DG units located near the loads significantly reduce the power losses in distribution networks. However, non-optimal siting and sizing of DG units together with continuously changing load demand has introduced numerous challenges in distribution networks that comprise voltage limit violation, enhancement in power losses, relay co-ordination issues, low voltage stability index etc.

The problem of optimal siting and sizing of DGs in distribution networks deals with mixed integer variables. While sizing of solar-based energy resources deals with continuous variables, those of wind-based generators involves discrete ones. As reported in Chapter 2, several optimization techniques for optimal siting and sizing of DGs are available. These include analytical, nature inspired, heuristic, meta-heuristic variables. In addition, not all of them are parameter independent. Some of these

---

This Chapter is based on the following published paper

I. A. Quadri, S. Bhowmick and D. Joshi, "A comprehensive technique for optimal allocation of distributed energy resources in radial distribution systems," *Applied Energy,* Vol. 211, pp. 1245-1260, 2018.

algorithms are not equally adept at handling both continuous and discrete variables and are observed to be prone to local extrema trappings, which may lead to non-optimal solutions. This chapter presents a CTLBO technique for the optimal placement of DERs in distribution networks, which is both parameter independent as well as capable of handling mixed integer variables. This optimization technique also possesses strong immunity to local extrema trappings. To highlight exclusively the diverse applicability and robustness of the algorithm, at the outset, the proposed algorithm is first validated through eight standard mathematical benchmark functions. Comparative results in the form of mean value and standard deviation (SD) validate the superiority of the proposed optimization technique over several existing ones. Subsequently, to demonstrate the applicability of the proposed algorithm to a specific application, a deterministic problem of optimal DG sizing and placement in many RDNs is considered. Both single and multi-objective criterion is considered for optimal allocation of DERs. Unlike some existing works [53, 111, 153, 154], which have considered a manual weight factor estimation approach for multi-objective formulations, the proposed technique is based on the weight factor estimation and ε-constraint approaches. The latter is independent of weight factors. The results obtained validate the superiority or equivalency of the proposed method over existing algorithms like TLBO and QOTLBO for both mathematical benchmark functions as well as optimal allocation of DGs in distribution networks.

4.2 DEVELOPMENT OF CTLBO ALGORITHM

This section details the development of the CTLBO algorithm based on teaching–learning based optimization (TLBO) algorithm. First, a TLBO algorithm has been explained in detail. Subsequently, some modifications in the TLBO algorithm have been

recommended. Finally, CTLBO algorithm is presented in this section.

4.2.1 Description of teaching–learning based optimization algorithm

TLBO algorithm was first introduced by Rao [155]. It is a meta-heuristic algorithm based on the teaching learning process, is adopted to improve the knowledge of the student, where the best learner of the class i.e. the teacher, improves the performance of the remaining learners. This is known as the '*teaching phase'* while each learner improves his knowledge by interacting with other fellow learners in the '*learning Phase*'.

In this manner, with proper interaction in *teaching and learning phase*, the TLBO proceeds towards the acquiring the best knowledge. The process of TLBO technique can be better understood using enhancement of students' subject knowledge in the class analogy. The variables of SV in TLBO techniques corresponds to the different courses offered to a student and the total marks obtained by each student in all the courses correspond to the 'fitness'. The marks of the student in all the courses corresponds to one solution of the TLBO. The students having maximum in total marks or knowledge (fitness) among the students considered as a 'teacher' in that class. The teacher tries to improve the knowledge of remaining students and helps them to score better marks in the entire subject, as per his knowledge. The students also learn or enhance its knowledge from their own effort by discussing between themselves. The complete process of TLBO is carried out in two phases as detailed below:

Teacher Phase: The teacher tries to improve the mean marks (knowledge) of a particular course (variable) to the best of his capacity. Therefore, a random process takes place for the generation of new variable for a solution in order to get better knowledge

(fitness). For each individual variable of old solution '$X_{old,i}^{SVS}$', a new variable of solution '$X_{new,i}^{SVS}$' is generated using mathematical formulation given below:

$$X_{new,i}^{SVS} = X_{old,i}^{SVS} + rand * \left(X_{Teacher,i} - T_F * M_i\right) \quad (4.1)$$

The value of 'T_F' corresponds to the knowledge transferred to the learner decided randomly with equal probability. It can be either 1 or 2 [155]. So, a new solution 'X_{new}^{SVS}' generated using Eqn. (4.1) is accepted if its knowledge (fitness) corresponding to new solution 'X_{new}^{SVS}' is better than the old solution 'X_{old}^{SVS}'.

Learner Phase: This is an alternative way to improve the knowledge by one's own efforts without the teacher. Students randomly interact with other students of the class and improve their understanding about a particular subject. The learner phase is mathematically explained as below:

$$X_{new,i}^{SVS} = X_{old,i}^{SVS} + rand * \left(X_{old,i}^{f} - X_{old,i}^{k}\right) \quad \text{if } F\left(X_{old}^{f}\right) < F\left(X_{old}^{k}\right) \quad (4.2a)$$

$$X_{new,i}^{SVS} = X_{old,i}^{SVS} + rand * \left(X_{old,i}^{k} - X_{old,i}^{f}\right) \quad \text{if } F\left(X_{old}^{f}\right) > F\left(X_{old}^{k}\right) \quad (4.2b)$$

Where 'SVS', 'f ', 'k' are learners in the class in such a way that SVS ≠ f ≠ k. If the fitness corresponding to new solution'X_{new}^{SVS}' is found to be better than old solution 'X_{old}^{SVS}', 'X_{new}^{SVS}' is accepted otherwise it is rejected.

The two stages i.e. *teaching and learning phases* comprise an iteration. After several iterations, the TLBO algorithm reaches the global solution or best knowledge. Although this algorithm has the minimum number of parameters to be tuned as compared to other population-based optimization techniques, it suffers from premature convergence due to strong local minima trappings of the objective function [65] when number of solution

variables increases.

The following modifications are proposed to improve the performance of the TLBO to avoid premature convergence issues:

4.2.2 Modification in teaching phase

In conventional TLBO, the new solution variables 'X_{new}^{SVS}' is generated based on the mean of the particular variable of all the solutions in the SVM. In the proposed technique, instead of the mean of the variable, the solution having minimum fitness in the SVM is selected. As shown in Eqn. (4.1), for any given 'T_F', the value of the bracketed term on the right-hand side will be more if the mean is replaced by the minimum or worst fitness solution 'X_{worst}^{SVS}'. This results in a wider search space for the new solution 'X_{new}^{SVS}' and a having higher probability of reaching the global solution. This modification is mathematically shown below to generate each variable of solution vector,

$$X_{new,i}^{SVS} = X_{old,i}^{SVS} + rand * \left(X_{Teacher,i} - T_F * X_{worst,i}\right) \quad (4.3)$$

4.2.3 Modification in the teaching factor

TLBO technique considers 'T_F' value either 1 or 2 [155], which corresponds to a transfer of either 0% or 100% knowledge from the teacher to the learner, respectively. However, practically this assumption is incorrect as it should be between 0-100 %. Hence, the 'T_F' is modified as given below.

$$T_F = \left({}^{1}/_{rand}\right)^{a} \quad (4.4)$$

If value of 'a' is high, it increases the search space and hence having enhanced probability of reaching the global solution. It is observed that keeping the value of 'a' between 0-5 yields better results with several objective functions, as highlighted in the case studies and results. Hence, this modification results in a better transfer of knowledge than conventional TLBO technique.

4.2.4 Comprehensive teaching–learning based optimization algorithm

The proposed technique 'CTLBO' comprises two phases i.e. *teaching phase and learning phase.* The '*teaching phase'* in the proposed CTLBO uses Eqn. (4.3) for the generation of new solution 'X_{new}^{SVS}' using Eqn. (4.4) for 'T_F'. The '*learning phase'* of the proposed CTLBO remains the same and the variables of new solution is generated as using Eqn. (4.2a) and (4.2b). Subsequently the SVM is updated as detailed in section 3.10 of chapter 3, if the fitness corresponding to new solution 'X_{new}^{SVS}' is better than old solution 'X_{old}^{SVS}' in both the '*teaching phase and learning phase'*.

A new solution vector generation and updating process occurs in each iteration. Then, in each iteration the fitness of the new generated solution vector greatly improves ultimately converges to global solution vector.

4.3 OBJECTIVE FUNCTION FORMULATION

The CTLBO technique is implemented on a deterministic problem of optimal DG sizing and placement in RDNs addressing some core issues like APL, VD and VSI [53, 111, 153, 154]. To enhance the network operational issues i.e. APL, VD, or VSI, first formulated as single objective functions and later multi-objective formulations, where all the single objective functions considered simultaneously, have been carried out.

The analysis is based on the following assumptions:

a. The radial distribution network under consideration is balanced.
b. Constant power load at nominal load level is assumed.
c. All DGs are assumed Type-I DGs i.e. their power factors are unity.
d. The uncertainty associated with the power outputs of solar / wind based DGs is not considered.

4.3.1 Single objective function

The objective of DG allocation in distribution networks is to reduce the active power loss, improve voltage profile of the network, and enhance the voltage stability while satisfying all operating constraints. In this section, only one criterion is selected as the objective function i.e. single objective function (SOF), are described below:

4.3.1.1 Active power loss minimization

The optimal DGs placement problem is mainly concerned with the minimization of APL in the distribution network. Several methods include Exact loss method, forward-backward methods etc., [147, 156, 157] are available in literature for power flow calculation in distribution networks. The APL of the distribution network is calculated as per section 3.2 of chapter 3 and single objective function (F_1) for APL is defined as,

$$F_1 = \text{minimize}(\text{APL}) \tag{4.5}$$

4.3.1.2 Voltage deviation minimization

DGs are connected near the load to supply the power requirement of the distribution networks. Subsequently power injection in the network modify the voltage profile of

the network. Therefore, to minimize the VD in the network, single objective function (F_2) is defined as shown below [65]:

$$F_2 = \text{minimize (VD)} \tag{4.6}$$

4.3.1.3 Voltage stability index maximization

The voltage profile of a distribution network is characterized by its VSI [158], which should always be near to unity. So, maximization of VSI is considered as single objective function to make the VSI value close to unity, as shown in Eqn. (4.7).

$$F_3 = \text{maximize (VSI)} \tag{4.7}$$

4.3.2 Multi-objective formulation

A multi-objective function optimizes all the single objective functions simultaneously subject to the equality and inequality constraints. In this chapter, a multi-objective function (MOF) is used in line with [44], which simultaneously reduces the APL (F_1) and VD (F_2) while improves the VSI (F_3) is formulated using two approaches as detailed below:

4.3.2.1 Weighted sum approach

In this approach [159] , each single objective functions is assigned a weight coefficient to convert multi valued functions to single value function. This can be mathematically represented as follows,

$$\text{MOF} = \text{Minimize}\left(a_1 * F_1 + a_2 * F_2 + a_3 * {}^{1}/_{F_3}\right) \tag{4.8}$$

In this formulation, a weighted sum approach for multi-objective function in line with [65], is used which simultaneously reduces the APL (F_1) and VD (F_2) while improves the VSI (F_3) where 'a_1', 'a_2' and 'a_3' are the weight coefficient associated with each single objective functions respectively. If DGs are implemented with the objective of mitigating a specific problem, the corresponding weight coefficient is increased. Any value of weight coefficient can be chosen depending upon the importance of the objective function. However, for a normalized objective function, the sum of the weight factors should be unity as shown below.

$$a_i \in ([0,1]) \quad \text{and} \quad \sum_{i=1}^{ob} a_i = 1$$

4.3.2.2 ε-constraints approach

In ε-constraints approach, detailed in [159], the multi-objective optimization problem is solved by targeting one of the objective function as main objective function and restricting the rest of the objective functions as constraints. Mathematically it can be represented as below,

$$MOF = \text{Minimize } F\mu(X) \tag{4.9}$$

$$\text{Subject to } F_m(X) \leq \varepsilon_m \qquad m = 1,2,3 \ldots M. \text{ and } m \neq \mu;$$

$$g_j(X) \geq 0, \quad j = 1,2,3 \ldots .;$$

$$h_l(X) = 0, \quad l = 1,2,3 \ldots .;$$

$$X_{min,i} \leq X_i \leq X_{max,i}, \quad i = 1,2,3 \ldots .;$$

In this chapter, $F\mu(x)$ corresponds to the APL, considered as main objective function while $F_m(x)$ comprises both the VD and the inverse of VSI as constraints.

4.3.3 Constraints

The above single and multi-objective function are subject to following constraints while allocating DGs in the radial distribution network.

4.3.3.1 Active and reactive power balance constraints

$$P_{sub} + \sum_{k=1}^{nDG} P_{DG,k} = P_{loss} + \sum_{k=1}^{n} P_{L,k} \quad \& \quad Q_{sub} = Q_{con} + \sum_{k=1}^{n} Q_{L,k} \tag{4.10}$$

4.3.3.2 Voltage constraint

The voltage must be maintained between V_{max} $(1.05\ \text{p.u.})$ and V_{min} $(0.95\ \text{p.u.})$ at all the network buses.

$$V_{min} \leq |V_k| \leq V_{max} \qquad k = 1,2,3,4 \ldots \ldots n \tag{4.10}$$

4.3.3.3 Thermal limit [160]

$$|I_j| \leq |I_j^{max}| \tag{4.11}$$

4.3.3.4 DG capacity limit [53]

$$P_{DG,k}^{min} \leq P_{DG,k} \leq P_{DG,k}^{max} \tag{4.12}$$

4.4 CASE STUDIES AND RESULTS

Initially the developed CTLBO algorithm has been mathematically validated and results have been compared with existing algorithms. Subsequently, the CTLBO have been used to allocated DGs in many distribution networks for single and multi-objective

Table 4.1: Mathematical benchmark functions [161] .

No.	Function	Formulation	N	Search range
1.	Sphere	$F(x)_{min} = \sum_{i=1}^{N} x_i^2$	10	[-100,100]
2.	Rosenbrock	$F(x)_{min} = \sum_{i=1}^{N} [100(x_i^2 - x_{i+1})^2 + (1 - x_i)^2]$	10	[-2.048,2.048]
3.	Ackley	$F(x)_{min} = -20e^{\left(-0.2\sqrt{\frac{1}{N}\sum_{i=1}^{N} x_i^2}\right)} - e^{\left(\frac{1}{N}\sum_{i=1}^{N}\cos(2\pi x_i)\right)} + 20 + e^1$	10	[-32.768,32.768]
4.	Griewank	$F(x)_{min} = \frac{1}{4000}\sum_{i=1}^{N} x_i^2 - \prod_{i=1}^{N}\cos\left(\frac{x_i}{\sqrt{i}}\right) + 1$	10	[-600,600]
5.	Weierstrass	$F(x)_{min} = \sum_{i=1}^{N}\left(\sum_{k=0}^{k_{max}}\left[a^k \cos\left(2\pi b^k (x_i + 0.5)\right)\right]\right) - N\sum_{k=0}^{k_{max}}\left[a^k \cos\left(2\pi b^k (0.5)\right)\right]$ $a = 0.5, \quad b = 3 \text{ and } \quad k_{max} = 20$	10	[-0.5,0.5]
6.	Rastrigin	$F(x)_{min} = \sum_{i=1}^{N} [x_i^2 - 10\cos(2\pi x_i) + 10]$	10	[-5.12,5.12]
7.	NCRastrigin	$F(x)_{min} = \sum_{i=1}^{N} [y_i^2 - 10\cos(2\pi y_i) + 10]\, y_i$ $= \begin{cases} x_i & \lvert x_i\rvert < 0.5 \\ \frac{\text{round}(2x_i)}{2} & \lvert x_i\rvert > 0.5 \end{cases}$	10	[-5.12,5.12]
8.	Schwefel	$F(x)_{min} = 418.9829 * N - \sum_{i=1}^{N}\left(-x_i \sin\left(\sqrt{\lvert x_i\rvert}\right)\right)$	10	[-500,500]

Table 4.2: Comparative results of CTLBO algorithm with other algorithms [161].

	Sphere	Rosenbrock	Ackley	Griewank
	Mean ± SD	Mean ± SD	Mean ± SD	Mean ± SD
PSO–w	7.96E−051 ± 3.56E−050	3.08E+000 ± 7.69E−001	1.58E−014 ± 1.60E−014	9.69E−002 ± 5.01E−002
PSO–cf	9.84E−105 ± 4.21E−104	6.98E−001 ± 1.46E+000	9.18E−001 ± 1.01E+000	1.19E−001 ± 7.11E−002
UPSO	9.84E−118 ± 3.56E−117	1.40E+000 ± 1.88E+000	1.33E+000 ± 1.48E+000	1.04E−001 ± 7.10E−002
ABC	7.09E−017 ± 4.11E−017	2.08E+000 ± 2.44E+000	4.58E−016 ± 1.76E−016	1.57E−002 ± 9.06E−003
Modified ABC	7.04E−017 ± 4.55E−017	4.42E−001 ± 8.67E−001	3.32E−016 ± 1.84E−016	1.52E−002 ± 1.28E−002
TLBO	0.00 ± 0.00	1.72E+00 ± 6.62E−01	3.55E−15 ± 8.32E−31	0.00 ± 0.00
I-TLBO (NT=4)	0.00 ± 0.00	2.00E−01 ± 1.42E−01	1.42E−15 ± 1.83E−15	0.00 ± 0.00
CTLBO	2.322E−209 ±1.752E−209	2.7847E-03±2.523E-03	2.4409E-16±1.567E-16	0.00 ± 0.00

	Weierstrass	Rastrigin	NCRastrigin	Schwefel
	Mean ± SD	Mean ± SD	Mean ± SD	Mean ± SD
PSO–w	2.28E−003 ± 7.04E−003	5.82E+000 ± 2.96E+000	4.05E+000 ± 2.58E+000	3.20E+002 ± 1.85E+002
PSO–cf	6.69E−001 ± 7.17E−001	1.25E+001 ± 5.17E+000	1.20E+001 ± 4.99E+000	9.87E+002 ± 2.76E+002
UPSO	1.14E+000 ± 1.17E+00	1.17E+001 ± 6.11E+000	5.85E+000 ± 3.15E+000	1.08E+003 ± 2.68E+002
ABC	9.01E−006 ± 4.61E−005	1.61E−016 ± 5.20E−016	6.64E−017 ± 3.96E−017	7.91E+000 ± 2.95E+001
Modified ABC	0.00E+000 ± 0.00E+000	1.14E−007 ± 6.16E−007	1.58E−011 ± 7.62E−011	3.96E+000 ± 2.13E+001
TLBO	2.42E−05 ± 1.38E−20	6.77E−08 ± 3.68E−07	2.65E−08 ± 1.23E−07	2.94E+02 ± 2.68E+02
I-TLBO (NT=4)	0.00 ± 0.00	0.00 ± 0.00	0.00 ± 0.00	1.10E+02 ± 1.06E+02
CTLBO	0.00 ± 0.00	0.00 ± 0.00	0.00 ± 0.00	0.92779E+02±0.41E+02

problems as follows.

4.4.1 Mathematical validation of the CTLBO algorithm

The proposed technique (CTLBO) is first implemented on eight standard mathematical benchmark functions for validation. The details of these functions and the results are shown in Tables 4.1 and 4.2, respectively. Comparative results in the form of mean and standard deviation of eight mathematical benchmark functions, when subjected to 30000 maximum function evaluations for 30 independent runs, validate that the proposed optimization technique is superior or equivalent to [161]. A comparison of the CTLBO vis-à-vis other algorithms is shown in Table 4.2. It is observed that the CTLBO gives the best results with Rosenbrock, Ackley and Schwefel functions, while it yields results identical to ITLBO (Improved TLBO) with Griewank, Rastrigin and NCRastrigin functions. However, it is observed that for the Sphere functions, ITLBO gives the best result. Subsequent to the validation of the CTLBO on standard mathematical benchmark functions, it is applied to the optimal placement and sizing of DGs in distribution networks. Three radial test distribution networks have been used for the implementation of CTLBO for optimal DG allocation.

4.4.2 33-bus RDN

The description of 33-bus is given in chapter 3 and network data is detailed in Table A.1**.** Subsequently, 3 DGs (Type –I) are considered for optimal allocation in this DN. It may be noted that 3 DGs have been chosen for economy [114]. The aspect of the selection of the number of DGs are elaborated at the end of this section. Results obtained with the CTLBO algorithm for optimal allocation of DGs to minimize the APL as the SOF are shown in Table 4.3. From Table 4.3, it is observed that as compared to TLBO

Table 4.3: Results of 33-bus for APL minimization

	TLBO		QOTLBO		CTLBO	
	Optimal DG		Optimal DG		Optimal DG	
	Location	Size (MW)	Location	Size (MW)	Location	Size (MW)
	10	0.8246	12	0.8808	13	0.8017
	24	1.0311	24	1.0592	24	1.0913
	31	0.8862	29	1.0714	30	1.0536
APL (kW)	75.540		74.101		72.787	
VD (p.u.)	0.0222		0.0160		0.0151	
VSI (p.u.)	0.8365		0.8656		0.8805	

Table 4.4: Results of 33-bus for VD minimization

	TLBO		QOTLBO		CTLBO	
	Optimal DG		Optimal DG		Optimal DG	
	Location	Size (MW)	Location	Size (MW)	Location	Size (MW)
	14	1.1320	14	1.0744	13	1.1894
	29	1.1980	27	1.200	25	0.7139
	30	1.0081	33	1.200	30	1.9221
APL (kW)	126.496		115.425		110.410	
VD (p.u.)	0.0010		0.0009		0.0004	
VSI (p.u.)	0.9302		0.9324		0.9480	

Table 4.5: Results of 33-bus for VSI maximization

	TLBO		QOTLBO		CTLBO	
	Optimal DG		Optimal DG		Optimal DG	
	Location	Size (MW)	Location	Size (MW)	Location	Size (MW)
	8	1.1993	6	1.1998	11	1.6046
	12	1.1996	11	1.200	25	0.7685
	31	1.1992	29	1.1983	31	1.4520
APL (kW)	132.691		104.878		110.008	
VD (p.u.)	0.0023		0.0016		0.0007	
VSI (p.u.)	0.9604		0.9618		0.9756	

Table 4.6: Results of 33-bus for simultaneous optimization of APL, VD and VSI

	TLBO		QOTLBO		CTLBO		CTLBO	
			Weight coefficient		(a_1=1.0 a_2=0.6 a_3=0.35)		(ε-constraints Method)	
	Optimal DG		Optimal DG		Optimal DG		Optimal DG	
	Location	Size (MW)	Location	Size (MW)	Location	Size (MW)	Location	Size (MW)
	12	1.1826	13	1.0834	13	1.0364	13	1.1926
	28	1.1913	26	1.1876	24	1.1630	25	0.8706
	30	1.1863	30	1.1992	30	1.5217	30	1.6296
APL (kW)	124.695		103.403		85.9595		96.1732	
VD (p.u.)	0.0011		0.0011		0.0026		0.0009	
VSI (p.u.)	0.9503		0.9530		0.9481		0.9638	

and QOTLBO [65], results with proposed CTLBO gives reduction in APL to 72.787 kW (from 210.998 kW in the base case), reduction in VD to 0.0151 p.u. (from 0.1338 p.u. in the base case) and improvement in VSI to 0.8805 (from 0.6672 p.u. in the base case). Subsequently, the proposed CTLBO is applied to allocate the DGs with the SOF for minimization of VD, Table 4.4 shows the results. From Table 4.4, it is observed that the proposed CTLBO results in values of APL, VD and VSI i.e. 110.410 kW, 0.0004 p.u. and 0.9480 p.u. respectively, which are superior to both TLBO and QOTLBO. Further, the proposed CTLBO is applied for the optimal allocation of DGs with the SOF for maximization of VSI. From Table 4.5, it is again observed that the proposed CTLBO results in improved APL, VD and VSI i.e. 110.008 kW, 0.0007 p.u. and 0.9756 p.u respectively, as compared to TLBO [44]. However, as compared to QOTLBO, the APL are slightly more. Finally, the proposed CTLBO is applied to the optimal siting and sizing of DGs with the MOF for improvement in all the three quantities i.e. reduction of both APL and VD along with improvement in VSI. The values of the individual objective function weights ('a_1', 'a_2' and 'a_3') have been adopted from [65] and are detailed in Table 4.6. From Table 4.6, it is observed that with a_1 = 1, a_2 = 0.65 and a_3 = 0.35, the CTLBO results only in improved APL (85.9595 kW). However, when the

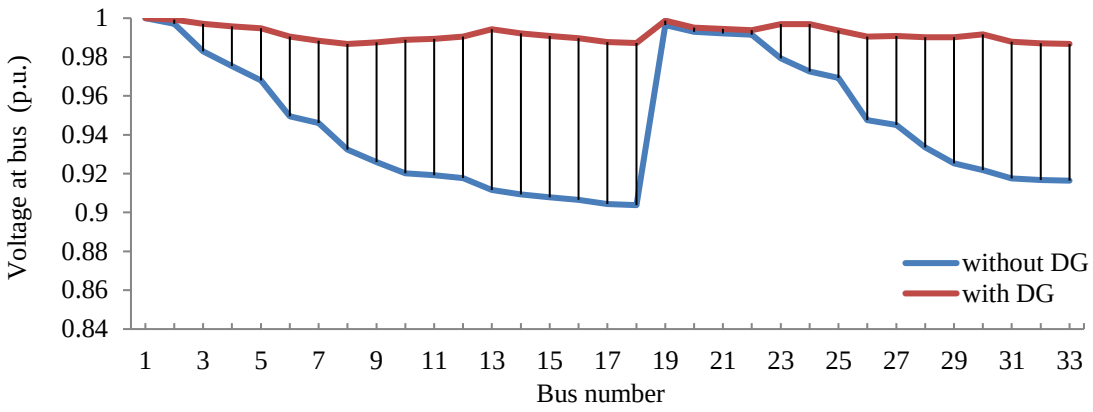

Fig. 4.1 (a): Bus voltage profile of the 33-bus without and with DG

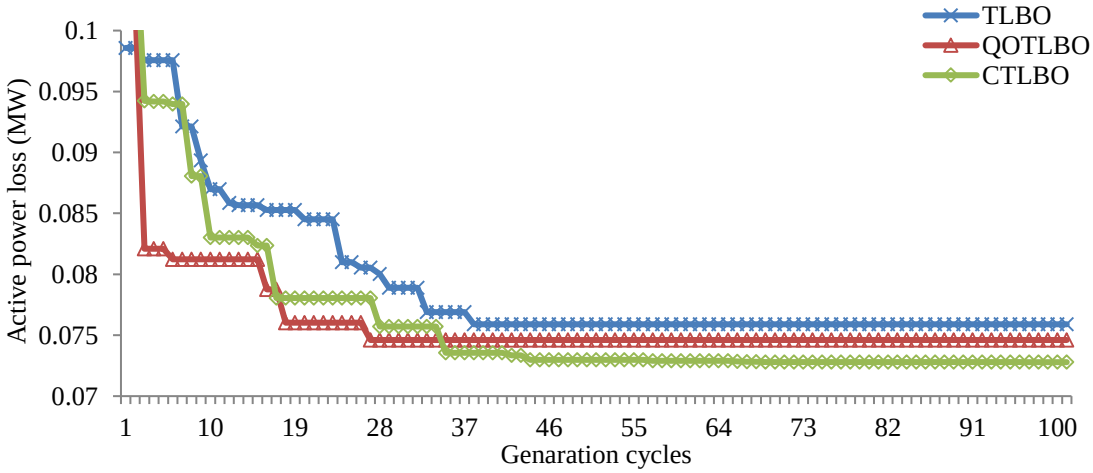

Fig. 4.1 (b): APL minimization convergence characteristics with DG for 33-bus

formulation is carried out using the ε-constraints method, CTLBO shows remarkable improvement in all the three target objectives i.e. APL, VD and VSI i.e. 96.1732 kW, 0.0009 p.u. and 0.9638 p.u. respecti-vely, over both TLBO and QOTLB [65]. The bus voltage profile of the 33-bus without and with DGs is shown in Fig. 4.1 (a). From Fig.4.1 (a), it is observed that in the presence of DGs, the bus voltage profile shows a marked improvement than that without any DG. The convergence characteristic for single objective and multi objective formulations of the proposed CTLBO algorithm vis-à-vis TLBO and QTLBO is shown in Fig. 4.1(b) and Fig. 4.1(c) for APL minimization (single objective formulation) and fitness function value (multi-objective formulation), respect-tively. Fig. 4.1 (d) shows the line loading margins incorporated in the 33-bus. From

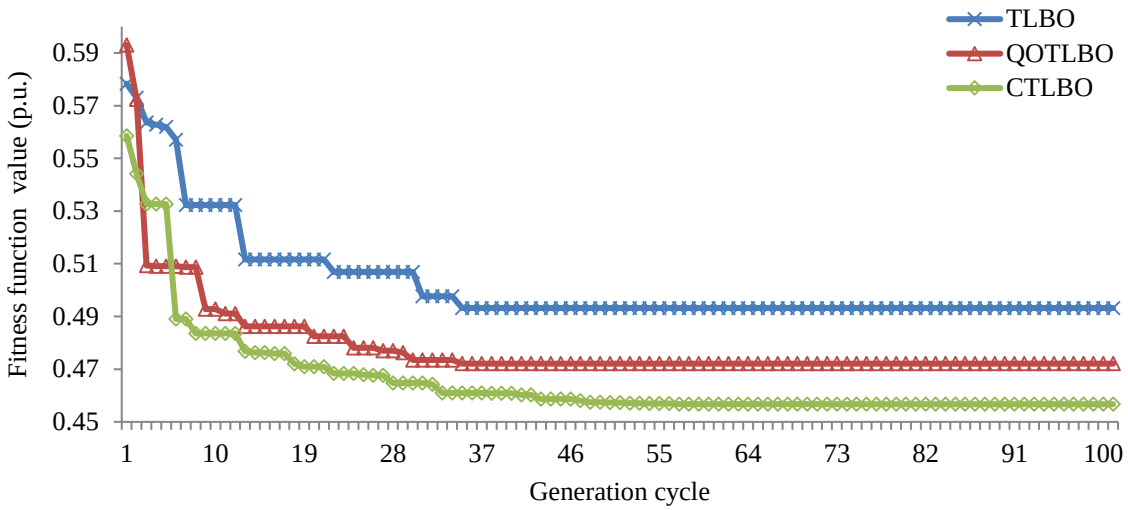

Fig. 4.1 (c): Fitness function convergence characteristics with for 33-bus

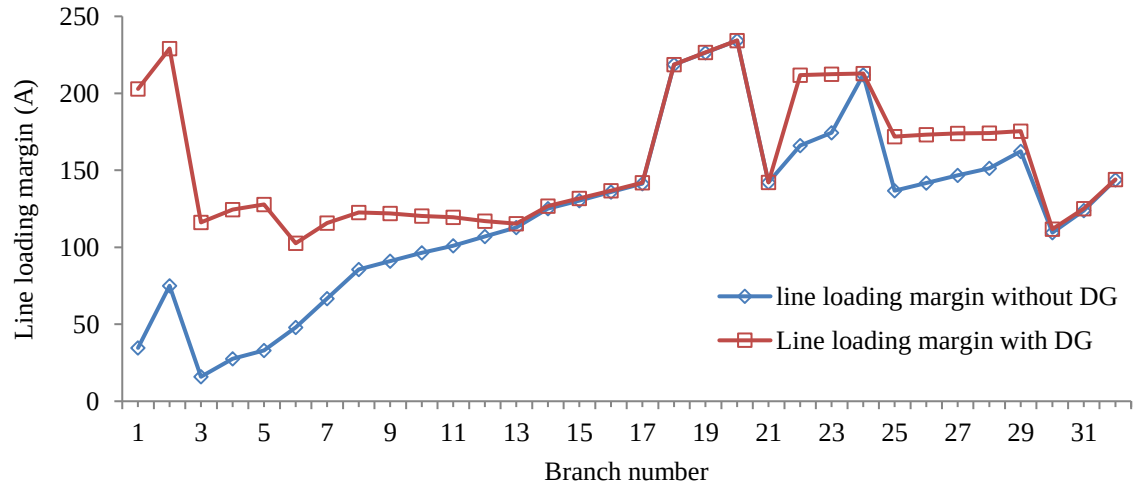

Fig. 4.1 (d): Available loading margins with 3 DGs in 33-bus

the Fig. 4.1 (d), it can be observed that DGs are very effective in relieving network congestion, particularly, in lines 1-13 and 21-29 in the 33-bus.

4.4.3 69-bus RDN

The proposed algorithm is now applied to the problem of optimal sizing and placement of DGs in the 69-bus RDN. The data for this network is detailed in appendix Table A.2

and chapter 3**.** Subsequently, 3 DGs (Type–I) are considered for optimal sizing and placement in this network**.** The aspect of the selection of the number of DGs are again elaborated at the end of this section. Results obtained with the CTLBO algorithm applied to the optimal allocation of DGs with the SOF for minimization of APL are shown in Table 4.7. From Table 4.7, it is observed that as compared to TLBO and QOTLBO [44], the proposed method results in improved values of APL and VD i.e. 69.388 kW and 0.0052 p.u., respectively. However, the values of VSI (0.9185 p.u.) is superior to that with TLBO but slightly inferior to that with QOTLBO. Table 4.8 shows the results with the proposed CTLBO again applied to the optimal allocation of DGs with the SOF for minimization of VD. From Table 4.8, it is observed that the proposed CTLBO results in values of APL, VD and VSI i.e. 83.154 kW, 0.0001 p.u. and 0.9771 p.u. respectively, which are superior to both TLBO and QOTLBO. Table 4.9 shows the results with the proposed CTLBO applied to the SOF for maximization of VSI. From Table 4.9, it is observed that CTLBO results in improved values of all the three quantities i.e. APL, VD and VSI i.e. 83.919 kW, 0.0003 p.u. and 0.9852 p.u. respectively, as compared to either TLBO or QOTLBO. Subsequently, the proposed CTLBO is applied to the MOF for improvement in all the three quantities i.e. minimization of both

Table 4.7: Results of 69-bus for APL minimization

	TLBO		QOTLBO		CTLBO	
	Optimal DG		Optimal DG		Optimal DG	
	Location	Size (MW)	Location	Size (MW)	Location	Size (MW)
	15	0.5919	18	0.5334	11	0.5268
	61	0.8188	61	1.1986	18	0.3796
	63	0.9003	63	0.5672	61	1.7190
APL (kW)	72.406		71.625		69.388	
VD (p.u.)	0.0063		0.0062		0.0052	
VSI (p.u.)	0.9167		0.9196		0.9185	

Table 4.8: Results of 69-bus for VD minimization

	TLBO		QOTLBO		CTLBO	
	Optimal DG		Optimal DG		Optimal DG	
	Location	Size (MW)	Location	Size (MW)	Location	Size (MW)
	14	0.9762	13	1.1764	10	1.0054
	59	1.1388	60	1.1177	20	0.4185
	64	1.1635	62	1.1962	61	2.2051
APL (kW)	90.102		90.670		83.154	
VD (p.u.)	0.0003		0.00022		0.00011	
VSI (p.u.)	0.9770		0.9197		0.9771	

Table 4.9: Results of 69-bus for VSI maximization

	TLBO		QOTLBO		CTLBO	
	Optimal DG		Optimal DG		Optimal DG	
	Location	Size (MW)	Location	Size (MW)	Location	Size (MW)
	27	0.7026	22	1.1931	14	0.8878
	60	1.1716	61	1.1967	50	0.7067
	61	1.1630	62	1.1914	61	2.2908
APL (kW)	88.891		110.507		83.919	
VD (p.u.)	0.0009		0.0072		0.0003	
VSI (p.u.)	0.9762		0.9770		0.9852	

Table 4.10: Results of 69-bus for simultaneous optimization of APL, VD and VSI

	TLBO		QOTLBO		CTLBO		CTLBO	
	Weight coefficient				(a_1=1.0 a_2=0.6 a_3=0.35)		(ε-constraints Method)	
	Optimal DG		Optimal DG		Optimal DG		Optimal DG	
	Location	Size (MW)	Location	Size (MW)	Location	Size (MW)	Location	Size (MW)
	13	1.0134	15	0.8114	11	0.5603	12	0.9658
	61	0.9901	61	1.1470	18	0.4274	25	0.2307
	62	1.1601	63	1.0022	61	2.1534	61	2.1336
APL (kW)	82.172		80.585		76.372		79.660	
VD (p.u.)	0.0008		0.0007		0.0008		0.0003	
VSI (p.u.)	0.9745		0.9769		0.9770		0.9770	

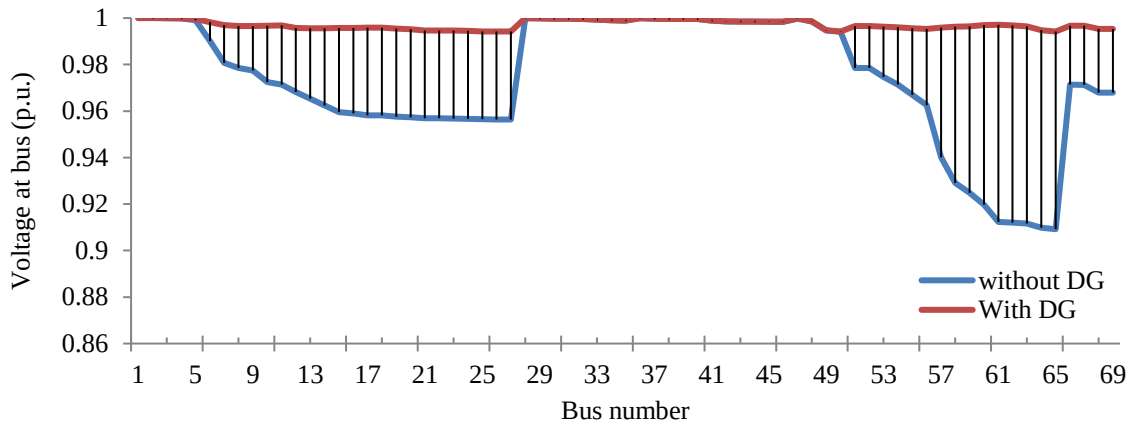

Fig. 4.2 (a): Voltage profile of 69-bus without and with DGs

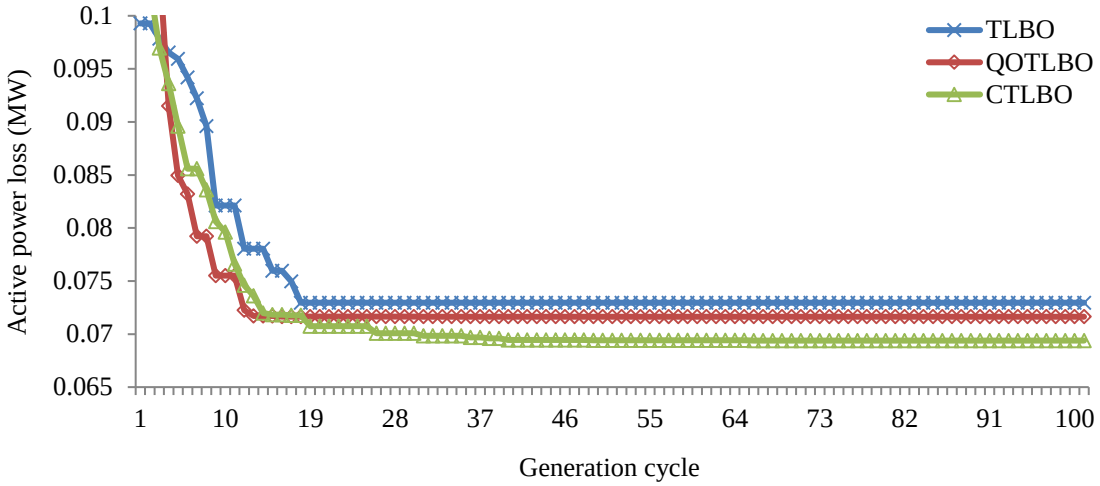

Fig. 4.2 (b): APL minimization convergence characteristics for 69-bus

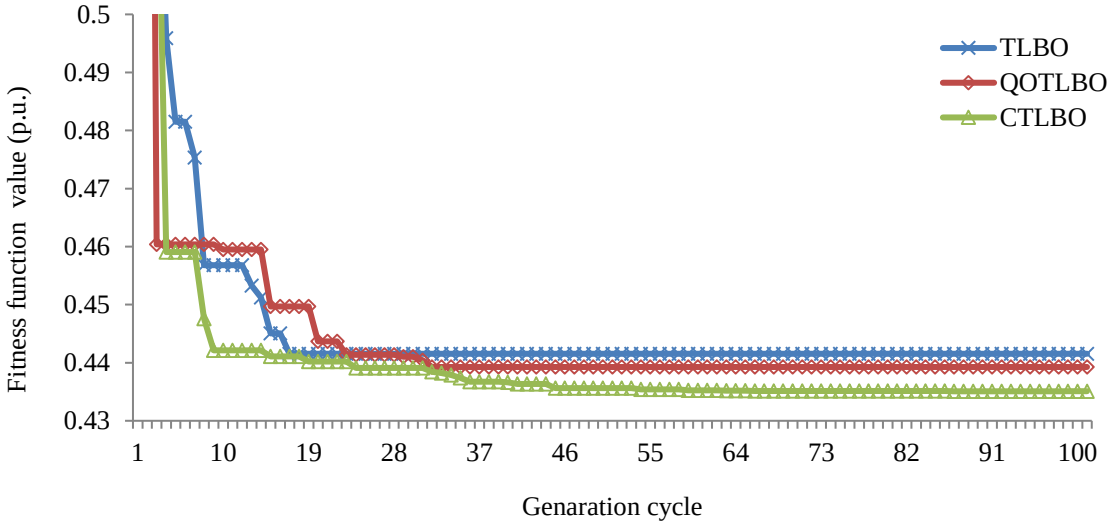

Fig. 4.2 (c): Fitness convergence characteristics for 69-bus

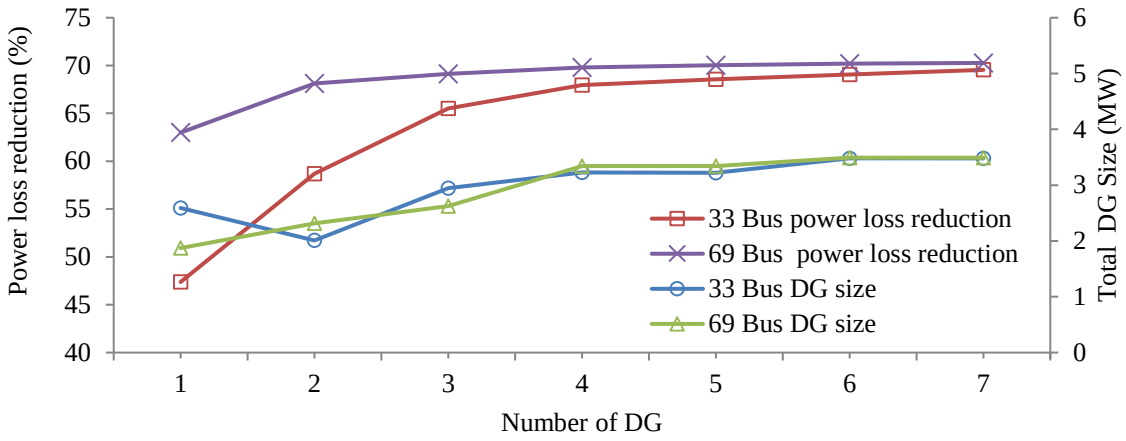

Fig. 4.2 (d): Impact of number of DGs on APL and Total DG size for 33-bus and 69-bus

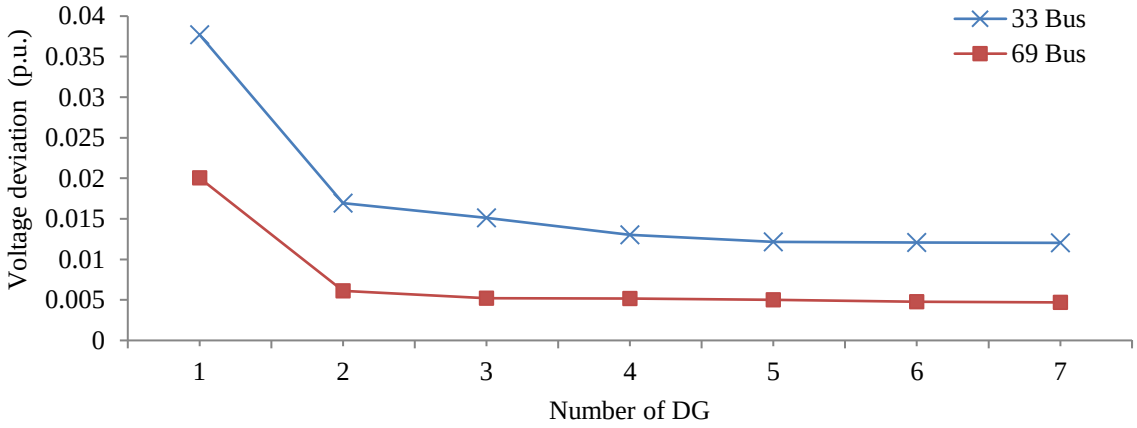

Fig. 4.2 (e): Impact of number of DGs on VD of 33-bus and 69-bus

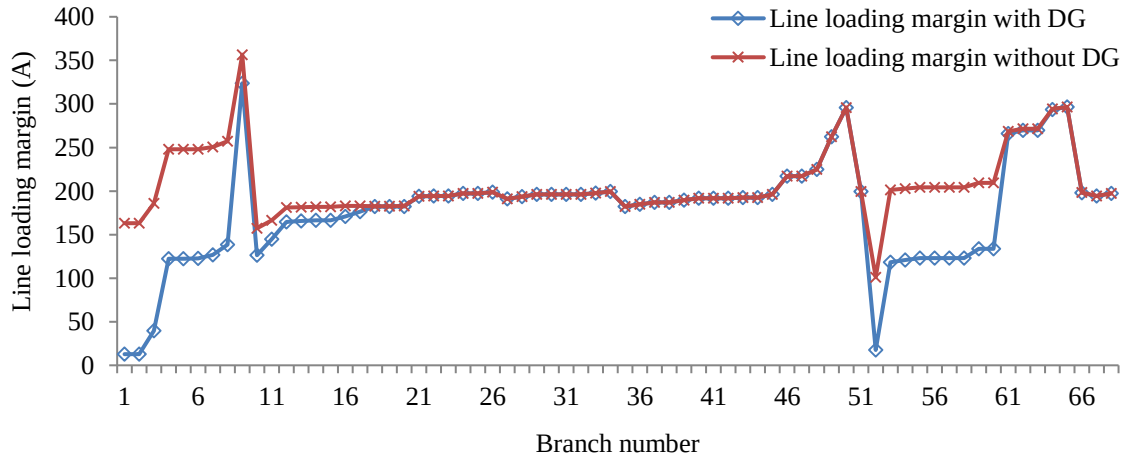

Fig. 4.2 (f): Available loading margins with 3 DGs in 69-bus

APL and VD along with the maximization of VSI. The values of the individual objective function weights ('a_1', 'a_2' and 'a_3') are given in Table 4.10 to demonstrate the superiority of the proposed method. From Table 4.10, it is observed that with $a_1 = 1$, $a_2 = 0.65$ and $a_3 = 0.35$, the proposed CTLBO results in the improvement of both APL and VSI i.e. 76.372 kW and 0.9770 p.u. respectively. The VD i.e. 0.0008 p.u., is observed to be inferior to QOTLBO. However, using the ε-constraints method, CTLBO shows improvement in all the three quantities i.e. APL, VD and VSI i.e. 76.660 kW, 0.0003 p.u. and 0.9770 p.u. respectively, as compared to either TLBO or QOTLBO. The bus voltage profile of the 69-bus without and with DGs is shown in Fig.4.2 (a). From Fig. 4.2(a), it is observed that in the presence of DGs, the bus voltage profile shows amarked improvement over that without DG. The convergence characteristics for SOFs and MOF of the CTLBO vis-à-vis TLBO and QTLBO is shown in Fig. 4.2 (b) and Fig. 4.2(c) for APL minimization and multi-objective fitness function value respectively. The effect of the number of DGs on the APL reduction and VD are shown in Fig. 4.2(d) and 4.2(e), respectively. From Fig. 4.2(d) and 4.2(e), it can be observed that for both the 33 and 69-bus, although the network APL and the bus VD decreases while increasing number of DGs from 3 to 4, the impact of the fourth DG is marginal. Hence, only 3 DGs have been considered for both 33 and 69-bus networks. Fig. 4.2(f) shows the line loading margins without and with DGs incorporated in the 69-bus. From the above Fig. 4.2(f), it can again be observed that DGs are very effective in relieving network congestion, particularly in lines 1-10 and 51-61 in the 69-bus network.

4.4.4 118-bus RDN

The effectiveness of the proposed CTLBO algorithm is reiterated by implementing it on the 118-bus test network. The branch and load data is taken from [138] and detailed

in appendix Table A.3 and chapter 3**.** Subsequently, 7 DGs of Type–I are considered for optimal sizing and placement. The aspect of the selection of the number of DGs are again elaborated at the end of this section. Results obtained with the CTLBO algorithm applied to the optimal allocation of DGs with the SOF for minimization of APL are shown in Table 4.11. From Table 4.11, it is observed that as compared to TLBO and QOTLBO [65], the proposed CTLBO gives improved result in APL, VD and VSI i.e. 516.256 kW, 0.0572 p.u. and 0.8291 p.u. respectively. Results obtained with the CTLBO algorithm applied for the optimal allocation of DGs with the SOF for minimization of VD are shown in Table 4.12. From Table 4.12, it is observed that the proposed CTLBO yields improved values of both VD and VSI i.e. 0.0070 p.u. and 0.9075 p.u. respectively, over TLBO and QOTLB. However, the APL (826.844 kW) is slightly inferior to that obtained with TLBO. Table 4.13 shows the results obtained with the CTLBO algorithm applied to the optimal allocation of DGs with the SOF for maximization of VSI. From Table 4.13, it is obser ved that the proposed CTLBO results in improvement of both VD and VSI 0.0269 p.u. and 0.9205 p.u. respectively, as compared to either TLBO or QOTLB. However, the APL (1145.143 kW) is slightly

Table 4.11: Results of 118-bus for APL minimization

	TLBO		QOTLBO		CTLBO	
	Optimal DG		Optimal DG		Optimal DG	
	Location	Size (MW)	Location	Size (MW)	Location	Size (MW)
	8	1.7553	24	1.2463	20	1.8176
	10	0.5910	42	0.7322	44	1.2764
	36	1.5368	47	3.5392	52	2.7671
	49	2.6865	74	2.6792	75	2.5333
	71	2.5014	78	1.2483	83	2.0949
	79	2.4941	94	1.0865	100	1.6631
	110	2.6628	108	3.2432	114	3.1199
APL (kW)	590.697		576.182		516.256	
VD (p.u.)	0.0939		0.0629		0.0572	
VSI (p.u.)	0.7988		0.8269		0.8291	

Table 4.12: Results of 118-bus for VD minimization

	TLBO		QOTLBO		CTLBO	
	Optimal DG		Optimal DG		Optimal DG	
	Location	Size (MW)	Location	Size (MW)	Location	Size (MW)
	33	3.0918	33	3.5158	23	1.4808
	45	1.5553	45	1.8064	44	1.8910
	49	4.4919	49	4.4480	51	6.4081
	71	4.1287	72	3.6721	76	3.5791
	86	3.5000	87	3.9364	85	3.0644
	96	2.9346	89	3.7719	100	2.5052
	110	3.9804	110	3.9690	114	4.6081
APL (kW)	820.6794		890.3024		826.844	
VD (p.u.)	0.0143		0.0134		0.0070	
VSI (p.u.)	0.8823		0.8829		0.9075	

Table 4.13: Results of 118-bus for VSI maximization

	TLBO		QOTLBO		CTLBO	
	Optimal DG		Optimal DG		Optimal DG	
	Location	Size (MW)	Location	Size (MW)	Location	Size (MW)
	35	3.2536	21	3.2536	26	0.4541
	54	4.2454	43	1.4154	45	0.8362
	58	3.5129	54	4.2454	52	4.9067
	74	3.8290	74	4.9614	65	0.2214
	75	4.4863	80	3.5129	71	9.1134
	81	0.8286	94	3.2396	81	4.9382
	111	3.3889	111	3.9253	115	3.3851
APL (kW)	1840.075		1031.8933		1145.143	
VD (p.u.)	0.1398		0.0301		0.0269	
VSI (p.u.)	0.8695		0.9009		0.9205	

inferior to that obtained with QOTLBO. Subsequently, CTLBO is applied to the MOF for improvement of all the three quantities i.e. reduction of both APL and VD along with the improvement of VSI. The values of the individual objective function weights ('a_1', 'a_2' and 'a_3') given in Table 4.14 have been selected in line with [65]. From Table 4.14, it is observed that for $a_1 = 1$, $a_2 = 0.65$ and $a_3 = 0.35$, the proposed CTLBO results in the improvement of both VD and VSI i.e 0.0110 p.u. and 0.8838 p.u. respectively

Table 4.14: Results of 118-bus for simultaneous optimization of APL, VD, VSI

	TLBO		QOTLBO		CTLBO		CTLBO	
	Weight coefficient		(a_1=1.0 a_2=0.6 a_3=0.35)				(ε-constraints Method)	
	Optimal DG		Optimal DG		Optimal DG		Optimal DG	
	Location	Size (MW)	Location	Size (MW)	Location	Size (MW)	Location	Size (MW)
	35	3.2462	43	1.5880	43	3.2693	22	2.0515
	48	2.8864	49	3.8459	51	5.9000	44	1.1333
	65	2.4307	54	0.9852	61	1.3302	51	4.4872
	72	3.3055	74	3.1904	76	3.4981	77	2.6457
	86	1.9917	80	3.1632	84	3.0069	81	4.6408
	99	1.6040	94	1.9524	100	2.4184	93	3.7585
	111	3.5984	111	3.6013	115	4.0687	115	3.2820
APL (kW)	705.8980		677.5881		781.789		655.767	
VD (p.u.)	0.0327		0.0233		0.0110		0.0228	
VSI (p.u.)	0.8548		0.8794		0.8838		0.8948	

over TLBO or QOTLBO. On the other hand, the APL (781.789 kW) is observed to be inferior to both TLBO and QOTLBO. However, with the ε-constraints method, the proposed method shows marked improvement in all the three quantities i.e. APL, VD and VSI (655.767 kW, 0.0228 p.u. and 0.8948 p.u. respectively), as compared to either TLBO or QOTLBO. The bus voltage profile of the 118-bus without and with DGs is shown in Fig. 4.3(a). From Fig. 4.3 (a), it is observed that in the presence of DGs, the bus voltage profile shows a marked improvement than that without DG. The convergence characteristic for the single objective and multi objective formulation of the proposed CTLBO algorithm vis-à-vis TLBO and QTLBO is shown in Fig. 4.3(b) and Fig. 4.3(c) for APL minimization and multi objective fitness function value, respectively. Fig. 4.3(d) and 4.3(e) shows the effect of increase in the number of DGs on the APL reduction and bus VD in the 118-bus. From Fig. 4.3(d) and 4.3(e), it can be observed that although the network APL nd the bus VD decreases while increasing number of DGs from 7 to 8, the impact of the eighth DG is marginal. Hence, only 7 DGs have been considered for 118-bus networks.

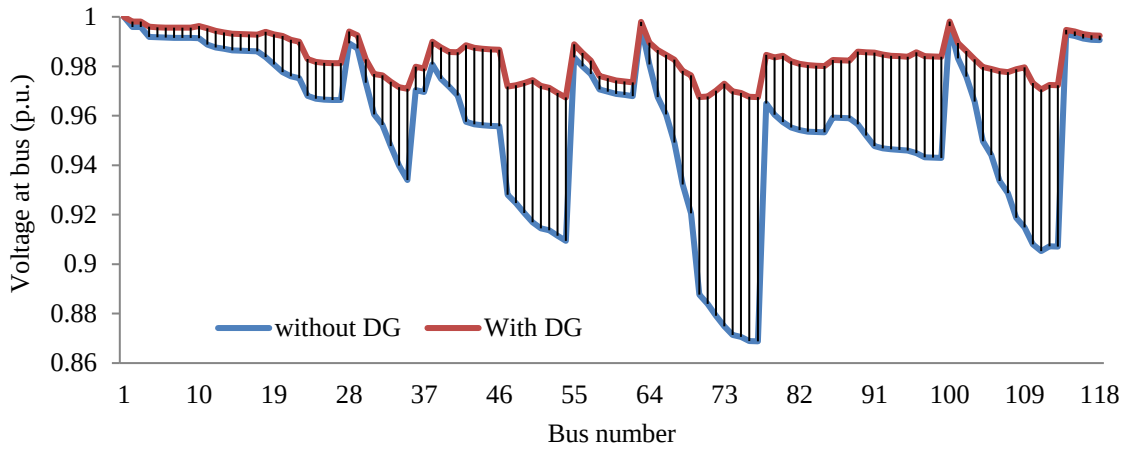

Fig. 4.3 (a): Voltage profile of 118-bus with and without DG

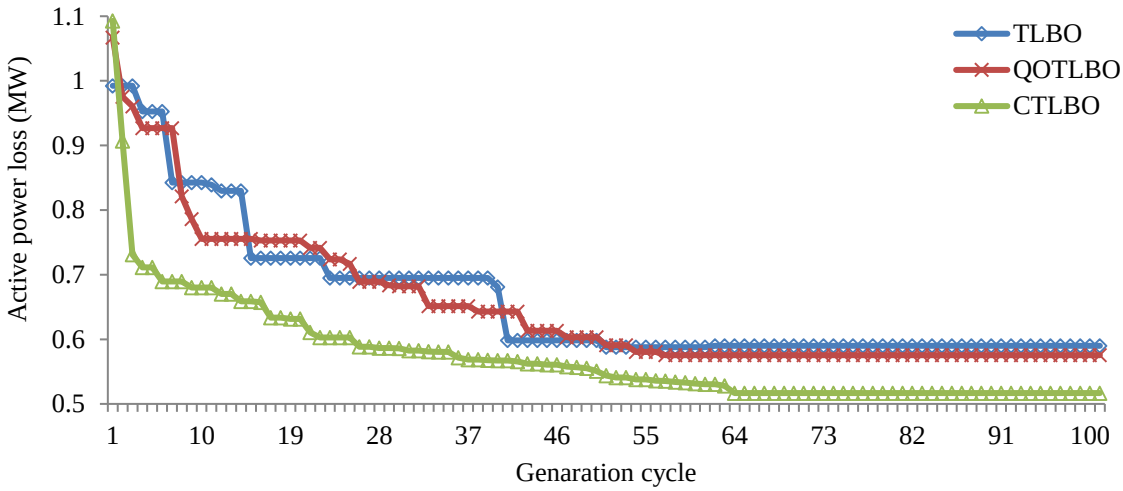

Fig. 4.3 (b): Power loss convergence characteristics of 118-bus for APL minimization

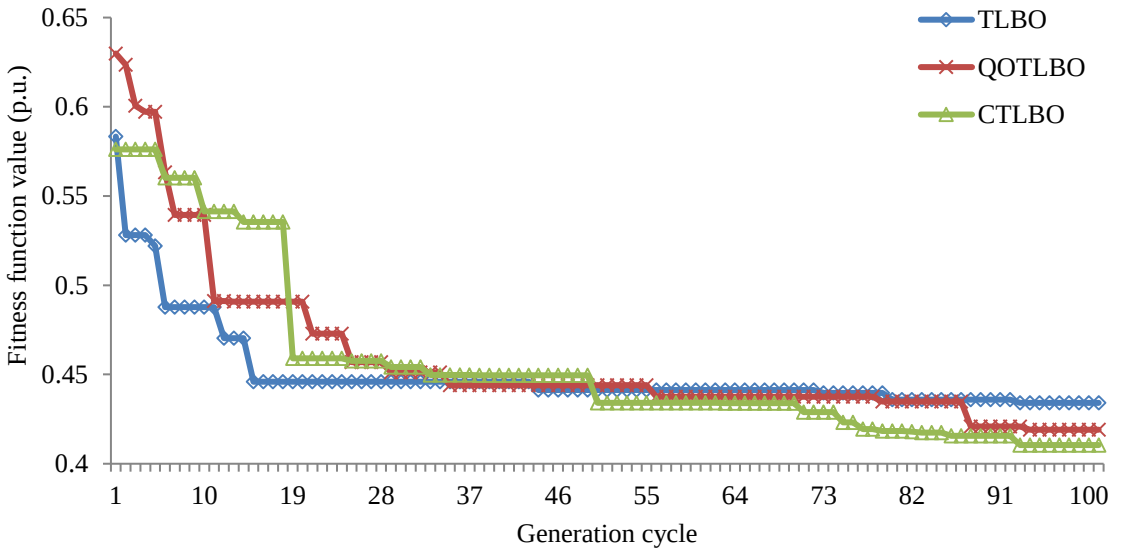

Fig. 4.3 (c): Fitness convergence characteristics for 118-bus

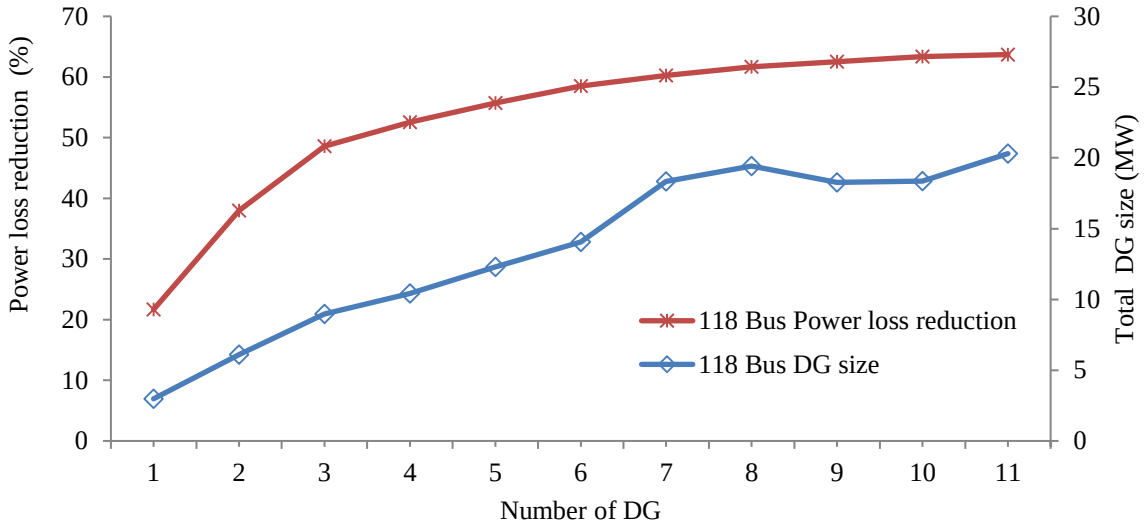

Fig. 4.3 (d): Impact of number of DGs on APL and Total DG size for 118-bus

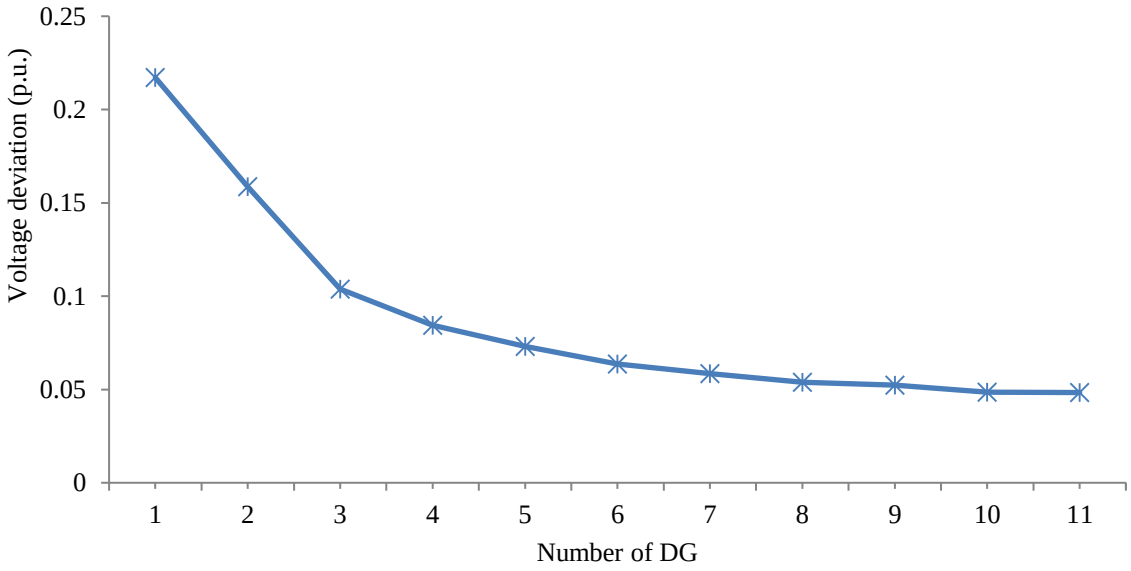

Fig. 4.3 (e): Impact of number of DGs on voltage deviation for 118-bus

4.5 IMPACT OF OPTIMAL DG ALLOCATION ON THE ANNUAL ENERGY LOSS

The effects of the allocation of DGs in the 33-bus and 69-bus are shown in Table 4.15. It is to be noted that only one DG is considered in order to compare and demonstrate the superiority of the proposed technique over the analytical method reported in [35].

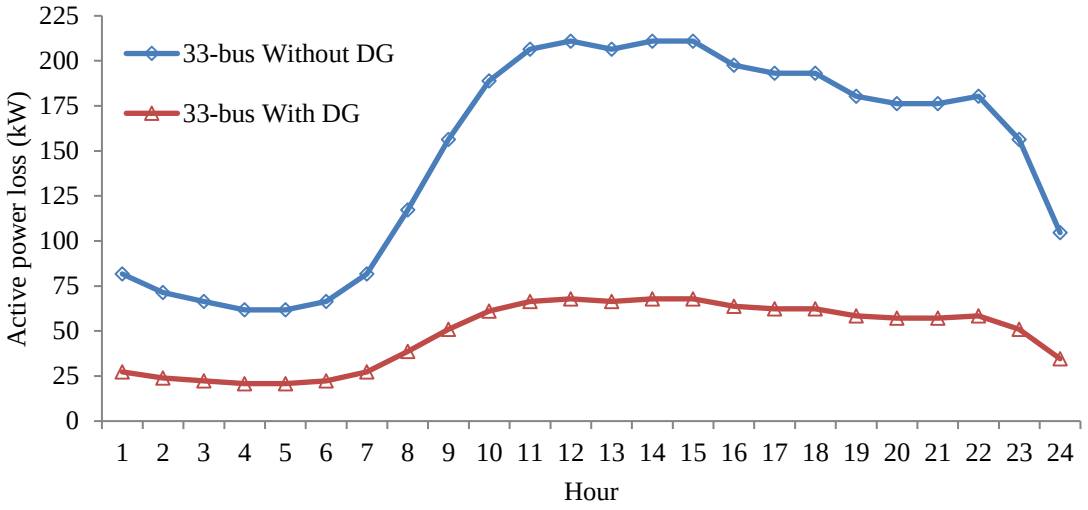

Fig. 4.4 (a): Hourly power loss of 33-bus without and with DG

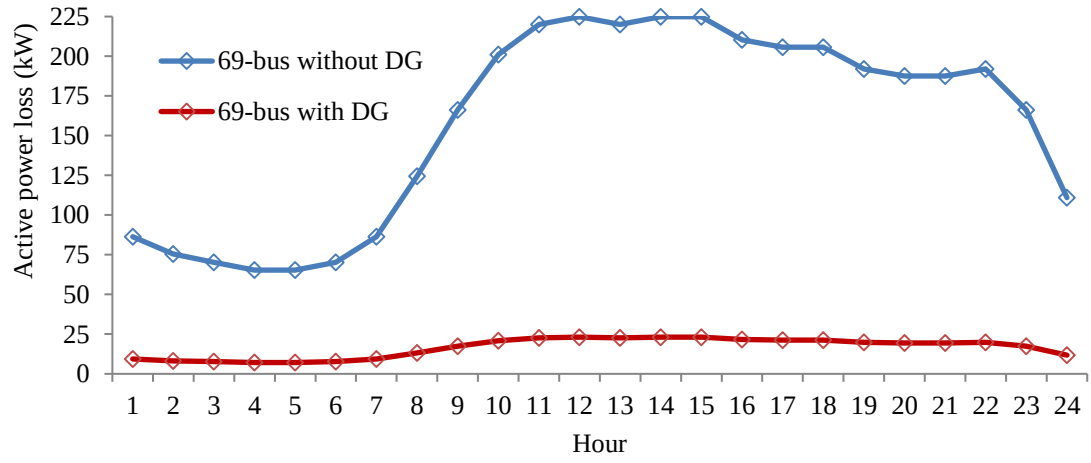

Fig. 4.4 (b): Hourly power loss of 69-bus without and with DG

Table 4.15: Results of DG placement for annual energy loss

Distribution network	33-bus		69-bus	
Optimization method	Analytical [35]	CTLBO	Analytical [35]	CTLBO
Location (Bus)	6	6	61	61
Size(MVA)	3.025	3.106	2.222	2.244
Optimal power factor	0.82	0.825	0.82	0.823
DG penetration (%)	69.31	71.09	47.73	48.16
EL before DG (MWh)	1299.59	1299.59	1381.53	1381.53
EL after DG (MWh)	423.13	422.658	144.35	144.165
EL reduction (%)	67.44	67.453	89.55	89.57
Saving($) (tariff@$ 0.12 /kWh)	105175.2	105231.84	148461.6	148483.8

The hourly APL in the 33 and 69-bus without and with DG are shown in Fig. 4.4(a) and 4.4(b), respectively, corresponding to practical daily load profile data reported in [35]. The EL for both the networks, without and with DGs, are calculated as shown in Fig. 4.4(a) and 4.4(b) respectively. From Table 4.15, it is observed that using the CTLBO technique, proper sizing (3.106 MW for 33-bus and 2.224 MW for the 69-bus) considering single DG installation results in 772 kWh and 185 kWh more annual energy savings, respectively, than the analytical approach reported in [35]. This results in an annual cost savings of $ 56.64 and $ 22.20 more in the 33 and 69-bus, respectively, as compared to [35].

4.6 SUMMARY

A comprehensive teaching-learning based optimization technique (CTLBO) has been developed in this chapter. The CTLBO is able to handle mix integer variables very efficiently and is immune to local extrema trappings. At first its validation is tested on mathematical benchmark functions. Comparative results of mathematical benchmark functions in the form of mean value and standard deviation validate the superiority of the proposed optimization technique over several existing ones. Subsequently, the proposed method is implemented for optimal DG sizing and placement in various radial distribution networks considering SOFs of power loss and VD minimization and maximization of VSI. The results demonstrate the superiority of the proposed optimization technique over TLBO and QOTLBO. Subsequently, multi-objective formulations have been considered using two methodologies - the weighted sum and the ε-constraints approaches. The latter is independent of weight coefficients for optimal allocation of DGs. The result obtained with ε-constraints approach validates the exploration and exploitation capability of the proposed technique over TLBO and

QOTLBO. It is also observed that the optimal placement of DGs results in marked reduction of network energy losses and VD up to a certain level of DG penetration, along with better network congestion management.

CHAPTER 5

HYBRID TEACHING-LEARNING BASED OPTIMIZATION TECHNIQUE

5.1 INTRODUCTION

Optimal DG allocation in distribution networks is a major concern of utilities due to its impact on the operational revenue. Optimal allocation of DGs can minimize power flows in distribution networks. This improves the network capacity release, voltage profile, cost saving and emission reduction. Increased dissemination of DG units accompanied by load variations has brought together numerous operational issues in distribution networks such as power instabilities, voltage limit violations, high power losses and low voltage stability because of reverse power flow in the network.

In Chapter 4, CTLBO algorithm [113] has been developed, which is almost independent of optimization parameters and possesses excellent convergence characteristics for mixed integer variables. CTLBO is used to allocate Type-I DGs in several distribution networks for single as well as multi-objective functions and yields improved results over QOTLBO and TLBO algorithms. However, it has the tendency to be trapped in strong local minima when the number of variables increases and may give non-optimal solutions. It is observed that CTLBO exhibits good search space exploitation capability while harmony search algorithm [162] has good exploration capability. Therefore, a proper integration of the merits of CTLBO and HSA is expected to result in a better optimization technique for high-dimensional and multimodality problems. To get a

---

This Chapter is based on the following published paper

I. A. Quadri, S. Bhowmick and D. Joshi, "A Hybrid Teaching-learning Based Optimization Technique for Optimal DG Sizing and Placement in Radial Distribution Systems", ***Soft Computing,*** Springer, pp. 1-19, 2018.

good balance of exploration and exploitation capabilities of the search space, a new optimization algorithm based on the hybridization of HSA and CTLBO has been presented in this chapter. In this algorithm, at first the HSA is utilized to explore the search space with a high probability of finding the global solution. Subsequently, CTLBO carries out exploitation of the search space for the global solution. For choice of CTLBO or HSA, the proposed algorithm uses self-adaptive selection probability. The details of this hybrid technique has been explained in the next section.

5.2 DEVELOPMENT OF HYBRID TEACHING-LEARNING BASED OPTIMIZATION TECHNIQUE

This section details the development of the HTLBO algorithm based on the CTLBO and the harmony search algorithms. At first, a summary of the TLBO algorithm is presented along with the harmony search algorithm. Finally, the HTLBO algorithm is detailed in this section.

5.2.1 Comprehensive teaching-learning based optimization algorithm

CTLBO [113] is a meta-heuristic algorithm and comprises of two stages - the *teaching phase* and the *learning Phase.* In the '*teaching phase',* the best learner i.e. teacher, transfers his knowledge to the other remaining learners to enhance their knowledge. Subsequently, in the '*learning phase',* each learner interacts with other fellow learners to further improve his/her own knowledge. These two stages are repeated till the CTLBO proceeds towards the global best knowledge (global solution). The details of the CTLBO algorithm has already been explained in Chapter 4.

5.2.2 Harmony search algorithm

Geem, first introduced HSA in 2001 [162], which mimics the improvisation of music players to improve the acceptability of their creation. The sounds for better aesthetic estimation can be improved through more and more practice just as the value of an objective function improves iteration by iteration. The steps of the HSA are as follows:

Step 1. Initialize the SVM and algorithm parameters

At the beginning, a matrix of SVM is formed, where each row represents a solution vector (X_{old}^{SVS}) for the objective function fitness 'F (X_{new}^{SVS})' defined for the optimization problem. Initially, each solution vector (X_{old}^{SVS}) is computed using Eqn. (3.29) and SVM matrix is obtained as per Eqn. (3.30). Initialized other variables of the HSA.

Step 2. Improvise new solution

A new solution 'X_{new}^{SVS}' will depend on the three parameters:

1. Harmony memory consideration rate (HMCR) represents the probability of the selection of solution variables for SVM. The probability of HMCR varies between '0' and '1'. (1-HMCR) is the probability of selecting the variable from outside the SVM.
2. Pitch adjustment rate (PAR) represents the probability of shifting the solution variables to neighboring values within the possible range.
3. Random selection.

The generation of the new solution variables of SVM is known as improvisation. HMCR decides whether to adjust the pitch of each solution variable or not. After considering the solution variable by HMCR, the pitch adjustment is decided by PAR value as follows:

if rand $<$ HMCR

$$X_{new,i}^{SVS} \leftarrow X_{old,i}^{SVS} \in \{X_1^{SVS} \quad X_2^{SVS} \quad \cdots \quad \cdots \quad \cdots \quad X_N^{SVS}\} \tag{5.1a}$$

if rand $<$ PAR

$$X_{new,i}^{SVS} \leftarrow X_{old,i}^{SVS} + \text{rand} * BW \tag{5.1b}$$

Else

$$X_{new,i}^{SVS} \leftarrow X_{old,i}^{SVS} - \text{rand} * BW \tag{5.1c}$$

end

else Random selection

$$X_{new,i}^{SVS} = X_{min,i} + \text{rand} * (X_{max,i} - X_{min,i}) \quad \text{where i,} = 1,2,3 \ldots N \tag{5.1d}$$

end

Where the value of BW (Bandwidth) lies between '0' and '1'. So, steps are repeated to generate new solution variables as detailed in Eqn. 5.1a to 5.1d and fitness 'F (X_{new}^{SVS})' corres-ponding to new generated solution vector 'X_{new}^{SVS}' is calculated.

Step 3. Update SVM

If fitness F **(**X_{new}^{SVS}**)** of the new solution 'X_{new}^{SVS}' gives better objective function values than the worst solution in SVM, the worst solution is replaced by the new solution '**(**X_{new}^{SVS}**)**' otherwise discarded.

Step 4. Termination

The HSA keeps on repeating steps 1, 2 and 3, until maximum number of improvisation (NI) are met, which is set during the parameter initialization process.

In basic HSA, the parameters HMCR, PAR and BW are constant values. The proposed

algorithm adopts dynamic strategies to select the values of HMCR and PAR. Dynamic selection of HMCR and PAR provide better balance in exploration and exploitation of search space in the hybrid algorithm. The suggested modification detailed in [26] as shown below.

$$\mathrm{HMCR} = \mathrm{HMCR}_{\max} - (\mathrm{HMCR}_{\max} - \mathrm{HMCR}_{\min}) * (\frac{\mathrm{currentiteration}}{\mathrm{maxiteration}}) \quad (5.2a)$$

$$\mathrm{PAR} = \mathrm{PAR}_{\max} - (\mathrm{PAR}_{\max} - \mathrm{PAR}_{\min}) * (\frac{\mathrm{currentiteration}}{\mathrm{maxiteration}}) \quad (5.2b)$$

$$\mathrm{BW} = \mathrm{BW}_{\max} * \exp[\ln\left(\frac{\mathrm{BW}_{\max}}{\mathrm{BW}_{\min}}\right) * \frac{\mathrm{currentiteration}}{\mathrm{maxiteration}}\ ] \quad (5.2c)$$

5.2.3 Hybridization of CTLBO and HS algorithm

It is observed that the characteristics of TLBO and HS algorithms are complimentary to each other i.e. HSA has excellent exploratory behavior but slow in convergence while TLBO exhibits very good exploitation characteristics and fast convergence. Hence, the proposed method aims to utilize the merits of both algorithms and reach the global solution quickly. So, for the maximum exploration of the search space, initially, HSA is employed and then exploitation of the search space is done with the help of TLBO. In the proposed method, selection of the teaching phase of the TLBO algorithm and local pitch adjustment by HMCR of HSA is based on the ratio ASR (Auto selection rate) defined as

$$\mathrm{ASR} = \frac{\text{Best fitness of SVM}}{\text{Worst fitness of SVM}} \quad (5.3)$$

As the value of ASR changes in each iteration, ASR is dynamic in nature and is self adaptive for the selection of either of these two algorithms for the improvisation of the

Harmony vector. For minimization problems, as the value of best fitness will always be less than the worst fitness value, ASR will be less than 1. For maximization problems, ASR is obtained by minimizing the inverse of the fitness function values, which will also lead to ASR less than 1. Initially ASR will be low which gives preference to the HS algorithm for better exploration of the search space. As ASR moves towards unity, teaching phase is selected for better tuning of the variables.

To minimize the demerits of HS and CTLBO, the HTLBO initially utilizes the exploration characteristics of HS. Subsequently, the CTLBO algorithm is implemented for better tuning and fast convergence of the solution vector. The following steps are considered for the HTLBO algorithm.

A. Target vector selection: $X_{new}^{SVS}=X_{old}^{SVS}$ from the SVM.

B. Generation of target vector X_{new}^{SVS} in each iteration comprises of four steps.

Step 1. Auto selection rate.

The selection of Teaching phase or HMCR for the generation of target vector X_{new}^{SVS}depends upon the ASR is found using Eqn. (5.3).

Step 2. Teaching phase / HMCR and local pitch adjustment/ mutation phase

When ASR is less than 'r', ('r' is a number between 0 and 1) the teaching phase is selected and Eqn. (4.3) is used to generate '$X_{new,i}^{SVS}$' of ASR is more than 'r,' HSA is selected for the generation of X_{new}^{SVS} . The probability of tuning the target vector is decided by the HMCR. If the random number is less than HMCR, local pitch adjustment of '$X_{new,i}^{SVS}$' is carried otherwise mutation phase is carried out according to Eqn. (5.1d) to generate the new target vector 'X_{new}^{SVS}'in the feasible space. If the fitness of the target vector

'$X_{new,i}^{SVS}$'is better than that of the worst fitness vector, then 'X_{worst}' is replaced by 'X_{new}^{SVS}'.

Step 3. Learning phase.

This phase enhances the knowledge (fitness) of the target vector'$X_{new,i}^{SVS}$'by interacting with the randomly selected harmony vector from solution vector matrix. Improvement of 'X_{new}^{SVS}' is done according to Eqn. (4.2a & 4.2b). If the fitness of the target vector 'X_{new}^{SVS}' is better than the fitness of the worst fitness vector, then X_{worst} is replaced by 'X_{new}^{SVS}'.

Step 4. Dynamic adjustment of parameters

For the efficient operation of the HTLBO algorithm, the HMCR, PAR and the BW parameters are dynamically tuned, in each iteration, as per Eqn. (5.2a), (5.2b), & (5.2c).

C. If the target vector generated has better fitness, then the SVM is updated otherwise the next iteration is started. If the number of iterations satisfies the condition for termination, the algorithm is terminated and the best solution of SVM is selected as the solution of the objective function.

5.3 OBJECTIVE FUNCTION FORMULATION

The proposed work has considered the following assumptions:

(a) All RDNs are balanced.
(b) Unity power factor DGs have been employed in RDN.
(c) Nominal load level and constant power load model is assumed.
(d) The outputs of all DGs are time invariant.

5.3.1 Multi-objective function

A multi-objective function optimizes all the SOFs simultaneously, subject to the equality and inequality constraints. In this chapter, a MOF is used in line with [65], which simultaneously reduces the APL (F_1) and VD (F_2) while improves the VSI (F_3) is formulated using two approaches as detailed below,

5.3.1.1 Weighted sum approach

In this approach [159], each single objective functions is assigned a weight factor to convert multi valued functions to single value function. This can be mathematically represented as shown below,

$$\mathrm{MOF} = \mathrm{Minimize}(a_1 * F_1 + a_2 * F_2 + a_3 * 1/F_3) \tag{5.4}$$

In this formulation, a weighted sum approach for MOF in line with [65], is used which simultaneously reduces the APL (F_1) and VD (F_2) while improves the VSI (F_3) where 'a_1', 'a_2' and 'a_3' are the weight coefficient associated with each SOFs respectively. If DGs are implemented with the objective of mitigating a specific problem, the corresponding weight coefficient is increased. Any value of weight coefficient can be chosen depending upon the significance of the objective function. But, for a normalized objective function, the sum of the weight coefficient should be unity as shown below,

$$a_i \in ([0,1]) \quad \text{and} \quad \sum_{i=1}^{m} a_i = 1 \tag{5.5}$$

5.3.1.2 ε-constraints approach

In this optimization approach, detailed in [159], the multi-objective optimization problem is solved by targeting one of the objective functions as main objective function

and restricting the rest of the objective functions as constraints. Mathematically it can be represented as follows,

$$MOF = \text{Minimize } F\mu(X) \tag{5.6}$$

$$\text{Subject to } F_m(X) \leq \varepsilon_m \quad m = 1,2,3 \ldots M. \text{ and } m \neq \mu;$$

$$g_j(X) \geq 0, \quad j = 1,2,3 \ldots .;$$

$$h_l(X) = 0, \quad l = 1,2,3 \ldots .;$$

$$X_{min,i} \leq X_i \leq X_{max,i}, \quad i = 1,2,3 \ldots . N;$$

In this chapter, $F\mu(x)$ corresponds to the APL, considered as main objective function while $F_m(x)$ comprises both the VD and the inverse of VSI as constraints.

5.3.2 Constraints

The SOFs and the MOF are subject to the following constraints for the optimal allocation of DGs in the RDN as given below.

5.3.2.1 Active and reactive power balance constraints

$$P_{sub} + \sum_{k=1}^{nDG} P_{DG,k} = P_{loss} + \sum_{k=1}^{n} P_{L,k} \;\; \& \;\; Q_{sub} = Q_{con} + \sum_{k=1}^{n} Q_{L,k} \tag{5.7}$$

5.3.2.2 Voltage limit constraint

The voltage magnitudes (V_k) of all the buses of RDN must be within limits of V_{max} (1.05 p. u.) and V_{min} (0.95 p. u.)

$$V_{min} \leq |V_k| \leq V_{max} \quad k = 1, 2, 3, 4 \ldots \ldots n \tag{5.8}$$

5.3.2.3 Thermal limit [75]

$$|I_j| \leq |I_j^{max}| \qquad j = 1,2,3,4 \ldots \ldots nb \tag{5.9}$$

5.3.2.4 Real power limit [53]

$$P_{DG,k}^{min} \leq P_{DG,k} \leq P_{DG,k}^{max} \quad (5.10)$$

5.3.2.5 Maximum penetration of DG units in the network [163]

$$\sum_{k=1}^{nDG} \mathbf{P_{DG,k}} = \% \mathbf{J} * \sum_{k=1}^{nb} \mathbf{P_{L,k}} \quad (5.11)$$

5.4 CASE STUDIES AND RESULTS

The proposed algorithm (HTLBO) is first validated on standard mathematical benchmark functions. The HTLBO algorithm parameters are detailed in Table 5.6. HTLBO is tested for 20, 30 and 50 variables and the results are shown in Table 5.1. Subsequently, the suggested HTLBO was used for optimal allocation of Type-1 DGs in the 33-bus, 69-bus and 118-bus using ε-constraints method for the MOF. The MOF considers all the three SOFs simultaneously. Results obtained are better than TLBO and QOTLBO respectively, as shown in subsequent tables.

5.4.1 Mathematical benchmark functions validation

The performance of the proposed HTLBO algorithm is validated on eleven mathematical benchmark test functions [64] as given in Table 5.1. A comparison of the proposed HTLBO vis-à-vis other algorithms [155] is shown in Table 5.3 and Table 5.4. It is observed that the proposed method gives the best results with Penalized, Penalized 2 & Rosenbrock functions, while it yields results identical to ITLBO (improved TLBO) with Sphere, Schwefel 2.22, Schwefel 1.2, Griewank, Ackley & Rastrigin functions. However, it is observed that for the Schwefel 2.21 and Step 2 functions, ITLBO gives the best result. For the purpose of demonstration, Pareto sets are obtained for some

Table 5.1: Mathematical benchmark functions for HTLBO

S.No.	Function	Formulation	N	Search range
1	Sphere	$F(x)_{min} = \sum_{i=1}^{N} x_i^2$	30	[-100,100]
2	Schwefel 2.22	$F(x)_{min} = \sum_{i=1}^{N} \lvert x_i \rvert + \prod_{i=1}^{N} \lvert x_i \rvert$	30	[-10,10]
3	Schwefel 1.2	$F(x)_{min} = \sum_{i=1}^{N} \left(\sum_{j=1}^{i} x_j \right)^2$	30	[-100,100]
4	Schwefel 2.21	$F(x)_{min} = \max_{1 \le i \le N} \lvert x_i \rvert$	30	[-100,100]
5	Rosenbrock	$F(x)_{min} = \sum_{i=1}^{N} [100(x_i^2 - x_{i+1})^2 + (1 - x_i)^2]$	30	[-2.048,2.048]
6	Step 2	$F(x)_{min} = \sum_{i=1}^{N} ([x_i + 0.5])^2$	30	[-100,100]
7	Rastrigin	$F(x)_{min} = \sum_{i=1}^{N} [x_i^2 - 10\cos(2\pi x_i) + 10]$	30	[-5.12,5.12]
8	Ackley	$F(x)_{min} = -20e^{\left(-0.2\sqrt{\frac{1}{N}\sum_{i=1}^{N} x_i^2}\right)} - e^{\left(\frac{1}{N}\sum_{i=1}^{N}\cos(2\pi x_i)\right)} + 20 + e^1$	30	[-32.768,32.768]
9	Griewank	$F(x)_{min} = \frac{1}{4000}\sum_{i=1}^{N} x_i^2 - \prod_{i=1}^{N} \cos\left(\frac{x_i}{\sqrt{i}}\right) + 1$	30	[-600,600]
10	Penalized	$F(x) = \frac{\pi}{N}\left[10\sin^2(\pi y_1) + \sum_{i=1}^{N-1}(y_i - 1)^2\{1 + 10\sin^2(\pi y_{i+1})\} + (y_N - 1)^2\right] + \sum_{i=1}^{N} u(x_i, 10, 100, 4)$ $u(x_i, ak, m) = \begin{cases} k(x_i - a)^m, & x_i > a, \\ 0, -a \le x_i \le a, y_i = 1 + 1/4(x_i + 1) \\ k(-x_i - a)^m & x_i < -a \end{cases}$	30	[-50,50]
11	Penalized 2	$F(x) = 0.1\left[10\sin^2(\pi x_1) + \sum_{i=1}^{N-1}(x_i - 1)^2\{1 + \sin^2(3\pi x_{i+1})\} + (x_N - 1)^2 + \left(1 + \sin^2(2\pi x_N)\right)\right] + \sum_{i=1}^{N} u(x_i, 5, 100, 4)$ $u(x_i, ak, m) = \begin{cases} k(x_i - a)^m, & x_i > a, \\ 0, & -a \le x_i \le a \\ k(-x_i - a)^m & x_i < -a \end{cases}$	30	[-50,50]

Table 5.2: Multi-objective mathematical benchmark functions

S.No.	Function	Objective function	N	Search range	Comment
1	SCH	$f_1(x) = x^2$ $f_2(x) = (x-2)^2$	1	$[-10^3, 10^3]$	Convex
2	KUR	$f_1(x) = \sum_{i=1}^{N-1}\left[-10\exp\left(-0.2\sqrt{x_i^2 + x_{i+1}^2}\right)\right]$ $f_2(x) = \sum_{i=1}^{N-1}(\lvert x_i\rvert^{0.8} + 5\sin x_i^3)$	3	[-5,5]	Nonconvex
3	ZDT3	$f_1(x) = x_1$ $f_2(x) = g(x)[1 - \sqrt{x_1/g(x)} - \frac{x_1}{g(x)}\sin(10\pi x_1)$ $g(x) = 1 + 9\left(\sum_{i=2}^{N} x_i\right)/(n-1)$	30	[0,1]	Convex, disconnected
4	ZDT4	$f_1(x) = x_1$ $f_2(x) = g(x)\left[1 - \sqrt{x_1/g(x)}\right]$ $g(x) = 1 + 10(N-1) + \sum_{i=2}^{N}[x_i^2 - 10\cos(4\pi x_i)]$	10	$x_1 \in [0,1]$ $x_i \in [-5,5]$, $i = 2,3..,n$	Nonconvex
5	BNH	$f_1(x) = 4x_1^2 + 4x_2^2$ $f_2(x) = (x_1-5)^2 + (x_2-5)^2$ Subject to $C_1(x) = (x_1-5)^2 + x_2^2 \le 25$, $C_2(x) = (x_1-8)^2 + (x_2+3)^2 \ge 7.7$	2	$0 \le x_1 \le 5$, $0 \le x_2 \le 3$.	Convex
6	TNK	$f_1(x) = x_1$ $f_2(x) = x_2$ Subject to $C_1(x) = x_1^2 + x_2^2 - 1 - 0.1\cos(16\tan^{-1}(x_1/x_2)) \ge 0$, $C_2(x) = (x_1-0.5)^2 + (x_2-0.5)^2 \le 0.5$	2	$0 \le x_1 \le \pi$, $0 \le x_2 \le \pi$.	Discontinuous
7	OSY	$f_1(x) = -[25(x_1-2)^2 + (x_2-2)^2 + (x_3-1)^2 + (x_4-4)^2 + (x_5-1)^2]$ $f_2(x) = x_1^2 + x_2^2 + x_3^2 + x_4^2 + x_5^2 + x_6^2$ Subject to $C_1(x) = x_1 + x_2 - 2 \ge 0$, $C_2(x) = 6 - x_1 - x_2 \ge 0$ $C_3(x) = 2 + x_1 - x_2 \ge 0$ $C_4(x) = 2 - x_1 + 3x_2 \ge 0$ $C_5(x) = 4 - (x_3-3)^2 - x_4 \ge 0$ $C_6(x) = (x_5-3)^2 + x_6 - 4 \ge 0$	6	$0 \le x_1, x_2, x_6 \le 10$ $1 \le x_3, x_5 \le 5$ $0 \le x_4 \le 6$	Continuous

multi-objective test functions (unconstrained and constrained) shown in Table 2, when HTLBO is integrated with 'non-dominating sorting algorithm' [159]. From Fig 5.1(a), it is observed that for unconstrained problems, HTLBO yields similar results with SCH and KUR, inferior results with ZDT3 and better results with ZDT4, as compared to

TNK, while better results are obtained with BNH and OSY than NSGA- II, as shown in Fig. 5.1 (b). Table 5.5 shows the impact of variations of HTLBO parameters on the solution of the Sphere function. The parameters considered are ‘a’, ‘SVS’, ‘IN’, ‘N’. It

Table 5.3: Comparative results of HTLBO algorithm with other algorithms.

F.No	N	G-ABC		PS-ABC		TLBO	
		Mean	SD	Mean	SD	Mean	SD
1	20	3.1943E-16	7.3909E-17	0.00	0.00	0.00	0.00
	30	6.2643E-16	1.0859E-16	0.00	0.00	0.00	0.00
	50	1.2546E-5	6.0511E-9	0.00	0.00	0.00	0.00
2	20	9.3611E-16	1.3278E-16	0.00	0.00	0.00	0.00
	30	1.3019E-10	4.6859E-11	0.00	0.00	0.00	0.00
	50	2.3671E-05	6.1889E-06	0.00	0.00	0.00	0.00
3	20	2.6919E3	1.4619E3	0.00	0.00	0.00	0.00
	30	1.0939E4	2.5670E3	0.00	0.00	0.00	0.00
	50	4.1236E4	5.8269E3	0.00	0.00	0.00	0.00
4	20	0.3325	1.0786	0.00	0.00	0.00	0.00
	30	12.6211	2.6556	8.59E-115	4.71E-114	4.9E-324	0.00
	50	45.3075	4.3151	19.6683	6.341E+00	9.9E-324	0.00
5	20	1.6769	2.9037	.5190	1.0764	15.0536	2.28E−01
	30	7.47961	19.0926	1.5922	4.4066	25.4036	3.50E−01
	50	25.7164	31.75811	34.4913	30.3412	45.8955	2.89E−01
6	20	3.3386E-16	1.0154E-16	2.6147E-16	3.8684E-17	9.24E−33	4.36E−33
	30	6.4499E-16	1.1126E-16	5.7169E-16	8.2549E-17	1.94E−29	1.88E−29
	50	5.6529E-09	3.6854E-09	1.1674E-15	1.4114E-16	3.26E−13	5.11E−13
7	20	0.00	0.00	0.00	0.00	6.41E−14	6.16E−14
	30	3.3165E-02	1.8165E-01	0.00	0.00	6.95E−13	1.64E−12
	50	2.1733	1.0728	0.00	0.00	7.90E−13	1.89E−12
8	20	2.7533E-14	3.5832E-15	8.8817E-16	0.00	3.55E−15	8.32E−31
	30	7.7828E-10	2.9817E-10	8.8817E-16	0.00	3.55E−15	8.32E−31
	50	1.1137E-04	3.8873E-05	8.8817E-16	0.00	3.55E−15	8.32E−31
9	20	6.0279E-04	2.2313E-03	0.00	0.00	0.00	0.00
	30	6.9655E-04	2.2609E-03	0.00	0.00	0.00	0.00
	50	1.0470E-03	2.7482E-03	0.00	0.00	0.00	0.00
10	20	3.2621E-16	6.6721E-17	2.5576E-16	4.9715E-17	4.00E−08	6.85E−24
	30	5.8570E-16	1.1349E-16	5.5312E-16	8.6858E-17	2.67E−08	6.79E−12
	50	9.3017E-11	7.9664E-11	1.0252E-15	1.5815E-16	5.18E−05	1.92E−04
11	20	6.5528E-08	2.4413E-07	2.3456E-18	2.2088E-18	2.34E−08	6.85E−24
	30	2.1724E-07	5.6676E-07	6.0601E-18	5.6064E-18	2.37E−08	4.91E−10
	50	8.8776E-07	1.5324E-06	5.0541E-17	1.5350E-16	1.52E−03	5.29E−03

is observed from Table 5.5 that for SVS=10 and Maximum iteration=6000, HTLBO algorithm gives best results for all 'a'. Similarly, for SVS=20 and 30, HTLBO gives best results with 'a=0.2'. For SVS=40 and 50, HTLBO gives best results with 'a=0.1'while considering N=20. On the other hand, with N=30 and 50, 'a=0.2' gives better result.

Table 5.4: Comparative results of HTLBO algorithm with other algorithms.

F.No	N	ITLBO		HTLBO	
		Mean	SD	Mean	SD
1	20	0.00	0.00	0.00	0.00
	30	0.00	0.00	0.00	0.00
	50	0.00	0.00	0.00	0.00
2	20	0.00	0.00	0.00	0.00
	30	0.00	0.00	0.00	0.00
	50	0.00	0.00	0.00	0.00
3	20	0.00	0.00	0.00	0.00
	30	0.00	0.00	0.00	0.00
	50	0.00	0.00	0.00	0.00
4	20	0.00	0.00	4.9407E-324	0.00
	30	0.00	0.00	4.9407E-324	0.00
	50	0.00	0.00	4.9407E-324	0.00
5	20	1.3785	8.49E−01	0.1332	0.14021
	30	15.032	1.2E+00	16.141	1.4042
	50	38.7294	7.57E−01	42.447	1.1164
6	20	0.00	0.00	0.00	0.00
	30	0.00	0.00	2.5063e-32	7.0518e32
	50	1.51E−32	8.89E−33	1.8917e-14	4.3031e-14
7	20	0.00	0.00	0.00	0.00
	30	0.00	0.00	0.00	0.00
	50	0.00	0.00	0.00	0.00
8	20	7.11E−16	0.00	2.2201e-15	0.00
	30	7.11E−16	0.00	2.2201e-15	0.00
	50	7.11E−16	0.00	2.2201e-15	0.00
9	20	0.00	0.00	0.00	0.00
	30	0.00	0.00	0.00	0.00
	50	0.00	0.00	0.00	0.00
10	20	2.42E−16	1.09E−16	2.355e-32	8.4989e-48
	30	4.98E−16	2.14E−16	3.2337E-29	6.4289E-29
	50	9.19E−16	5.38E−16	3.4659E-16	2.9939E-16
11	20	1.93E−18	1.12E−18	1.3498E-32	0
	30	5.92E−18	4.74E−18	3.1884E-28	4.0023E-28
	50	4.87E−17	4.26E−17	5.1175E-15	3.2346E-16

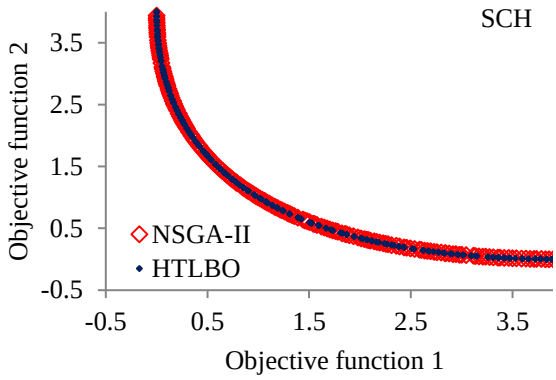

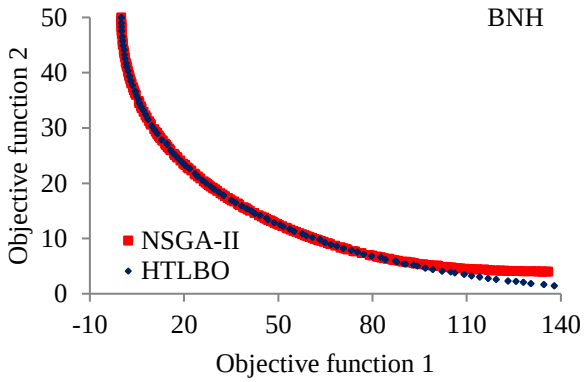

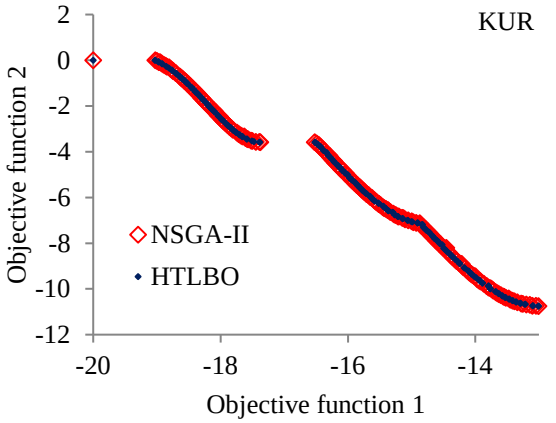

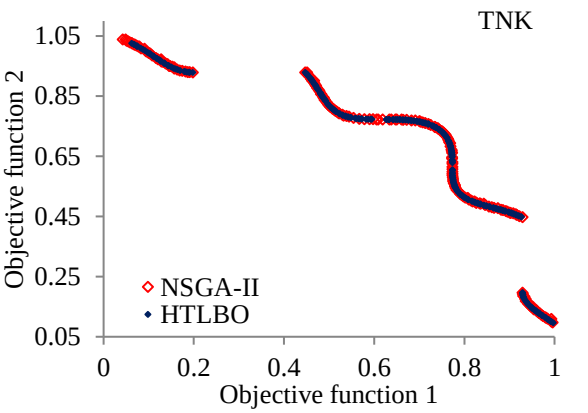

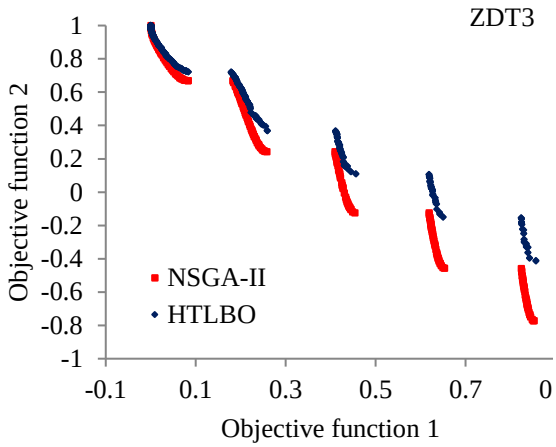

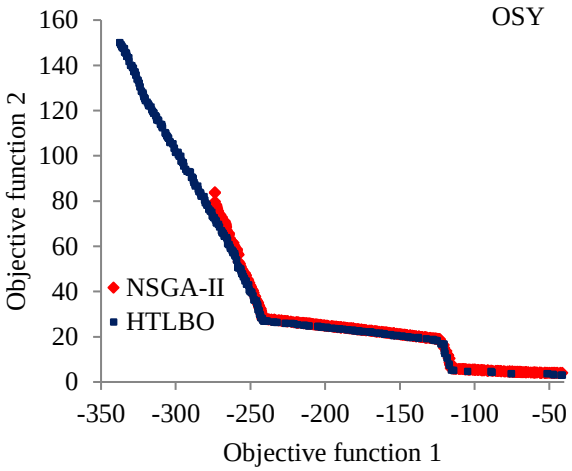

Fig. 5.1 (a): Results of unconstrained multi-objective functions by NSGA-II and HTLBO for

[1] SCH
[2] KUR
[3] ZDT3
[4] ZDT4

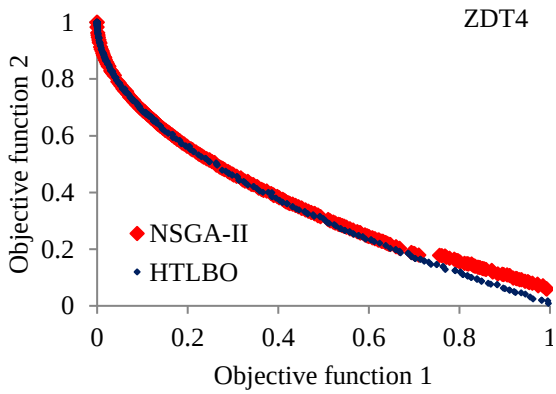

Fig. 5.1 (b): Results of constrained multi-objective functions by NSGA-II and HTLBO for

[1] BNH
[2] TNK
[3] OSY

Table 5.5: Impact of algorithm parameters on mathematical benchmark function.

Sphere function			Teaching factor rate (a)							
SVS	IN	N	0.1		0.2		0.3		0.4	
			Mean	SD	Mean	SD	Mean	SD	Mean	SD
10	6000	20	0	0	0	0	0	0	0	0
		30	0	0	0	0	0	0	0	0
		50	0	0	0	0	0	0	0	0
20	3000	20	1.32E-220	0	3.11E-233	0	8.64E-223	0	1.95E-198	0
		30	1.69E-174	0	5.21E-191	0	2.74E-174	0	6.10E-155	1.30E-154
		50	1.40E-142	1.97E-142	1.47E-154	3.22E-154	1.31E-141	2.92E-141	1.29E-120	2.37E-120
30	2000	20	2.61E-119	5.29E-119	1.44E-121	2.99E-121	4.18E-111	9.33E-111	5.53E-102	1.06E-101
		30	6.89E-90	9.66E-90	3.00E-91	6.62E-91	2.37E-84	5.28E-84	8.63E-76	9.88E-76
		50	5.96E-67	1.29E-66	1.63E-73	3.27E-73	8.72E-67	6.04E-67	3.53E-55	4.40E-55
40	1500	20	5.72E-78	8.55E-78	1.18E-76	2.45E-76	3.01E-71	4.27E-71	7.46E-64	1.64E-63
		30	2.65E-56	2.08E-56	1.72E-57	1.28E-57	5.83E-53	5.64E-53	5.94E-45	1.20E-44
		50	5.46E-39	1.16E-38	1.15E-42	1.07E-42	5.09E-38	9.58E-38	3.43E-32	2.45E-32
50	1200	20	2.97E-55	3.02E-55	4.81E-53	1.02E-52	5.80E-49	1.27E-48	1.29E-44	1.29E-44
		30	3.98E-38	2.64E-38	5.34E-39	5.18E-39	5.65E-35	6.93E-35	1.03E-30	1.24E-30
		50	9.07E-27	7.55E-27	3.74E-28	5.55E-28	2.53E-25	2.61E-25	1.32E-20	1.03E-20

Table 5.6: HTLBO algorithm parameters

Parameter	Values
a	0.2
$HMCR_{min}$	0.7
$HMCR_{max}$	0.95
PAR_{min}	0.3
PAR_{max}	0.5
r	0.9
BW_{min}	0.0001
BW_{max}	0.1
Maxiteration	500
SVS	90

5.4.2 33-bus RDN

The suggested HTLBO is first implemented for optimal allocation of DGs in the 33-bus RDN using two methods. The first one is the weighted sum method, where the MOF is formulated as a weighted sum of the three SOFs. The second approach comprises the modification of the MOF into a SOF using the ε-constraints method [159]. In both the

methods, the objective is simultaneous minimization of the network APL and VD together with VSI maximization. The detailed network data is given in appendix Table A.1 and chapter 3. Three DGs (Type –I) are selected for optimal allocation in this RDN. The HTLBO parameters are selected as given in Table 5.6 .The weight factors 'a1', 'a2' and 'a3' corresponding to the three SOFs are shown in Table 5.7. As shown in Table 5.7, when a1 = 1.0 a2 = 0.6 and a3 = 0.35, the suggested HTLBO shows reduction in the APL to 82.815 kW (from 210.998 kW in the base case). On the other hand, results of MOF with ε-constraints Method, gives simultaneous improvement in all three SOFs i.e. F1, F2 and F3 (97.5330 kW, 0.0009 p.u. and 0.9653 p.u., respectively), in comparison to both TLBO and QOTLBO, as shown in Table 5.7 that without DG. From Fig. 5.2 (a), minimum network voltage magnitude of 0.9836 p.u. at node 33, is noticed in presence of DGs. The network voltage profile shows a remarkable improvement than that without DG (voltage magnitude of 0.9038 p.u. at bus 18). Fig. 5.2 (b) shows the convergence characteristics of the MOF corresponding to the TLBO, QTLBO and the proposed HTLBO algorithm. It is observed from Fig. 5.2 (b) that the proposed algorithm (HTLBO) has the lowest fitness value i.e. 0.4590 p.u. and the fastest convergence rate.

5.4.3 69-bus RDN

The HTLBO is now implemented on the 69-bus for optimal allocation of DGs. Again, three DGs (Type –I) have been considered. Similar to the case of the 33-bus RDN above, the MOF (for minimization of the network APL and VD together with maximization of VSI) is evaluated using both the weighted sum method and the ε-constraints method. The HTLBO parameters are again selected as shown in Table 5.6. The detailed network data is given in appendix A.2 and chapter 3. As shown in Table 5.8,

Table 5.7: Results for optimal DG allocation in 33-bus

	TLBO		QOTLBO		HTLBO		HTLBO	
	Weight coefficient				(a_1=1.0 a_2=0.6 a_3=0.35)		ε-constraints Methods	
	Optimal DG		Optimal DG		Optimal DG		Optimal DG	
	Location	Size (MW)	Location	Size (MW)	Location	Size (MW)	Location	Size (MW)
	12	1.1826	13	1.0834	13	1.0229	13	1.2043
	28	1.1913	26	1.1876	25	0.9016	25	0.8573
	30	1.1863	30	1.1992	30	1.4567	30	1.6480
APL (kW)	124.695		103.403		82.815		97.5330	
VD (p.u.)	0.0011		0.0011		0.0026		0.0009	
VSI (p.u.)	0.9503		0.9530		0.9360		0.9653	
MOF (p.u.)	0.4936		0.4713		0.4590		0.4590	

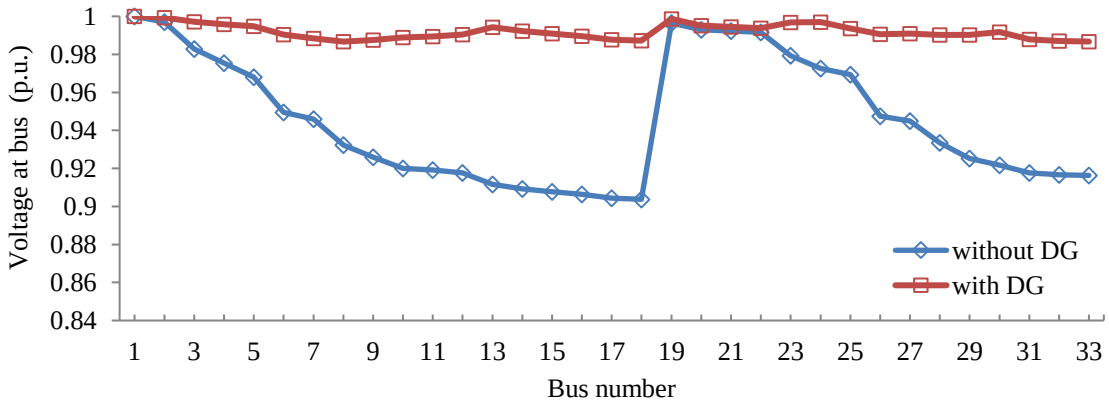

Fig. 5.2 (a): Bus voltage profile of the 33-bus without and with DG

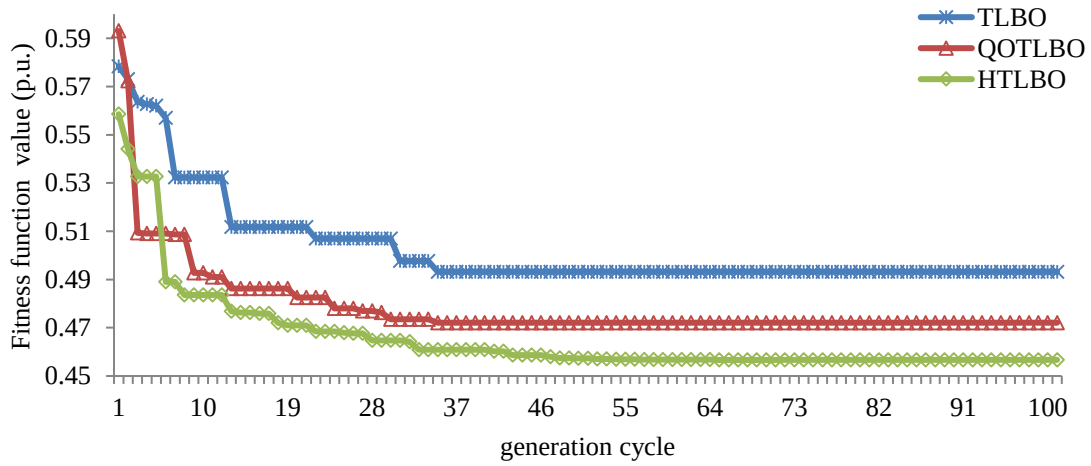

Fig. 5.2 (b):Fitness convergence characteristics in 33-bus for MOF

Table 5.8: Results for MOF in 69-bus

	TLBO		QOTLBO		HTLBO		HTLBO	
	Weight coefficient				(a_1=1.0 a_2=0.6 a_3=0.35)		ε-constraints Method	
	Optimal DG		Optimal DG		Optimal DG		Optimal DG	
	Location	Size (MW)	Location	Size (MW)	Location	Size (MW)	Location	Size (MW)
	13	1.0134	15	0.8114	12	0.9424	12	0.9956
	61	0.9901	61	1.1470	25	0.2306	20	0.2398
	62	1.1601	63	1.0022	61	2.0508	61	2.1123
APL (kW)	82.172		80.585		76.938		79.431	
VD (p.u.)	0.0008		0.0007		0.0006		0.0003	
VSI (p.u.)	0.9745		0.9769		0.9677		0.9770	
MOF (p.u.)	0.4418		0.4393		0.4389		0.4389	

when a_1=1.0 a_2=0.6 and a_3=0.35, HTLBO shows reduction in APL to 76.938 kW and improvement in the VDI to 0.0006 p.u. On the other hand, results of MOF with ε-constraints method, gives simultaneous improvement in all the three SOFs (F_1, F_2 and F_3) to 79.431 kW, 0.0003 p.u. and 0.9770 p.u. respectively, in comparison to both TLBO and QOTLBO, as shown in Table 5.8. Fig.5.3 (a) shows the voltage profile enhancement of the 69-bus with DGs over that without DG. From Fig.5.3 (a), it is observed that the minimum network voltage magnitude with DGs is 0.9942 p.u., occurs at bus 50. Thus, with DGs, the network voltage profile shows a notable improvement than that without DG (0.9092 p.u. at bus 65). Fig. 5.3 (b) shows the convergence characteristics of the MOF corresponding to the TLBO, QTLBO and the HTLBO algorithm. It is observed from Fig. 5.3 (b) that the proposed algorithm (HTLBO) has the lowest fitness value i.e. 0.4389 p.u. and the fastest convergence rate.

5.4.4 118-bus RDN

The proposed algorithm (HTLBO) is now implemented on the 118-bus for optimal allocation of DGs. Seven DGs (Type –I) have been considered. Similar to the case of

the 33 and 69-bus above, the MOF (for minimization of the network APL and VD together with maximization of VSI) is evaluated using both the weighted sum method and the ε-constraints method. The HTLBO parameters are again selected as shown in Table 5.6. The detailed network data is given in appendix A.3 and chapter 3**.** As shown in Table 5.8, when a_1=1.0 a_2=0.6 and a_3=0.35, HTLBO shows improvement in both VDI and VSI as compared to both TLBO and QOTLBO, although the APL are inferior to both TLBO and QOTLBO. On the other hand, results of MOF with ε-constraints method, gives simultaneous improvement in all the three SOFs (F_1, F_2 and F_3) to 658.756 kW, 0.0225 p.u. and 0.8978 p.u. respectively, in comparison to both TLBO and QOTLBO, as shown in Table 5.9. Fig.5.4 (a) shows the voltage profile enhancement of the 118-bus with DGs over that without DG. From Fig.5.4 (a), it is observed that the minimum network voltage magnitude of 0.97344 p.u. occurs at node 56, in the presence of DGs. The network voltage profile again shows a remarkable improvement over that without any DG (voltage magnitude of 0.86879 p.u. at bus 80). Fig. 5.4(b) shows the convergence characteristics of the MOF corresponding to the TLBO, QTLBO and the

Table 5.9: Results for MOF of 118-bus

	TLBO		QOTLBO		HTLBO		HTLBO	
	Weight coefficients				(a_1=1.0 a_2=0.6 a_3=0.35)		ε-constraints method	
	Optimal DG		Optimal DG		Optimal DG		Optimal DG	
	Location	Size (MW)	Location	Size (MW)	Location	Size (MW)	Location	Size (MW)
	35	3.2462	43	1.5880	25	2.0833	22	2.0526
	48	2.8864	49	3.8459	43	1.2457	44	1.1217
	65	2.4307	54	0.9852	52	4.9877	51	4.5526
	72	3.3055	74	3.1904	80	2.6429	77	2.6456
	86	1.9917	80	3.1632	82	34.6417	81	4.6412
	99	1.6040	94	1.9524	93	3.8135	93	3.7620
	111	3.5984	111	3.6013	115	3.2830	115	3.2836
APL (kW)	705.8980		677.5881		774.946		658.756	
VD (p.u.)	0.0327		0.0233		0.0172		0.0225	
VSI (p.u.)	0.8548		0.8794		0.9017		0.8978	
MOF (p.u.)	0.4361		0.4187		0.4062		0.4104	

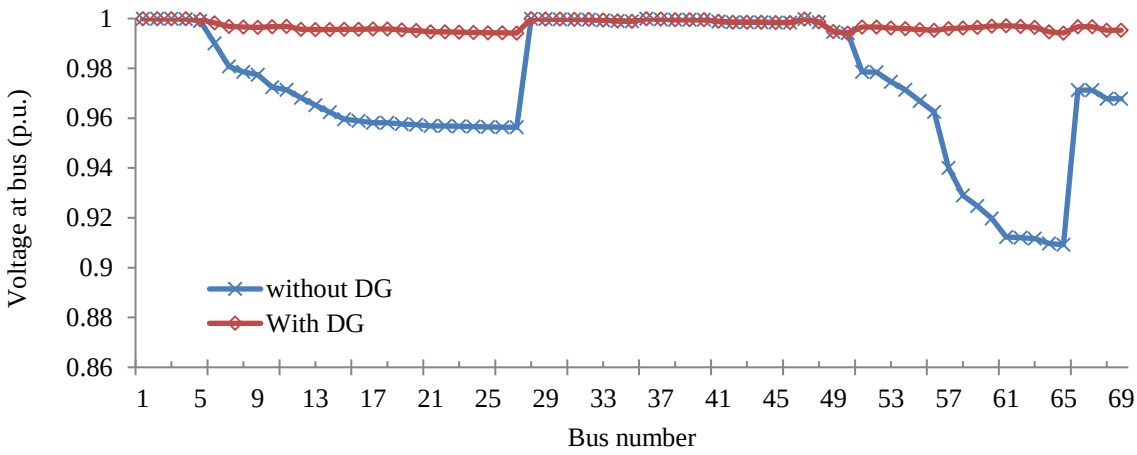

Fig. 5.3 (a): Bus voltage profile of 69-bus with and without DG

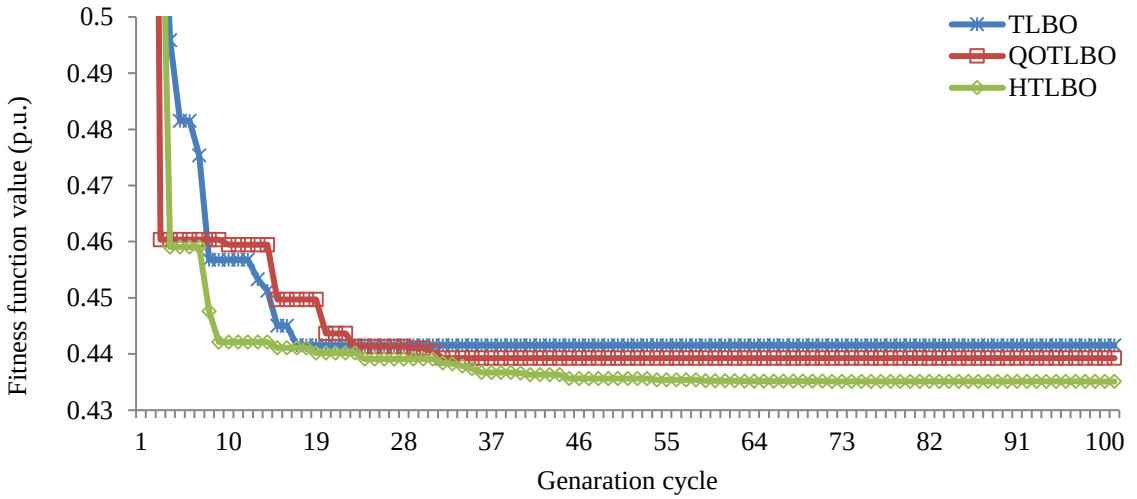

Fig. 5.3 (b): Fitness convergence characteristics of 69-bus for MOF

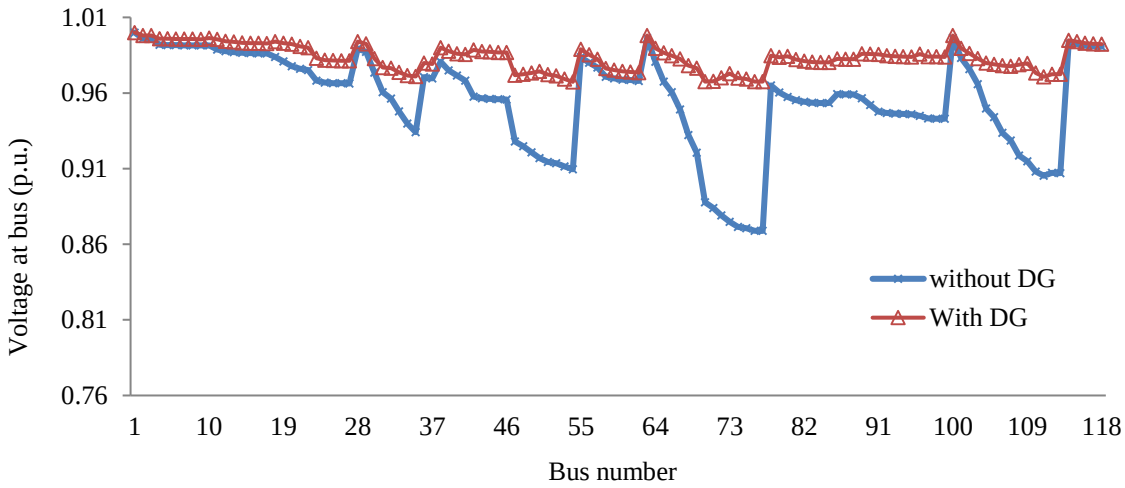

Fig. 5.4 (a): Bus voltage profile of 118-bus with and without DG

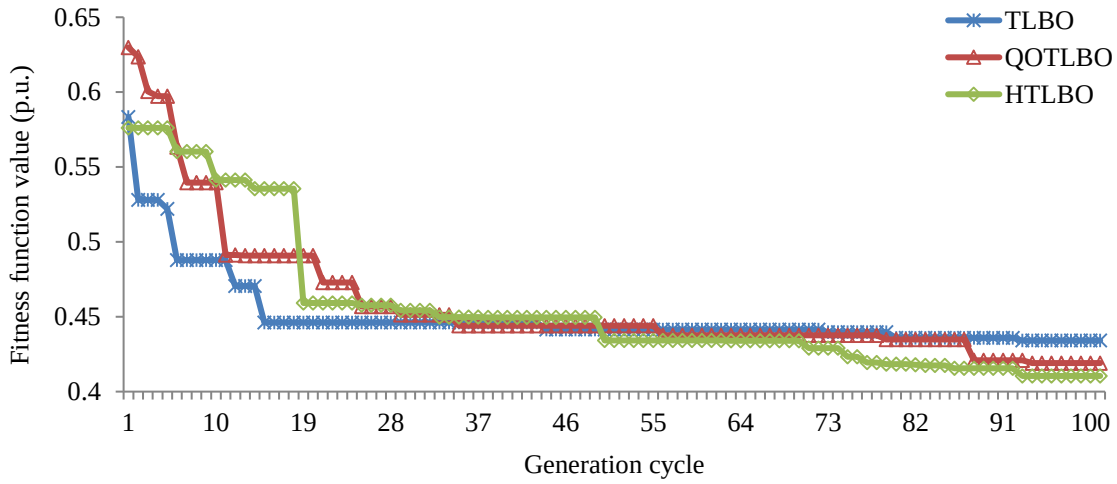

Fig. 5.4 (b): Fitness convergence characteristics of 118-bus for MOF

proposed HTLBO algorithm. It is observed from Fig. 6 (b) that the proposed algorithm (HTLBO) has the lowest fitness value of 0.4104 p.u.

5.5 SUMMARY

A HTLBO technique has been presented in this chapter. Its computational capability with continuous variables is first demonstrated on standard mathematical benchmark functions in the form of mean value and standard deviations. Subsequently, the proposed algorithm is implemented for optimal allocation of multiple DGs in the 33, 69 and 118-bus to validate its capability with mixed integer variables (i.e. DGs sizes belong to continuous domain while DG locations are in the discrete domain). The allocation of DGs in RDS are carried out using two methodologies i.e. weighted sum approach and ε-constraints method to solve the MOF, which includes the minimization of real power losses and voltage deviations along with maximization of VSI. The ε-constraints approach yields better results than the weighted sum approach in all the objectives over TLBO and QOTLBO. The results authenticate the global convergence competence of the HTLBO. The impact of the various parameters of the proposed algorithm is also

investigated. It is observed that for a certain level of DG penetration, a proper tuning of the algorithm parameters ensures global solution. It is also observed that optimal allocation of DGs results in substantial performance improvement of RDS, along with better network congestion management.

CHAPTER 6

REACTIVE POWER MANAGEMENT IN DISTRIBUTION NETWORKS FOR ENERGY, COST AND EMISSION SAVING

6.1 INTRODUCTION

DG integration in the distribution networks results in power loss reduction, voltage profile enhancement, improvement in VSI, network operational cost reduction and emission saving. However, integration of renewable energy sources based on solar and wind result in degradation of power supply reliability and enhancement of power quality issues because of uncertainty in solar and wind availability. It is observed in chapters 4 and 5 that only active power injection in the distribution network doesn't ensure power quality and network reliability. In recent years, these issues compelled the DNOs to take some remedial measures to mitigate these challenges. It is observed from the literature review that reactive power management in distribution networks is one of the measures to mitigate the challenges. However, published literature is available on reactive power management in distribution networks is limited.

This chapter is aimed to present a detailed analysis on the impact of the integration of reactive power compensatory device in the DNs. DSTATCOM is a shunt device, which constitutes an energy storage device, an inverter, and a transformer. Their fast dynamic response in respect of injection and absorption of reactive power makes their acceptability inevitable in distribution networks [55]. This investigation aims to provide a complete solution of 1) optimal DSTATCOM locations and sizes and 2)

This Chapter is partially based on the following published paper

I. A. Quadri, S. Bhowmick and D. Joshi, "Analytical Approach for Multiple DSTATCOM Allocation in Radial Distribution Systems for Enhancement of Energy, Cost and Emission Savings," *2nd IEEE International Conference on Power Electronics, Intelligent Control and Energy Systems (ICPEICES)*, Delhi, pp. 1-6, 2018.

optimal network topologies vis-à-vis varying load conditions, addressing multiple issues of power loss reduction, reduction of TACS and enhanced savings in energy and green-house gas emission. This chapter has adopted both analytical and meta-heuristic approaches, for optimal DSTATCOM allocations in different distribution networks considering single as well as multi-objective criteria. The impact of DSTATCOM on the technical issues, operational economy and environmental benefits in several distribution networks is investigated.

6.2 ANALYTICAL APPROACH FOR OPTIMUM ALLOCATION OF DSTATCOMS

The proposed technique is implemented for a deterministic problem of optimal DSTATCOM sizing and placement in RDNs addressing some core issues like APL, yearly energy loss, total cost saving.

The case studies assumptions are as following:

a. All the RDN are balanced.
b. The load shedding and line interruption are not considered.
c. Daily load profile is considered for EL, cost calculation and emission saving.
d. DSTATCOMs are considered for injecting reactive power only.

6.2.1 Problem formulation

The proposed method for computing the optimum size and location of DSTATCOM uses the BIBC and BCBV matrices. Development of BIBC and BCBV matrices are detailed in [38], using the topological configuration of the distribution systems. The proposed method for multi-DSTATCOMs requires executing only power flow for the

determination of the optimum size and location of DSTATCOMs in the RDS.

The total active power loss (APL) of the network is based on the equivalent current-injection at all the buses and total current flowing through the branch without or with DSTATCOMs. The expression of the total network APL [42] is given as follows:

$$P_{loss} = \sum_{j=1}^{nb} R_j[(\sum_{k=2}^{n} BIBC(j,k-1).MM)^2 + (\sum_{k=2}^{n} BIBC(j,k-1).NN)^2]$$

$$\text{Where } MM = {P_k \cos(\theta_k) + Q_k \sin(\theta_k)}\Big/{|V_k|} \quad \&$$

$$NN = {P_k \sin(\theta_k) - Q_k \cos(\theta_k)}\Big/{|V_k|} \tag{6.1}$$

6.2.1.1 Loss sensitivity factor approach

The objective is to find the capacity of DSTATCOM at any bus 'k' to minimize total APL of the network. The derivative of the j^{th} branch power loss per k^{th} bus injected reactive power i.e. $\partial P_{loss,j}/\partial Q_k$, can be obtained as below,

$$\frac{\partial P_{loss_j}}{\partial Q_k} = 2R_j.\sum_{k=2}^{n}(BIBC(j,k-1).MM).BIBC(j,k-1)\frac{\sin(\theta_k)}{|V_k|} + 2R_j.\sum_{k=2}^{n}(BIBC(j,k-1).NN).BIBC(j,k-1).\frac{-\cos(\theta_k)}{|V_k|} \tag{6.2a}$$

Summation of the above expression for all the branches leads to the derivation of the total power losses per k^{th} bus injected real power $\partial P_{loss,j}/\partial Q_k$, can be expressed as,

$$\frac{\partial P_{loss}}{\partial Q_k} = 2\sum_{j=1}^{nb}\left[R_j.(\sum_{k=2}^{n} BIBC(j,k-1).MM).BIBC(j,k-1)\frac{\sin(\theta_k)}{|V_k|}\right] + 2\sum_{j=1}^{nb}\left[R_j.\sum_{k=2}^{n}(BIBC(j,k-1).NN).BIBC(j,k-1).\frac{-\cos(\theta_k)}{|V_k|}\right] \tag{6.2b}$$

The objective is to find the size of DSTATCOM at any bus 'k' to minimize the total APL of the network. To calculate the optimum size of DSTATCOM at bus 'k', the Eqn. (6.2b) is equated to zero as:

$$\frac{\partial P_{loss}}{\partial Q_k} = 0 \tag{6.3a}$$

By solving Eqn. (6.3a), the reactive power injected at bus 'k' can be expressed as below:

$$Q_k = \frac{|V_k|.\sum_{j=1}^{nb}[R_j.\{PP..BIBC(j,k-1).\cos(\theta_k) - QQ.BIBC(j,k-1)\sin(\theta_k)\}]}{\sum_{j=1}^{nb} R_j.(BIBC(j,k-1))^2} \tag{6.3b}$$

Where $PP = \left(\sum_{\substack{m=2 \\ m\neq k}}^{n} BIBC(j, m-1).Im(I_m)\right)$ and $QQ = \left(\sum_{\substack{m=2 \\ m\neq k}}^{n} BIBC(j, m-1).re(I_m)\right)$

The Eqn. (6.3b) is the reactive power absorbed or injected into each bus 'k' in the network. The optimum size of added DSTATCOM at k^{th} bus can be obtained as follows:

$$Q_k = Q_{DG,k} + Q_{L,k} \tag{6.4}$$

6.2.1.2 The procedure to find optimal sizes and locations of multiple DSTATCOMs

The objective is to minimize the network APL, in the system by injecting or absorbing reactive power ($Q_{DG,k}$). In the proposed method, the following steps are used to determine the optimal size and placement of multi-DSTATCOMs:

Step 1. Execute the base case power flow.

Step 2. Find the optimum capacity of the new DSTATCOM for each bus except the source (substation) bus using Eqns. (6.3b) and (6.4)

Step 3. Determine the total active power losses from Eqn. (6.1) by placing the DSTAT-

COM of optimum capacity at each bus.

Step 4. Go for the bus, which has the least network APL after allocating DSTATCOM in step 3, as optimum location and corresponding ($Q_{DG,k}$) capacity as optimum size.

Step 5. Check whether the bus voltages in the network are within the acceptable range. If the bus voltage is not within the acceptable range, then the DSTATCOM is removed from the bus and we return to Step 4. Steps 1 to 4 determine the first optimal allocation of DSTATCOM in the network.

Step 6. The network data is updated by injecting reactive power of amount $Q_{DG,k}$ at the optimum location for computing the location and the size of the next DSTATCOM

Step 7. Steps 1 to 7 are repeated for finding the optimal locations and sizes of multiple DSTATCOMs.

6.2.1.3 Cost of DSTATCOM

The cost of investment of the DSTATCOM can be computed as detailed in Eqn. 3.22(a)-3.22(d) of chapter 3. This section deals with a computational procedure to utilize DSTATCOM units in the distribution networks for minimizing the energy loss and cost savings. At first DSTATCOM size and location is calculated for minimizing the power losses at the peak load as previously mentioned. The DSTATCOM output is calculated as per the load demand curve as detailed in load modelling of chapter 3. Finally, the EL and TACS are calculated using Eqns. (3.13) and (3.22a-3.22d), respectively, based on the DSTATCOM output pattern. The following steps are followed to compute the annual energy savings for 24-hour load demand [111],

Step 1. Find out the optimal size and location of a DSTATCOM unit at the

maximum load level using the procedure discussed in section 6.2.1.2.

Step 2. Find the optimal output of the DSTATCOM unit at the optimal location at time 't' as given below as shown below,

$$Q_{DG,k} = \text{Load}(t) * Q_{DG,k}^{max} \quad (6.5)$$

Where Load (t) is the total load demanded (p.u.) at time duration't' [111]

Step 3. Run power flow with each DSTATCOM output i.e. $Q_{DG,k}$ calculated in Step 2 for each period and calculate the total EL, as per Eqn. (3.13) of chapter 3.

Step 4. Calculate the TACS using Eqn. 3.22(a)-3.22(d). TACS data is given in Table A.4.

6.2.1.4 Emission saving

ES is the annual emission saving due to placement of DSTATCOM(s). The details for calculation of ES are detailed in section 3.4 of chapter 3.The data of ER of grid is given in Table A.5 [109]. The impact of DSTATCOM allocation in the distribution network is evaluated on the basis of indices as detailed in chapter 3. VSI indicates the vulnerability of the distribution network to voltage collapse, So VSI must be improved toward unity. VDI represents the overall voltage fluctuation at all the buses in the network. Ideally VDI should be zero. QLI describes the loadability of the network and it should be as high as possible. TBVVB indicates the number of buses in the network having voltage magnitudes beyond permissible limit.

6.2.2 Constraints

Following constraints are taken in consideration while allocating DSTATCOMs in the radial distribution network.

6.2.2.1 Active and reactive power balance constraints

$$P_{sub} = P_{loss} + \sum_{k=1}^{n} P_{L,k} \;\; \& \;\; Q_{sub} + \sum_{k=1}^{nDG} Q_{DG,k} = Q_{con} + \sum_{k=1}^{n} Q_{L,k} \qquad (6.6a)$$

6.2.2.2 Voltage constraint

The voltage magnitude at all the buses must be maintained between V_{max} (1.05 p. u.) 0and V_{min} (0.90 p. u.).

$$V_{min} \leq |V|_k \leq V_{max} \qquad k = 1,2,3,4 \ldots \ldots n \qquad (6.6b)$$

6.2.2.3 Line thermal limit

$$\left|I_j\right| \leq \left|I_j^{max}\right| \qquad (6.6c)$$

6.2.2.4 Reactive power limit of DSTATCOM

$$Q_{DG,k}^{min} \leq Q_{DG,k} \leq Q_{DG,k}^{max} \qquad (6.6d)$$

6.2.3 Impact of number of DSTATCOMs placement in 33-bus, 69-bus and 118-bus distribution networks

The effect of DSTATCOM allocation in RDN on APL and TACS is investigated by increasing the number of DSTATCOM. From Fig. 6.1 (a) and 6.1 (b), it can be observed that for both 33 and 69-bus, although the network APL reduce when the number of DSTATCOMs are increased from 1 to 5, but yearly cost savings are maximum at $ 17291.85 and 21429.78, for 33-bus and 69-bus, respectively with two DSTATCOMs in both the RDNs. Hence, only two DSTATCOMs are considered in both 33 and 69-bus.

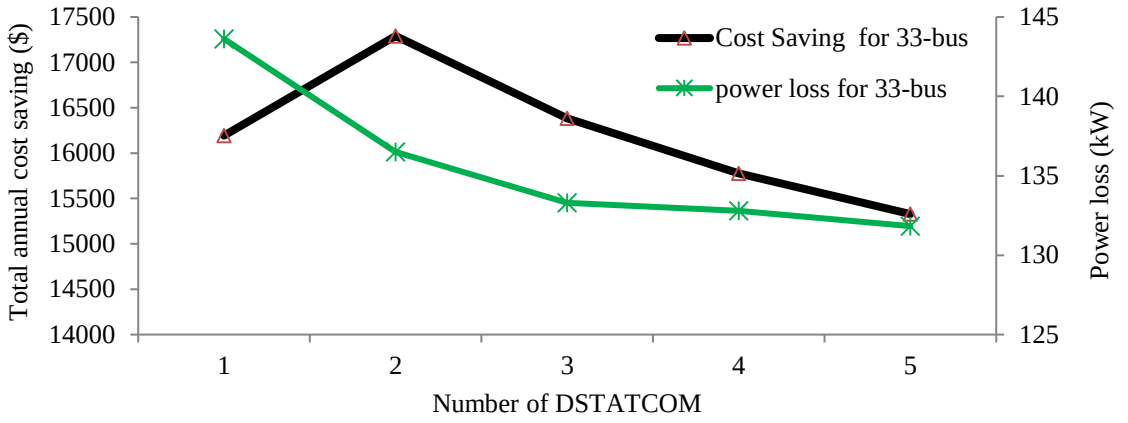

Fig. 6.1 (a): Impact of number of DSTATCOMs on APL and TACS for 33-bus

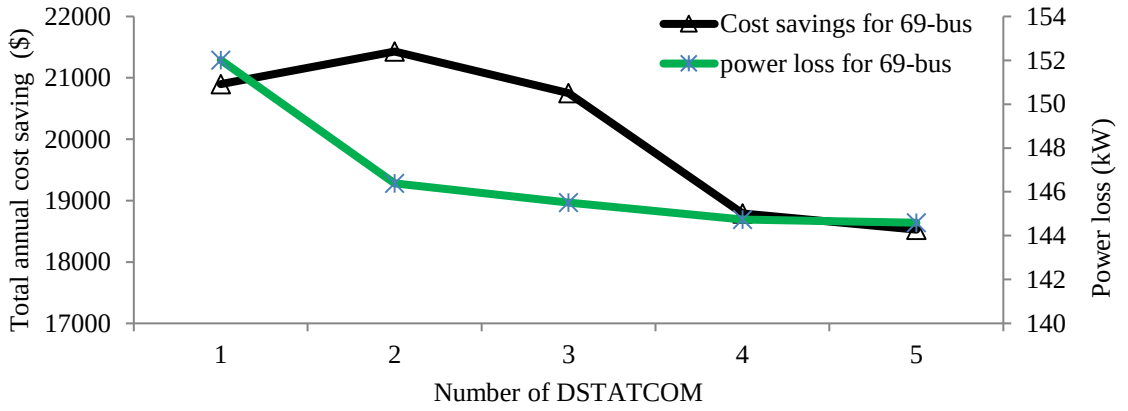

Fig. 6.1 (b): Impact of number of DSTATCOMs on APL and TACS in 69-bus

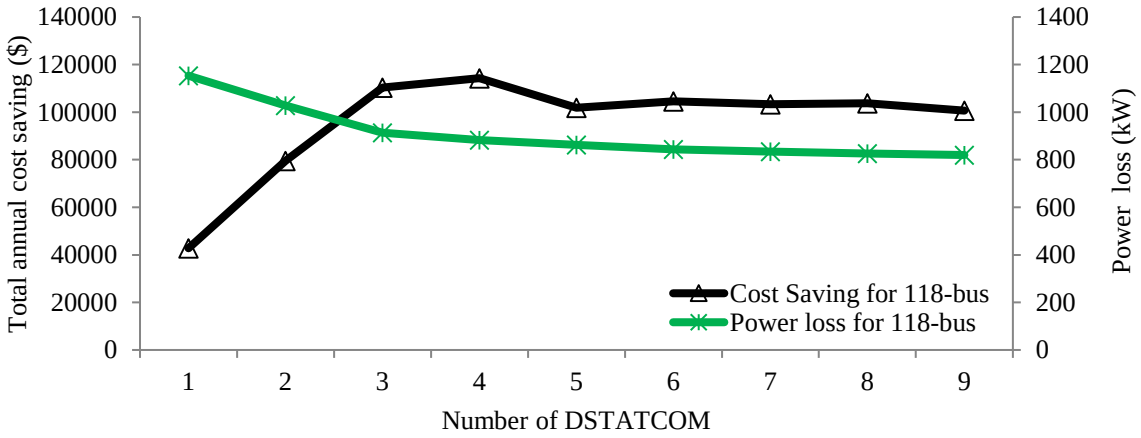

Fig. 6.1 (c): Impact of number of DSTATCOMs on APL and TACS in 118-bus

Fig. 6.1 (c) shows that APL reduces with increase in the number of DSTATCOMs from 1 to 9 in the 118-bus. But it is observed that TACS is maximum at $ 114300.64 with four DSTATCOMs in the 118-bus. So, four DSTATCOMs are considered for placement in the 118-bus.

6.2.4 Case studies and results

The proposed method is primarily used to optimally allocate the single DSTATCOM in 33-bus, 69-bus, and 118-bus to illustrate the computational procedure involve in to finding optimum location and size of DSTATCOM under peak load condition. Thereafter, annual ES and TACS is computed. Subsequently, the proposed method is used for multiple DSTATCOMs placement optimally in the 33-bus, 69-bus, and 118-bus. At first, the optimal number of DSTATCOMs is selected based on maximum TACS for 33-bus, 69-bus, and 118-bus. Subsequently, multiple DSTATCOM are placed by considering optimal number of DSTATCOM for RDNs under consideration.

6.2.4.1 33-bus RDN

The proposed analytical method is first implemented for optimal allocation of DSTATCOMs in the 33-bus RDN. The detailed network data is given in Table A.1 and chapter 3. DSTATCOM size at each bus is calculated using Eqn. (6.4) and APL is calculated in the network after placing the DSTATCOM of the computed size at the respective bus using Eqn. (6.3d)), as shown in Fig. 6.2 (a). It is observed from Fig. 6.2 (a) that optimal location is bus 30 and size is 1226.72 kVAr of DSTATCOM. The APL is minimum at 143.62 kW in the network. It is observed from Fig. 6.2 (b) that DSTATCOM placement to meet the reactive power demand of the load locally results

in reversal of reactive power flow in several lines in the network. This local reactive power management enhances the active power flow capability of the distribution network. Fig. 6.2 (c) and 6.2 (d) shows that magnitudes of the branch currents change marginally but their phase angles change markedly with reactive power compensation in the network. From Fig. 6.2 (e), it is observed that the minimum voltage in the network without DSTATCOM is 0.9131 p.u at bus 18, which improves to 0.9254 p.u. after placement of one DSTATCOM. Placement of two DSTATCOMs of sizes 336 kVAr (at bus 13) and 1226.72 kVAr (at bus 30) results in APL of 136.51 kW and a minimum voltage of 0.93693 p.u. (at bus 18) in the network.

After placing DSTATCOM of optimal size in the network at the optimal location, the reactive power injected by the DSTATCOM for actual loading of the line for a day is shown in Fig. 6.2 (f). The 24-hour variation of the load has already been shown in Fig. 3.4 in Chapter 3. Fig. 6.2 (g) shows the APL of the network without and with DSTATCOM for the 24-hour period. The yearly energy losses and TACS of the network are calculated using Eqns. (3.13) and (3.22a) – (3.22d) corresponding to the parameters provided in annexure Table A.4 It is observed from Table 6.1 that the cost savings is $ 16194.476 and $ 17291.8592, corresponding to DSTATCOMs 1 and 2, respectively. Fig. 6.2 (e) depicts the voltage profile without any DSTATCOM in the distribution network. It is observed from Tables 6.2 and 6.3 that all the indices undergo improvement except the TACS, with placement of two DSTATCOMs resulting in a maximum cost saving of $ 17291.8592. Hence, optimal number of DSTATCOMs must be selected. Allocation of two DSTATCOMs result in 373.393 tons of emission savings yearly. From Tables 6.2 and 6.3, it is observed that QLI improves by 1.55 %, VDI increases by 5.61 % while VSI reduces to 0.0547 p.u., APLR and RPLR are 32.645 % and 32.448 %, respectively. The minimum network voltage is 0.9369p.u. corresponding

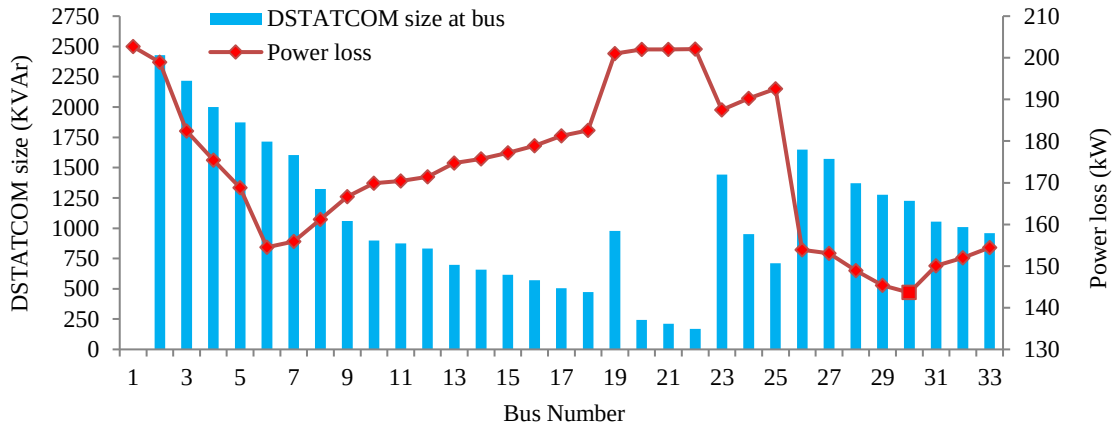

Fig. 6.2 (a): The optimal size at each bus and APL with DSTATCOM in 33-bus

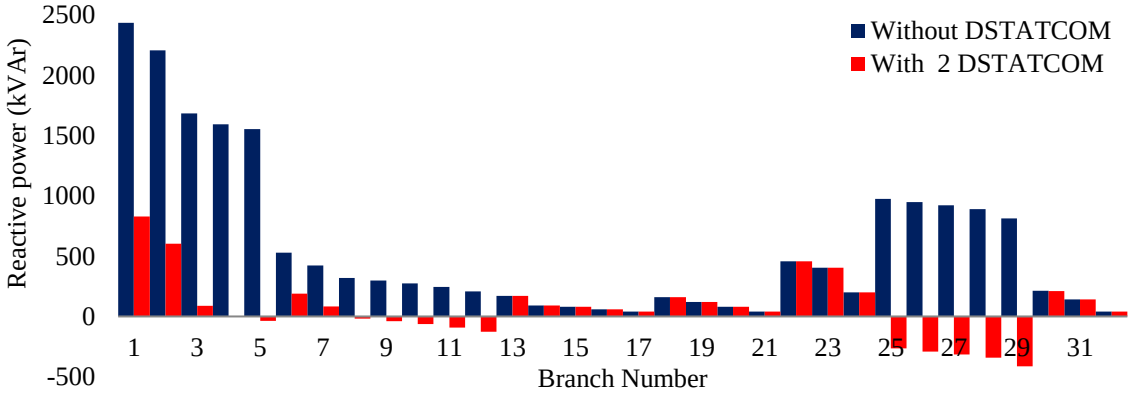

Fig. 6.2 (b): Reactive power flow in each line without and with DSTATCOMs for 33-bus

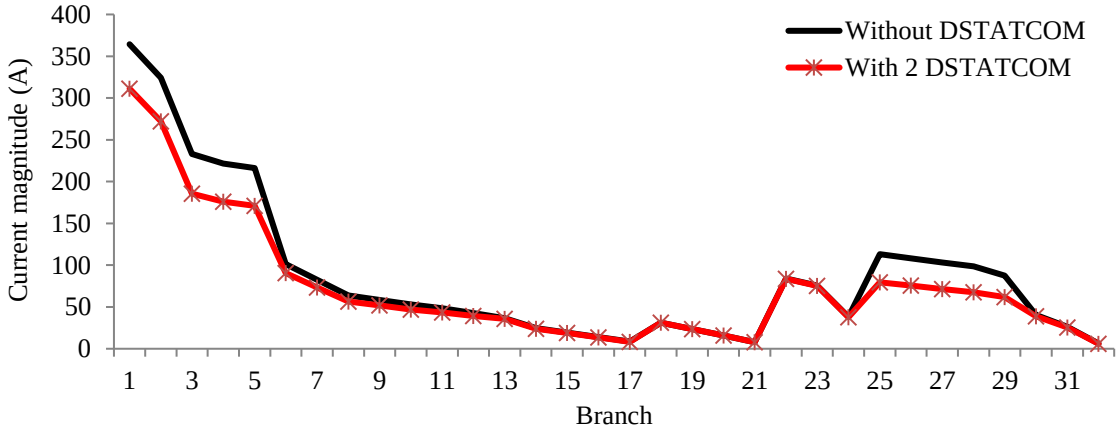

Fig. 6.2 (c): Branch current magnitude in each line without and with DSTATCOMs in 33-bus

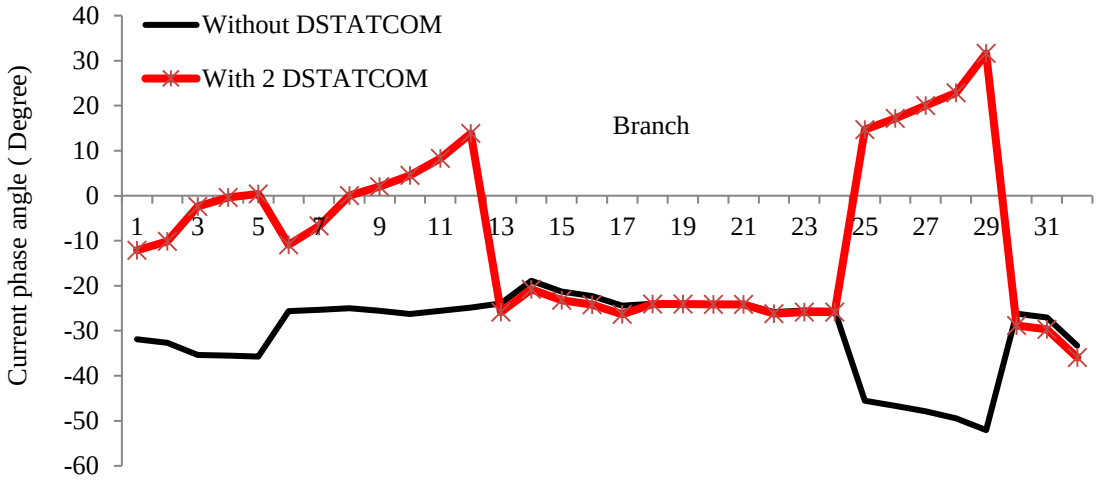

Fig. 6.2 (d): Branch current phase angle without and with DSTATCOMs in 33-bus

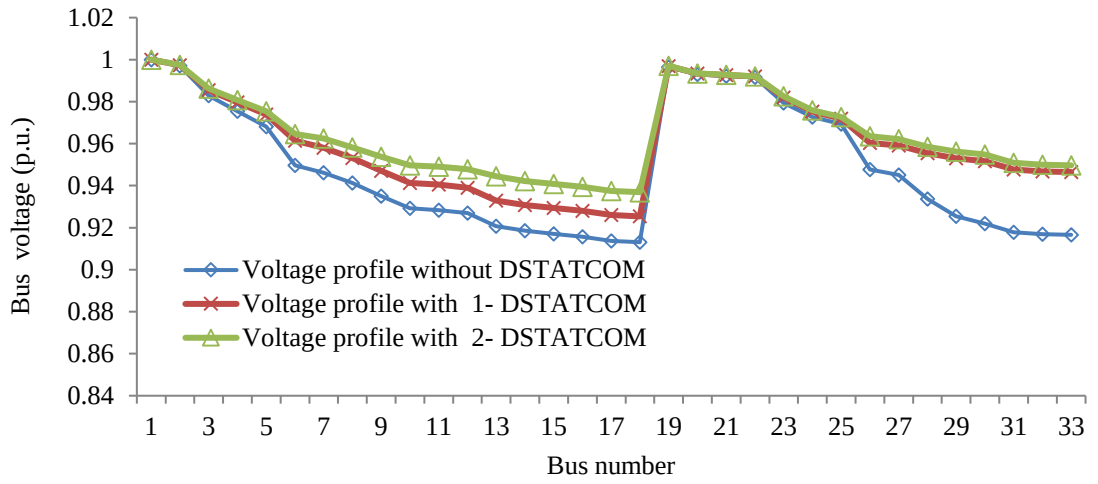

Fig. 6.2 (e): Voltage profile of network without and with DSTATCOMs in 33-bus

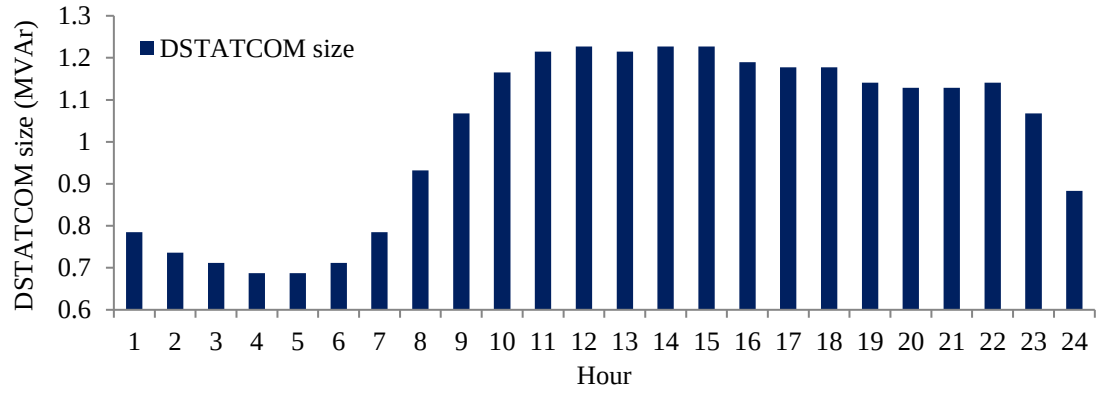

Fig. 6.2 (f): Hourly reactive power injected by the optimally placed DSTATCOM in 33-bus

to bus 18. It is observed from Table 6.7 that the proposed method results in 130 % increase in the TACS. On the other hand, the computational time is only 1.38 second instead of 21.22 second, in comparison to the IA [100] with allocation of only 1 DSTATCOM. However, allocation of 2 DSTATCOMs in the network results in 8.97 % increase in the TACS, with a computational time of only 1.49 second against 11.06 second for bat algorithm (BA) [164].

6.2.4.2 69-bus RDN

The proposed analytical approach is now implemented on the 69-bus for optimal allocation of DSTATCOMs. The detailed network data is given in appendix Table A.2 and chapter 3. The DSTATCOM size at each bus is calculated using Eqn. (6.4) and the network APL is calculated after placing this DSTATCOM at the respective bus using Eqn. (6.1). Fig. 6.3 (a) shows the DSTATCOM size and the network APL. It is observed from Fig. 6.3 (a) that optimal location and size of the DSTATCOM is at bus 61 and 1298 kVAr, respectively. The network APL is minimum at 152.01 kW. It is observed from Fig.6.3 (b) that placement of DSTATCOM in the network helps to meet the reactive power demand of the load locally and results in reversal of reactive power flows in several lines in the network. This local reactive power management enhances the active power flow capability of the distribution network. Fig. 6.3(c) and 6.3 (d) shows that the magnitude of branch currents change marginally while their phase angles change markedly with reactive power compensation in the network. From Fig. 6.3 (e), the minimum voltage magnitude in the network without DSTATCOM is 0.9092 p.u at bus 65, while after the placement of one DSTATCOM, the minimum network voltage is 0.9302 p.u (at bus 65). Placement of two DSTATCOMs of sizes 349.45 kVAr at bus 17 and 1291.80 kVAr at bus 61 results in network APL of 136.51 kW. The minimum

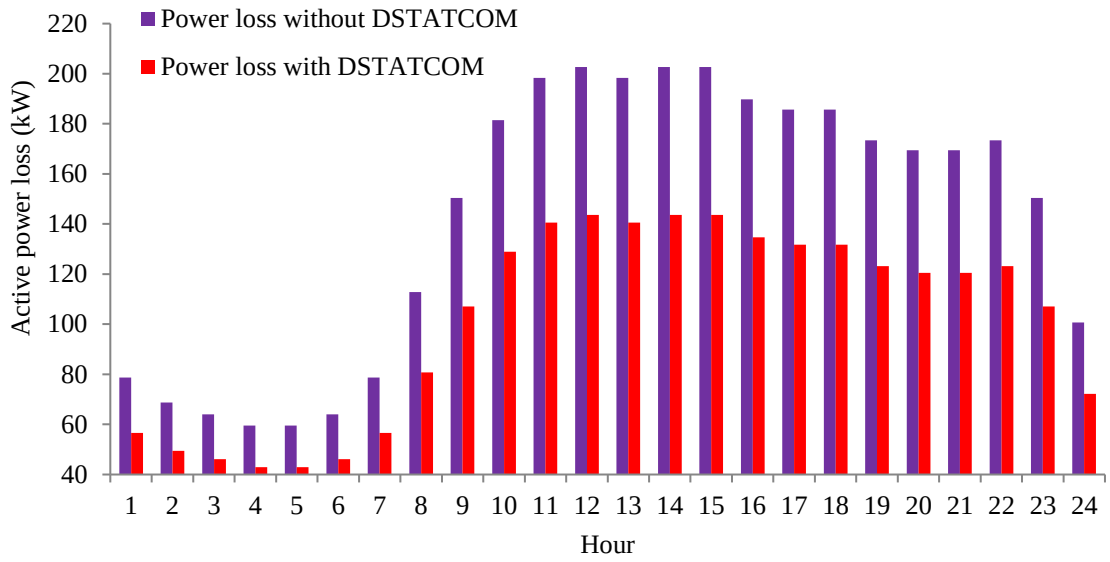

Fig. 6.2 (g): Hourly APL in the network without and with DSTATCOMs in 33-bus

Table 6.1: Results using analytical method in 33-bus

		Number of DSTATCOM		
	Base case	1	2	3
Size (Location) kVAr (Bus No.)		1226.7215 (30)	336.0017 (13) 1226.7215 (30)	336.0017 (13) 474.3026 (24) 1226.7215 (30)
APL (kW)	202.677	143.6255	136.5114	133.2929
RPC (kVAr)	135.140	96.3025	91.2947	89.2414
EL (kWh)	1248443.0528	888619.1100	845701.1946	826079.5294
TAC ($)	74906.5831	53317.1466	50742.0716	49564.7717
Dcost ($)	-	5394.9605	6872.6521	8958.5732
TACS ($)	-	16194.4760	17291.8592	16383.2381
Emission (Ton)	26175.015	25841.412	25801.6215	25783.4297

Table 6.2: Results of performance indices with DSTATCOM for 33-bus

		Number of DSTATCOM		
	Base case	1	2	3
ES (Ton)	-	333.6030	373.3930	391.5850
QLI (p.u.)	3.5311	3.5732	3.5861	3.5911
VSI (p.u.)	0.6951	0.7247	0.7341	0.7682
VDI (p.u.)	0.1171	0.0709	0.0547	0.0522
TBVVB	0	0	0	0
APLR	-	29.135	32.645	34.2337
RPCR	-	28.739	32.448	33.9641
Vmin (Bus)	0.9131 (18)	0.9254 (18)	0.9369 (18)	0.9378 (18)
CT (Second)	-	1.2544	1.3003	1.3361

voltage magnitude in the network is 0.9313 p.u (at bus 65).

After optimally allocating the DSTATCOM in the network, the reactive power injected by the DSTATCOM is shown in Fig. 6.3 (f) corresponding to the actual loading of the line for a day (shown in Fig. 3.4). Fig.6.3 (g) shows the APL of the network without and with the DSTATCOM. Energy losses and TACS of the network is calculated using Eqns. (3.13) and (3.22a - 3.22d) corresponding to the data provided in appendix Table A.4. It is observed from Table 6.3 that the cost savings are $ 20899.31 and 21429.78 for 1 and 2 DSTATCOMs, respectively. Fig. 6.3 (e) depicts the voltage profile without and with DSTATCOM placed optimally in the distribution network. It is observed from Table 6.3 and 6.4 that all the indices undergo improvement except the TACS, with placement of two DSTATCOMs resulting in a maximum cost savings of $ 21429.7825. So optimal number of DSTATCOMs must be selected. Optimal allocation of 2 DSTATCOMs result in 442.6704 tons of emission savings yearly. It is observed that QLI has 1.21 % improvement, VDI increases by 10.21 %, VSI reduces to 0.0572 p.u.,

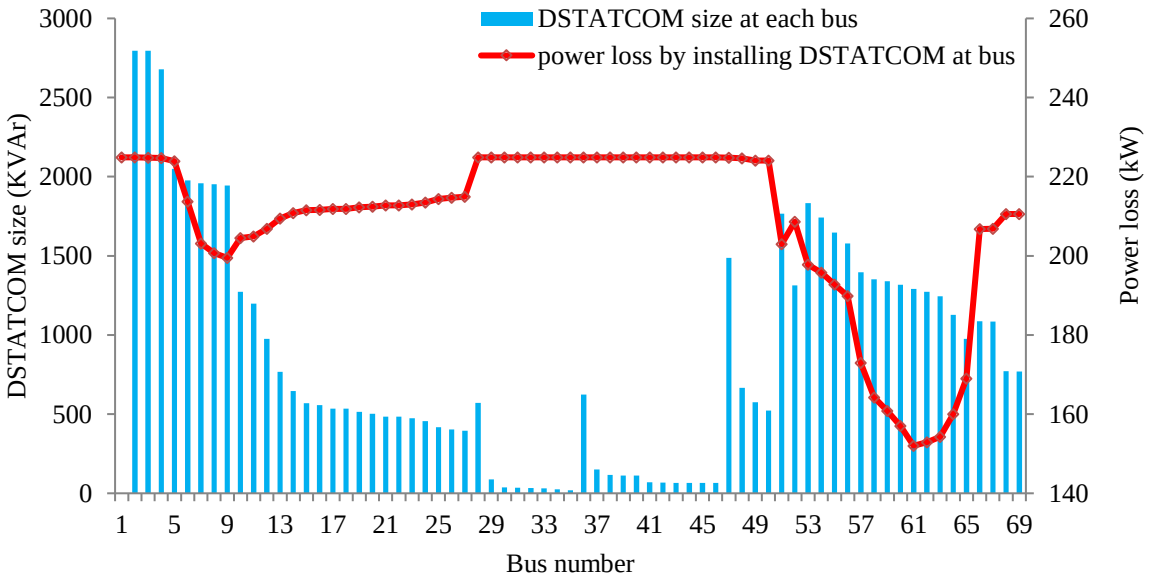

Fig. 6.3 (a): The optimal size at each bus and APL with DSTATCOM in 69-bus

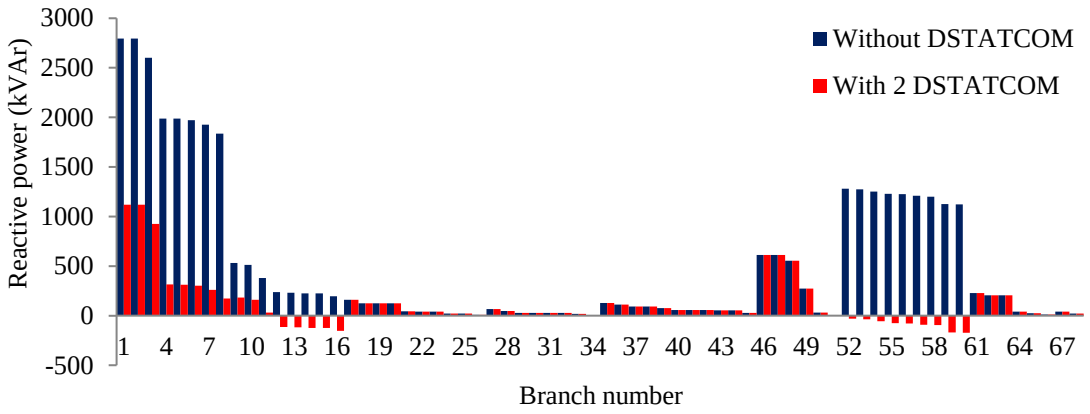

Fig. 6.3 (b): Reactive power flow in each line without and with 2 DSTATCOMs in 69-bus

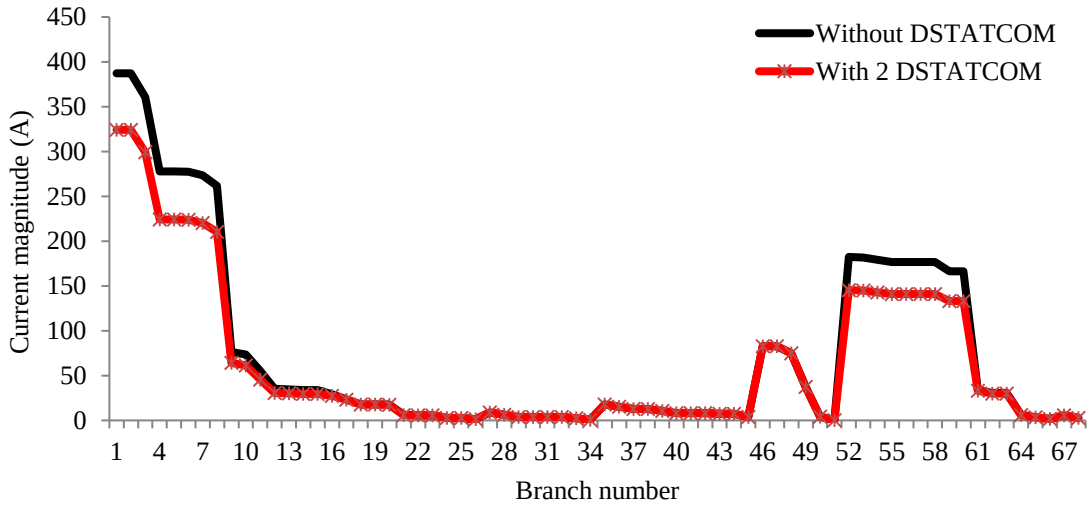

Fig. 6.3 (c): Branch current magnitude without and with DSTATCOMs in 69-bus

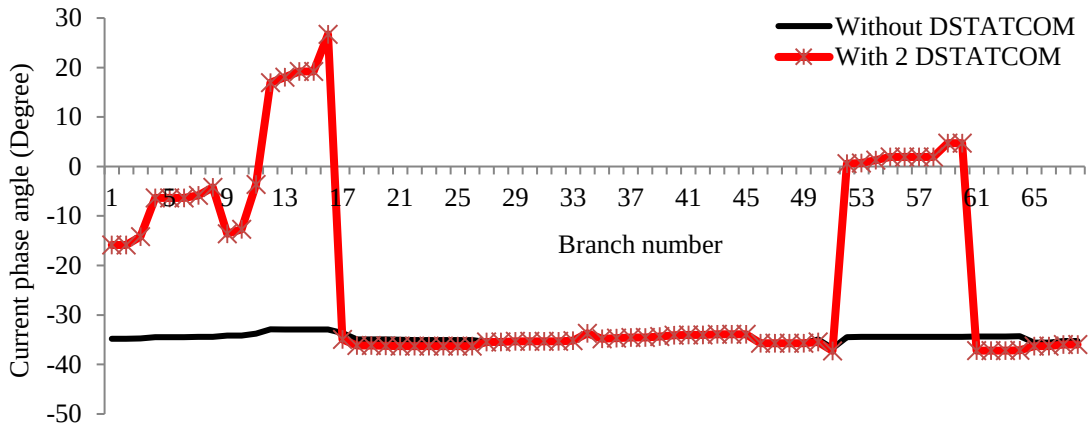

Fig. 6.3 (d): Branch current phase angle without and with 2- DSTATCOMs in 69-bus

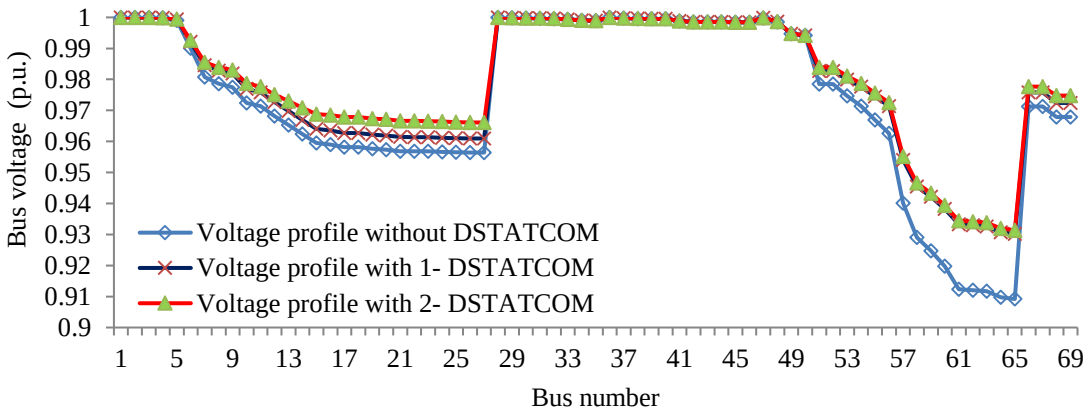

Fig. 6.3 (e): Voltage profile of network without and with DSTATCOM in 69-bus

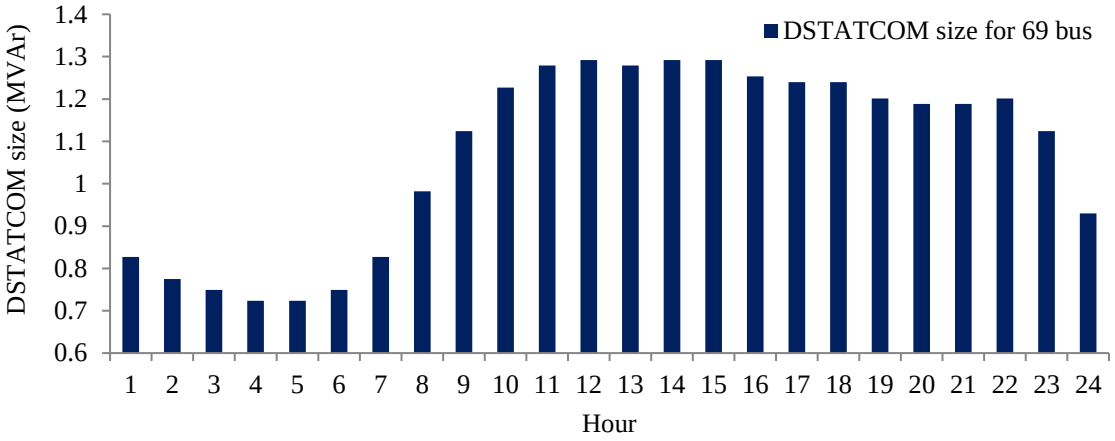

Fig. 6.3 (f): Hourly reactive power supplied by the optimally placed DSTATCOM for 69-bus

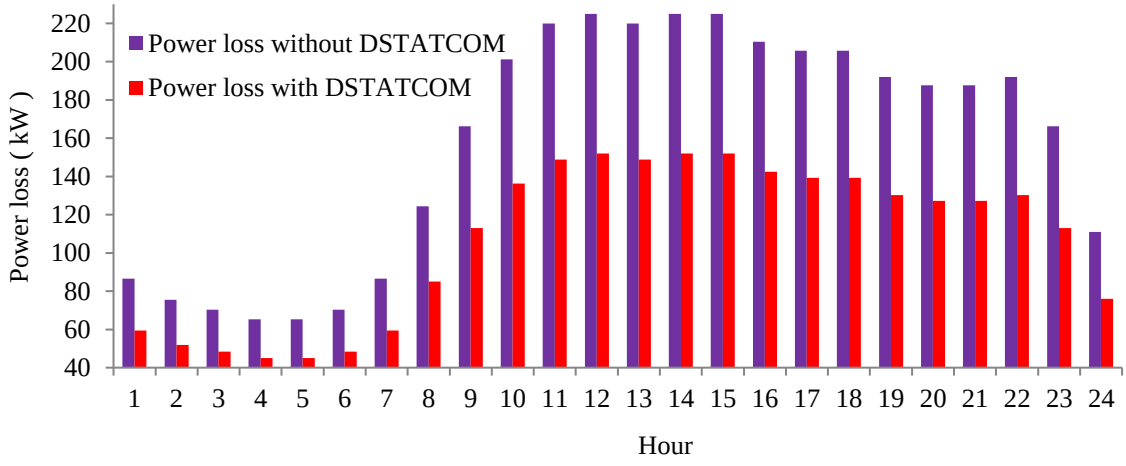

Fig. 6.3 (g): Hourly APL in the network without and with DSTATCOM in 69-bus

Table 6.3: Results using analytical method in 69-bus

		Number of DSTATCOM			
	Base case	1	2	3	4
Size (Location)		1291.8064 (61)	349.4544 (17)	225.3594 (11)	225.3594 (11)
kVAr (Bus No.)			1291.8064 (61)	349.4544 (17)	349.4544 (17)
				1291.8064 (61)	511.8633 (50)
					1291.8064 (61)
APL (kW)	224.8974	152.0148	146.3932	145.5146	144.7323
RPC (kVAr)	102.115	70.528	68.2145	67.7996	65.8979
EL (kWh)	1381327.9423	938319.3798	903864.0621	898654.8759	893773.7625
TAC ($)	82879.6765	56299.1627	54231.8437	53919.2925	53626.4257
Dcost ($)	-	5681.1954	7218.0503	8209.1513	10460.2594
TACS ($)	-	20899.3183	21429.7825	20751.2325	18792.9913
Emission (ton)	26879.983	26469.258	26437.313	26432.4838	26427.9583

Table 6.4: Results of performance indices with DSTATCOM (s) in 69-bus

		Number of DSTATCOM			
	Base case	1	2	3	4
ES (Ton)	-	410.7259	442.6704	447.5000	452.0254
QLI (p.u.)	3.6184	3.6575	3.6624	3.6647	3.6674
VSI (p.u.)	0.6833	0.6913	0.7531	0.7539	0.7549
VDI (p.u.)	0.0992	0.0648	0.05718	0.0546	0.0545
TBVVB	0	0	0	0	0
APLR (%)	-	32.406	34.9058	35.2965	35.6444
RPCR (%)	-	30.933	33.1987	33.6049	35.4672
Vmin (Bus)	0.9092 (65)	0.9302 (65)	0.9314 (65)	0.9321 (65)	0.9321 (65)
CT (Second)	-	1.4080	1.8602	2.3296	2.8352

while the APLR and RPCR are 34.90 and 33.198 %, respectively. It is observed from Table 6.8 that the proposed method results in 22.64 % more yearly cost savings while the computational time is only 1.41 second instead of 32.30 second for the IA [100] with allocation of 1 DSTATCOM. However, allocation of 2 DSTATCOMs in the network results in 9.23 % more yearly cost savings while the computational time is only 1.86 second instead of 12.83 second, in comparison to BA [165].

6.2.4.3 118-bus RDN

The proposed analytical approach is now implemented on the 118-bus for optimal

allocation of DSTATCOMs. The detailed network data is given in appendix Table A.3 and chapter 3**.** Four DSTATCOMs are considered for optimal sizing and placement in this network for maximum economic benefits. The DSTATCOM size at each bus is calculated using Eqn. (6.4) and the network APL is calculated after placing the DSTATCOM of the estimated size at the respective bus using Eqn. (6.1). The optimal location and size for a single DSTATCOM in the 118-bus is found to be 2293.73 kVAr at bus 115 while the network APL is 1153.34 kW. Proceeding in a similar way, multiple DSTATCOM locations and their corresponding sizes are shown in Table 6.5. It is observed from Table 6.5 that the network APL reduces i.e. 1298.09 kW (base case) to 882.7042 kW and the yearly cost savings increases to $ 114300.6412 with optimal allocation of 4 DSTATCOMs. However, beyond 4 DSTATCOMs, the network APL reduces but the yearly cost savings decreases. TACS of the network is calculated using Eqns. (3.13) and (3.22a - 3.22d) with the data provided in Appendix Table A.4 It is observed from Tables 6.5 and 6.6 that all the indices undergo improvement except the TACS, with placement of four DSTATCOMs resulting in maximum cost savings of $ 114300.6412. Hence, only four DSTATCOMs are considered for maximum economic benefits. Optimal allocation of 4 DSTATCOMs result in 2332.6237 tons of yearly emission savings. QLI has 3.02 % improvement, VDI increases by 18.34 % and VSI reduces to 0.1826 p.u. from 0.3576 p.u. The APLR and RPCR are 31.99 and 32.92 % respectively. It is observed from Fig.6.4 (a) that placement of DSTATCOMs in the network helps to meet the reactive power demand locally and results in the reversal of reactive power flows in several lines in the network. This local reactive power management enhances the active power flow capability of the distribution network. Fig. 6.4 (b) depicts the voltage profile without and with the allocation of DSTATCOMs in the network. Figs. 6.4(c) and 6.4 (d) show that the magnitudes of the branch currents

Table 6.5: Results using analytical method in 118-bus

		Number of DSTATCOM				
	Base case	1	2	3	4	5
Size (Location) kVAr (Bus No.)		2293.7979 (111)	1835.6452 (72) 2293.7979 (111)	2524.7477 (51) 1835.6452 (72) 2293.7979(111)	2524.7477 (51) 1835.6452 (72) 1681.0505 (81) 2293.7979(111)	4470.0866 (30) 2524.7477 (51) 1835.6452 (72) 1681.0505 (81) 2293.7979(111)
APL (kW)	1298.0918	1153.3395	1028.2326	913.6555	882.7042	862.9468
RPC (kVAr)	978.7359	900.6988	810.1418	686.8598	656.5030	643.7548
EL (kWh)	7968512.951	7087658.443	6340048.560	5641253.4511	5452547.2847	5331279.9330
TAC ($)	478110.777	425259.5065	380402.9136	338475.2070	327152.8370	319876.7959
Dcost ($)	-	10087.8224	18160.7494	29264.2589	36657.2987	56316.1533
TACS ($)	-	42763.4479	79547.1140	110371.3110	114300.6412	101917.8277
Emission (ton)	160319.600	159502.935	158809.8046	158161.9317	157986.9768	157874.5464

Table 6.6: Results of performance indices with DSTATCOM for 118-bus

	Number of DSTATCOM					
	Base case	1	2	3	4	5
ES (Ton)	-	816.6654	1509.7959	2157.668	2332.6237	2445.0541
QLI (p.u.)	21.2161	21.5953	21.699	21.8156	21.8583	21.8843
VSI (p.u.)	0.5697	0.5697	0.6627	0.6628	0.6742	0.6742
VDI (p.u.)	0.3576	0.3267	0.2530	0.2017	0.1826	0.1752
TBVVB	8	8	0	0	0	0
APLR	-	11.1511	20.7889	29.6155	31.999	33.5218
RPCR	-	7.9732	17.2256	29.82174	32.9238	34.2259
Vmin (Bus)	0.8687 (78)	0.8687 (78)	0.9022 (78)	0.9022 (78)	0.9061 (78)	0.9061 (78)
CT (Second)	-	3.4099	5.6983	7.9842	10.2021	12.3937

Table 6.7: Comparative results using analytical method for 33-bus

		IA [100]	Analytical method	BA [165]	Analytical method
No. of DSTATCOM	Base case	1	1	2	2
Size (Location) kVAr (Bus No.)	-	962.49 (12)	1226.72 (30)	600 (10) 1200 (30)	336.00 (13) 1226.72 (30)
Total DSTATCOM size (kVAr)	-	962.49	1226.72	1800	1562.72
APL (kW)	202.677	143.96	143.62	137.50	136.51
EL (kWh)	1248443.0528	1060621.54	888619.11	852028.45	845701.19
TAC ($)	74906.5831	63637.29	53317.14	51121.70	50742.07
Dcost ($)	-	4232.90	5394.96	7916.16	6872.65
TACS ($)	-	7036.38	16194.47	15868.71	17291.85
CT (Second)	-	21.22	1.38	11.06	1.49

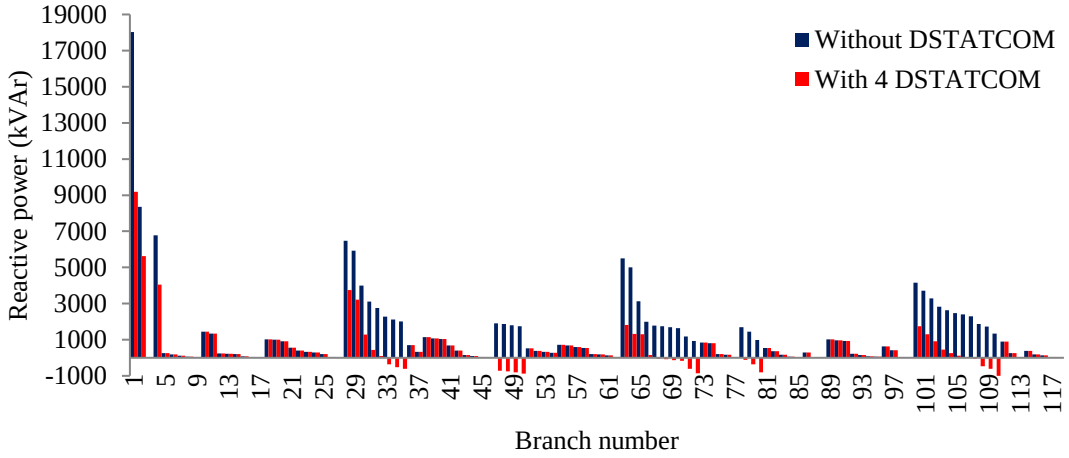

Fig. 6.4 (a): Reactive power flow in each line without and with 4 DSTATCOMs in 118-bus

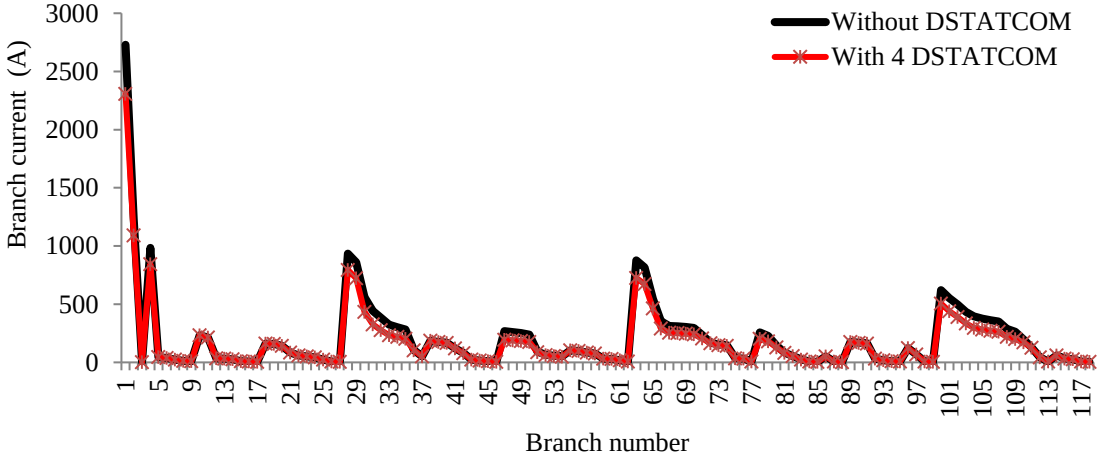

Fig. 6.4 (b): Branch current magnitude without and with 4- DSTATCOMs in 118-bus

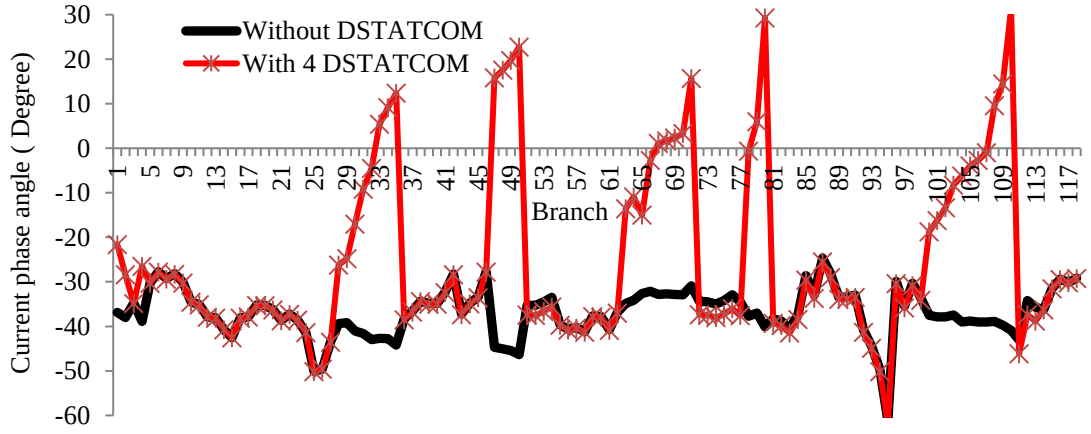

Fig. 6.4 (c): Branch current phase angle without and with 4 DSTATCOMs in 118-bus

Table 6.8: Comparative results using analytical method for 69-bus

		IA [100]	Analytical method	BA [165]	Analytical method
No. of DSTATCOM	Base case	1	1	2	2
Size (Location) kVAr (Bus No.)		1702.42 (61)	1291.81 (61)	480 (15) 1430 (61)	349.45 (17) 1291.81 (61)
Total DSTATCOM Size (kVAr)		1702.42	1291.81	1910	1641.26
APL (kW)	224.89	157.50	152.01	148.07	146.39
EL (kWh)	1381327.94	972395.33	938319.37	914371.81	903864.06
TAC ($)	82879.67	58343.71	56299.16	54862.30	54231.84
Dcost ($)	-	7495.81	5681.19	8399.92	7218.05
TACS ($)	-	17040.14	20899.31	19617.4	21429.78
CT (Second)	-	32.30	1.41	12.83	1.86

change marginally but the phase angles of the branch currents change markedly with reactive power compensation in the network. The minimum network bus voltage magnitude is 0.9061 p.u at bus 78.

6.3 CTLBO ALGORITHM BASED OPTIMAL ALLOCATION OF DSTATCOM(s)

CTLBO [113] is a meta-heuristic algorithm and comprises of two stages i.e. *teaching phase and learning phase.* In '*teaching phase',* the best learner i.e. teacher, transfers his knowledge to the other remaining learners to enhance their knowledge. Subsequently, in the '*learning phase',* each learner interacts with other fellow learners to further improve his/her own knowledge. These two stages are repeated till the CTLBO proceeds towards the global best knowledge (global solution). The detail of the CTLBO algorithm has been explained in chapter 4.

6.3.1 Objective function formulation

The efficiency of reactive power management in RDN can be increased drastically by network reconfiguration and optimal allocation of DSTATCOMs.

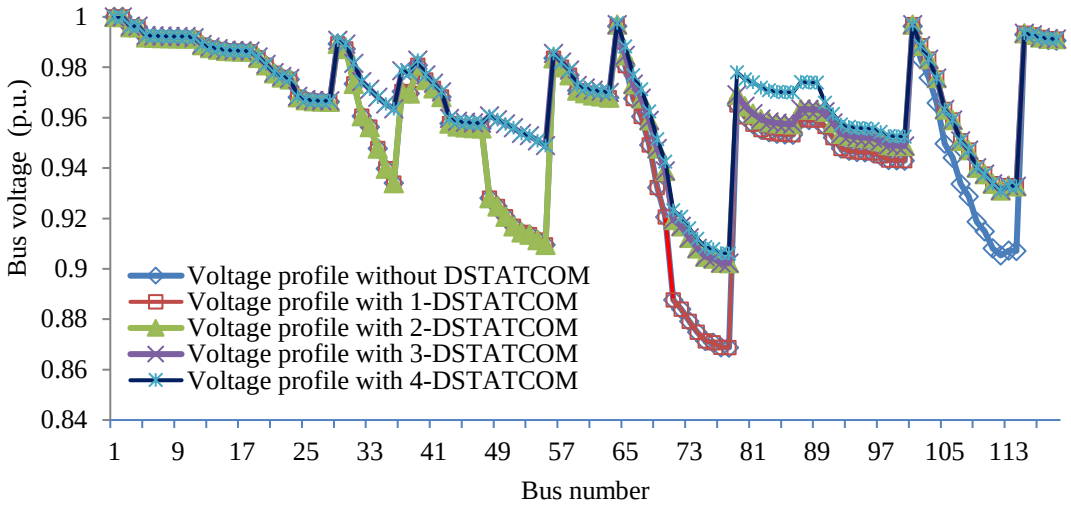

Fig. 6.4 (d): Voltage profile of 118-bus network without and with DSTATCOMs

The considered assumptions are given below:

a. All the RDN are balanced.

b. Load shedding and line interruptions are not considered.

c. Average 24-hour daily load pattern is taken into account for computing yearly energy losses, costs and emission savings.

d. DSTATCOMs are considered for injecting reactive power only.

e. Protection issues due to placement of DSTATCOMs are not considered.

6.3.1.1 Single objective function

The allocation of DSTATCOMs in RDN is to reduce the network APL, enhance the TACS and ES while satisfying all working constraints. Descriptions of these SOFs are given below:

6.3.1.1.1 Active power loss

The APL reduction of the DNs is of primary concern while allocating DSTATCOMs in RDN. Various formulations [35, 121, 141, 142, 143, 145] for power flow studies of

RDN exist in the literature. The APL can be calculated using Eqn. (3.12a). So, SOF F_1 to minimize APL is given as,

$$\mathrm{F_1} = \text{Minimize (APL)} \tag{6.7}$$

6.3.1.1.2 Total annual cost saving

Cost of investment can be calculated from the cost of DSTATCOM as detailed in Eqn. (3.22a-3.22d) of chapter 3. Therefore, SOF F_2 to maximize TACS is given as,

$$\mathrm{F_2} = \text{Maximization (TACS)} \tag{6.8}$$

6.3.1.2 Multi-objective function

A MOF consider entire SOFs at the same time, put through the inequality and the equality constraints. This chapter formulated a MOF based on two SOFs, which simultaneously reduces the APL (F_1) and improves the TACS (F_2) using weighted sum approach as detailed in chapter 4. Mathematically the MOF is shown below,

$$\mathrm{MOF} = \text{Minimize}\left[\left(\mathrm{a_1} * \frac{\mathrm{P_{loss}^{DG}}}{\mathrm{P_{loss}}}\right) + \left\{\mathrm{a_2} * 1/\left(\frac{\mathrm{TACS}}{\mathrm{TAC}}\right)\right\} + \sum_{\mathrm{k=1}}^{\mathrm{n}}\{(|\mathrm{V}|_k - \mathrm{V_{min}})^2 - (|\mathrm{V}|_k - \mathrm{V_{max}})^2\}\right] \tag{6.9}$$

Eqn. (6.9) results in single value of the MOF. However, to achieve multiple operating point in the network the a_i is increased or decreased in steps of 0.05 [i.e. a_1 and a_2 are (1, 0), (0.95, 0.05), (0.90, 0.10) to (0, 1) respectively] in such a way that sum of all the weight coefficient remain unity, is mathematically expressed as Eqn. (6.10),

$$\mathrm{a_i} \epsilon ([0,1]) \text{ and } \sum_{\mathrm{i=1}}^{\mathrm{ob}} \mathrm{a_i} = 1\,. \tag{6.10}$$

Therefore, changing weight coefficient in steps will give multiple operating point (Pareto solution) of the network. Since emission saving (ES) depends only on the network losses, So, ES is directly calculated using Eqn. (3.23a to 3.23c) instead of considering as separated SOF but Pareto solution as shown in Fig. 6.6(a) to 6.6(e) and Fig. 6.8 (a) to 6.8 (d), is depicting all the three SOFs i.e. APL, TACS and ES.

6.3.2 Constraints

The following constraints are taken into consideration while DSTATCOMs allocation in the RDN as detailed in Eqn. (6.6a to 6.6d).

6.3.3 Radiality of distribution network

Reconfiguration is the process to open/close the tie or isolation switches in such a way to maintain the radiality of the distribution network. In this chapter, the incidence matrix (A) is formed and its determinant ensures the radiality of DN as shown below.

$$\det(A) = 1 \; or \; -1 \; (radial \; system) \qquad or$$

$$\det(A) = 0 \; (\; not \; radial \; system) \tag{6.11}$$

6.3.4 Annual energy and cost savings of SOFs for varying loads

This section deals with a computational procedure to utilize DSTATCOM units in the distribution network for minimizing the EL and maximizing the TACS. At first the DSTATCOM sizes and locations are calculated for minimizing the APL at the nominal load. The DSTATCOM size ($Q_{DG,k}^{max}$) at k^{th} bus is calculated at nominal load (1 p.u.). The DSTATCOM outputs is calculated as per the load demand curve [111]. Finally, the

EL and TACS are determined based on the DSTATCOM output pattern. The following steps are followed to find out the ES for 24-hour load demand:

Step 1. Compute the optimal capacity and location of a DSTATCOM unit at the peak load level only, using CTLBO algorithm for the SOFs .

Step 2. Compute the optimal output of the DSTATCOM unit at the optimal location at time‘t’ as below, where p.u. Load (t) is the load demand in per unit at time‘t’.

$$Q_{DG,k} = \text{Load}(t) \text{ x } Q_{DG,k}^{max} \tag{6.12}$$

Step 3. Run the power flow algorithm with each DSTATCOM output i.e. $Q_{DG,k}$ obtained in Step 2 and calculate the APL using Eqn. (3.12), EL (E_{loss}^{DG}) using Eqn. (3.13), TACS using Eqn. (3.22a to 3.22d), ES using Eqn. (3.23).

6.3.5 CASE STUDIES AND RESULTS

In this Section, optimal allocation of multiple DSTATCOMs are carried out in the 33-bus and 69-bus. Primarily, the optimum locations and sizes of multiple DSTATCOMs are found out using CTLBO technique, considering peak load. Thereafter annual energy savings, TACS and ES are computed using Eqn. (3.13), (3.22a to 3.22d) and (3.23a to 3.23c), respectively. The optimal number of DSTATCOMs is selected based on the SOFs and MOF considered for the RDN. Two RDN i.e. 33-bus and 69-bus are analyzed to demonstrate the effectiveness of CTLBO technique. The results are compared using the following criteria:

Case 1: Base configuration of the network.

Case 2: Only network reconfiguration.

Case 3: Only DSTATCOM allocation.

Case 4: Allocation of DSTATCOMs after network reconfiguration.

Case 5: Simultaneous network reconfiguration and DSTATCOM allocation.

6.3.5.1 33-bus RDN

The CTLBO algorithm is first implemented for two SOFs in the 33-bus for all five cases. The detailed network specification is given in appendix Table A.1 and chapter 3**.** Table 6.9 shows the results corresponding to the APL minimization in the 33-bus. It is observed from Table 6.9 that the base case power loss in the network is 202.67 kW while all the tie switches are open in the network. Case 2 shows that for APL minimization objective, when switches 7, 9, 14, 32 and 37 are opened while maintaining the network radiality, the RDS has minimum APL of 139.55 kW and 355.74 tons of emission savings in the network. It is also observed that for case 3, when two DSTATCOMs of suitable capacities are placed, the network TACS is maximum at

Table 6.9: Results using CTLBO in 33-bus for APL minimization

	Case 1	Case 2	Case 3	Case 4	Case 5
Open Switch	33 34 35 36 377	9 14 32 37	33 34 35 36 37	7 9 14 32 37	7 9 14 36 37
No. of DSTATCOM	-	-	2	1	1
Size (Location)	-	-	468.86 (12)	1028.34 (30)	1070.23 (30)
kVAr (Bus No.)	-	-	1057.75 (30)		
APL (kW)	202.677	139.553	135.7530	101.818	101.0188
RPC (kVAr)	135.1409	102.3049	90.5464	77.3081	75.3696
EL (kWh)	1248443.0528	864733.1989	840960.3743	632642.3927	627806.5746
TAC ($)	74906.5831	51883.9919	50457.6224	37958.5435	37668.3944
Dcost ($)	-	-	6713.8693	4522.5000	4706.7518
TACS ($)	-	23022.5912	17735.0913	32425.5395	32531.4369
Emission (ton)	26175.015	25819.2666	25797.226	25604.0886	25599.6051
ES (ton)	-	355.7484	377.7888	570.9264	575.4098
QLI (p.u.)	3.5311	3.5841	3.5841	3.6087	3.6103
VSI (p.u.)	0.6951	0.7736	0.7683	0.7894	0.7933
VDI (p.u.)	0.1171	0.0487	0.0561	0.0343	0.0314
TBVVB	0	0	0	0	0
APLR	-	31.1466	33.020	49.7632	50.1577
RPCR	-	24.2649	32.998	42.7944	44.2288
Vmin (Bus)	0.9131 (18)	0.9378 (32)	0.9362 (18)	0.9475 (33)	0.9545 (18)

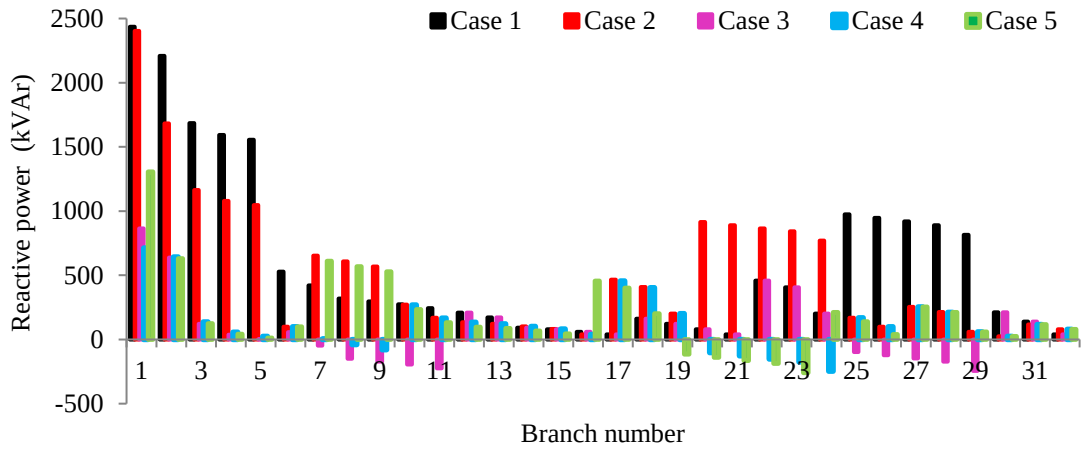

Fig. 6.5 (a): Line reactive power in 33-bus for APL minimization

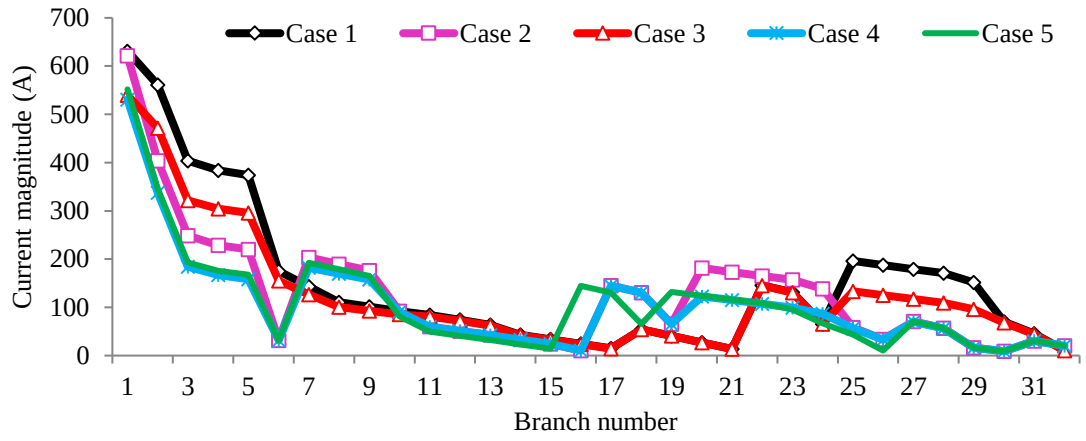

Fig. 6.5 (b): Branch current magnitudes in 33-bus for APL minimization

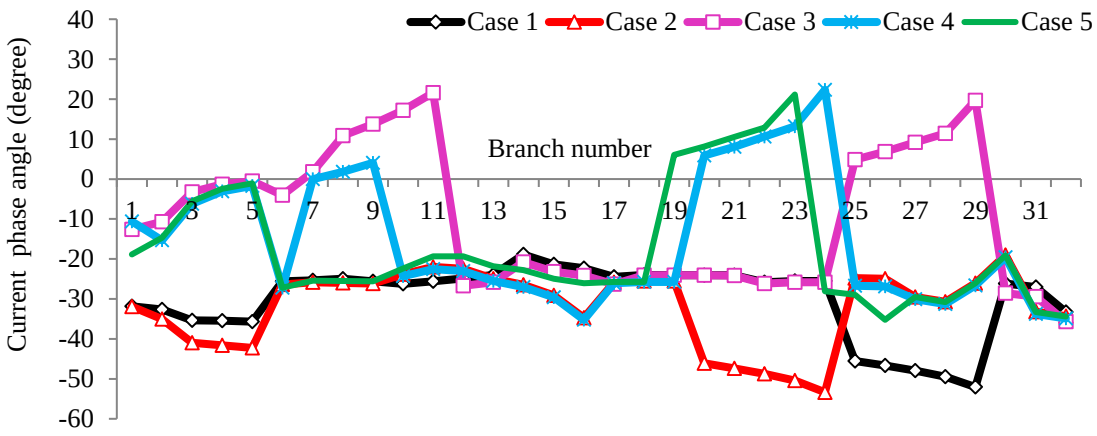

Fig. 6.5 (c): Branch current phase angles in 33-bus for APL minimization

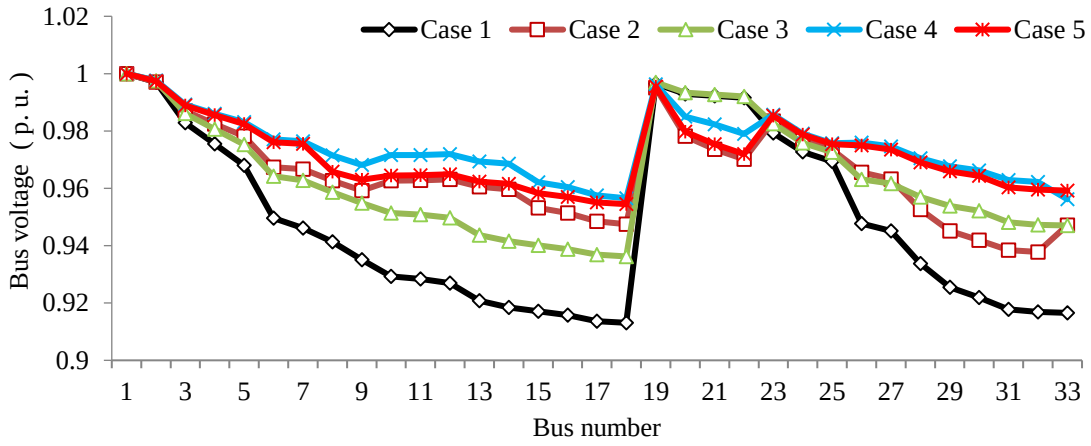

Fig. 6.5 (d): Voltage profile in 33-bus for APL minimization

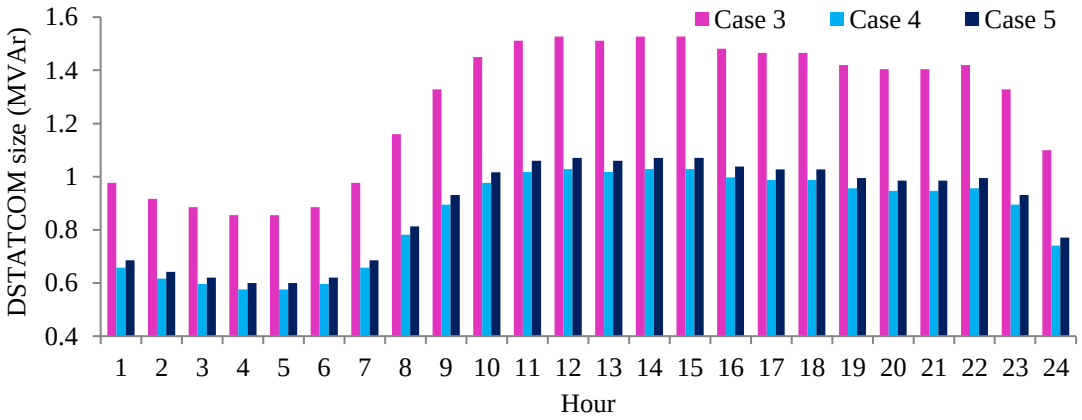

Fig. 6.5 (e): Hourly reactive power supplied by DSTATCOMs in 33-bus for APL minimization

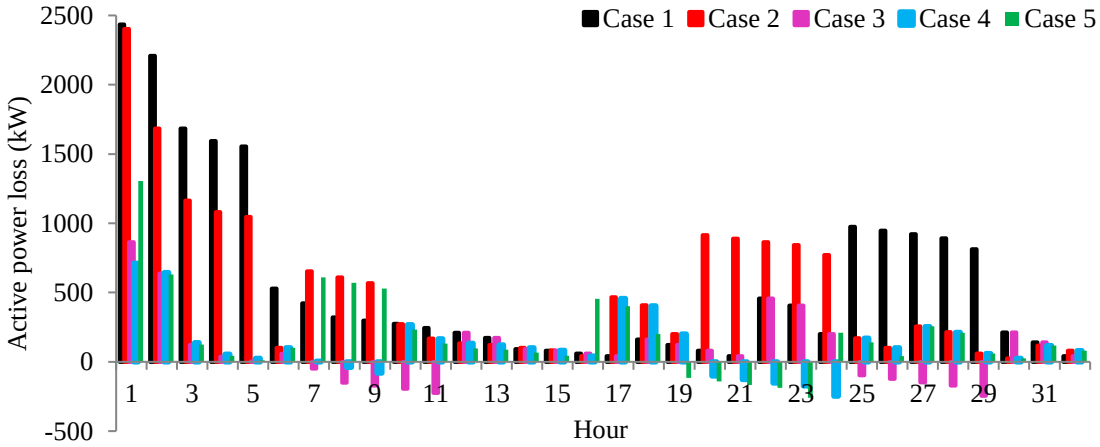

Fig. 6.5 (f): Hourly APL in 33-bus for APL minimization

Table 6.10: Results with DSTATCOMs for TACS maximization in 33-bus

	Case 3				
Open Switch			33 34 35 36 37		
No. of DSTATCOM	1	2	3	4	5
Size (Location)	1082.63 (30)	314.47 (14)	198.95 (8)	198.947 (8)	178.328 (8)
kVAr (Bus No.)		951.21 (30)	254.37 (14)	254.379 (14)	254.380 (14)
			894.02 (30)	699.390 (30)	138.438 (25)
				194.087 (32)	693.006 (30)
					194.088 (32)
APL (kW)	144.63079	137.1904	135.7712	135.3968	133.719
RPC (kVAr)	96.71742	91.3411	90.3221	89.9566	88.8626
EL (kWh)	894608.6125	849409.4762	840786.7641	838507.1302	828134.7484
TAC ($)	53676.5167	50964.5685	50447.2058	50310.4278	49688.0849
Dcost ($)	4761.2992	5566.2834	5925.4844	5923.0722	6413.1546
TACS ($)	16468.7671	18375.7311	18533.8928	18673.0830	18805.3435
Emission (ton)	25846.9649	25805.0595	25797.0652	25794.9516	25785.3351
ES (ton)	328.0500	369.9554	377.9498	380.0633	389.6798
QLI (p.u.)	3.5685	3.5771	3.5783	3.5790	3.5802
VSI (p.u.)	0.7291	0.7648	0.7654	0.7654	0.7651
VDI (p.u.)	0.0753	0.0624	0.0614	0.0608	0.0608
TBVVB	0	0	0	0	0
APLR	28.6398	32.3108	33.0110	33.1957	34.0232
RPCR	28.4322	32.4104	33.1644	33.4349	34.2444
Vmin (Bus)	0.9240 (18)	0.9352 (18)	0.9353 (18)	0.9353 (18)	0.9353 (18)

$ 17735.0913 while showing APL reduction and increased emission savings of 33%and 377.78 tons, respectively. Case 4 shows that single DSTATCOM placement after network reconfiguration gives maximum operational cost savings of $ 32425.53. However, simultaneous reconfiguration and DSTATCOM allocation shows further improvement in TACS of $ 32531.43 and reduction in APL of 101.0188 kW. It is also observed from tables 6.9, 6.10 and 6.11 that the APL reduction and TACS of the network keep on increasing with increasing number of DSTATCOMs at a substantial rate till three DSTATCOMs. It is observed from Fig. 6.5 (a) that placement of DSTATCOMs in the network help to meet the reactive power demand locally and results in the reversal of reactive power flow in several lines in the network. This local reactive power management enhances the active power flow capability of the RDS.

Table 6.11: Results of CTLBO algorithm for TACS maximization in 33-bus

	Case 4				
Open Switch	7 9 14 32 37				
No. of DSTATCOM	1	2	3	4	5
Size (Location)	854.68 (30)	178.88 (17)	142.69 (14)	141.403 (14)	55.6300 (9)
kVAr (Bus No.)		851.54 (30)	141.37 (18)	140.608 (18)	132.449 (14)
			849.70 (30)	135.403 (25)	114.094 (18)
				834.725 (30)	134.823 (25)
					834.439 (30)
APL (kW)	102.8491	98.6193	96.4796	94.7383	94.4560
RPC (kVAr)	77.7878	73.8687	71.7985	70.6681	70.4053
EL (kWh)	638935.0106	612952.9470	599777.5798	588978.5470	587248.5505
TAC ($)	38336.1006	36777.1768	35986.6547	35338.7128	35234.9130
Dcost ($)	3758.8017	4531.6866	4986.1689	8775.6716	5591.6148
TACS ($)	32811.6807	33597.7196	33933.7594	34061.1184	34080.0552
Emission (ton)	25609.9226	25585.8339	25573.6186	25563.6066	25562.0026
ES (ton)	565.0923	589.1810	601.3963	611.4084	613.0123
QLI (p.u.)	3.6047	3.6108	3.6133	3.6146	3.6149
VSI (p.u.)	0.7892	0.8223	0.8249	0.8266	0.8268
VDI (p.u.)	0.0366	0.0302	0.0283	0.0281	0.0279
TBVVB	0	0	0	0	0
APLR	49.2546	51.3416	52.3973	53.2565	53.3958
RPCR	42.4394	45.3394	46.8713	47.7078	47.9022
Vmin (Bus)	0.9475 (33)	0.9582 (33)	0.9583 (33)	0.9583 (32)	0.9583 (32)

Figs. 6.5 (b) and 6.5 (c) show that magnitude of the branch currents change marginally but their phase angles change widely due to reactive power compensation in the network. From Fig. 6.5 (d) the minimum bus voltage in the network without DSTATCOM is 0.9131 p.u (at bus no. 18), while it increases to 0.93621 p.u. (at bus no. 18) after the placement of two DSTATCOMs. However, with simultaneous network reconfiguration and DSTATCOM allocation, the minimum bus voltage is further enhanced to 0.9545 p.u. (bus no. 18). Fig. 6.5 (f) shows the reactive power injected by the DSTATCOMs after their allocation in the network, corresponding to the 24-hour load demand, as shown in Fig. 6.5 (e). Fig. 6.5 (g) shows the APL (24 hourly) of the network without and with DSTATCOMs, for Case 3. The energy losses and the TACS of the network are calculated using Eqn. (3.15) and (3.22) corresponding to the parameters provided in appendix Table A.5. Fig. 6.5 (d) depicts the voltage profile for

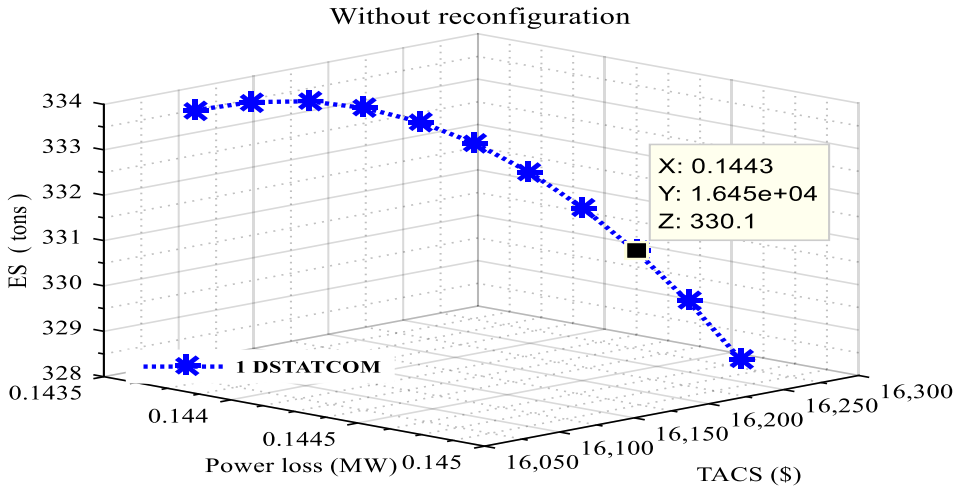

Fig. 6.6 (a): Pareto solutions with 1 DSTATCOM for case 3 in 33-bus

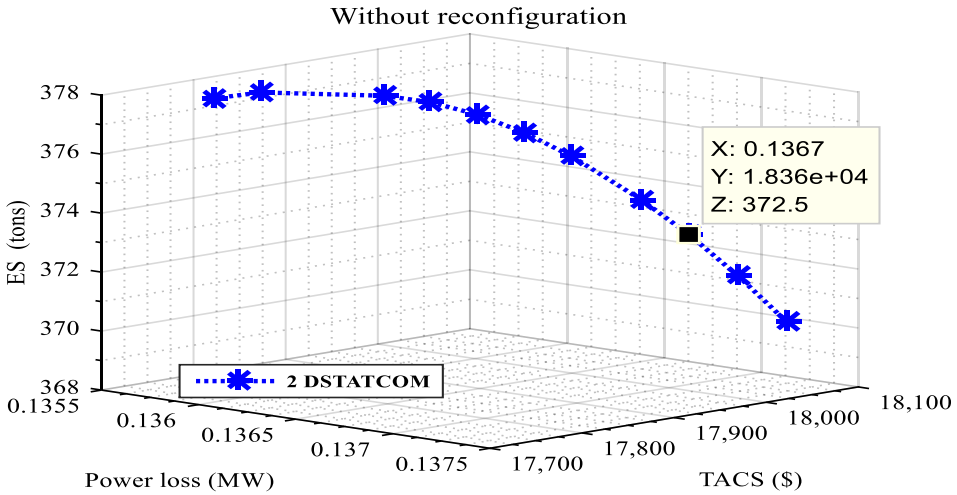

Fig. 6.6 (b): Pareto solutions with 2 DSTATCOMs for case 3 in 33-bus

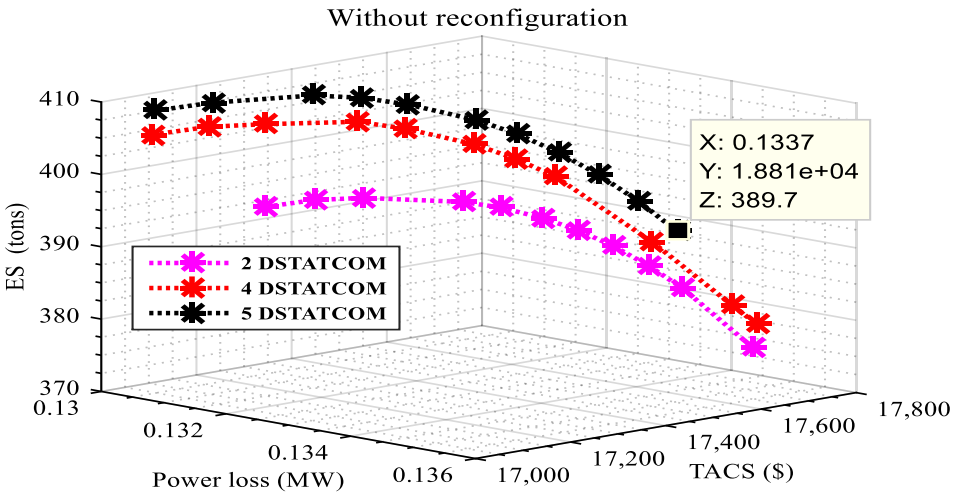

Fig. 6.6 (c): Pareto solutions with 3, 4 and 5 DSTATCOMs for case 3 in 33-bus

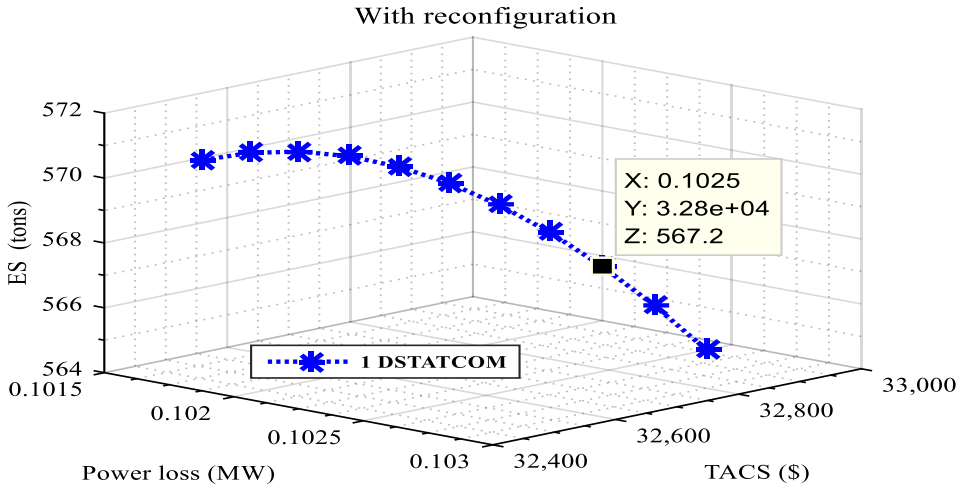

Fig. 6.6 (d): Pareto solutions with 1 DSTATCOM for case 4 in 33-bus

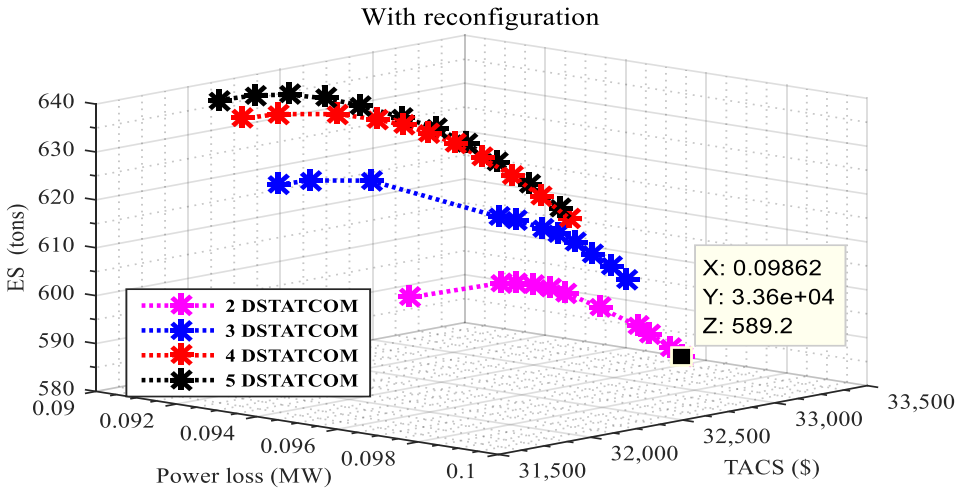

Fig. 6.6 (e): Pareto solutions with 2, 3, 4 and 5 DSTATCOMs for case 4 in 33-bus

Table 6.12: Comparative results of CTLBO based DSTATCOM allocation in 33-bus

	Case 3			
Algorithm	BFOA [166]	IA [100]	BA [165]	CTLBO
Open Switch	33 34 35 36 37			
No. of DSTATCOM	1	1	1	1
Size (Location) kVAr (Bus No.)	1102.7 (30)	962.49 (12)	1150 (30)	1252.71 (30)
APL (kW)	144.38	171.79	143.97	143.6016
RPC (kVAr)		115.26	96.47	96.3378
QLI (p.u.)	-			3.5740
VSI (p.u.)	0.7228	0.79311	0.7242	0.7340
VDI (p.u.)	-	-	-	0.0701
APLR	28.76	15.24	28.97	29.147
RPCR	-	14.78	28.67	28.713
Vmin (Bus)	0.9240	0.9258	0.9244	0.9256 (18)

Table 6.13: Comparison of CTLBO Algorithm based DSTATCOM allocation in 33-bus for case 3

	Case 3			
Algorithm	ICA [167]	BFOA [166]	BA [165]	CTLBO
Open Switch		33 34 35 36 37		
No. of DSTATCOM	2	2	2	2
Size (Location)	455 (10)	600 (10)	450 (10)	468.86 (12)
kVAr (Bus No.)	1005 (30)	1200 (30)	995 (30)	1057.75 (30)
APL (kW)	140.24	137.50	146.73	135.7530
RPC (kVAr)	93.67	92.01	95.63	90.5464
QLI (p.u.)	-	-	-	3.5841
VSI (p.u.)	-	-	-	0.7683
VDI (p.u.)	-	-	-	0.0561
APLR	30.31	32.15	27.60	33.020
RPCR	30.73	31.96	29.28	32.998
Vmin (Bus)	0.9301	0.9289	0.9299	0.9362 (18)

Table 6.14: Comparison of CTLBO algorithm based DSTATCOM allocation in 33-bus for case 5

	Case 5		
Algorithm	HFACO [105]	SFLA [168]	CTLBO
Open Switch	7 9 14 32 37	11 28 30 33 34	7 9 14 36 37
No. of DSTATCOM	1	1	1
Size (Location) kVAr (Bus No.)	980 (10)	1110.2 (10)	1070.23 (30)
APL (kW)	110.22	118.1	101.0188
RPC (kVAr)	-	-	75.3696
QLI (p.u.)	-		3.6103
VSI (p.u.)	-	-	0.7933
VDI (p.u.)	-	-	0.0314
APLR	45.61	41.73	50.1577
RPCR	-	-	44.2288
Vmin (Bus)	-	0.9423	0.9545 (18)

APL minimization of the RDS. Pareto solutions of multi-objective formulation by weighted sum approach [159] for APL, TACS and ES corresponding to cases 3 and 4 are presented in Figs. 6.6 (a) to 6.6 (e). The complete results of Pareto solutions for 69-bus are given in appendix Table A.7. The Pareto solutions make available multiple network operating conditions before the DNOs up to placement of five DSTATCOMs without and/or with reconfigu-ration of the RDS. It is possible to achieve APL

reduction, TACS and ES up to 55.74 %, $ 34080 and 456 tons, respectively, for 33-bus. It is observed from Table 6.11 and 6.12 that CTLBO algorithm yields minimum network losses of 143.60 kW and 135.753 kW after placement of one and two DSTATCOMs respectively, in the 33-bus for case 3 in comparison to BFOA [166], BA [165] and imperialist competitive algorithm (ICA) [167]. Table 6.13 shows that a marked reduction in the APL is achieved when proper tie switches/isolators are opened and optimal allocation of DSTATCOMs are carried out in the network simultaneously.

6.3.5.2 69-bus RDN

The CTLBO is now implemented for 69-bus for all the cases. The detailed network specification is given in appendix Table A.2 and chapter 3. Table 6.14 shows the results corresponding to the APL minimization in this RDS. It is noted from Table 6.14 that for Case 1, the APL in the network is 224.95 kW while all the tie switches are open in the network. Case 2 shows that for the APL minimization objective, when switches 14, 56, 61, 69 and 70 are opened to maintain network radiality, the RDS has APL, TACS and ES of 98.571 kW, $ 46194.86 and 713.80 tons, respectively. It is also observed that for case 3, with optimal allocation of two DSTATCOMs, the maximum network TACS, APLR and ES are $ 21462.48, 34.91% and 442.77 tons, respectively. Case 4 suggest that placement of two DSTATCOMs following network reconfiguration gives maximum TACS of $ 51646.6739. However simultaneous reconfiguration and allocation (Case 5) of two DSTATCOMs yield highest TACS of $ 51646.6739, which is same as that of case 4. It is observed from Tables 6.11 that APL reduction and TACS of the network keeps on increasing with increase in the number of DSTATCOMs but at a significant rate up to three DSTATCOMs. Table 6.13 shows that for the 69-bus , with the placement of a single DSTATCOM the APL is minimum with switches 14, 57, 63,

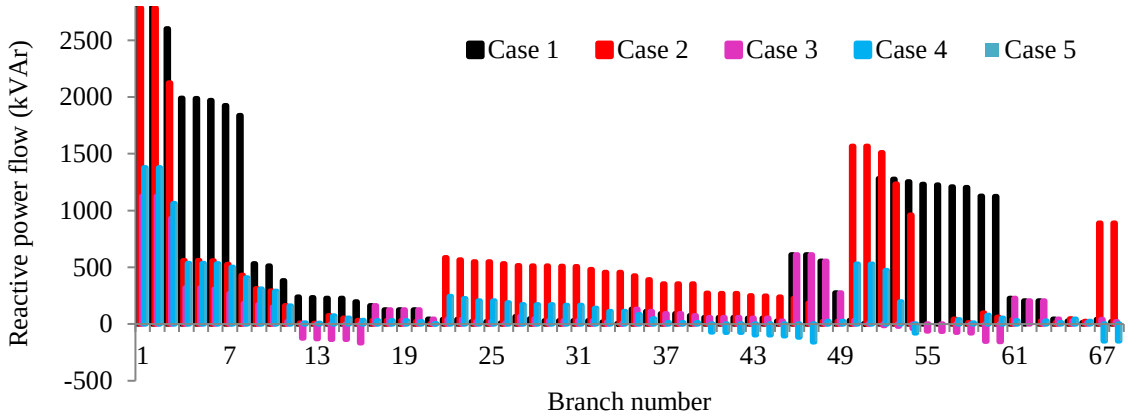

Fig. 6.7 (a): Reactive power flow in each line in 69-bus for APL minimization

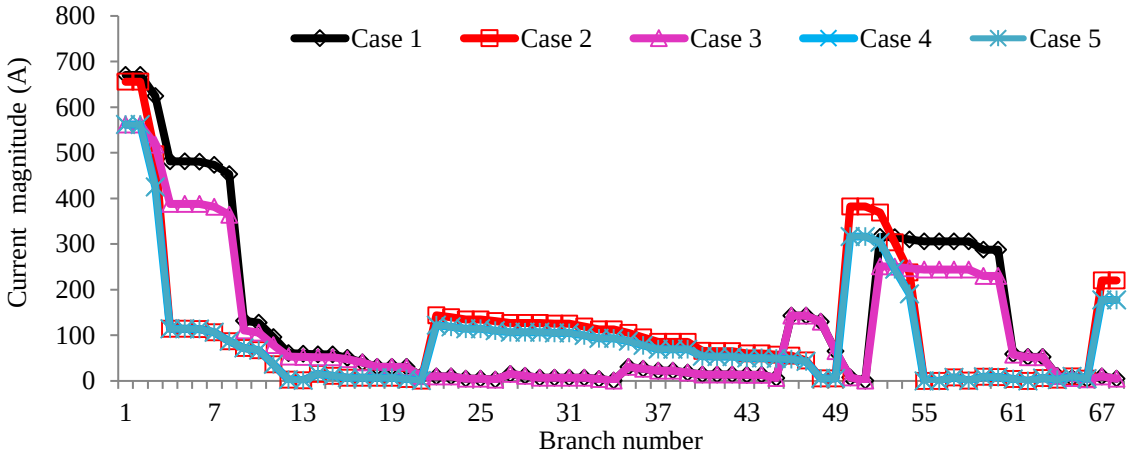

Fig. 6.7 (b): Branch current magnitude in 69-bus for APL minimization

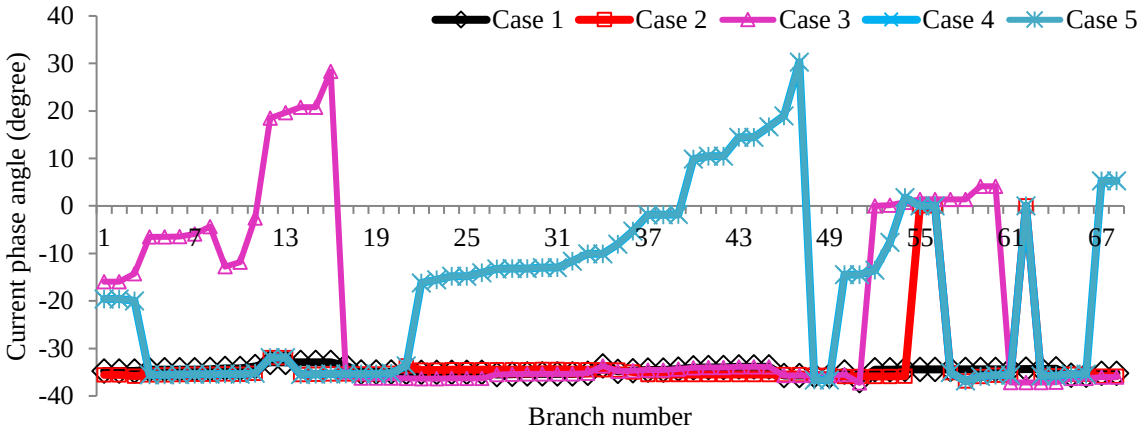

Fig. 6.7 (c): Branch current phase angle in 69-bus for APL minimization

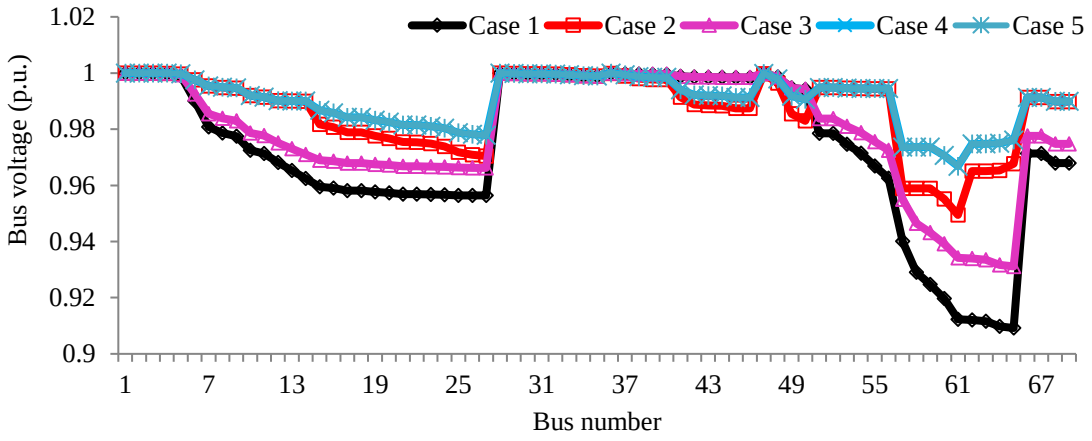

Fig. 6.7 (d): Voltage profile of network in 69-bus for APL minimization

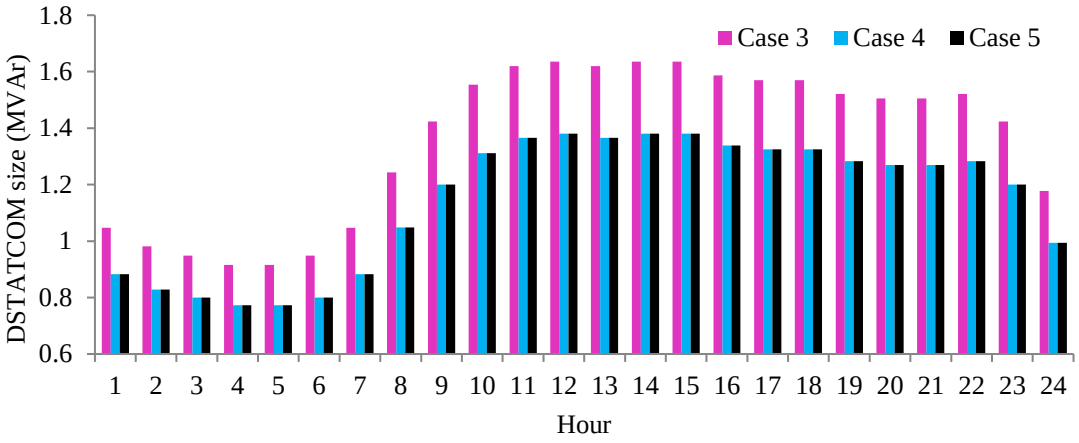

Fig. 6.7 (e): Hourly reactive power supplied by DSTATCOMs in 69-bus for APL minimization

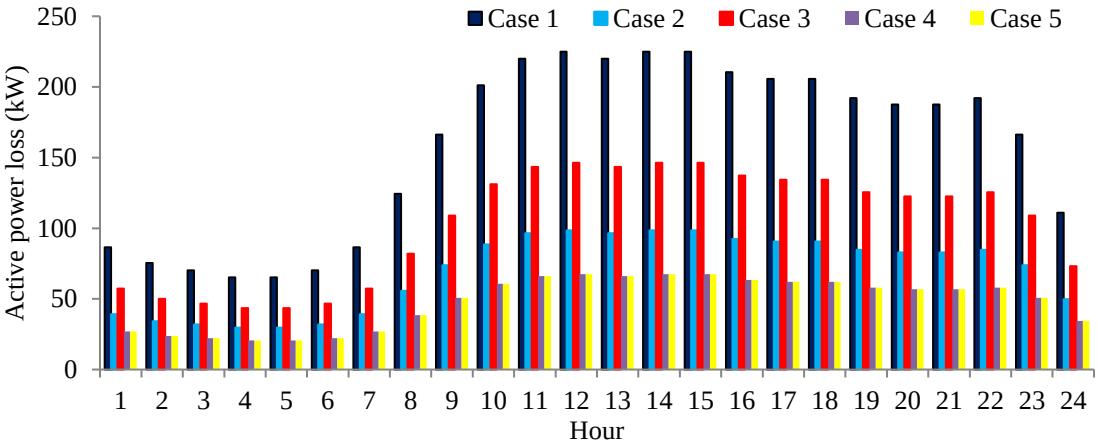

Fig. 6.7 (f): Hourly APL in 69-bus network for APL minimization

Table 6.15: CTLBO algorithm based DSTATCOMs allocation for APL minimization in 69-bus

	Case 1	Case 2	Case 3	Case 4	Case 5
Open Switch	69 70 71 72 73	14 56 71 69 70	69 70 71 72 73	14 56 61 69 70	14 56 61 69 70
No. of DSTATCOM	-	-	2	2	2
Size (Location)			360.41 (17)	1038.19 (61)	1038.19 (61)
kVAr (Bus No.)			1274.98 (61)	341.79 (64)	341.79 (64)
APL (kW)	224.8974	98.5717	146.379	67.3899	67.3899
RPC (kVAr)	102.1156	92.0240	68.2097	62.7666	62.7666
EL (kWh)	1381327.9423	611413.5998	903748.9191	419399.2101	419399.2101
TAC ($)	82879.6765	36684.8159	54224.9351	25163.9526	25163.9526
Dcost ($)	-		7192.2586	6069.0499	6069.0499
TACS ($)	-	46194.8606	21462.4827	51646.6739	51646.6739
Emission (ton)	26879.9838	26166.1742	26437.2066	25988.1521	25988.1521
ES (ton)	-	713.8096	442.7771	891.8316	891.8316
QLI (p.u.)	3.6184	3.6967	3.6621	3.7306	3.7306
VSI (p.u.)	0.6833	0.8308	0.7517	0.8865	0.8865
VDI (p.u.)	0.0992	0.0244	0.0573	0.0124	0.0124
TBVVB	0	0	0	0	0
APLR	-	56.1701	34.9121	70.0349	70.0349
RPCR	-	9.8825	33.2034	38.5337	38.5337
Vmin (Bus)	0.9092 (65)	0.9495 (61)	0.9311 (65)	0.9668 (61)	0.9668 (61)

69 and 70 open for loss minimization objective while switches 14, 56, 61, 59 and 70 should be opened for cost saving objective. . It is observed from Fig. 6.7 (a) that placement of DSTATCOMs in the network helps to meet the reactive power demand locally and results in the reversal of reactive power flow in several lines in the network. This local reactive power management enhances the active power flow capability of the DN. Fig. 6.7 (b) and 6.7 (c) shows that the magnitudes of the branch currents change marginally but their phase angles undergo marked changes with reactive power compensation in the network. From Fig. 6.7 (d), it is observed that the minimum bus voltage in the network without DSTATCOM is 0.9092 p.u (at bus no. 65), which increases to 0.93113 p.u. (at bus no. 65) after the placement of two DSTATCOMs. However, with simultaneous reconfiguration and DSTATCOM allocation the minimum bus voltage is enhanced to 0.9668 p.u. (at bus 61). After optimal allocation of two DSTATCOMs in the network, their reactive power injections is shown in Fig. 6.4 (d)

Table 6.16: CTLBO algorithm based DSTATCOM allocation for TACS maximization in 69-bus

	Case 3				
Open Switch	69 70 71 72 73				
No. of DSTATCOM	1	2	3	4	5
Size (Location)	1175.46 (61)	226.909 (21)	116.740 (17)	116.730 (17)	116.7310 (17)
kVAr (Bus No.)		1140.395 (61)	125.120 (21)	125.120 (21)	098.4990 (21)
			1138.09 (61)	931.195 (61)	026.6183 (26)
				206.632 (64)	931.1950 (61)
					206.6326 (64)
APL (kW)	152.9006	148.0530	147.8266	147.4894	147.4814
RPC (kVAr)	71.0191	69.0748	68.9811	68.8132	68.8105
EL (kWh)	943537.7406	913661.9055	912268.7359	910229.4586	910180.1856
TAC ($)	56612.2644	54819.7143	54736.1241	54613.7675	54610.8111
Dcost ($)	5169.5331	6013.2284	6068.8799	6067.6617	6067.6396
TACS ($)	21097.8789	22046.7337	22074.6724	22198.2472	22201.2257
Emission (ton)	26474.0959	26446.3972	26445.1055	26443.2149	26443.1692
ES (ton)	405.8878	433.5865	434.8782	436.7688	436.8146
QLI(p.u.)	3.6542	3.6566	3.6567	3.6569	3.6569
VSI (p.u.)	0.7429	0.7438	0.7438	0.7460	0.7460
VDI (p.u.)	0.0673	0.0627	0.0625	0.0623	0.0623
TBVVB	0	0	0	0	0
APLR	32.0123	34.1678	34.2685	34.4184	34.4220
RPCR	30.452	32.3562	32.4479	32.6125	32.6151
Vmin (p.u.)	0.9284 (65)	0.9287 (65)	0.9287 (65)	0.9294 (65)	0.9294 (65)

corresponding to the actual loading of the line for a 24-hour period, as shown in Fig. 3.4. Fig. 6.7 (e) shows the APL of the network without and with DSTATCOMs for bus voltage is enhanced to 0.9668 p.u. (at bus 61). After optimal allocation of two DSTATCOMs in the network, their reactive power injections is shown in Fig. 6.4 (d) corresponding to the actual loading of the line for a 24-hour period, as shown in Fig. 3.4. Fig. 6.7 (e) shows the APL of the network without and with DSTATCOMs for the 24-hour period. Energy losses, TACS and ES of the network are calculated using Eqns. (3.13), (3.22a-3.22d) and (3.23c) corresponding to the data provided in appendix Tables A.4 and A.5. Fig. 6.7 (d) depicts the VP with APL minimization objective for all the case studies with the 69-bus. From Fig. 6.7 (d), it can be observed that optimal network reconfiguration and allocation of DSTATCOMs improves the voltage profile of the RDS substantially. Pareto solutions of the multi-objective formulation using

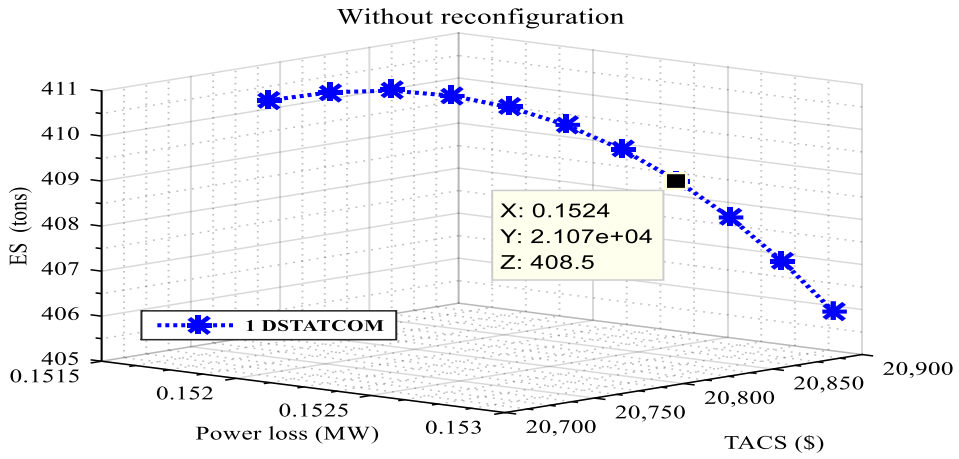

Fig. 6.8 (a): Pareto solutions with 1 DSTATCOM without reconfiguration in 69-bus

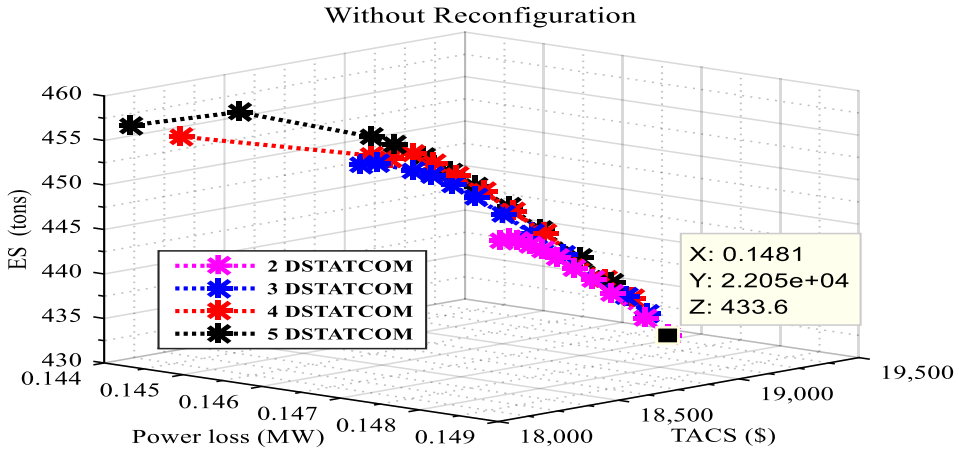

Fig. 6.8 (b): Pareto solutions with 2, 3, 4 and 5 DSTATCOMs without reconfiguration in 69-bus

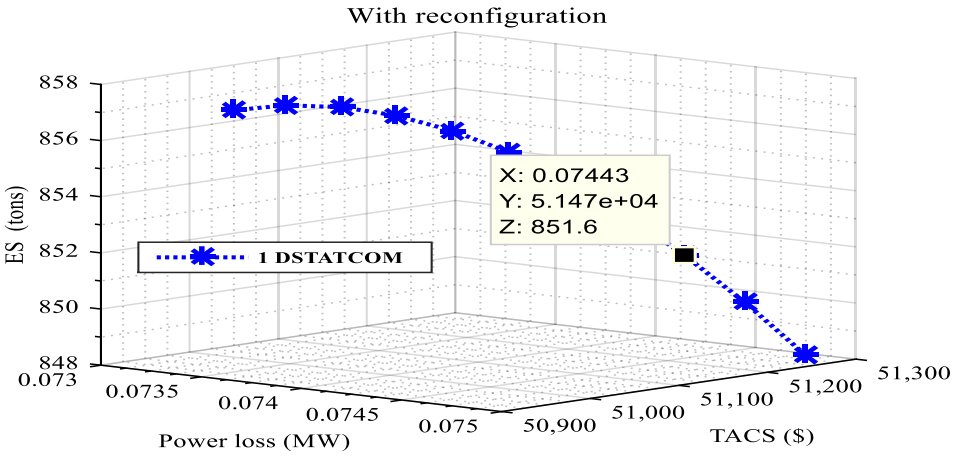

Fig. 6.8 (c): Pareto solutions with 1 DSTATCOMs with reconfiguration in 69-bus

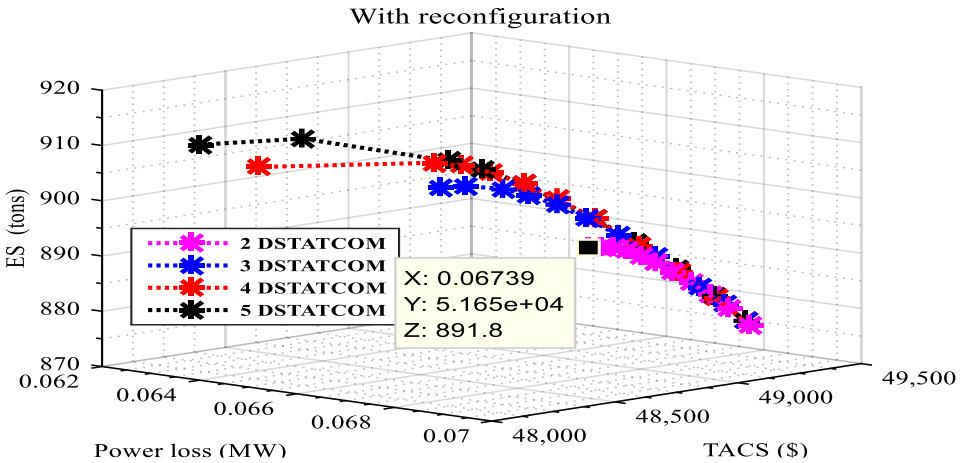

Fig. 6.8 (d): Pareto solutions with 2, 3, 4 and 5 DSTATCOMs with reconfiguration in 69-bus

Table 6.17: CTLBO algorithm based DSTATCOMs allocation for TACS maximization in 69-bus for case 4

	Case 4				
Open Switch	14 56 61 69 70				
No. of DSTATCOM	1	2	3	4	5
Size (Location) kVAr (Bus No.)	776.071(61)	776.00 (61) 226.17 (64)	776.00 (61) 185.22 (64) 47.59 (65)	776.00 (61) 23.00 (62) 1622.10 (64) 47.597 (65)	6.029 (27) 776.00 (61) 23.002 (62) 162.211 (64) 42.501 (65)
APL (kW)	74.9825	69.6318	69.5393	69.5361	69.5249
RPC (kVAr)	69.7641	66.1107	66.0412	66.0396	66.0307
EL (kWh)	466237.5460	433073.6797	432499.9906	432480.6710	432410.9368
TAC ($)	27974.2527	25984.4207	25949.9994	24100.6421	25944.6562
Dcost ($)	3413.0600	4407.4505	4436.6336	4436.6203	4440.7256
TACS ($)	51492.3637	52487.8052	52493.0434	52494.2159	52494.2946
Emission (ton)	26031.5773	26000.8301	26000.2982	26000.2803	26000.2157
ES (ton)	848.4064	879.1536	879.6855	879.7034	879.7680
QLI(p.u.)	3.7182	3.7218	3.7219	3.7219	3.7219
VSI (p.u.)	0.8674	0.8726	0.8726	0.8726	0.8726
VDI (p.u.)	0.0196	0.0154	0.0154	0.0154	0.0153
TBVVB	0	0	0	0	0
APLR	66.6588	69.0380	69.0792	69.0805	69.0855
RPCR	31.6812	35.2589	35.3270	35.3286	35.3372
Vmin (Bus)	0.9626 (61)	0.9626 (61)	0.9626 (61)	0.9626 (61)	0.9626 (61)

Table 6.18: CTLBO algorithm based DSTATCOM allocation in 69-bus for case 5

	Case 5			
	33 Bus	33 Bus	69 Bus	69 Bus
Objective function	Power loss	TACS	Power loss	TACS
Open Switch	7 9 14 36 37	7 9 14 36 37	14 57 63 69 70	14 56 61 59 70
No. of DSTATCOM	1	1	1	1
Size (Location) kVAr (Bus No.)	1070.23 (30)	896.92 (30)	1062.68 (61)	776.071 (61)
APL (kW)	101.0188	102.050	73.1664	74.9825
RPC (kVAr)	75.3696	75.8526	67.4086	69.7641
EL (kWh)	627806.5746	634075.4016	455185.7648	466237.5460
TAC ($)	37668.3944	38044.5240	27311.1458	27974.2527
Dcost ($)	4706.7518	3944.5341	4673.5533	3413.0600
TACS ($)	32531.4369	32917.5249	50894.9773	51492.3637
Emission (ton)	25599.6051	25605.4171	26021.3309	26031.5773
ES (ton)	575.4098	569.5978	858.6529	848.4064
QLI (p.u.)	3.6103	3.6061	3.7254	3.7182
VSI (p.u.)	0.7933	0.7931	0.8710	0.8674
VDI (p.u.)	0.0314	0.0336	0.0166	0.0196
TBVVB	0	0	0	0
APLR	50.1577	49.6488	67.4663	66.6588
RPCR	44.2288	43.8714	33.9878	31.6812
Vmin (Bus)	0.9545 (18)	0.9544 (33)	0.9661 (62)	0.9625 (61)

Table 6.19: Comparison of CTLBO algorithm based 1 DSTATCOM allocation in 69-bus for case 3

	Case 3			
Algorithm	CSOA [164]	IA [100]	BA [165]	CTLBO
Open Switch	68 69 70 71 72			
No. of DSTATCOM	1	1	1	1
Size (Location) kVAr (Bus No.)	1200 (61)	1704.4 (61)	1150 (61)	1329.82 (61)
APL (kW)	152.95	157.5	153.36	151.958
RPC (kVAr)	-	72.4	96.47	70.4638
QLI (p.u.)	-	-	-	3.6585
VSI (p.u.)	0.7375	0.7561	0.7356	0.7504
VDI (p.u.)	-	-	-	0.0639
APLR	32.02	30	31.9	32.4315
RPCR	-	29.2	30.27	30.9959
Vmin (Bus)	0.9285	0.9353	0.9278	0.9307 (65)

Table 6.20: Comparison of CTLBO algorithm based 2 DSTATCOMs allocation in 69-bus for case 3

	Case 3			
Algorithm	ICA [167]	BA [165]	BFOA [166]	CTLBO
Open Switch		68 69 70 71 72		
No. of DSTATCOM	2	2	2	2
Size (Location)	0375 (15)	0330 (15)	480 (15)	360.41 (17)
kVAr (Bus No.)	1280 (61)	1220 (61)	1430 (61)	1274.98 (61)
APL (kW)	147.35	146.73	148.07	146.379
RPC (kVAr)	72.382	68.73	68.76	68.2097
QLI (p.u.)	-			3.6621
VSI (p.u.)	-	0.7418	0.7512	0.7517
VDI (p.u.)	-	-	-	0.0573
APLR (%)	34.60	34.78	34.19	34.9121
RPCR (%)	29.17	33.04	32.72	33.2034
Vmin (Bus)	0.9324	0.9299	0.9332	0.9311 (65)

Table 6.21: Comparison of CTLBO algorithm based 1 DSTATCOM allocation in 69-bus for case 5

	Case 5	
Algorithm	DE [101]	CTLBO
Open Switch	13 59 63 70 71	14 57 63 69 70
No. of DSTATCOM	1	1
Size (Location) kVAr (Bus No.)	924 (61)	1062.68 (61)
APL (kW)	78.59	73.1664
RPC (kVAr)	84.23	67.4086
QLI (p.u.)	-	3.7254
VSI (p.u.)	-	0.8710
VDI (p.u.)	-	0.0166
APLR	55.64	67.4663
RPCR	17.51	33.9878
Vmin (Bus)	0.9632	0.9661 (62)

weighted sum approach for APL, TACS and ES are presented in Fig. 6.7 (a)-6.7 (e), corresponding to cases 3 and 4. The complete results of Pareto solutions for 69-bus are given in appendix Table A.7. It is observed from the Pareto solutions that several network operating conditions are available to the DNOs for placement of up to five DSTATCOMs without and/or with reconfiguration to achieve APL reduction, cost savings and emission savings up to 71.73 %, $52449 and 912 tons, respectively, in the

69-bus. It is observed from Table 6.18 and 6.19 that CTLBO algorithm yields minimum network losses of 151.958 kW and 146.379 kW after placement of one and two DSTATCOMs respectively, in the 69- bus for case 3 in comparison to BA [165], BFOA [166] and ICA [167]. Table 6.20 shows that a remarkable reduction in the APL is achieved when simultaneous network reconfiguration and optimal allocation of DSTATCOMs is carried out in the network.

6.4 SUMMARY

This chapter first presents an analytical approach for the optimal allocation of multiple DSTATCOMs in RDS for enhancing annual energy, cost and emission savings. This method is based on the power loss sensitivity and does not involve the solution of differential equations. This results in a significantly less computational time as compared to IA and BA, while maintaining the desired level of accuracy. The proposed work considers a 24-hour load profile for the all the distribution networks. The effectiveness of the proposed method is tested on small (33-bus), medium (69-bus) and large (118-bus) while considering optimal number of DSTATCOMs for each network. Various performance indices indicate that increasing number of DSTATCOMs in RDS improves all the indices except cost savings. So, the economic aspect is also considered for selecting the optimal number of DSTATCOMs for allocation in the RDS. Several performance indicators are used to give insight of the network performance. This will be helpful for the network operators. Comparative results of the proposed method show remarkable improvement in the yearly cost savings with reduction in computational time over IA and BA methods.

Subsequently, this chapter also implements a CTLBO algorithm based optimization

technique for network reconfiguration and optimal allocation of DSTATCOMs in the 33-bus and 69-bus. Both SOF and MOF are considered. Case studies show that simultaneous network reconfiguration and DSTATCOM allocation yields the best value for the objective function. It has been observed that in the presence of DSTATCOMs, reverse power flows in lines change significantly and improve the margin of power transfer capability. Analysis reveals that an optimal number of DSTATCOMs must be considered for minimizing the annual operational costs while considering power loss minimization as a constraint. Realistic 24-hour load profiles have been considered for both the DNs. Pareto solutions of the MOFs have been carried out to operate the DNs in several operational modes to satisfy different objectives. Comparative results show significant improvement in the annual energy, cost and emission savings with reduction in the computational time over several other existing soft computing techniques.

CHAPTER 7

MULTI-OBJECTIVE APPROACH TO MAXIMIZE LOADABILITY OF DISTRIBUTION NETWORKS

7.1 INTRODUCTION

Exponential load growth, renewable based DGs penetration, non-linearity in loads, network upgrade deferral causes serious network operational challenges like line thermal limit violations, voltage limit violations, voltage stability issues, relay co-ordination problem. Therefore, to mitigate these issues, several remedial steps has been reported in literature such as network reconfiguration, load balancing, reactive power compensation, allocation of different types of DERs according to the load demand profile, incentive-based policy etc., which enhance the overall network efficiency and prevent the limits violation of the distribution networks. The literature review also reveals that the operational challenges are also minimized by enhancing the loadability of distribution network to its maximum capacity without violating constraints. DG allocation and network reconfiguration both play a crucial role in enhancing the network loadability. Although non-optimal allocation of DGs and network reconfiguration although improves the loadability, the power loss of the distribution network increases. Several loadability enhancement approaches have been reported in [109, 118, 119, 120, 129] in respect of real power loss minimization only. So, this chapter intends to develop an approach to consider simultaneous loadability enhancement and power loss minimization. The objective of loadability enhancement taking into account loss minimization

---

This Chapter is based on the following published paper

I. A. Quadri, S. Bhowmick and D. Joshi, "Multi-objective Approach to Maximize Loadability of Distribution Networks by Simultaneous Reconfiguration and Allocation of Distributed Energy Resources", *IET Generation Transmission and Distribution*, Vol. 12, Issue 21, pp.5700-5712,2018.

of the distribution networks is achieved by implementing CTLBO algorithm [113] employing multi-objective ε-constraints approach [159]. In this chapter, the effectiveness of the CTLBO algorithm to improve the loadability of the distribution networks is demonstrated considering several case studies with the 33-bus and 69-bus RDN.

7.2 PROBLEM FORMULATION

The objective of optimal DGs allocation and/or reconfiguration of RDN is to improve the line loadability and reduce the network APL. Subsequently, enhance the voltage profile, VSI and QLI while satisfying all working constraints. Descriptions of multi-objective functions are given below:

7.2.1 Multi objective function

A MOF considers all the SOFs simultaneously for either maximization or minimization, while satisfying the equality and inequality constraints. In this work, a MOF simultaneously maximizes $F\mu(X)$ and minimizes $F_m(X)$ satisfying the bus voltage limits, line thermal limits and maintaining the network power balance using the ε-constraints [28] method as follows.

$$\text{MOF} = \text{Minimize } F\mu(X) \tag{7.1}$$

$$\text{Subject to } F_m(X) \leq \varepsilon_m \quad m = 1,2,3 \ldots . M \text{ and } c \neq \mu;$$

$$g_p(X) \geq 0, \quad p = 1,2,3 \ldots .;$$

$$h_q(X) = 0, \quad q = 1,2,3 \ldots .;$$

$$X_{min,i} \leq x_i \leq X_{max,i}, \quad i = 1,2,3 \ldots N;$$

where one of the objectives of the MOF problem is maximized/minimized while keeping the remaining objectives as constraints. Here in this optimization problem $F\mu(X)$ represents the loading factor, while $F_m(X)$ represents the APL as constraint. 'g_j' comprises the bus voltage and line thermal limits while 'h_k'comprises the power balance constraints, respectively.

The impact of DG allocation and / or reconfiguration of the distribution network is evaluated based on indices as detailed in chapter 3. Here, VSI indicates the vulnerability of the network to a voltage collapse. Therefore, VSI must be close to unity. VDI represents the overall voltage fluctuation at all the buses in the network. Ideally, VDI should be zero. QLI describes the loadability of the network and should be as high as possible.

7.2.2 Network loadability objective function

Optimal allocation of DGs and/or network reconfiguration enhances the network loadability. The primary objective is to maximize 'λ' till divergence is observed in the power flow analysis. Here, increment in 'λ' enhances the loads at all the buses as shown below,

$$\mathbf{S_{new,k}} = \lambda * \mathbf{S_{b,k}} \tag{7.2}$$

So, the objective is to maximize λ while P_{loss} kept as constraints as shown below ,

$$F\mu(X) = \lambda_{max} = \text{maximize } (\lambda) \tag{7.3a}$$

$$F_m(X) = P_{loss} \tag{7.3b}$$

7.2.3 Constraints

Following constraints are taken into consideration for DG allocation and/or reconfiguration of the distribution network.

7.2.3.1 Active and reactive power balance constraints

$$P_{sub} + \sum_{k=1}^{nDG} P_{DG,k} = P_{loss} + \sum_{k=1}^{n} P_{L,k} \quad \&$$

$$Q_{sub} + \sum_{k=1}^{nDG} Q_{DG,k} = Q_{con} + \sum_{k=1}^{n} Q_{L,k} \tag{7.4a}$$

7.2.3.2 Voltage limits

The voltage magnitude at each bus must be maintained within a specified limit, say 0.95-1.05 p.u. as recommended by IEEE or IEC standards, at all network buses.

At any network bus ‘k’,

$$0.95 \leq |V|_k \leq 1.05 \qquad k = 1,2,3,4 \ldots \ldots n \tag{7.4b}$$

7.2.3.3 Thermal limits

$$|I_j| \leq |I_j^{max}| \tag{7.4c}$$

7.2.3.4 Real power limit and reactive power limit of DGs

$$P_{DG,k}^{min} \leq P_{DG,k} \leq P_{DG,k}^{max} \quad \text{i.e. } 0 \leq P_{DG,k} \leq 4 \tag{7.4d}$$

$$Q_{DG,k}^{min} \leq Q_{DG,k} \leq Q_{DG,k}^{max} \text{ i.e. } 0 \leq Q_{DG,k} \leq 4 \tag{7.4e}$$

7.3 IMPLEMENTATION OF CTLBO ALGORITHM FOR MAXIMIZATION OF LOADABILITY

This section illustrates the application of the CTLBO algorithm for the optimal allocation of DGs and/ or network reconfiguration by opening/closing of tie/sectional switches to meet the objective function, while satisfying all constraints. In this chapter, several cases which include allocation of multiple DGs with/without reconfiguration in the RDN are taken to maximize 'λ' using CTLBO algorithm. The number of solution vector variables is selected and rest steps is followed as detailed in chapter 3. The new solution vectors for teaching and Learning phase is used using Eqn. (4.3) and (4.2a and 4.2b), respectively. The following parameter values are selected for the CTLBO algorithm: a = 2, NI=250, SVS=90. The best result over 10 runs has been reported for each of the following cases.

Case 1: Base case considering nominal load

Case 2: Only network reconfiguration

Case 3: Only DG allocation

Case 4: DG allocation followed by network reconfiguration

Case 5: simultaneous DG allocation and network reconfiguration

7.4 CASE STUDIES, RESULTS AND DISCUSSIONS

7.4.1 33-bus RDN

The detailed network data is given in appendix A.1 and chapter 3**.** This chapter demonstrates the effectiveness of the CTLBO algorithm for loadability enhancement of RDN by network reconfiguration and/ or optimal allocation of DGs. The results are presented in Tables 7.1 and 7.2. From Tables 7.1 and 7.2, it is observed that 'λ' increases while APL and RPC reduces with increase in the number of DGs allocated. The maximum

enhancement in 'λ' is observed to be 104.7 % for Case 5 (with respect to Case 1). Maximum reductions in APL and RPC are observed to be 73 % and 69 % respectively, with respect to case 1. The minimum bus voltage magnitude of the network improves from 0.9038 to 0.9928 p.u for case 5.

The maximum value of QLI occurs in Case 3 when the number of DGs is three. The maximum enhancement in QLI is 7.144 % for Case 3 with 3 DGs (in comparison to case 1). A remarkable improvement in the VSI is observed (from 0.6672 to 0.9636), while the VDI is rendered zero. The VPI increases to 0.5302 for case 3 from zero. Cases 4 and 5 are observed to have maximum KMML (26128.72 kVA) corresponding to λ_{max} = 6.98. It is observed from Table 7.1 that no solution is available for Cases 2 and 4 (with one DG) with lower voltage limit constraint (0.95 p.u). Hence, the lower voltage threshold is further reduced till a solution is obtained. It is observed from Table 7.2 that loadability improvement of the network remains identical for cases 4 and 5 with allocation of 2 or 3 DGs.

The reconfiguration of the network and DG allocation improves the loading limits of the network without violating the voltage constraints. It is observed from Fig. 7.2 (c) that allocation of 3 DGs in the network has the maximum effect. While Case 1 can cater to only 2359.45 kVA (λ=0.54) with-out violating any voltage or line limit constraints, the load proposed CTLBO based technique enhances the load carrying capability to 3713.95 kVA (λ=0.85), 8957.17 kVA (λ=2.05) and 9175.64 kVA (λ=2.10) in cases 2, 3 & 4, respectively. It may be noted that the load carrying capability in Case 5 is identical to that of Case 4.

The convergence characteristics with 2 DGs for Cases 2-5 are shown in Fig. 7.2 (d). The curves show that the number of iterations increases when reconfiguration is

involved as can be observed in Cases 2 and 5. It is observed from Table 7.3, 7.4 and 7.5 that CTLBO and DABC algorithms give same result which is marginally better than [134].

For case 3, comparison of Tables 7.3 and 7.5 shows that with CTLBO based optimal allocation of one, two and three DGs in the 33-bus results in significant improvements in the line loading factor (λ=5.07), KMML (17783.26 kVA), QLI (3.7745 p.u.) and VSI (0.9465 p.u.) along with reduction in the APL and RPC up to 60.23 and 56.67 % respectively, over DABC [129] and hybrid PSO (HPSO) [109]. From Tables 7.1 and 7.3, it is observed that the network loadability enhancement is more when the allocated DGs operate at different power factors. The topology of the reconfigured network with maximum loadability is shown in Fig. 7.1. It is generated using a graphical approach.

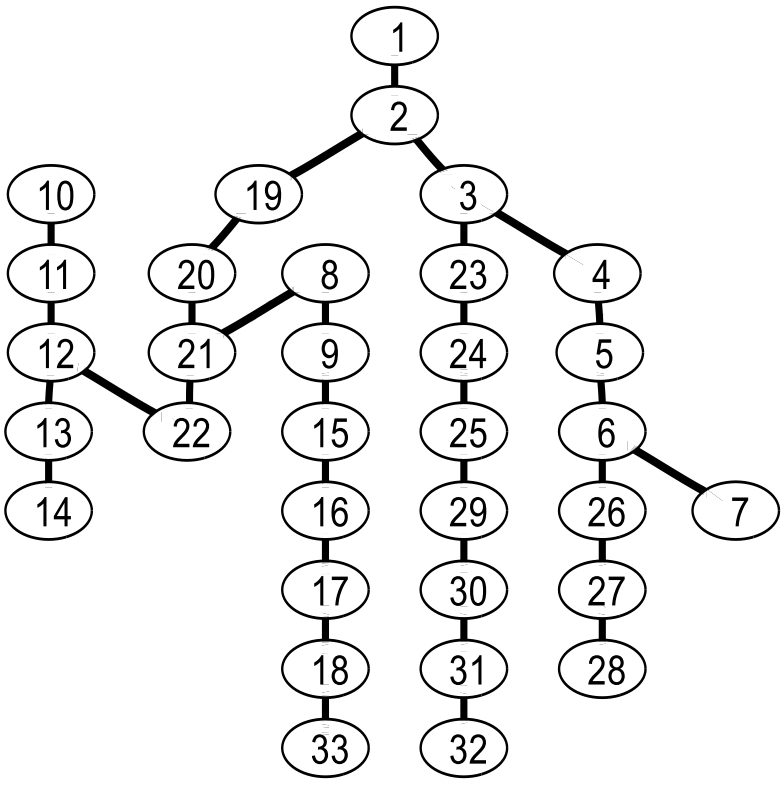

Fig. 7.1: Best reconfiguration for case 2 in 33-bus

Table 7.1: Results of 33-bus for loadability enhancement with 1 DG

	Without DG		1 DG		
	Case 1	Case 2	Case 3	Case 4	Case 5
Open tie/Sectional Switch	33 34 35 36 37	7 9 14 28 32	33 34 35 36 37	7 9 14 28 32	7 9 14 17 28
kVA (Bus)	-	-	3609.886 (8)	2149.001 (30)	2736.046 (30)
Power factor	-	-	0.8362	0.7307	0.7748
APL (kW)	210.9900	139.9781	130.8608	58.2302	57.4654
RPC (kVAr)	143.0329	104.8847	112.1985	50.6667	48.7508
λmax	3.4100	5.2500	4.31	5.9	6
KMML	10530.13	18569.74	14462.55	21409.82	21846.75
TBVVB	21	7	0	0	0
VDI	0.0245	0.0023	0	0.0003	0
VPI	0	0.1793	0.4412	0.2603	0.3232
QLI	3.5227	3.5803	3.7209	3.6674	3.6996
VSI	0.6671	0.7665	0.9117	0.8087	0.8335
APLR	-	33.6581	37.9791	72.4021	72.7645
RPCR	-	26.6709	21.5576	64.5768	65.9163
Vmin (Bus)	0.9037 (18)	0.9413 (32)	0.9771 (33)	0.9486 (33)	0.9645 (17)

Table 7.2: Results of 33-bus for loadability enhancement with 2 and 3 DGs

	2 DG			3 DG		
	Case 3	Case 4	Case 5	Case 3	Case 4	Case 5
Open tie or Sectional Switch	33 34 35 36 37	7 9 14 28 32	7 9 14 28 32	33 34 35 36 37	7 9 14 28 32	7 9 14 28 32
kVA (Bus)	1430.954 (15)	831.142 (16)	831.142 (16)	0967.774 (13)	669.504 (12)	669.504 (12)
	2568.624 (30)	2916.855 (30)	2916.855 (30)	0563.725 (16)	592.893 (17)	592.893 (17)
				2508.081 (30)	3069.255 (30)	3069.255 (30)
Power factor	0.9594	0.8949	0.8949	0.9692	0.9901	0.9901
	0.7569	0.7536	0.7536	0.9265	0.9365	0.9365
				0.7729	0.7515	0.7515
APL (kW)	86.5759	56.9016	56.9016	83.8966	56.8845	56.8845
RPC (kVAr)	66.5092	45.5439	45.5439	61.9705	44.3443	44.3443
λmax	5.0600	6.9000	6.9000	5.0700	6.9800	6.9800
KMML	17739.56	25779.17	25779.17	17783.26	26128.72	26128.72
TBVVB	0	0	0	0	0	0
VDI	0	0	0	0	0	0
VPI	0.5236	0.3778	0.3779	0.5302	0.3998	0.3998
QLI	3.7718	3.7333	3.7333	3.7744	3.7474	3.7474
VSI	0.9455	0.9213	0.9213	0.9465	0.9636	0.9636
APLR	58.9678	73.0318	73.0317	60.2376	73.0398	73.0398
RPCR	53.5007	68.1584	68.1584	56.6739	68.9971	68.9971
Vmin (Bus)	0.9861 (25)	0.9773 (14)	0.9773 (14)	0.9864 (25)	0.9928 (28)	0.9928 (28)

Fig. 7.3 shows the voltage profile of the network during different cases. It is observed that cases 1 and 2 show voltage constraint violation at nodes 21 and 7 of the network, respectively. However cases 3, 4 and 5 show significant improvement in the network voltage profile except case 4 (with one DG). Fig. 7.1 shows the topology of the 33-bus, corresponding to case 2. The comparison shows that for Case 5 with 2 DGs allocated, the best combination of open tie/sectional switch locations are 7, 9, 14, 28 and 32, which result in a maximum loading factor of λ=6.90 which pertains to loadability up to 25779.17 kVA, QLI up to 3.7333 and minimum network Bus voltage magnitude to 0.9773 p.u, with no voltage limit constraint violation. It is observed that Case 5 results in a substantial improvement of the evaluation indices and yields the highest loadability.

Table 7.3: Comparative results of 33-bus for loadability Enhancement

Algorithm	HPSO [109]	DABC [129]	CTLBO	HPSO	CTLBO
	Case 3	Case 3	Case 3	Case 5	Case 5
Open tie/Sectional Switch	33 34 35 36 37	33 34 35 36 37	33 34 35 36 37	7 10 14 28 32	7 9 14 28 32
kVA (Bus)	1637.100 (14)	1313.900 (16)	1430.954 (15)	956.600 (9)	831.142 (16)
	2072.000 (32)	2212.300 (22)	2568.624 (30)	3117.500 (25)	2916.855 (30)
Power factor	0.9500	0.8500	0.9594	0.95	0.8949
			0.7569		0.7536
APL (kW)	113.15	87.65	86.5759	58.86	56.9016
RPC (kVAr)	90.63	73,32	66.5093	46.54	45.5439
λmax	4.99	5.00	5.06	6.31	6.90
KMML	17433.71	17477.40	17739.56	23201.25	25779.17
TBVVB	0	0	0	0	0
VDI	0	0	0	0	0
VPI	0.5115	0.0700	0.5236	0.3462	0.3778
QLI	3.7600	3.7609	3.7718	3.72	3.7333
VSI	-	-	0.9456	-	0.9213
APLR	46.3710	58.4577	58.9678	72.103	73.0317
RPCR	36.6270	48.7308	53.5007	67.457	68.1584
Vmin (Bus)	-	-	0.9861 (25)	-	0.9773 (14)

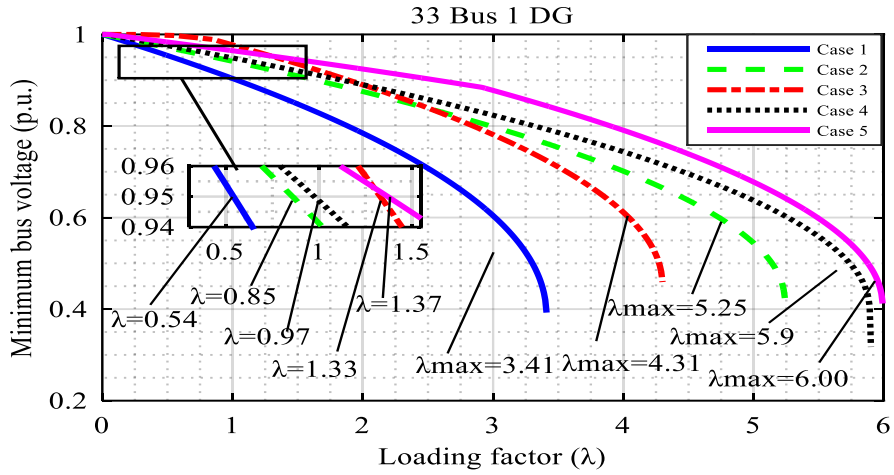

Fig. 7.2 (a): Maximum loading curves of 33-bus for 1 DG

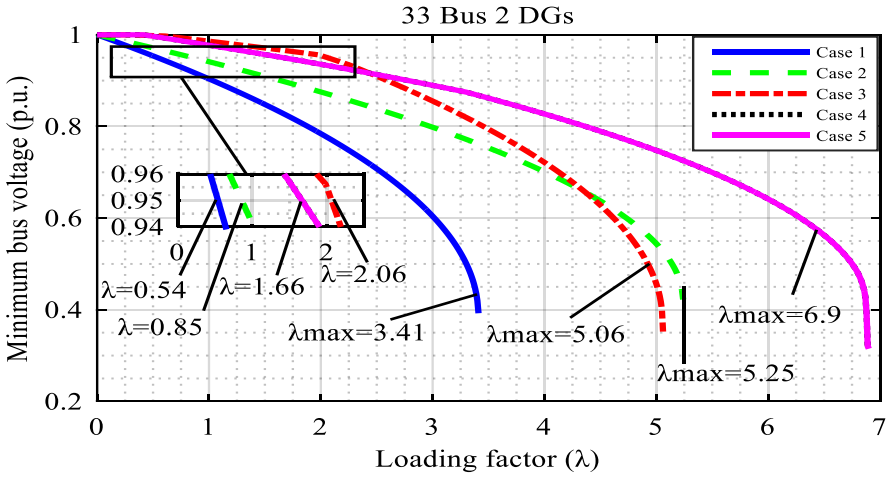

Fig. 7.3 (b): Maximum loading curves of 33-bus for 2 DGs

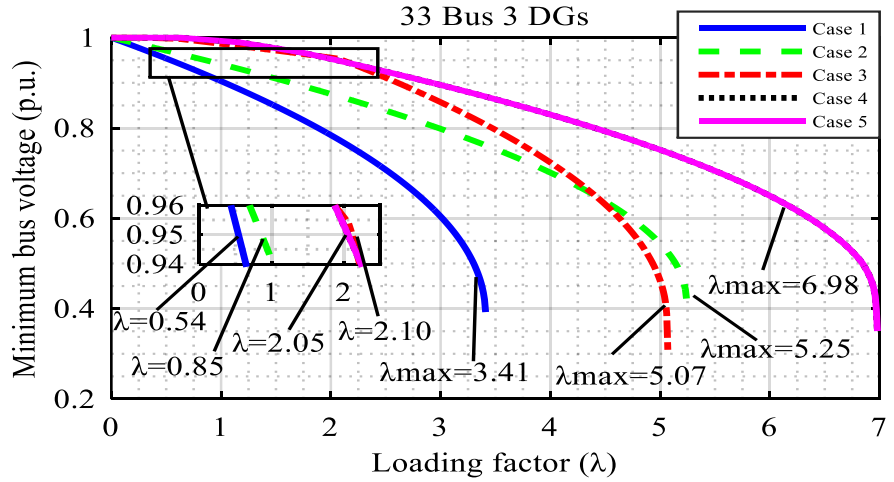

Fig. 7.4 (c): Maximum loading curves of 33-bus for 3 DGs

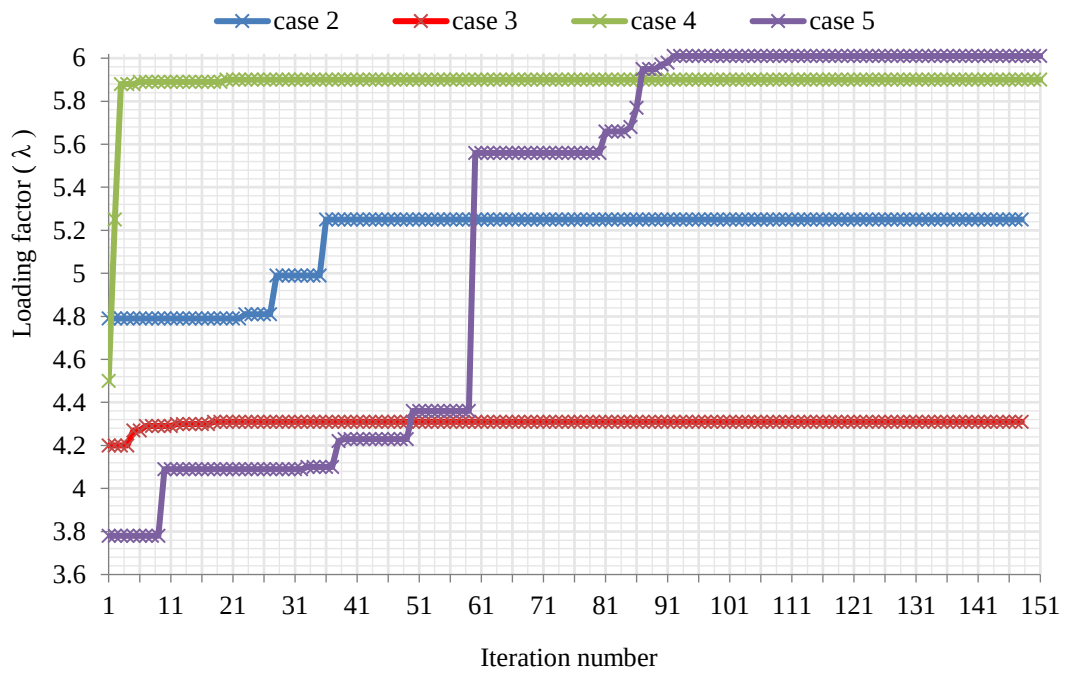

Fig. 7.5 (d): Convergence curves for maximum lodability with 2 DGs

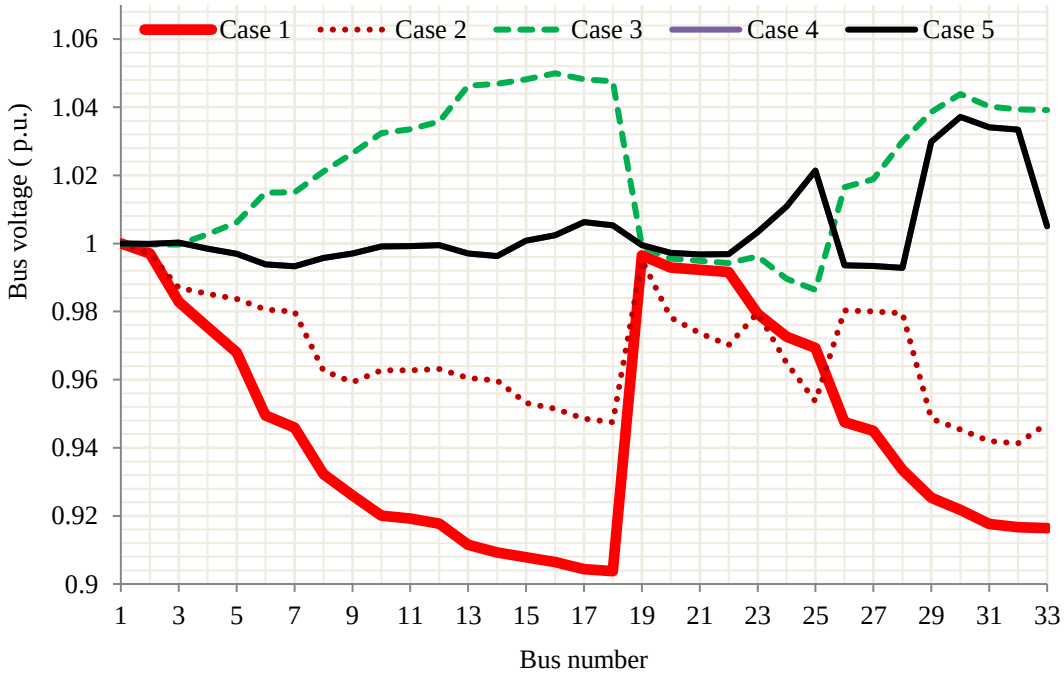

Fig. 7.6: Voltage profile for 3 DGs allocation in 33-bus

Table 7.4: Comparative results of loadability enhancement of 33-bus for case 2

Algorithm	DABC [129]	HS [134]	CTLBO
Open tie/ Sectional Switch	7 9 14 28 32	7 9 14 32 37	7 9 14 28 32
APL (kW)	139.97	144.5780	139.9781
RPC(kVAr)	104.87	100.5317	104.8847
λmax	5.23	5.07	5.25
KMML	18482.35	17783.25	18569.74
TBVVB	7	6	7
VDI	0.0023	0.0030	0.0023
VPI	0.1793	0.1866	0.1793
QLI	3.58	3.5788	3.5804
VSI	-	0.7769	0.7666
APLR	33.66	28.66	33.6581
RPCR	26.66	25.61	26.6709
Vmin (Bus)	-	0.9388 (32)	0.9413 (32)

Table 7.5: Comparative results of loadability enhancement of 69-bus

Algorithm	DABC [129]	CTLBO	DABC [129]	CTLBO
	Case 3	Case 3	Case 3	Case 3
Open tie/Sectional Switch	33 34 35 36 37	33 34 35 36 37	33 34 35 36 37	33 34 35 36 37
kVA (Bus)	3623.9 (8)	3609.88 (8)	1364.1 (15)	967.77 (13)
			444.0 (29)	563.72 (16)
			1973.0 (31)	2508.08 (30)
Power factor	0.85	0.836274	0.85	0.9692
				0.9265
				0.7729
APL (kW)	131.85	130.8608	84.16	83.8966
RPC (kVAr)	113.03	112.1985	68.02	61.9705
λmax	4.31	4.31	5.04	5.07
KMML	14462.55	14462.55	17652.18	17783.26
TBVVB	0	0	0	0
VDI	0	0	0	0
VPI	0.1757	0.4412	0.0643	0.5302
QLI	3.7213	3.7209	3.7713	3.7745
VSI	-	0.9117	-	0.9465
APLR	37.5089	37.9792	60.1119	60.2376
RPCR	20.9636	21.5576	52.4369	56.6739
Vmin (Bus)	-	0.9771 (33)	-	0.9864 (25)

The multi-objective ε-constraints approach simultaneously enhances the network loadability and reduce the APL, without violating the voltage and line limit constraints. However case studies with the 33-bus suggest that Cases 4 and 5 yield identical results with 2 and 3 DGs. Although maximum loadability is observed with 3 DGs allocated, however, compared to the case with 2 DGs allocated, only marginal improvement is observed. So in order to reduce the operational costs, it would be prudent to select the optimal number of DGs as 2.

7.4.2 69-bus RDN

The detailed network data is given in Appendix A.2 and chapter 3**.** The results are shown in Tables (7.6 and 7.7). From Table (7.6 and 7.7), it is observed that that 'λ' increases with increase in the number of DGs. The maximum enhancement in 'λ' is observed to be 141.93 % in Case 5 with three DGs allocated. The results also reveal that Case 3 yields maximum APL and RPC reduction. Maximum reductions of up to 63.47 and 63.24 % are observed for APL and RPC respectively, with respect to Case 1. The minimum bus voltage magnitude of the network improves from 0.9092 to 0.9943 p.u. for Case 3. The maximum value of QLI occurs in Case 3 when two DGs are allocated. The maximum enhancement in QLI is 7.342 % in Case 3 with 2 DGs (in comparison to Case 1). A remarkable improvement in the VSI is observed (from 0.6833 to 0.9775) in case 3 when 3 DGs are placed. Also, in Case 3, it is observed that with 2 DGs, the VDI is rendered zero while the VPI increases to 0.4463 from zero. Cases 4 & 5 are observed to have identical maximum KMML (31639.18 kVA) corresponding to λ_{max} = 7.79. It is observed from Table 7.6 that no solution is available in Case 2 with lower voltage limit constraint (0.95 p.u.). However, the lower voltage threshold is further reduced till a solution is obtained. It is also observed from Tables 7.6 and 7.7 that loadability of the

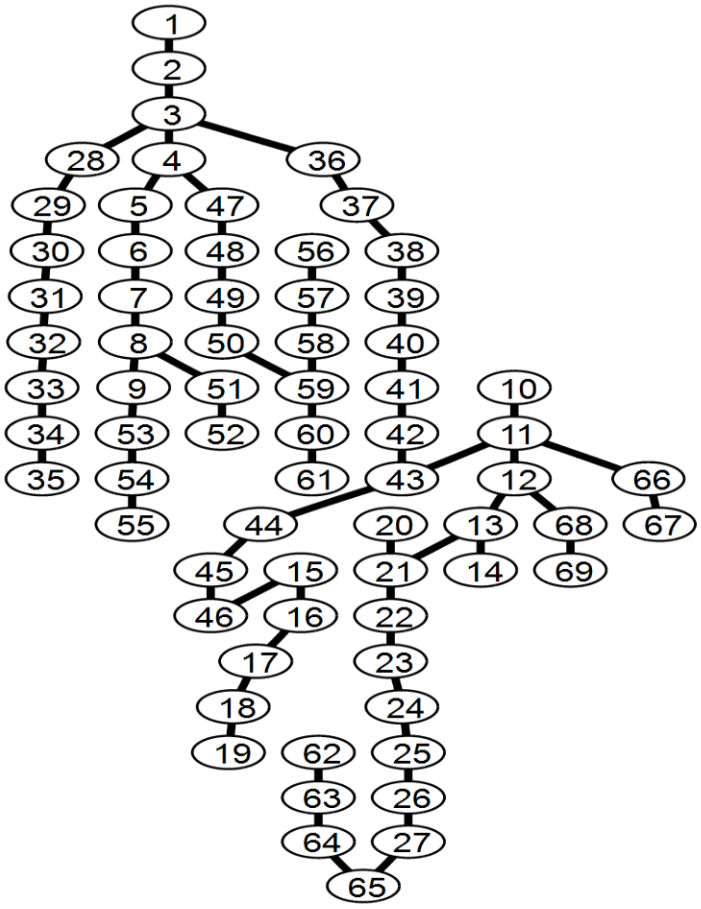

Fig. 7.7: Best reconfiguration topology for case 2 of 69-bus

Table 7.6: Results for loadability enhancement of 69-bus with 1 DG

	Without DG		1 DG		
	Case 1	Case 2	Case 3	Case 4	Case 5
Open tie/ Sectional Switch	69 70 71 72 73	14 58 61 69 70	69 70 71 72 73	14 58 61 69 70	14 58 61 69 70
kVA(Bus)			3684.153 (61)	3891.016 (61)	3891.016 (61)
Power factor			0.8394	0.8687	0.8687
APL (kW)	224.9515	98.5898	86.5685	117.0621	117.0621
RPC (kVAr)	102.1406	92.0378	38.0906	70.2688	70.2688
λmax	3.22	5.51	4.91	7.73	7.73
KMML	10344.47	21015.12	18219.32	31359.59	31359.59
TBVVB	9	1	0	0	0
VDI	0.0118	6.37E-05	0	0	0
VPI	-	0.1924	0.4059	0.2824	0.2824
QLI	3.6189	3.6972	3.8698	3.8468	3.8469
VSI	0.6833	0.8306	0.9286	0.8672	0.8672
APLR	-	56.1728	61.5168	47.9612	47.9612
RPCR	-	9.8911	62.7077	31.2038	31.2038
Vmin (Bus)	0.9092 (65)	0.9495 (61)	0.9817 (27)	0.9651 (62)	0.9651 (62)

Table 7.7: Results for loadability enhancement of 69-bus with 2 and 3 DGs

	2 DG			3 DG		
	Case 3	Case 4	Case 5	Case 3	Case 4	Case 5
Open tie/ Sectional Switch	69 70 71 72 73	14 58 61 69 70	10 14 18 56 61	69 70 71 72 73	14 58 61 69 70	9 14 19 55 61
kVA(Bus)	640.790 (16)	385.261 (10)	751.383 (27)	347.851 (22)	149.820 (32)	3857.816 (61)
	3681.781 (61)	3893.261 (61)	3856.998 (61)	426.426 (47)	3860.015 (61)	503.090 (64)
				3725.761 (61)	339.263 (65)	241.174 (68)
Power factor	0.9213	0.9929	0.8209	0.7833	0.8112	0.8077
	0.7695	0.8708	0.8033	0.9996	0.7999	0.8316
				0.7803	0.9988	0.7763
APL (kW)	82.1582	113.9611	94.8372	83.8425	102.1497	92.9965
RPC (kVAr)	37.5466	68.9080	56.5855	37.8812	59.8052	56.1681
λmax	4.92	7.73	7.79	4.93	7.73	7.79
KMML	18265.91	31359.59	31639.18	18312.51	33130.27	31639.18
TBVVB	0	0	0	0	0	0
VDI	0	0	0	0	0	0
VPI	0.4463	0.2884	0.3445	0.4285	0.3042	0.3463
QLI	3.8846	3.8493	3.8617	3.8792	3.8563	3.8606
VSI	0.9774	0.8672	0.9509	0.9775	0.9225	0.9397
APLR	63.4774	49.3397	57.8411	62.7286	54.5904	58.6673
RPCR	63.2403	32.5361	44.6004	62.9127	41.4482	45.0090
Vmin (Bus)	0.9943 (50)	0.9651 (62)	0.9895 (62)	0.9943 (50)	0.9801 (62)	0.9878 (20)

network remains identical with 2 and 3.DGs in Case 4. This trend is also observed in Case 5. However, both the APL and RPC of the network reduce as the number of DGs increase (from 2 to 3). Fig 7.5 (e) shows the convergence characteristics with 2 DGs allocated, for the different case studies (Cases 2-5).

It is observed from Table 7.10 that CPF [127], DABC [129] and CTLBO techniques give results which are almost identical, but marginally better than [127]. The topology of the reconfigured network with maximum loadability is shown in Fig. 7.4. It is again generated using a graphical approach. The reconfiguration and optimal DG allocation improves the loading limit of the loading limits of the network without violating the voltage constraints. From Fig. 7.5 (c), it is observed that placement of 3 DGs in the network gives the best result. While Case 1 can cater only up to 2656.013 kVA (λ=0.57) without violating the voltage and line limit constraints, the proposed CTLBO based

network reconfiguration and DG allocation technique enhances the load carrying capability up to 4613.074 kVA (λ=0.99), 8806.778 kVA (λ=1.89), 8527.198 kVA (λ=1.83) and 9878.503 kVA (λ=2.12), corresponding to cases 2, 3, 4 and 5, respectively. Fig 7.6 shows the voltage profile of the network during different cases. It is observed that cases 1 and 2 show voltage constraint violations at nodes 9 and 1 of the network, respectively. However, cases 3, 4 and 5 show significant voltage profile improvement of the network with no voltage limit violations. Fig. 7.4 shows the reconfigured network topology for the 69-bus corresponding to case 2. Comparative results in Table 7.8 and 7.9 show significant improvements in the line loading factor (λ=4.92), VSI (0.9775) and KMML (18312.51 kVA) with 3 DGs. It is observed that with 2 DGs, the maximum QLI is obtained (3.8846 p.u.) while APL and RPC reduction of up to 63.477 and 63.24 % respectively, occurs. The comparison also shows that corresponding to Case 5 with 1 DG allocated, the optimal combination of open tie/sectional switches are at locations 14, 58, 61, 69 and 70, which results in a maximum loading factor of λ=7.73 which enhances the loadability up to 31359.59 kVA. However, in Case 3, an improvement in QLI of up to 3.8698 and a network minimum bus voltage of 0.9817 p.u. is observed, without any voltage limit constraint violation. On the basis of the above, it can be concluded that highest loadability is observed with Case 5 while Case 3 provides better solutions in terms of other network indices. The multi-objective ε-constraint approach for maximum loadability is used to simultaneously enhance the network loadability and the APL, without violating any voltage or line limit constraints. Although it is observed from for Case 5 that maximum loadability is obtained by placing 3 DGs, but marginal improvement occurs by placing 3 DGs instead of 2 DGs. So in order to reduce the operational and maintenance costs, the optimal number of DGs can be selected as 2.

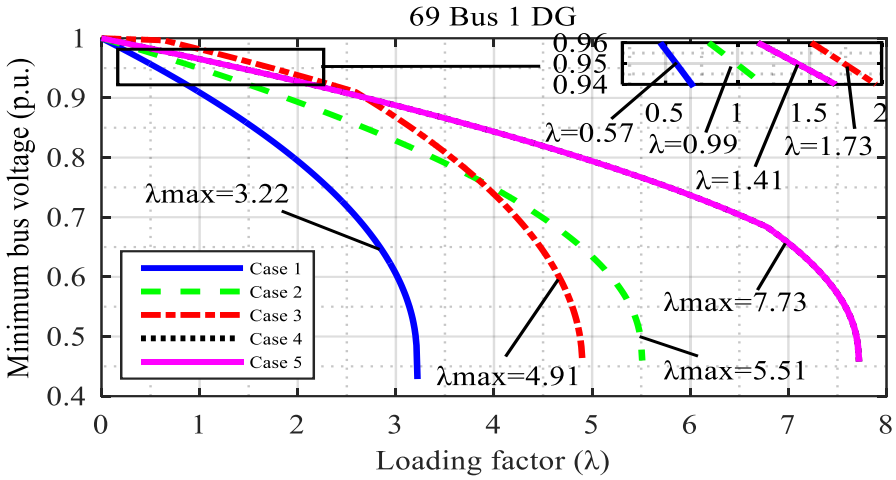

Fig. 7.5 (a): Maximum loading curves of 69-bus for 1 DG

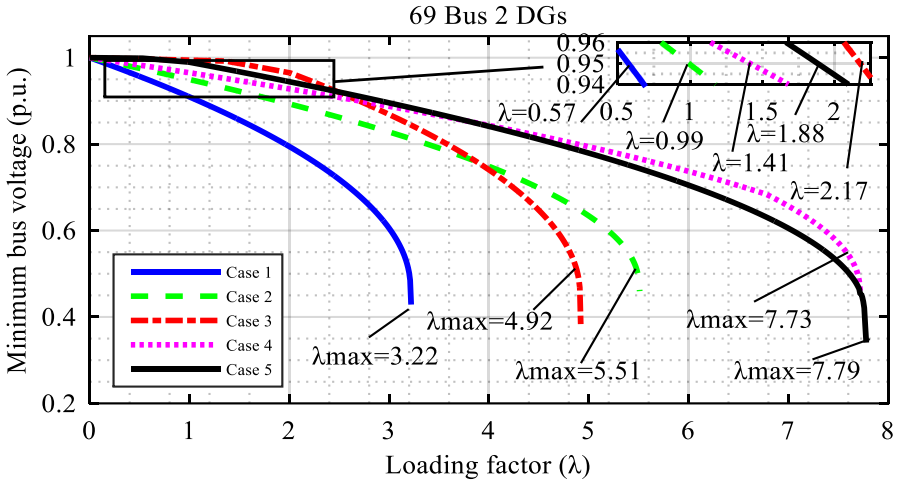

Fig. 7.5 (b): Maximum loading curves of 69-bus for 2 DGs

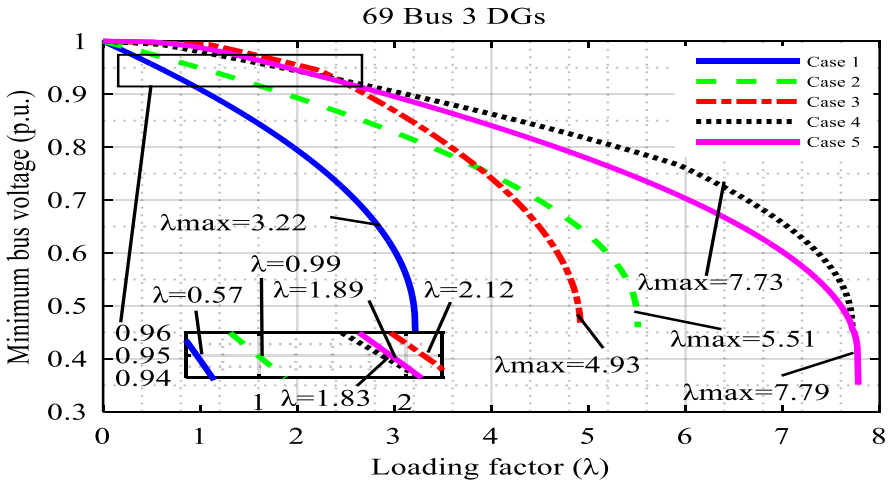

Fig. 7.5 (b): Maximum loading curves of 69-bus for 3 DGs

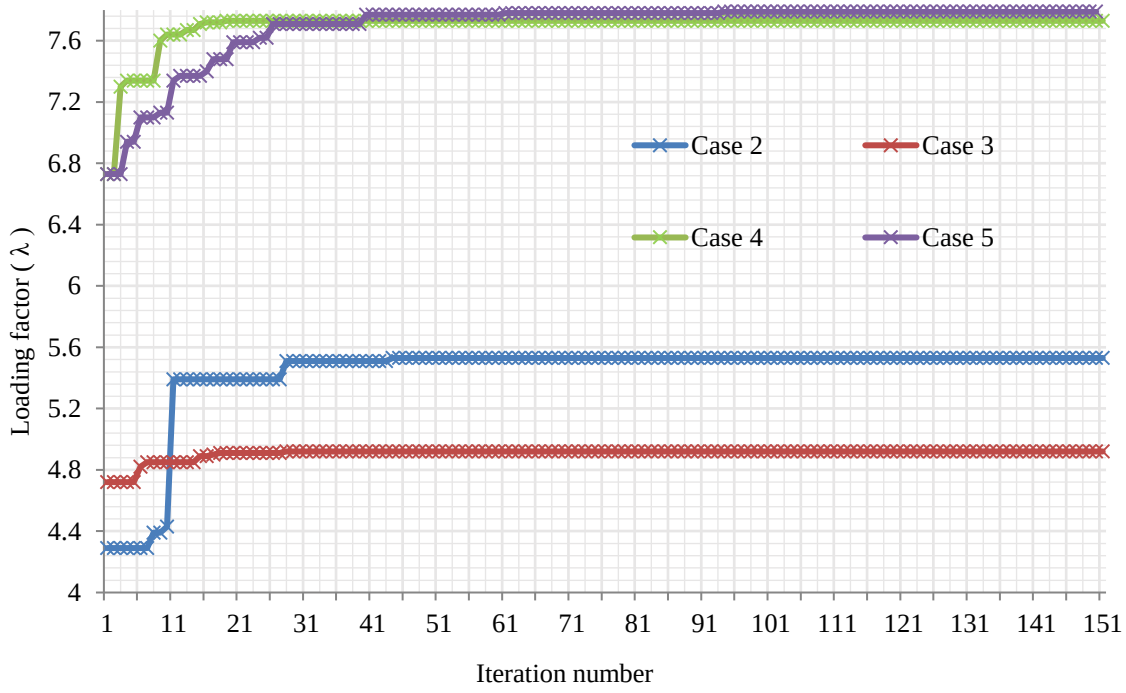

(d)

Fig. 7.8 (d): Convergence curves for maximum lodability with 2 DGs

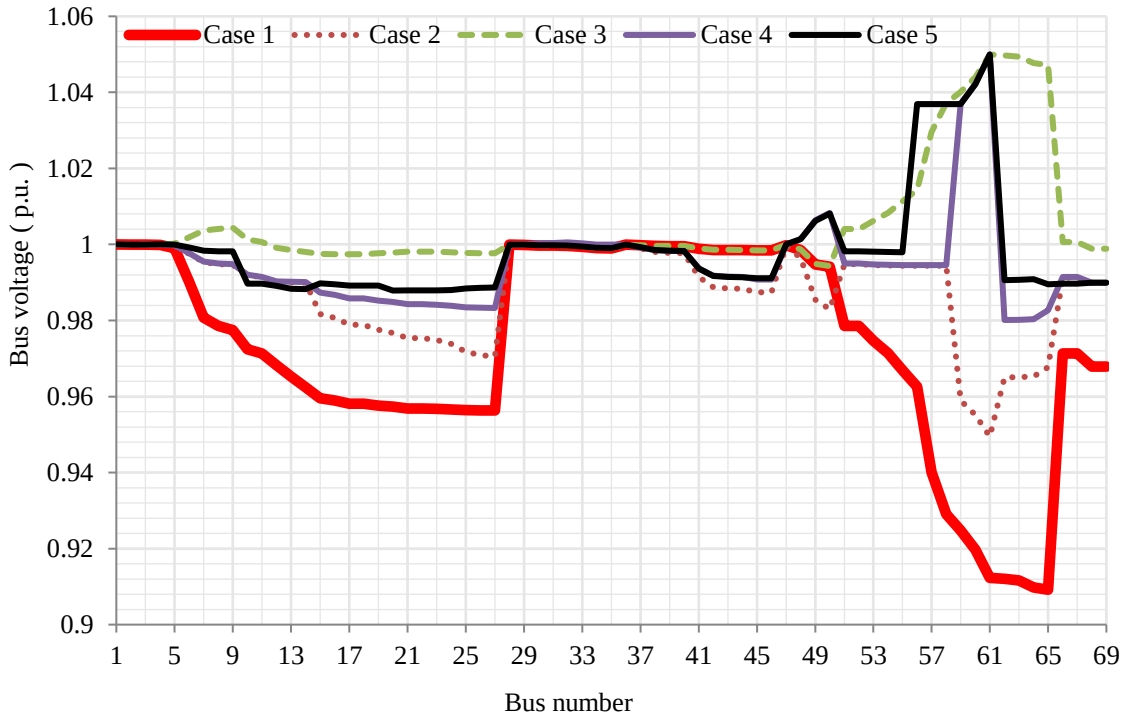

Fig. 7.9: Voltage profile for 3 DGs allocation in 69-bus

Table 7.8: Comparative results of loadability enhancement of 69-bus

	HPSO [109]	DABC [129]	CTLBO	HPSO [109]	CTLBO
	Case 3	Case 3	Case 3	Case 5	Case 5
Open tie/Sectional switch	69 70 71 72 73	69 70 71 72 73	69 70 71 72 73	13 17 38 57 63	14 58 61 69 70
kVA (Bus)	3635.000 (61)	3684.700 (61)	3684.153 (61)	4102.500 (61)	3891.016 (61)
Power factor	0.9500	0.8500	0.8394	0.9500	0.8687
APL (kW)	104.8600	87.1300	86.5685	160.81	117.0621
RPC (kVAr)	46.0200	38.3400	38.0906	91.85	70.2688
λmax	4.83	4.91	4.91	7.53	7.73
KMML	17846.54	18219.32	18219.32	30427.66	31359.59
TBVVB	0	0	0	0	0
VDI	0	-	0	0	0
VPI	0.4042	0.1459	0.4058	0.3317	0.2824
QLI	3.87	3.8713	3.8697	3.83	3.8468
VSI	-	-	0.9286	-	0.8672
APLR	53.385	61.2669	61.5167	28.513	47.9612
RPCR	54.949	62.4669	62.7076	10.083	31.2037
Vmin (Bus)	-	-	0.9817 (27)	-	0.9651 (62)

Table 7.9: Comparative results of loadability enhancement of 69-bus with 2 and 3 DGs

	DABC [129]	CTLBO	DABC [129]	CTLBO
	Case 3	Case 3	Case 3	Case 3
Open tie/Sectional Switch	69 70 71 72 73	69 70 71 72 73	69 70 71 72 73	69 70 7172 73
kVA(Bus)	547.600 (48) 3685.100 (61)	640.790 (16) 3681.780 (61)	0.152.900 (46) 3652.500 (61) 32.200 (63)	435.065 (22) 187.947 (25) 3857.656 (61)
Power factor	0.8500	0.9214 0.7694	0.8500	0.9932 0.7992 0.8558
APL (kW)	86.6800	82.1582	87.0000	83.8425
RPC (kVAr)	37.1700	37.5466	38.1800	37.8812
λmax	4.91	4.92	4.91	4.92
KMML	18219.32	18265.91	18219.32	18312.51
TBVVB	0	0	0	0
VDI	0	0	0	0
VPI	0.1459	0.4463	0.1459	0.4285
QLI	3.8713	3.8846	3.8713	3.8792
VSI	-	0.9774	-	0.9775
APLR	61.4669	63.4774	61.3247	62.7286
RPCR	63.6123	63.2403	62.6236	62.9127
Vmin (Bus)	-	0.9943 (50)	-	0.9943 (50)

Table 7.10: Comparative results of loadability enhancement of 69-bus with 2 and 3 DGs for case 2

	CPF [127]	DABC [129]	HS [134]	CTLBO
Open tie/ Sectional Switch	14 55 61 59 70	14 57 6159 70	14 58 63 69 70	14 58 61 69 70
APL (kW)	98.5900	98.5900	99.6100	98.5800
RPC (kVAr)	-	92.0400	93.4320	92.0378
λmax	5.50	5.49	5.45	5.51
KMML	20968.52	20921.93	20735.54	21015.12
TBVVB	0	1	3	1
VDI	0	0.0001	0.3522E-04	6.37E-05
VPI	-	0.1834	0.1867	0.19241
QLI	-	3.7	3.6960	3.6972
VSI	-	-	0.8087	0.8306
APLR	56.172	56.172	56.1723	56.1729
RPCR	-	9.892	8.525	9.8911
Vmin	0.9495	-	0.9483	0.9495 (61)

Table 7.11: Computational time (second) for loadability enhancement with 2 DGs

Network	33 Bus	Ref.		69 Bus	Ref.
Case 2	54.7756	NA		77.7164	NA
Case 3	125.8425	NA		173.5123	NA
Case 4	126.7248	NA		175.6153	NA
Case 5	252.0567	470.639	[TS]	566.1415	NA
		1772.240	[GWO]		
		2146.489	[IHS] [128]		

7.5 COMPARISON OF COMPUTATIONAL PERFORMANCE

Table 7.5 shows the computational times of the proposed approach for different case studies while considering two DGs. The results shown in Table 7.11 are the average computational time for 150 iterations and 10 runs. The comparison of Case 5 for 33-Bus RDN shows that the computational time of the proposed approach is almost half that of [128] and is drastically reduced in comparison to gray wolf optimization (GWO) and IHS algorithms.

7.6 SUMMARY

This chapter presents a ε-constraint based multi-objective approach using CTLBO algorithm for optimal network reconfiguration and DG allocation to improve the loadability of the 33-bus and 69-bus. The results demonstrate that the proposed technique is more effective than DABC and HPSO. Results show that simultaneous network reconfiguration and DG allocation results in maximum loadability enhancement, followed by the case with only DG allocation. A comparison of Cases 3 and 5 demonstrates better results in terms of evaluation indices like KMML, QLI, VSI, VPI, APLR, RPCR and voltage profile, when power factors of the DGs are all different. A graphical approach for network reconfiguration is adopted, which is more interactive than other methods. It is also observed that violations of voltage limits occur before that of line thermal limits. The computational time taken by the proposed approach is drastically reduced in comparison GWO and IHS algorithms.

CHAPTER 8

CONCLUSIONS AND SUGGESTIONS FOR FUTURE SCOPE OF WORK

8.1 INTRODUCTION

Integration of different types of DGs in distribution networks together with variations in load necessitates proper planning and operation of DG units. As an integral part of the planning and operation of distribution networks, for smart integration of DGs, proper siting (location) and sizing of DGs is essential. This calls for techniques to optimally allocate the DG resources. This thesis investigates the development and implementation of two optimization techniques for DG allocation in radial distribution systems to improve the network performance, operational costs and environmental emission. The techniques are specifically aimed for high penetration of DGs together with an efficient use of the existing infrastructure of distribution networks. The research work is also intended to highlight the operation of DGs at optimal power factors to maximize technical, economic and environmental benefits. The work carried out in this thesis can be summarized along with its outcomes from each chapter as given below:

Chapter 1, details the various types of distributed generation resources in the global and Indian scenario. Various type of DG resources, their available sizes and implications on account of their integration in the distribution networks have been discussed. Finally, the potential of different DG resources, ongoing projects and research facilities in the Indian context have also been presented.

Chapter 2 presents an extensive literature survey on the different types of optimization

techniques available for allocation of different types of DG resources in distribution networks in the context of fulfilling specific objectives like reduction of power losses, operational costs or environmental emission, improvement of voltage profile or voltage stability etc. The contributions and the limitations of different research works in the literature in respect of development and implementation of diverse optimization techniques based on analytical, heuristic, meta-heuristic, nature-inspired and hybrid approaches have been detailed, along with the research gaps.

Chapter 3 first details the power flow technique and the load modelling followed in this thesis. Subsequently, the different types of DGs, network reconfiguration technique as well as the computational steps in the optimization algorithm(s) for DG allocation, are discussed. The details of three test radial distribution networks - the 33-bus, 69-bus and the 118-bus RDS, which are employed to investigate the efficacy of the proposed optimization techniques, are also presented.

Chapter 4 addresses the development of the CTLBO technique. The major advantages of the CTLBO e.g. its parameter independence and capability of handling both continuous as well as discrete variables, are discussed. The CTLBO is first validated on eight standard mathematical benchmark functions and is observed to give same or better results than TLBO, I-TLBO, PSO and ABC. Subsequently, CTLBO is implemented for optimal allocation of Type-I DGs in the 33-bus, 69-bus and 118-bus radial distribution networks to minimize power losses, minimize network voltage variations and maximize the VSI. Both single and multi-objective formulations are used. The multi-objective formulation uses the weighted sum and the ε-constraints methods. It is observed that CTLBO gives better result in comparison to QOTLBO and I-TLBO. Finally, CTLBO is used for optimal allocation of Type-I DGs to improve annual energy savings in the

33-bus and 69-bus.

Chapter 5 addresses the development of the HTLBO technique to mitigate the challenges posed by the CTLBO technique. The HTLBO is the hybrid of the HSA and the TLBO. While HSA explores the solution search space better, the TLBO possesses better exploitation capability thereof. Both these qualities are incorporated in the hybrid HTLBO technique. The developed optimization technique is first validated using standard mathematical benchmark functions. It is observed that HTLBO yields better or same results than TLBO, I-TLBO, PSO and ABC for single objective functions while better or comparable results for multi-objective problem than NSGA-II. Additionally, the impact of parameter variations on convergence characteristics of HTLBO is demonstrated. Subsequently, the HTLBO algorithm is used for optimal siting and sizing of Type-I DGs in the 33-bus, 69-bus and 118-bus for MOFs where minimization of power losses and VD along with maximization of VSI is achieved. It is observed that this optimization technique proves to be better than QOTLBO and TLBO.

Chapter 6 addresses the optimal allocation of Type-II DGs in the 33-bus, 69-bus and 118-bus using analytical as well as meta-heuristic approaches. It is observed that analytical approaches based on the loss sensitivity factor results in reduction in the power losses, network operational costs and environmental emission for smaller number of DGs. However, when number of DGs and objective functions increase, analytical approach for DGs allocation may result in non-optimal solutions. In light of this, CTLBO is used for network reconfiguration and optimal DG allocation in RDS. Both single as well as multi-objective formulations are used. It is observed that this results in better network voltage profile, VSI and environmental emission savings as compared to other optimization techniques like IA, BA, BFOA etc. Pareto analysis has been carried

out for the optimal allocation of Type-II DGs corresponding to different case studies to maximize the benefits for the network operators.

Chapter 7 details the analysis and investigation of maximizing the loadability of existing distribution networks. Network loadability enhancement has been carried out using Type-III DGs having varying power factors. The loadability enhancement of 33-bus and 69-bus distribution networks is achieved using multi-objective approach based on ε-constraints method. It is observed that simultaneous allocation of Type-III DGs and network reconfiguration results in maximum loadability enhancement. It is also found that this network loadability enhancement approach results in better values of network loadability indices like KMML, QLI and voltage profile with significant reduction in the network APL and computational time.

8.2 FUTURE SCOPE OF WORK

Some of the suggestions for future work as follows:

1. Performance analysis by allocating renewable energy-based DG resources (solar and wind-based sources).
2. Investigation of reliability analysis of the network by integrating dispatchable and non-dispatchable DG resources.
3. Analysis involving simultaneous uncertainty of the DG resources and the load.
4. Development of a framework for distribution network planning by simultaneously considering renewable DGs, battery energy networks, network reconfiguration, electric vehicles, capacitor banks etc.
5. Development of a coordination control policy for collaboration of renewable energy based DGs and electric vehicle units accompanied by reactive power control devices like tap changing transformers, shunt capacitors, FACTS devices etc.

List of research publications

List of papers (s) published in peer reviewed referred international journals:

1. I. A. Quadri, S. Bhowmick and D. Joshi, "A Comprehensive Technique for Optimal Allocation of Distributed Energy Resources in Radial Distribution Systems," *Applied Energy*, Vol. 211, pp. 1245-1260, 2018.
2. I. A. Quadri, S. Bhowmick and D. Joshi, "Multi-objective Approach to Maximize Loadability of Distribution Networks by Simultaneous Reconfiguration and Allocation of Distributed Energy Resources," *IET Generation Transmission and Distribution*, Vol. 12, Issue 21, pp.5700-5712, 2018.
3. I. A. Quadri, S. Bhowmick and D. Joshi, "A Hybrid Teaching-learning Based Optimization Technique for Optimal DG Sizing and Placement in Radial Distribution Systems," *Soft Computing*, pp.1-19, 2018.

List of paper(s) published in international/national conferences:

1. I. A. Quadri, S. Bhowmick and D. Joshi, "Potential of Distributed Generation Resources in India," *IEEE 1st International Conference on Power Electronics, Intelligent Control and Energy Systems (ICPEICES)*, Delhi, pp. 1-6, 2016.
2. I. A. Quadri, S. Bhowmick and D. Joshi, "Analytical Approach for Multiple DSTATCOM Allocation in Radial Distribution Systems for Enhancement of Energy, Cost and Emission Savings," *2nd IEEE International Conference on Power Electronics, Intelligent Control and Energy Systems (ICPEICES)*, Delhi, pp. 1-6, 2018.

References

[1] I. A. Quadri, S. Bhowmick and D. Joshi, "Potential of Distributed Generation Resources in India," *IEEE 1st International Conference on Power Electronics, Intelligent Control and Energy Systems (ICPEICES)*, Delhi,India, 4-6 June 2016.

[2] "Distributed Generation in Liberalized Electricity Markets," IEA, France, 2002.

[3] T. Ackermann, G. Andersson and L. Soder, "Distributed Generation: A Definition," *Electric Power Systems Research*, vol. 57, no. 3, pp. 195-204, 2001.

[4] P. Dondi, D. Bayoumi, C. Haederli, D. Julian and M. Suter, "Network Integration of Distributed Power Generation," *Journal of Power Sources*, vol. 106, no. 1-2, pp. 1-9, 2002.

[5] T. Basso and N. R. Friedman , "IEEE 1547 National Standard for Interconnecting Distributed Generation: How Could It Help my Facility?," National Renewable Energy Laboratory, Golden, Colorado, 2003.

[6] T. N. Preda, K. Uhlen and D. E. Nordgard, "An Overview of the Present Grid Codes for Integration of Distributed Generation," *CIRED 2012 Workshop: Integration of Renewables into the Distribution Grid*, Lisbon, Portugal, 29-30 May 2012.

[7] "Special Report on Renewable Energy Sources and ClimateChange Mitigation," *IPCC*,Cambridge University Press, Cambridge, United Kingdom and New York, NY, USA, 2012.

[8] H. Ritchie and M. Roser, "https://ourworldindata.org/renewable-energy," University of Oxford, UK, 2016.

[9] M. Hoogwijk and W. Graus, "Global Potential of Renewable Energy Sources: a Literature Assessment," REN21, 2008.

[10] S. N. Singh, J. Ostergaard and N. Jain, "Distributed Generation in Power Systems: An Overview and Key Issues," *24rth Indian Engineering Congress* , NIT Surathkal, Kerala, December 10-13, 2009.

[11] M. Cruz, Y. Adriana , C. Sanchez , M. Francy , B. Grimoni, J. Aquiles and L. B. Reis, "Analysis of Sub-transmission Networks With Distributed Generation," *International Conference on Renewable Energy Research and Applications*, Madrid, Spain, 20-23 October,2013.

[12] L. Aleixo, T. Solvang, M. Istad and D. E. Nordgard, "Experiences From Integrating Distributed Generation in Norway: Results From a DSO Survey 2010/2011," *CIRED 2012 Workshop: Integration of Renewables into the Distribution Grid*, Lisbon, Portugal, 29-30 May 2012.

[13] B. L. Schenkman, D. G. Wilson, R. D. Robinett and K. Kukolich, "Photovoltaic Distributed Generation for Lanai Power Grid Real-time Simulation and Control Integration Scenario," *International Symposium on Power Electronics*,

Electrical Drives, Automation and Motion:SPEEDAM 2010, Pisa, Italy, 14-16 June 2010.

[14] H. Ying, E. Eriksson and A. Holm, "Application Study of Distributed Generation Its Impact on Reliability of a Vattenfall's Distribution System," *2010 IEEE 11th International Conference on Probabilistic Methods Applied to Power Systems (PMAPS)*, Singapore, 14-17 June 2010.

[15] N. G. A. Hemdan and M. Kurrat, "Effect of Integration of Distributed Wind Generation into a Real MV Distribution Network: A Case Study using Measured Wind Data and Simulated Load Profiles," *IEEE PES General Meeting*, Providence, RI, USA, 25-29 July 2010.

[16] P. S. Georgilakis and N. D. Hatziargyriou, "Optimal Distributed Generation Placement in Power Distribution Networks: Models, Methods and Future Research," *IEEE Transactions on Power Systems*, vol. 28, no. 3, pp. 3420-3428, 2013.

[17] M. R. Miveh, M. Gandomkar, S. Mirsaeidi and M. R. Gharibdoost, "A Review on Protection Challenges in Microgrids," *2012 Proceedings of 17th Conference on Electrical Power Distribution*, Tehran, Iran, 2-3 May 2012.

[18] S. C. Jangam and H. T. Jadhav , "Protective Systems for Wind Farms and Its Interconnection to Grid- A Review," *2012 Green Technologies (ICGT) International Conference*, Trivandrum, Kerala, India., 8-20 December 2012.

[19] L. F. F. Gutierres , G. Cardoso and G. Marchesan, "Recloser-fuse Coordination Protection for Distributed Generation Systems: Methodology and Priorities for Optimal Disconnections," *12th IET International Conference on Developments in Power System Protection (DPSP 2014)*, Copenhagen, Denmark, 31 March-3 April 2014.

[20] C. Gonzalez, R. Ramirez, R. Villafafila and A. Sumper, "Assess the Impact of PhotoVoltaic Generation Systems on Low-voltage Network: Software Analysis Tool Development," *9th International Conference on Electrical Power Quality and Utilisation*, Barcelona, 9-11 October 2007.

[21] S. K. Khadem, M. Basu and M. F. Conlon, "Integration of UPQC for Power Quality Improvement in Distributed Generation Network – A Review," *2011 2nd IEEE PES International Conference and Exhibition on Innovative Smart Grid Technologies*, Manchester, UK, 5-7 December 2011.

[22] R. A. F. Currie, G. W. Ault, C. E. T. Foote, N. M. McNeill and A. K. Gooding, "Smarter Ways to Provide Grid Connections for Renewable Generators," *IEEE PES General Meeting*, Providence, RI, USA, 25-29 July 2010.

[23] P. K. Olulope, K. A. Folly, S. Chowdhury and S. P. Chowdhury, "Dynamic Impact and Assessment of Stability of Power Systems with DG Penetration: A review," *45th International Universities Power Engineering Conference UPEC2010*, Cardiff, Wales, UK, 31 August-3 September 2010.

[24] "Annual Report," Ministry of Renewable Energy,Govenrment of India, Delhi, India, 2017-18.

[25] D. Goenka and S. Guttikunda, "Coal Kills: An Assessment of Death and Disease Caused by India's Dirtiest Energy Source," Conservation Action Trust, Mumbai.2013

[26] A. Zervos, "Renewables 2017 Global Status Report," REN21 Secretariat, Paris, 2017.

[27] S. N. Singh, J. Ostergaard and N. Jain, "Distributed Generation in Power Systems: An Overview and Key Issues," *24th Indian Engineering Congress*, NIT Surathkal;Kerala, 2009.

[28] L. H. Loong, V. P. Sabev and K. J. Jaromir, "Regional Renewable Energy and Resource Planning," *Applied Energy*, vol. 88, no. 2, pp. 545-550, 2011.

[29] C. Paola, M. Massimiliano and C. Gaia, "Paradigm Shift in Urban Energy Systems Through Distributed Generation: Methods and Models," *Applied Energy*, vol. 88, no. 4, pp. 1032-1048, 2011.

[30] H. L. Willis, "Analytical Methods and Rules of Thumb for Modeling DG-Distribution Interaction," *2000 Power Engineering Society Summer Meeting*, Seattle, WA, USA, 2000.

[31] C. Wang and M. H. Nehrir, "Analytical Approaches for Optimal Placement of Distributed Generation Sources in Power Systems," *IEEE Transactions on Power Systems*, vol. 19, no. 4, pp. 2068-2076, 2004.

[32] N. Acharya, P. Mahat and N. Mithulananthan, "An Analytical Approach for DG Allocation in Primary Distribution Network," *International Journal of Electrical Power & Energy Systems*, vol. 28, no. 10, pp. 669-678, 2006.

[33] T. Gozel and M. HakanHocaoglu, "An Analytical Method for the Sizing and Siting of Distributed Generators in Radial Systems," *Electric Power Systems Research*, vol. 79, no. 6, pp. 912-918, 2009.

[34] S. Elsaiah , M. Benidris and J. Mitra, "Analytical Approach for Placement and Sizing of Distributed Generation on Distribution Systems," *IET Generation, Transmission & Distribution*, vol. 8, no. 6, pp. 1039-1049, 2014.

[35] D. Q. Hung, N. Mithulananthan and R. C. Bansal, "Analytical Expressions for DG Allocation in Primary Distribution Networks," *IEEE Transactions on Energy Conversion*, vol. 25, no. 3, pp. 814-820, 2010.

[36] S. G. Naik, D. K. Khatod and M. P. Sharma, "Optimal Allocation of Combined DG and Capacitor for Real Power Loss Minimization in Distribution Networks," *International Journal of Electrical Power & Energy Systems*, vol. 53, pp. 967-973, 2013.

[37] M. M. Aman, G. B. Jasmon, H. Mokhlis and A. H. Bakar, "Optimal Placement and Sizing of a DG Based on a New Power Stability Index and Line Losses," *International Journal of Electrical Power & Energy Systems*, vol. 43, no. 1, pp. 1296-1304, 2012.

[38] V. Murthy and A. Kumar, "Comparison of Optimal DG Allocation Methods in Radial Distribution Systems Based on Sensitivity Approaches," *International Journal of Electrical Power & Energy Systems,* vol. 53, pp. 450-467, 2013.

[39] J. H. Teng, T. S. Luor and Y. H. Liu, "Strategic Distributed Generator Placements for Service Reliability Improvements," *IEEE Power Engineering Society Summer Meeting,*, Chicago, IL, USA, USA, 21-25 July 2002.

[40] G. Carpinelli, G. Celli, F. Pilo and A. Russo, "Distributed Generation Siting and Sizing Under Uncertainty," *2001 IEEE Porto Power Tech Proceedings*, Porto, Portugal, Portugal, 10-13 September 2001.

[41] T. S. Chung, Y. Z. Li and Z. Y. Wang, "Optimal Generation Expansion Planning via Improved Genetic Algorithm Approach," *International Journal of Electrical Power & Energy Systems,* vol. 26, no. 8, pp. 655-659, 2004.

[42] G. Mokryani and P. Siano, "Optimal Wind Turbines Placement Within a Distribution Market Environment," *Applied Soft Computing,* vol. 13, no. 10, pp. 4038-4046, 2013.

[43] F. Ugranlı and E. Karatepe, "Optimal Wind Turbine Sizing to Minimize Energy Loss," *International Journal of Electrical Power & Energy Systems,* vol. 53, pp. 656-663, 2013.

[44] S. A. Eroshenko, A. I. Khalyasmaa, S. A. Dmitriev, A. V. Pazderin and A. A. Karpenko, "Distributed Generation Siting and Sizing With Implementation Feasibility Analysis," *2013 International Conference on Power, Energy and Control (ICPEC),* Sri Rangalatchum Dindigul, India, 6-8 February 2013.

[45] W. Sheng, K.Y. Liu, Y. Liu, X. Meng and Y. Li, "Optimal Placement and Sizing of Distributed Generation via an Improved Nondominated Sorting Genetic Algorithm II," *IEEE Transactions on Power Delivery,* vol. 30, no. 2, pp. 569 - 578, 2015.

[46] I. C. d. Silva, S. Carneiro, E. J. d. Oliveira, J. d. S. Costa, J. L. R. Pereira and P. A. N. Garcia, "A Heuristic Constructive Algorithm for Capacitor Placement on Distribution Systems," *IEEE Transactions on Power Systems,* vol. 23, no. 4, pp. 1619 - 1626, 2008.

[47] T. Gozel, M. Hocaoglu, U. Eminoglu and A. Balikci, "Optimal Placement and Sizing of Distributed Generation on Radial Feeder With Different Static Load Models," *2005 International Conference on Future Power Systems,* Amsterdam, Netherlands, 18-18 November 2005.

[48] S. Kansal, V. Kumar and B. Tyagi, "Optimal Placement of Different Type of DG Sources in Distribution Networks," *International Journal of Electrical Power & Energy Systems,* vol. 53, pp. 752-760, 2013.

[49] R. S. Maciel, M. Rosa, V. Miranda and P. F. Antonio, "Multi-objective Evolutionary Particle Swarm Optimization in the Assessment of the Impact of Distributed Generation," *Electric Power Systems Research,* vol. 89, pp. 100-108, 2012.

[50] M. Gomez-Gonzalez, A. Lopez and F. Jurado, "Optimization of Distributed Generation Systems Using a New Discrete PSO and OPF," *Electric Power Systems Research,* vol. 84, no. 1, pp. 174-180, 2012.

[51] H. Nasiraghdam and S. Jadid, "Optimal Hybrid PV/WT/FC Sizing and Distribution System Reconfiguration Using Multi-objective Artificial Bee Colony (MOABC) Algorithm," *Solar Energy,* vol. 86, no. 10, pp. 3057-3071, 2012.

[52] T. Niknam, S. I. Taheri, J. Aghaei, S. Tabatabaei and M. Nayeripour, "A Modified Honey Bee Mating Optimization Algorithm for Multiobjective Placement of Renewable Energy Resources," *Applied Energy,* vol. 88, no. 12, pp. 4817-4830, 2011.

[53] Z. Moravej and A. Akhlaghi, "A Novel Approach Based on Cuckoo Search for DG Allocation in Distribution Network," *International Journal of Electrical Power & Energy Systems,* vol. 44, no. 1, pp. 672-679, January 2013.

[54] I. A. Mohamed and M. Kowsalya , "Optimal Size and Siting of Multiple Distributed Generators in Distribution System Using Bacterial Foraging Optimization," *Swarm and Evolutionary Computation,* vol. 15, pp. 58-65, 2014.

[55] S. Devi and M. Geethanjali, "Application of Modified Bacterial Foraging Optimization Algorithm for Optimal Placement and Sizing of Distributed Generation," *Expert Systems with Applications,* vol. 41, no. 6, pp. 2772-2781, 2014.

[56] M. H. Sulaiman, M. W. Mustafa, A. Azmi, O. Aliman and S. R. A. Rahim, "Optimal Allocation and Sizing of Distributed Generation in Distribution System via Firefly Algorithm," *2012 IEEE International Power Engineering and Optimization Conference*, Melaka, Malaysia, 6-7 June 2012.

[57] M. Gandomkar, M. Vakilian and M. Ehsan, "Optimal Distributed Generation Allocation in Distribution Network Using Hereford Ranch Algorithm," *2005 International Conference on Electrical Machines and Systems*, Nanjing, China, 27-29 September 2005.

[58] M. N. Dehghani, M. B. Farhang and k. Hamed, "Optimal Allocation and Sizing of Distributed Generation in Distribution Network Using Modified Shuffled Leaping Algorithm," *SAUSSUREA,* vol. 5, no. 6, pp. 75-86, 2015.

[59] S. Saha and V. Mukherjee, "Optimal Placement and Sizing of DGs in RDS Using Chaos Embedded SOS Algorithm," *IET Generation, Transmission & Distribution,* vol. 10, no. 14, pp. 3671 - 3680, 2016 .

[60] S. H. Lee and J.W. Park, "Selection of Optimal Location and Size of Multiple Distributed Generations by Using Kalman Filter Algorithm," *IEEE Transactions on Power Systems,* vol. 24, no. 3, pp. 1393 - 1400, 2009.

[61] W. Sheng, K.Y. Liu, Y. Liu, X. Ye and K. He, "Reactive Power Coordinated Optimisation Method With Renewable Distributed Generation Based on

Improved Harmony Search," *IET Generation, Transmission & Distribution,* vol. 10, no. 13, pp. 3152 - 3162, 2016.

[62] T. Niknam, M. Bornapour and A. Gheisari, "Combined Heat, Power and Hydrogen Production Optimal Planning of Fuel Cell Power Plants in Distribution Networks," *Energy Conversion and Management,* vol. 66, pp. 11-25, 2013.

[63] B. Mohanty and S. Tripathy, "A Teaching Learning Based Optimization Technique for Optimal Location and Size of DG in Distribution Network," *Journal of Electrical Systems and Information Technology,* vol. 3, no. 1, pp. 33-44, 2016.

[64] J. A. Garcia and A. J. Mena, "Optimal Distributed Generation Location and Size Using a Modified Teaching–learning Based Optimization Algorithm," *International Journal of Electrical Power & Energy Systems,* vol. 50, pp. 65-75, 2013.

[65] S. Sultana and P. K. Roy, "Multi-objective Quasi-oppositional Teaching Learning Based Optimization for Optimal Location of Distributed Generator in Radial Distribution Systems," *International Journal of Electrical Power & Energy Systems,* vol. 63, pp. 534-545, 2014.

[66] N. Kanwar, N. Gupta, K. R. Niazi and A. Swarnkar, "Simultaneous Allocation of Distributed Resources using Improved Teaching Learning Based Optimization," *Energy Conversion and Management,* vol. 103, pp. 387-400, 2015.

[67] Q. K. Pan, P. N. Suganthan, M. F. Tasgetiren and J. J. Liang, "A Self-adaptive Global Best Harmony Search Algorithm for Continuous Optimization Problems," *Applied Mathematics and Computation,* vol. 216, no. 3, pp. 830-848, 2010.

[68] M. Mahdavi, M. Fesanghary and E. Damangir, "An Improved Harmony Search Algorithm for Solving Optimization Problems," *Applied Mathematics and Computation,* vol. 188, no. 2, pp. 1567-1579, 2007.

[69] P. Yadav, R. Kumar, S. K. Panda and C. S. Chang, "An Intelligent Tuned Harmony Search Algorithm for Optimisation," *Information Sciences,* vol. 196, pp. 47-72, 2012.

[70] S. Das, A. Mukhopadhyay, A. Roy, A. Abraham and B. K. Panigrahi, "Exploratory Power of the Harmony Search Algorithm: Analysis and Improvements for Global Numerical Optimization," *IEEE Transactions on Systems, Man, and Cybernetics, Part B (Cybernetics),* vol. 41, no. 1, pp. 89-106, 2011.

[71] D. Zou, L. Gao, J. Wu and S. Li, "Novel Global Harmony Search Algorithm for Unconstrained Problems," *Neurocomputing,* vol. 73, no. 16-18, pp. 3308-3318, 2010.

[72] S. Tuo, J. Zhang, L. Yong, X. Yuan, B. Liu, X. Xu and F. Deng, "A Harmony Search Algorithm for High-dimensional Multimodal Optimization Problems," *Digital Signal Processing,* vol. 46, pp. 151-163, 2015.

[73] J. Chen, Q. k. Pan and J. Q. Li, "Harmony Search Algorithm With Dynamic Control Parameters," *Applied Mathematics and Computation,* vol. 219, no. 2, pp. 592-604, 2012.

[74] A. Kattan and R. Abdullah, "A Dynamic Self-adaptive Harmony Search Algorithm for Continuous Optimization Problems," *Applied Mathematics and Computation,* vol. 219, no. 16, pp. 8542-8567, 2013.

[75] N. Kanwar, N. Gupta, K. R. Niazi, A. Swarnkar and R. C. Bansal, "Simultaneous Allocation of Distributed Energy Resource using Improved Particle Swarm Optimization," *Applied Energy,* vol. 185, no. 2, pp. 1684-1693, 2017.

[76] S. F. Santos, D. Z. Fitiwi, M. R. Cruz, C. M. Cabrita and J. P. Catalao, "Impacts of Optimal Energy Storage Deployment and Network Reconfiguration on Renewable Integration Level in Distribution Systems," *Applied Energy,* vol. 185, no. 1, pp. 44-55, 2017.

[77] B. C. Ampimah, M. Sun, D. Han and X. Wang, "Optimizing Sheddable and Shiftable Residential Electricity Consumption by Incentivized Peak and Off-peak Credit Function Approach," *Applied Energy,* vol. 210, pp. 1299-1309, 2018.

[78] M. A. Kazemi, M. Sedighizadeh, M. J. Mirzaei and O. Homaee, "Optimal Siting and Sizing of Distribution System Operator Owned EV Parking Lots," *Applied Energy,* vol. 179, pp. 1176-1184, 2016.

[79] M. Farhoodnea, A. Mohamed, H. Shareef and H. Zayandehroodi, "Optimum D-STATCOM Placement using Firefly Algorithm for Power Quality Enhancement," *2013 IEEE 7th International Power Engineering and Optimization Conference (PEOCO)*, Langkawi, Malaysia, 3-4 June 2013.

[80] F. Shahnia, R. P. Chandrasena, A. Ghosh and S. Rajakaruna, "Application of DSTATCOM for Surplus Power Circulation in MV and LV Distribution Networks With Single-phase Distributed Energy Resources," *2014 IEEE PES General Meeting | Conference & Exposition*, National Harbor, MD, USA, 27-31 July 2014.

[81] C.S. Chen, C. H. Lin, W. L. Hsieh, C. T. Hsu and T. T. Ku, "Enhancement of PV Penetration With DSTATCOM in Taipower Distribution System," *IEEE Transactions on Power Systems,* vol. 28, no. 2, pp. 1560 - 1567, 2013.

[82] D. Das, "Optimal Placement of Capacitors in Radial Distribution System using a Fuzzy-GA Method," *International Journal of Electrical Power & Energy Systems,* vol. 30, no. 6-7, pp. 361-367, 2008.

[83] V. Haldar and N. Chakraborty, "Power Loss Minimization by Optimal Capacitor Placement in Radial Distribution System using Modified Cultural Algorithm,"

International Transactions on Electrical Energy Systems, vol. 25, no. 1, pp. 54-71, 2015.

[84] N. Kanwar, N. Gupta, A. Swarnkar, K. R. Niazi and R. C. Bansal, "New Sensitivity Based Approach for Optimal Allocation of Shunt Capacitors in Distribution Networks using PSO," *Energy Procedia,* vol. 75, pp. 1153-1158, 2015.

[85] A. R. Jordehi, "Brainstorm Optimisation Algorithm (BSOA): An Efficient Algorithm for Finding Optimal Location and Setting of FACTS Devices in Electric Power Systems," *International Journal of Electrical Power & Energy Systems,* vol. 69, pp. 48-57, 2015.

[86] P. W. Lehn, "A Benchmark System for Simulation of the D-STATCOM," *2002 IEEE Power Engineering Society Winter Meeting. Conference Proceedings*, New York, NY, USA, USA, 27-31 January 2002.

[87] E. Acha, C. R. Fuerte-Esquivel, H. Ambriz-Perez and C. Angeles-Camacho, "FACTS: Modelling and Simulation in Power Networks," John Wiley & Sons, 2004.

[88] S. Devi and M. Geethanjali, "Optimal Location and Sizing Determination of Distributed Generation and DSTATCOM using Particle Swarm Optimization Algorithm," *International Journal of Electrical Power & Energy Systems,* vol. 62, pp. 562-570, 2014.

[89] R. Majumder, "Reactive Power Compensation in Single-Phase Operation of Microgrid," *IEEE Transactions on Industrial Electronics,* vol. 60, no. 4, pp. 1403-1416, 2013.

[90] R. Sirjani and A. R. Jordehi, "Optimal Placement and Sizing of Distribution Static Compensator (D-STATCOM) in Electric Distribution Networks: A review," *Renewable and Sustainable Energy Reviews,* vol. 77, pp. 688-694, 2017.

[91] G. Mokhtari, G. Nourbakhsh, F. Zare and A. Ghosh, "A New Distributed Control Strategy to Coordinate MultipleDSTATCOMS in LV Network," *2013 4th IEEE International Symposium on Power Electronics for Distributed Generation Systems (PEDG)*, Rogers, AR, USA, 8-11 July 2013.

[92] R. E. Brown , Electric Power Distribution Reliability, USA: CRC press, 2008.

[93] M. H. Bollen , Understanding power quality problems, New York: IEEE Press, 2000.

[94] S. M. S. S M Suhail Hussain and M. Subbaramiah, "An Analytical Approach for Optimal Location of DSTATCOM in Radial Distribution System,"*2013 International Conference on Energy Efficient Technologies for Sustainability*, Nagercoil, India, 10-12 April 2013.

[95] A. Bagherinasab, M. Zadehbagheri, S. A. Khalid, M. Gandomkar and N. A. Azli, "Optimal Placement of D-STATCOM Using Hybrid Genetic and Ant Colony

Algorithm to Losses Reduction," *International Journal of Applied Power Engineering*, vol. 2, no. 2, pp. 53-60, 2013.

[96] A. R. Gupta and A. Kumar, "Energy Saving Using D-STATCOM Placement in Radial Distribution System Under Reconfigured Network," *Energy Procedia*, vol. 90, pp. 124-136, 2016.

[97] S. M. Hussain and N. Visali, "Identification of Weak Buses Using Voltage Stability Indicator and Its Voltage Profile Improvement by Using DSTATCOM in Radial Distribution Systems," *IOSR Journal of Electrical And Electronics Engineering (IOSRJEEE)*, vol. 2, no. 4, pp. 17-23, 2012.

[98] A. R. Gupta and A. Kumar, "Optimal Placement of D-STATCOM in Distribution Network Using New Sensitivity Index With Probabilistic Load Models," *2015 2nd International Conference on Recent Advances in Engineering & Computational Sciences (RAECS)*, Chandigarh, India, 21-22 December 2015.

[99] A. R. Gupta and A. Kumar, "Optimal Placement of D-STATCOM Using Sensitivity Approaches in Mesh Distribution System With Time Variant Load Models Under Load Growth," *Ain Shams Engineering Journal*, vol. 9, no. 4, pp. 783-799, 2018.

[100] S. A. Taher and S. A. R. Afsari, "Optimal Location and Sizing of DSTATCOM in Distribution Dystems by Immune Algorithm," *International Journal of Electrical Power & Energy Systems*, vol. 60, pp. 34-44, 2014.

[101] S. Jazebi, S. H. Hosseinian and B. Vahidi, "DSTATCOM Allocation in Distribution Networks Considering Reconfiguration Using Differential Evolution Algorithm," *Energy Conversion and Management*, vol. 52, no. 7, pp. 2777-2783, 2011.

[102] S. Nesrallh, A. Mohamed and H. Shareef, "Reliability Improvement in Distribution Systems by Optimal Placement of DSTATCOM Using Binary Gravitational Search Algorithm," *Przeglad Elektrotechniczny*, vol. 88, no. 2, pp. 295-299, 2012.

[103] N. Kanwar, N. Gupta, K. R. Niazi and A. Swarnkar, "Improved Cat Swarm Optimization for Simultaneous Allocation of DSTATCOM and DGs in Distribution Systems," *Journal of Renewable Energy*, p. 10, 2015.

[104] T. Yuvaraj, K. R. Devabalaji and K. Ravi, "Optimal Placement and Sizing of DSTATCOM Using Harmony Search Algorithm," *Energy Procedia*, vol. 79, pp. 759-765, 2015.

[105] B. H. Tolabi, H. M. Ali and M. Rizwan, "Simultaneous Reconfiguration, Optimal Placement of DSTATCOM, and Photovoltaic Array in a Distribution System Based on Fuzzy-ACO Approach," *IEEE Transactions on Sustainable Energy*, vol. 6, no. 1, pp. 210 - 218, 2015.

[106] B. S. Chabok and A. Ashouri, "Optimal Placement of D-STATCOMs into the Radial Distribution Networks in the Presence of Distributed Generations,"

American Journal of Electrical and Electronic Engineering, vol. 4, no. 2, pp. 40-48, 2016.

[107] J. Yaghoobi, M. Islam and N. Mithulananthan, "Analytical Approach to Assess the Loadability of Unbalanced Distribution Grid With Roof Top PV Units," *Applied Energy,* vol. 211, pp. 358-367, 2018.

[108] Q. D. Hung and N. Mithulananthan, "Loss Reduction and Loadability Enhancement With DG: A dual-Index Analytical Approach," *Applied Energy,* vol. 115, pp. 233-241, 2014.

[109] M. M. Aman, G. B. Jasmon, A. H. Bakar and H. Mokhlis, "A New Approach for Optimum Simultaneous Multi-DG Distributed Generation Units Placement and Sizing Based on Maximization of System Loadability Using HPSO (Hybrid Particle Swarm Optimization) Algorithm," *Energy,* vol. 66, pp. 202-215, 2014.

[110] L. Luo, W. Gu, X. P. Zhang, G. Cao, W. Wang, G. Zhu, D. You and Z. Wu, "Optimal Siting and Sizing of Distributed Generation in Distribution Systems With PV Solar Farm Utilized as STATCOM (PV-STATCOM)," *Applied Energy,* vol. 210, pp. 1092-1100, 2018.

[111] D. Q. Hung, N. Mithulananthan and R. C. Bansal, "Analytical Strategies for Renewable Distributed Generation Integration Considering Energy Loss Minimization," *Applied Energy,* vol. 105, pp. 75-85, 2013.

[112] J. H. Braslavsky, J. R. Wall and L. J. Reedman, "Optimal Distributed Energy Resources and the Cost of Reduced Greenhouse Gas Emissions in a Large Retail Shopping Centre," *Applied Energy,* vol. 155, pp. 120-130, 2015.

[113] I. A. Quadri, S. Bhowmick and D. Joshi, "A Comprehensive Technique for Optimal Allocation of Distributed Energy Resources in Radial Distribution Systems," *Applied Energy,* pp. 1245-1260, 2018.

[114] R. S. Rao, K. Ravindra, K. Satish and S. V. L. Narasimham, "Power Loss Minimization in Distribution System Using Network Reconfiguration in the Presence of Distributed Generation," *IEEE Transactions on Power Systems,* vol. 28, no. 1, pp. 317 - 325, 2013.

[115] M. Ali, A. Dymarsky and K. Turitsyn, "Transversality Enforced Newton–Raphson Algorithm for Fast Calculation of Maximum Loadability," *IET Generation, Transmission & Distribution,* vol. 12, no. 8, pp. 1729 - 1737, 2018.

[116] R. S. Al Abri, E. F. El-Saadany and Y. M. Atwa, "Optimal Placement and Sizing Method to Improve the Voltage Stability Margin in a Distribution System Using Distributed Generation," *IEEE Transactions on Power Systems,* vol. 28, no. 1, pp. 326-334, 2013.

[117] N. Ghanbari, H. Mokhtari and S. Bhattacharya , "Optimizing Operation Indices Considering Different Types of Distributed Generation in Microgrid Applications," *Energies,* vol. 11, no. 894, 2018.

[118] R. B. Prada and L. J. Souza, "Voltage Stability and Thermal Limit: Constraints on the Maximum Loading of Electrical Energy Distribution Feeders," *IEE*

Proceedings - Generation, Transmission and Distribution, vol. 145, no. 5, pp. 573-577, 1998.

[119] M. H. Moradi and M. Abedini, "A Combination of Genetic Algorithm and Particle Swarm Optimization for Optimal DG Location and Sizing in Distribution Systems," *International Journal of Electrical Power & Energy Systems,* vol. 34, no. 1, pp. 66-74, 2012.

[120] S. Sivanagaraju, N. Visali, V. Sankar and T. Ramana, "Enhancing Voltage Stability of Radial Distribution Systems by Network Reconfiguration," *Electric Power Components and Systems,* vol. 33, no. 5, pp. 539-550, 2005.

[121] D. Das, "Maximum Loading and Cost of Energy Loss of Radial Distribution Feeders," *International Journal of Electrical Power & Energy Systems,* vol. 26, no. 4, pp. 307-314, 2004.

[122] A. Augugliaro, L. Dusonchet, S. Favuzza, M. G. Ippolito and E. R. Sanseverino, "A Simple Method to Assess Loadability of Radial Distribution Networks," *2005 IEEE Russia Power Tech,* St. Petersburg, Russia, 27-30 June 2005.

[123] M. Moghavvemi and M. O. Faruque, "Technique for Assessment of Voltage Stability in Ill-conditioned Radial Distribution Network," *IEEE Power Engineering Review,* vol. 21, no. 1, pp. 58-60, 2001.

[124] B. Venkatesh, R. Ranjan and H. B. Gooi, "Optimal Reconfiguration of Radial Distribution Systems to Maximize Loadability," *IEEE Transactions on Power Systems,* vol. 19, no. 1, pp. 260 - 266, 2004.

[125] J. Yu, W. Li and W. Yan, "Letter to the Editor: A New Line Loadability Index for Radial Distribution Systems," *Electric Power Components and Systems,* vol. 36, no. 11, pp. 1245-1252, 2008.

[126] Y. T. Hsiao and C. Y. Chien, "Multiobjective Optimal Feeder Reconfiguration," *IEE Proceedings - Generation, Transmission and Distribution,* vol. 148, no. 4, pp. 333-336, 2001.

[127] M. M. Aman, G. B. Jasmon, A. H. Bakar and H. Mokhlis, "Optimum Network Reconfiguration Based on Maximization of System Loadability Using Continuation Power Flow Theorem," *International Journal of Electrical Power & Energy Systems,* vol. 54, pp. 123-133, 2014.

[128] A. Tyagi, A. Verma and P. R. Bijwe, "Reconfiguration for Loadability Limit Enhancement of Distribution Systems," *IET Generation, Transmission & Distribution,* vol. 12, no. 1, pp. 88-93, 2018.

[129] M. M. Aman, G. B. Jasmon, H. Mokhlis and A. H. A. Bakar, "Optimum Tie Switches Allocation and DG Placement Based on Maximisation of System Loadability Using Discrete Artificial Bee Colony Algorithm," *IET Generation, Transmission & Distribution,* vol. 10, no. 10, pp. 2277-2284, 2016.

[130] M. Nuri, M. R. Miveh, S. Mirsaeidi and M. R. Gharibdoost, "Distributed Generation Placement to Maximize the Loadability of Distribution System

Using Genetic Algorithm," *2012 Proceedings of 17th Conference on Electrical Power Distribution*, Tehran, Iran, 2-3 May 2012.

[131] N. C. Hien, N. Mithulananthan and R. C. Bansal, "Location and Sizing of Distributed Generation Units for Loadabilty Enhancement in Primary Feeder," *IEEE Systems Journal,* vol. 7, no. 4, pp. 797-806, 2013.

[132] K. R. Guerriche and T. Bouktir, "Maximum Loading Point in Distribution System With Renewable Resources Penetration," *2014 International Renewable and Sustainable Energy Conference (IRSEC),* Ouarzazate, Morocco, 17-19 October 2014.

[133] M. Zarei and A. Zangeneh, "Multi-objective Optimization Model for Distribution Network Reconfiguration in the Presence of Distributed Generations," *International Transactions on Electrical Energy Systems,* vol. 27, no. 12, e2425, 2017.

[134] I. Ali , M. S. Thomas and P. Kumar, "Energy Efficient Reconfiguration for Practical Load Combinations in Distribution Systems," *IET Generation, Transmission & Distribution,* vol. 9, no. 11, pp. 1051-1060, 2015.

[135] P. Kumar, I. Ali , M. S. Thomas and S. Singh, "Imposing Voltage Security and Network Radiality for Reconfiguration of Distribution Systems Using Efficient Heuristic and Meta-heuristic Approach," *IET Generation, Transmission & Distribution,* vol. 11, no. 10, pp. 2457-2467, 2017.

[136] Y.Y. Fu and H. D. Chiang, "Toward Optimal Multi-period Network Reconfiguration for Increasing the Hosting Capacity of Distribution Networks," *2017 IEEE Power & Energy Society General Meeting*, Chicago, IL, USA, 16-20 July 2017.

[137] M. E. Baran and F. F. Wu, "Network Reconfiguration in Distribution Systems for Loss Reduction and Load Balancing," *IEEE Transactions on Power Delivery,* vol. 4, no. 2, pp. 1401-1407, 1989.

[138] D. Zhang, Z. Fu and L. Zhang, "An Improved TS Algorithm for Loss-minimum Reconfiguration in Large-scale Distribution Systems," *Electric Power Systems Research,* vol. 77, no. 5-6, pp. 685-694, 2007.

[139] W. D. Stevenson, Elements of Power System Analysis, India: McGraw-Hill, 1982.

[140] W. F. Tinney and C. E. Hart, "Power Flow Solution by Newton's Method," *IEEE Transactions on Power Apparatus and Systems,* Vol. PAS-86, no. 11, pp. 1449 - 1460, 1967.

[141] B. Stott and O. Alsac, "Fast Decoupled Load Flow," *IEEE Transactions on Power Apparatus and Systems,* Vol. PAS-93, no. 3, pp. 859-869, 1974.

[142] T. H. Chen, M. S. Chen, K. J. Hwang, P. Kotas and E. A. Chebli, "Distribution System Power Flow Analysis-A Rigid Approach," *IEEE Transactions on Power Delivery,* vol. 6, no. 3, pp. 1146-1152, 1991.

[143] D. Shirmohammadi, H. W. Hong, A. Semlyen and G. X. Luo, "A Compensation-Based Power Flow Method for Weakly Meshed Distribution and Transmission Networks," *IEEE Transactions on Power Systems,* vol. 3, no. 2, pp. 753-762, 1988.

[144] R. D. Zimmerman and H. D. Chiang, "Fast Decoupled Power Flow for Unbalanced Radial Distribution Systems," *IEEE Transactions on Power Systems,* vol. 10, no. 4, pp. 2045-2052, 1995.

[145] J. H. Teng, "A Network-Topology-based Three-Phase Load Flow for Distribution Systems," *Proceedings of the National Science Council, Republic of China,* vol. 24, no. 4, pp. 259-264, 2000.

[146] R. Rajaram, K. S. Kumar and N. Rajasekar, "Power System Reconfiguration in a Radial Distribution Network for Reducing Losses and to Improve Voltage Profile Using Modified Plant Growth Simulation Algorithm With Distributed Generation (DG)," *Energy Report,* vol. 1, pp. 116-122, 2015.

[147] S. K. Goswami and S. K. Basu, "Direct Solution of Distribution Systems," *IEE Proceedings C - Generation, Transmission and Distribution,* vol. 138, no. 1, pp. 78-88, 1991.

[148] M. Esmaeili, M. Sedighizadeh and M. Esmaili, "Multi-objective Optimal Reconfiguration and DG (Distributed Generation) Power Allocation in Distribution Networks Using Big Bang-Big Crunch Algorithm Considering Load Uncertainty," *Energy,* vol. 103, pp. 86-99, 2016.

[149] M. Ettehadi, H. Ghasemi and S. Vaez-Zadeh, "Voltage Stability-Based DG Placement in Distribution Networks," *IEEE Transactions on Power Delivery,* vol. 28, no. 1, pp. 171-178, 2013.

[150] S. G. Asper, C. O. Nwankpa, R. W. Bradish, H.D. Chiang, C. Concordia, J. V. Staron, C. W. Taylor, E. Vaahedi and G. Wu, "Bibliography on Load Models for Power Flow and Dynamic Performance Simulation," *IEEE Transactions on Power Systems,* vol. 10, no. 1, pp. 523-538, 1995.

[151] N. Jenkins, R. Allan, P. Crossley, D. Kirschen and G. Strbac, "Embedded Generation," *The Institution of Electrical Engineers,* London, 2000.

[152] S. K. Injeti and N. P. Kumar, "A Novel Approach to Identify Optimal Access Point and Capacity of Multiple DGs in a Small, Medium and Large Scale Radial Distribution," *International Journal of Electrical Power & Energy Systems,* vol. 45, no. 1, pp. 142-151, 2013.

[153] A. R. Malekpour, "Multi-Objective Stochastic Distribution Feeder Reconfiguration in Systems With Wind Power Generators and Fuel Cells Using the Point Estimate Method," *IEEE Transcations on Power Systems,* vol. 28, no. 2, pp. 1483-1492, 2013.

[154] A. A. El-Ela, S. M. Allam and M. M. Shatla, "Maximal Optimal Benefits of Distributed Generation Using Genetic Algorithms," *Electric Power Systems Research,* vol. 80, no. 7, pp. 869-877, 2010.

[155] R. V. Rao, V. J. Savsani and D. P. Vakharia, "Teaching–learning-based Optimization: A Novel Method for Constrained Mechanical Design Optimization Problems," *Computer-Aided Design*, vol. 43, no. 3, pp. 303-315, 2011.

[156] D. Das, H. S. Nagi and D. P. Kothari, "Novel Method for Solving Radial Distribution Networks," *IEE Proceedings - Generation, Transmission and Distribution*, vol. 141, no. 4, pp. 291-298, 1994.

[157] T. Gozel and M. H. Hocaoglu, "An Analytical Method for the Sizing and Siting of Distributed Generators in Radial Systems," *Electric Power Systems Research*, vol. 79, no. 6, pp. 912-918, 2009.

[158] M. Chakravorty and D. Das, "Voltage Stability Analysis of Radial Distribution Networks," *International Journal of Electrical Power & Energy Systems*, vol. 23, no. 2, pp. 129-135, 2001.

[159] K. Deb, Multiobjective Optimization Using Evolutionary Algorithm, Chichester: Wiley, 2001.

[160] N. Kanwar, N. Gupta, K. R. Niazi and A. Swarnkar, "Optimal Allocation of DGs and Reconfiguration of Radial Distribution Systems Using an Intelligent Search-based TLBO," *Electric Power Components and Systems*, vol. 45, no. 5, pp. 476-490, 2017.

[161] R. V. Rao and V. Patel, "An Improved Teaching-learning-based Optimization Algorithm for Solving Unconstrained Optimization Problems," *Scientia Iranica*, vol. 20, no. 3, pp. 710-720, 2013.

[162] Z. W. Geem, J. H. Kim and G. V. Loganathan, "A New Heuristic Optimization Algorithm:Harmony Search," *SIMULATION*, vol. 76, no. 2, pp. 60-68, 2001.

[163] L. Zhang, W. Tang, Y. Liu and T. Lv, "Multiobjective Optimization and Decision-making for DG Planning Considering Benefits Between Distribution Company and DGs Owner," *International Journal of Electrical Power & Energy Systems*, vol. 73, pp. 465-474, 2015.

[164] T. Yuvaraj, K. Ravi and K. R. Devabalaji, "Optimal Allocation of DG and DSTATCOM in Radial Distribution System Using Cuckoo Search Optimization Algorithm," *Modelling and Simulation in Engineering*, vol. Article ID 2857926, p. 11, 2017.

[165] T. Yuvaraj, K. Ravi and K. R. Devabalaji, " DSTATCOM Allocation in Distribution Networks Considering Load Variations Using Bat Algorithm," *Ain Shams Engineering Journal*, vol. 8, no. 3, pp. 391-403., 2017.

[166] K. R. Devabalaji, K. Ravi and D. P. Kothari, "Optimal Location and Sizing of Capacitor Placement in Radial Distribution System Using Bacterial Foraging Optimization Algorithm," *International Journal of Electrical Power & Energy Systems*, vol. 71, pp. 383-390, 2015.

[167] M. Sedighizadeh and A. Eisapour-Moarref, "The Imperialist Competitive Algorithm for Optimal Multi-Objective Location and Sizing of DSTATCOM in

Distribution Systems Considering Loads Uncertainty," *INAE Letters,* vol. 2, no. 3, pp. 83-95, 2017.

[168] H. D. Dehnavi and S. Esmaeili, "A New Multiobjective Fuzzy Shuffled Frog-leaping Algorithm for Optimal Reconfiguration of Radial Distribution Systems in the Presence of Reactive Power Compensators," *Turkish Journal of Electrical Engineering & Computer Sciences,* vol. 21, pp. 864-881, 2013.

Appendices

Table A.1: System data of 33-bus test distribution system

Branch	Bus number		Resistance (Ω)	Reactance (Ω)	Load at receiving end		Maximum loading capacity (A)
	Sending	Receiving			P (kW)	Q (kVAr)	
1	1	2	0.0922	0.047	0	0	400
2	2	3	0.493	0.2511	100	60	400
3	3	4	0.366	0.1864	90	40	250
4	4	5	0.3811	0.1941	120	80	250
5	5	6	0.819	0.707	60	30	250
6	6	7	0.1872	0.6188	60	20	150
7	7	8	0.7114	0.2351	200	100	150
8	8	9	1.03	0.74	200	100	150
9	9	10	1.044	0.74	60	20	150
10	10	11	0.1966	0.065	60	20	150
11	11	12	0.3744	0.1238	45	30	150
12	12	13	1.468	1.155	60	35	150
13	13	14	0.5416	0.7129	60	35	150
14	14	15	0.591	0.526	120	80	150
15	15	16	0.7463	0.545	60	10	150
16	16	17	1.289	1.721	60	20	150
17	17	18	0.732	0.574	60	20	150
18	2	19	0.164	0.1565	90	40	250
19	19	20	1.5042	1.3554	90	40	250
20	20	21	0.4095	0.4784	90	40	250
21	21	22	0.7089	0.9373	90	40	150
22	3	23	0.4512	0.3083	90	40	250
23	23	24	0.898	0.7091	90	50	250
24	24	25	0.896	0.7011	420	200	250
25	6	26	0.203	0.1034	420	200	250
26	26	27	0.2842	0.1447	60	25	250
27	27	28	1.059	0.9337	60	25	250
28	28	29	0.8042	0.7006	60	20	250
29	29	30	0.5075	0.2585	120	70	250
30	30	31	0.9744	0.963	200	600	150
31	31	32	0.3105	0.3619	150	70	150
32	32	33	0.341	0.5302	210	100	150
33	8	21	2	2	60	40	150
34	9	15	2	2	0	0	150
35	12	22	2	2	0	0	150
36	18	33	0.5	0.5	0	0	150
37	25	29	0.5	0.5	0	0	150

Table A.2: System data of 69-bus test distribution system

Branch	Bus number		Resistance (Ω)	Reactance (Ω)	Load at receiving end		Maximum loading capacity (A)
	Sending	Receiving			P (kW)	Q (kVAr)	
1	1	2	0.0005	0.0012	0	0	400
2	2	3	0.0005	0.0012	0	0	400
3	3	4	0.0015	0.0036	0	0	400
4	4	5	0.0251	0.0294	0	0	400
5	5	6	0.366	0.1864	0	0	400
6	6	7	0.381	0.1941	2.6	2.2	400
7	7	8	0.0922	0.047	40.4	30	400
8	8	9	0.0493	0.0251	75	54	400
9	9	10	0.819	0.2707	30	22	400
10	10	11	0.1872	0.0619	28	19	200
11	11	12	0.7114	0.2351	145	104	200
12	12	13	1.03	0.34	145	104	200
13	13	14	1.044	0.34	8	5	200
14	14	15	1.058	0.3496	8	5	200
15	15	16	0.1966	0.065	0	0	200
16	16	17	0.3744	0.1238	45	30	200
17	17	18	0.0047	0.0016	60	35	200
18	18	19	0.3276	0.1083	60	35	200
19	19	20	0.2106	0.0696	0	0	200
20	20	21	0.3416	0.1129	1	0.6	200
21	21	22	0.014	0.0046	114	81	200
22	22	23	0.1591	0.0526	5	3.5	200
23	23	24	0.3463	0.1145	0	0	200
24	24	25	0.7488	0.2475	28	20	200
25	25	26	0.3089	0.1021	0	0	200
26	26	27	0.1732	0.0572	14	10	200
27	3	28	0.0044	0.0108	14	10	200
28	28	29	0.064	0.1565	26	18.6	200
29	29	30	0.3978	0.1315	26	18.6	200
30	30	31	0.0702	0.0232	0	0	200
31	31	32	0.351	0.116	0	0	200
32	32	33	0.839	0.2816	0	0	200
33	33	34	1.708	0.5646	14	10	200
34	34	35	1.474	0.4873	19.5	14	200
35	3	36	0.0044	0.0108	6	4	200
36	36	37	0.064	0.1565	26	18.55	200
37	37	38	0.1053	0.123	26	18.55	200
38	38	39	0.0304	0.0355	0	0	200
39	39	40	0.0018	0.0021	24	17	200
40	40	41	0.7283	0.8509	24	17	200
41	41	42	0.31	0.3623	1.2	1	200

Branch	Bus number		Resistance (Ω)	Reactance (Ω)	Load at receiving end		Maximum loading capacity (A)
	Sending	Receiving			P (kW)	Q (kVAr)	
42	42	43	0.041	0.0478	0	0	200
43	43	44	0.0092	0.0116	6	4.3	200
44	44	45	0.1089	0.1373	0	0	200
45	45	46	0.0009	0.0012	39.22	26.3	200
46	4	47	0.0034	0.0084	39.22	26.3	300
47	47	48	0.0851	0.2083	0	0	300
48	48	49	0.2898	0.7091	79	56.4	300
49	49	50	0.0822	0.2011	384.7	274.5	300
50	8	51	0.0928	0.0473	384.7	274.5	300
51	51	52	0.3319	0.114	40.5	28.3	200
52	9	53	0.174	0.0886	3.6	2.7	200
53	53	54	0.203	0.1034	4.35	3.5	300
54	54	55	0.2842	0.1447	26.4	19	300
55	55	56	0.2813	0.1433	24	17.2	300
56	56	57	1.59	0.5337	0	0	300
57	57	58	0.7837	0.263	0	0	300
58	58	59	0.3042	0.1006	0	0	300
59	59	60	0.3861	0.1172	100	72	300
60	60	61	0.5075	0.2585	0	0	300
61	61	62	0.0974	0.0496	1244	888	300
62	62	63	0.145	0.0738	32	23	300
63	63	64	0.7105	0.3619	0	0	300
64	64	65	1.041	0.5302	227	162	300
65	11	66	0.2012	0.0611	59	42	300
66	66	67	0.0047	0.0014	18	13	200
67	12	68	0.7394	0.2444	18	13	200
68	68	69	0.0047	0.0016	28	20	200
69	11	43	0.5	0.5	28	20	200
70	13	21	0.5	0.5	0	0	200
71	15	46	1	0.5	0	0	200
72	50	59	2	1	0	0	200
73	27	65	1	0.5	0	0	200

Table A.3: System data of 118-bus test distribution system

Branch	Bus number		Resistance (Ω)	Reactance (Ω)	Load at receiving end	
	Sending	Receiving			P (kW)	Q (kVAr)
1	1	2	0	0	0	0
2	2	3	0.036	0.01296	0	0
3	3	4	0.033	0.01188	133.84	101.14
4	3	5	0.045	0.0162	16.214	11.292
5	5	6	0.015	0.054	34.315	21.845
6	6	7	0.015	0.054	73.016	63.602
7	7	8	0.015	0.0125	144.2	68.604
8	8	9	0.018	0.014	104.47	61.725
9	9	10	0.021	0.063	28.547	11.503
10	3	11	0.166	0.1344	87.56	51.073
11	11	12	0.112	0.0789	198.2	106.77
12	12	13	0.187	0.313	146.8	75.995
13	13	14	0.142	0.1512	26.04	18.687
14	14	15	0.18	0.118	52.1	23.22
15	15	16	0.15	0.045	141.9	117.5
16	16	17	0.16	0.18	21.87	28.79
17	17	18	0.157	0.171	33.37	26.45
18	12	19	0.218	0.285	32.43	25.23
19	19	20	0.118	0.185	20.234	11.906
20	20	21	0.16	0.196	156.94	78.523
21	21	22	0.12	0.189	546.29	351.4
22	22	23	0.12	0.0789	180.31	164.2
23	23	24	1.41	0.723	93.167	54.594
24	24	25	0.293	0.1348	85.18	39.65
25	25	26	0.133	0.104	168.1	95.178
26	26	27	0.178	0.134	125.11	150.22
27	27	28	0.178	0.134	16.03	24.62
28	5	29	0.015	0.0296	26.03	24.62
29	29	30	0.012	0.0276	594.56	522.62
30	30	31	0.12	0.2766	120.62	59.117
31	31	32	0.21	0.243	102.38	99.554
32	32	33	0.12	0.054	513.4	318.5
33	33	34	0.178	0.234	475.25	456.14
34	34	35	0.178	0.234	151.43	136.79
35	35	36	0.154	0.162	205.38	83.302
36	31	37	0.187	0.261	131.6	93.082
37	37	38	0.133	0.099	448.4	369.79
38	30	39	0.33	0.194	440.52	321.64
39	39	40	0.31	0.194	112.54	55.134
40	40	41	0.13	0.194	53.963	38.998
41	41	42	0.28	0.15	393.05	342.6

Branch	Bus number		Resistance (Ω)	Reactance (Ω)	Load at receiving end	
	Sending	Receiving			P (kW)	Q (kVAr)
42	42	43	1.18	0.85	326.74	278.56
43	43	44	0.42	0.2436	536.26	240.24
44	44	45	0.27	0.0972	76.247	66.562
45	45	46	0.339	0.1221	53.52	39.76
46	46	47	0.27	0.1779	40.328	31.964
47	36	48	0.21	0.1383	39.653	20.758
48	48	49	0.12	0.0789	66.195	42.361
48	48	49	0.12	0.0789	66.195	42.361
49	49	50	0.15	0.0987	73.904	51.653
50	50	51	0.15	0.0987	114.77	57.965
51	51	52	0.24	0.1581	918.37	1205.1
52	52	53	0.12	0.0789	210.3	146.66
53	53	54	0.405	0.1458	66.68	56.608
54	54	55	0.405	0.1458	42.207	40.184
55	30	56	0.391	0.141	433.74	283.41
56	56	57	0.406	0.1461	62.1	26.86
57	57	58	0.406	0.1461	92.46	88.38
58	58	59	0.706	0.5461	85.188	55.436
59	59	60	0.338	0.1218	345.3	332.4
60	60	61	0.338	0.1218	22.5	16.83
61	61	62	0.207	0.0747	80.551	49.156
62	62	63	0.247	0.8922	95.86	90.758
63	2	64	0.028	0.0418	62.92	47.7
64	64	65	0.117	0.2016	478.8	463.74
65	65	66	0.255	0.0918	120.94	52.006
66	66	67	0.21	0.0759	139.11	100.34
67	67	68	0.383	0.138	391.78	193.5
68	68	69	0.504	0.3303	27.741	26.713
69	69	70	0.406	0.1461	52.814	25.257
70	70	71	0.962	0.761	66.89	38.713
71	71	72	0.165	0.06	467.5	395.14
72	72	73	0.303	0.1092	594.85	239.74
73	73	74	0.303	0.1092	132.5	84.363
74	74	75	0.206	0.144	52.699	22.482
75	75	76	0.233	0.084	869.79	614.775
76	76	77	0.591	0.1773	31.349	29.817
77	77	78	0.126	0.0453	192.39	122.43
78	65	79	0.559	0.3687	65.75	45.37
79	79	80	0.186	0.1227	238.15	223.22
80	80	81	0.186	0.1227	294.55	162.47
81	81	82	0.26	0.139	485.57	437.92

Branch	Bus number		Resistance (Ω)	Reactance (Ω)	Load at receiving end	
	Sending	Receiving			P (kW)	Q (kVAr)
82	82	83	0.154	0.148	243.53	183.03
83	83	84	0.23	0.128	243.53	183.03
84	84	85	0.252	0.106	134.25	119.29
85	85	86	0.18	0.148	22.71	27.96
86	80	87	0.16	0.182	49.513	26.515
87	87	88	0.2	0.23	383.78	257.16
88	88	89	0.16	0.393	49.64	20.6
89	66	90	0.669	0.2412	22.473	11.806
90	90	91	0.266	0.1227	62.93	42.96
91	91	92	0.266	0.1227	30.67	34.93
92	92	93	0.266	0.1227	62.53	66.79
93	93	94	0.266	0.1227	114.57	81.748
94	94	95	0.233	0.115	81.292	66.526
95	95	96	0.496	0.138	31.733	15.96
96	92	97	0.196	0.18	33.32	60.48
97	97	98	0.196	0.18	531.28	224.85
98	98	99	0.1866	0.122	507.03	367.42
99	99	100	0.0746	0.318	26.39	11.7
100	2	101	0.0625	0.0265	45.99	30.392
101	101	102	0.1501	0.234	100.66	47.572
102	102	103	0.1347	0.0888	456.48	350.3
103	103	104	0.2307	0.1203	522.56	449.29
104	104	105	0.447	0.1608	408.43	168.46
105	105	106	0.1632	0.0588	141.48	134.25
106	106	107	0.33	0.099	104.43	66.024
107	107	108	0.156	0.0561	96.793	83.647
108	108	109	0.3819	0.1374	493.92	419.34
109	109	110	0.1626	0.0585	225.38	135.88
110	110	111	0.3819	0.1374	509.21	387.21
111	111	112	0.2445	0.0879	188.5	173.46
112	111	113	0.2088	0.0753	918.03	898.55
113	113	114	0.2301	0.0828	305.08	215.37
114	101	115	0.6102	0.2196	54.38	40.97
115	115	116	0.1866	0.127	211.14	192.9
116	116	117	0.3732	0.246	67.009	53.336
117	117	118	0.405	0.367	162.07	90.321
118	118	119	0.489	0.438	48.785	29.156
119	28	47	0.5258	0.2925	33.9	18.98
120	18	28	0.5258	0.2916		
121	9	25	0.4272	0.1539		
122	44	55	0.48	0.1728		

Branch	Bus number		Resistance (Ω)	Reactance (Ω)	Load at receiving end	
	Sending	Receiving			P (kW)	Q (kVAr)
123	50	63	0.36	0.1296		
124	38	63	0.57	0.572		
125	10	41	0.53	0.3348		
126	59	97	0.3957	0.1425		
127	74	92	0.68	0.648		
128	76	89	0.4062	0.1464		
129	78	100	0.4626	0.1674		
130	84	109	0.651	0.234		
131	87	106	0.8125	0.2925		
132	111	119	0.7089	0.2553		
133	26	36	0.5	0.5		

Table A. 4: Data for cost calculation [47]

$Cost_{DG}$ (US$/kVAr)	n_{DG} (year)	AR	K_e (US$/kWh)
50	30	0.1	0.06

Table A. 5: Emission data

Source	Emission rate (ER) (kg/MWh)		
Grid	NOx	CO_2	SO_2
	2.2952	921.25	3.5834

Table A. 6: Normalized average daily load demand

Hour	Load demand (p.u.)	Hour	Load demand (p.u.)	Hour	Load demand (p.u.)
1	0.64	9	0.87	17	0.96
2	0.60	10	0.95	18	0.96
3	0.58	11	0.99	19	0.93
4	0.56	12	1.00	20	0.92
5	0.56	13	0.99	21	0.92
6	0.58	14	1.00	22	0.93
7	0.64	15	1.00	23	0.87
8	0.76	16	0.97	24	0.72

Table A.7: Pareto solutions for DSTATCOMs allocation in 33-bus and 69-bus network

33-bus DSTATCOM allocation without reconfiguration	Location	Size(MVAr)	Loss (MW)	TACS ($)	ES (ton)
Open tie/Sectional switches 33 34 35 36 37	30	1.25271	0.143602	16086.76	333.7047
	30	1.235594	0.143612	16159.69	333.6685
	30	1.218512	0.143643	16224.82	333.5141
	30	1.201465	0.143695	16282.19	333.2421
	30	1.184451	0.143767	16331.82	332.8528
	30	1.167467	0.143859	16373.76	332.3466
	30	1.150514	0.143972	16408.01	331.7239
	30	1.133589	0.144105	16434.62	330.9848
	30	1.11669	0.144259	16453.6	330.1298
	30	1.099818	0.144433	16464.98	329.159
	30	1.082969	0.144627	16468.77	328.0725

Location		Size (MVAr)		Loss (MW)	TACS ($)	ES (ton)
12	30	0.468867	1.057751	0.135753	17735.09	377.7888
12	30	0.458522	1.04487	0.135767	17834.55	377.7473
13	30	0.389479	1.055923	0.135878	18052.79	377.1788
13	30	0.3817	1.042073	0.135944	18125.82	376.8375
13	30	0.373934	1.028254	0.136036	18189.01	376.3469
13	30	0.36618	1.014462	0.136154	18242.38	375.7075
13	30	0.358438	1.000698	0.136297	18285.98	374.9198
14	30	0.3357	0.993098	0.136538	18333.06	373.5855
14	30	0.328618	0.979122	0.13673	18356.78	372.521
14	30	0.321545	0.96517	0.136947	18371	371.3119
14	30	0.314481	0.95124	0.13719	18375.73	369.9584

Location			Size (MVAr)			Loss (MW)	TACS ($)	ES (ton)
13	24	30	0.378685	0.544211	1.036665	0.132172	17151.6	398.194
13	24	30	0.372906	0.501929	1.026376	0.132208	17399.04	398.0521
13	24	30	0.367136	0.459813	1.016111	0.132312	17619.56	397.5078
13	25	30	0.36486	0.345707	1.012074	0.132655	18027.08	395.6216
13	25	30	0.358441	0.317762	1.000659	0.132848	18159.92	394.5633
14	25	30	0.336835	0.291755	0.99528	0.133138	18289.17	392.9595
14	25	30	0.330967	0.263942	0.983699	0.133437	18380.02	391.2874
14	25	30	0.325106	0.236225	0.97214	0.13379	18450.47	389.3087
14	25	30	0.319254	0.2086	0.960601	0.134196	18500.65	387.0249
14	25	30	0.313409	0.181065	0.949081	0.134654	18530.68	384.4376
8	14	30	0.198951	0.25438	0.894023	0.135771	18533.89	377.9498

Location				Size (MVAr)				Loss (MW)	TACS ($)	ES (ton)
7	14	24	30	0.44246	0.276537	0.482557	0.903932	0.130688	17038.8	406.3674
7	14	24	30	0.414794	0.276455	0.444269	0.902136	0.130729	17327.37	406.2168
7	14	24	30	0.387237	0.276372	0.406127	0.900335	0.130851	17584.46	405.5968
7	14	25	30	0.372487	0.276289	0.311238	0.899344	0.131075	17994.16	404.4039
7	14	25	30	0.342257	0.276207	0.286199	0.89735	0.131317	18161.14	403.0871
8	14	25	30	0.275878	0.254763	0.268203	0.918126	0.131762	18376.92	400.6421
8	14	25	30	0.256272	0.254686	0.242076	0.912009	0.132106	18481.42	398.7282
8	14	25	30	0.236717	0.25461	0.216038	0.905903	0.132512	18562.45	396.4617
14	25	30	32	0.319253	0.208605	0.765924	0.194117	0.133822	18639.87	389.1384
8	14	30	32	0.222196	0.254456	0.70663	0.194102	0.135044	18666.18	382.0348
8	14	30	32	0.198948	0.254379	0.69939	0.194088	0.135397	18673.08	380.0633

Location					Size (MVAr)					Loss (MW)	TACS ($)	ES (ton)
7	14	24	30	32	0.442451	0.276537	0.482567	0.709084	0.194235	0.130315	17178.33	408.4819
7	14	24	30	32	0.414785	0.276455	0.444279	0.70731	0.19422	0.130355	17466.84	408.3308
7	14	25	30	32	0.402823	0.276371	0.336372	0.706528	0.194205	0.130527	17940.16	407.439
7	14	25	30	32	0.372479	0.276289	0.311244	0.704561	0.194191	0.130701	18133.53	406.517
7	14	25	30	32	0.342249	0.276207	0.286205	0.702588	0.194176	0.130943	18300.46	405.2
8	14	25	30	32	0.275873	0.254762	0.268209	0.723385	0.194161	0.131388	18516.2	402.7549
8	14	25	30	32	0.256268	0.254686	0.242082	0.71729	0.194147	0.131733	18620.68	400.8411
8	14	25	30	32	0.236712	0.25461	0.216043	0.711205	0.194132	0.132138	18701.68	398.5746
8	14	25	30	32	0.217205	0.254534	0.190092	0.705129	0.194117	0.132605	18759.36	395.9577
8	14	25	30	32	0.197745	0.254457	0.164224	0.699063	0.194103	0.133132	18793.87	392.9922
8	14	25	30	32	0.178328	0.25438	0.138439	0.693006	0.194088	0.13372	18805.34	389.6799

33-bus DSTATCOM allocation with reconfiguration	Location	Size (MVAr)	Loss (MW)	TACS ($)	ES (ton)
Open tie/Sectional switches 7 9 14 32 37	30	1.028339	0.101818	32425.54	570.9264
	30	1.010746	0.101829	32499.59	570.8751
	30	0.993209	0.10186	32565.61	570.7035
	30	0.975724	0.101912	32623.67	570.4124
	30	0.958291	0.101985	32673.83	570.0028
	30	0.940908	0.102079	32716.14	569.4753
	30	0.923574	0.102192	32750.65	568.8305
	30	0.906286	0.102326	32777.41	568.0693
	30	0.889043	0.102481	32796.48	567.1921
	30	0.871844	0.102655	32807.89	566.1996
	30	0.854687	0.102849	32811.68	565.0923

Location		Size (MVAr)		Loss (MW)	TACS ($)	ES (ton)
21	30	0.642543	1.017259	0.095906	31818.13	604.4526
8	30	0.434077	1.003214	0.095979	32773.99	604.1017
8	30	0.412788	0.986041	0.096048	32919.28	603.733
8	30	0.391595	0.96892	0.096163	33046.93	603.1017
8	30	0.370493	0.95185	0.096323	33157.1	602.21
8	30	0.34948	0.934828	0.096527	33249.95	601.0601
9	30	0.293076	0.918463	0.097024	33387.9	598.2466
16	30	0.224117	0.902362	0.09765	33531.87	594.6908
16	30	0.213459	0.885304	0.097898	33562.56	593.2816
17	30	0.18795	0.868545	0.098324	33591.95	590.8633
17	30	0.178883	0.851546	0.098619	33597.72	589.1811

Location			Size (MVAr)			Loss (MW)	TACS ($)	ES (ton)
8	24	30	0.445616	0.523925	0.96284	0.092585	31853.63	623.5248
8	24	30	0.425034	0.481341	0.950273	0.09263	32172.59	623.3068
8	25	30	0.406013	0.360249	0.946343	0.092913	32703.97	621.7291
12	17	30	0.264341	0.1832	0.967922	0.094373	33466.62	613.321
12	17	30	0.248924	0.177411	0.950854	0.094533	33576.99	612.4254
13	17	30	0.20327	0.178404	0.934238	0.094846	33732.52	610.6646
13	17	30	0.191896	0.171782	0.917214	0.095077	33802.37	609.364
13	17	30	0.180567	0.165183	0.900236	0.095348	33856.5	607.8284
13	18	30	0.171424	0.152162	0.883377	0.095696	33900.33	605.8536
14	18	30	0.1531	0.147575	0.866574	0.0961	33926.34	603.5569
14	18	30	0.142692	0.141372	0.849706	0.09648	33933.76	601.3963

Location				Size (MVAr)				Loss (MW)	TACS ($)	ES (ton)
12	16	24	30	0.29573	0.216744	0.520984	0.961979	0.090817	32229.34	633.6153
12	17	24	30	0.288799	0.192381	0.478856	0.949545	0.090872	32589.63	633.3481
12	17	25	30	0.274888	0.187164	0.358587	0.945527	0.091149	33120.46	631.8046
13	17	25	30	0.222761	0.189754	0.331089	0.931916	0.091458	33407.37	630.0778
13	17	25	30	0.211585	0.183252	0.302795	0.917902	0.091709	33579.83	628.6664
13	17	25	30	0.200455	0.176774	0.274608	0.903927	0.092029	33725.17	626.8504
13	17	25	30	0.18937	0.170319	0.246524	0.889992	0.092419	33843.6	624.633
13	17	25	30	0.178328	0.163886	0.218541	0.876093	0.092879	33935.36	622.0173
13	18	25	30	0.169439	0.151122	0.190778	0.862291	0.093441	34006.12	618.8145
14	18	25	30	0.151548	0.146656	0.163131	0.848534	0.094086	34048.38	615.1346
14	18	25	30	0.141404	0.140609	0.135403	0.834725	0.094738	34061.12	611.4084

Location					Size (MVAr)					Loss (MW)	TACS ($)	ES (ton)
6	12	16	25	30	0.301391	0.294977	0.216399	0.379063	0.852396	0.090257	32220.06	636.7874
6	12	17	25	30	0.266807	0.288087	0.192116	0.354982	0.852312	0.090314	32597.93	636.5156
6	12	17	25	30	0.231986	0.273178	0.186526	0.330741	0.852229	0.090456	32897.93	635.7388
7	12	17	25	30	0.183871	0.258437	0.180994	0.3082	0.857528	0.090713	33181.81	634.3062
7	12	17	25	30	0.154036	0.24363	0.175433	0.283575	0.855536	0.091034	33402.77	632.5003
7	13	17	25	30	0.125009	0.19977	0.176377	0.259602	0.853585	0.091533	33650.54	629.6781
8	13	18	25	30	0.115332	0.167263	0.121197	0.245259	0.889369	0.091921	33840.77	627.458
8	14	18	25	30	0.102925	0.151899	0.121173	0.217571	0.875616	0.092457	33948.11	624.4116
8	14	18	25	30	0.08632	0.144913	0.12115	0.189864	0.861841	0.093039	34020.01	621.099
9	14	18	25	30	0.068294	0.140556	0.114112	0.16242	0.848184	0.093754	34066.34	617.0223
9	14	18	25	30	0.055631	0.132449	0.114094	0.134824	0.83444	0.094456	34080.06	613.0123

69-bus DSTATCOM allocation without reconfiguration	Location	Size (MVAr)	Loss (MW)	TACS ($)	ES (ton)
Open tie/Sectional switches 69 70 71 72 73	61	1.329822	0.151958	20748.73	410.9825
	61	1.314274	0.151967	20815.4	410.9561
	61	1.298753	0.151996	20874.94	410.8213
	61	1.283259	0.152043	20927.38	410.5787
	61	1.26779	0.15211	20972.75	410.2285
	61	1.252345	0.152195	21011.07	409.7711
	61	1.236924	0.152299	21042.38	409.2069
	61	1.221527	0.152421	21066.69	408.5362
	61	1.206151	0.152562	21084.03	407.7593
	61	1.190797	0.152722	21094.42	406.8764
	61	1.175463	0.152901	21097.88	405.8878

Location		Size (MVAr)		Loss (MW)	TACS ($)	ES (ton)
17	61	0.36041	1.274986	0.146379	21462.48	442.7772
17	61	0.34838	1.261186	0.146395	21572.79	442.7262
17	61	0.336391	1.247412	0.146442	21671.15	442.4955
17	61	0.324444	1.233665	0.14652	21757.67	442.0863
18	61	0.312419	1.219961	0.14663	21832.71	441.4973
18	61	0.300562	1.206263	0.14677	21895.74	440.7347
18	61	0.288745	1.192587	0.14694	21947.16	439.7969
18	61	0.276967	1.178935	0.147142	21987.04	438.6849
18	61	0.265227	1.165305	0.147373	22015.44	437.3997
21	61	0.237083	1.154209	0.147776	22041.36	435.1337
21	61	0.22691	1.140395	0.148053	22046.73	433.5866

Location			Size (MVAr)			Loss (MW)	TACS ($)	ES (ton)
11	21	61	0.41259	0.230187	1.232413	0.145057	20887.88	450.1938
11	21	61	0.369176	0.230183	1.223284	0.145089	21111.37	450.0763
12	21	61	0.297971	0.207262	1.221846	0.145264	21472.31	449.1595
12	21	61	0.267479	0.207256	1.210871	0.14539	21611.46	448.4913
12	21	61	0.237114	0.20725	1.199918	0.145565	21731.51	447.5381
12	21	61	0.20687	0.207245	1.188989	0.14579	21832.63	446.3022
12	21	61	0.176744	0.207239	1.178074	0.146063	21915.02	444.7859
12	21	61	0.146737	0.207233	1.167181	0.146385	21978.82	442.992
12	21	61	0.116846	0.207227	1.156308	0.146755	22024.2	440.9227
21	61	64	0.237074	0.947303	0.206636	0.147439	22164.94	437.0243
21	61	64	0.226901	0.933496	0.206633	0.147716	22170.31	435.4774

Location				Size (MVAr)				Loss (MW)	TACS ($)	ES (ton)
11	21	50	61	0.412002	0.230187	0.517446	1.232292	0.144274	18908.23	454.7197
11	12	21	61	0.217575	0.174421	0.207268	1.223281	0.14496	21159.48	450.813
11	12	21	61	0.174378	0.174398	0.207262	1.214172	0.145055	21358.39	450.3302
12	21	61	64	0.267451	0.207256	1.003926	0.206658	0.145053	21735.12	450.3806
12	21	61	64	0.237084	0.20725	0.992979	0.206654	0.145229	21855.14	449.4272
12	21	61	64	0.20684	0.207244	0.982054	0.206651	0.145453	21956.26	448.1912
12	21	61	64	0.176716	0.207239	0.971149	0.206647	0.145727	22038.62	446.6751
12	21	61	64	0.146709	0.207233	0.960263	0.206644	0.146048	22102.41	444.8813
12	21	61	64	0.116819	0.207227	0.949397	0.20664	0.146418	22147.79	442.812
16	21	61	64	0.111446	0.145945	0.944185	0.206636	0.147163	22191.31	438.6005
17	21	61	64	0.116732	0.125122	0.931196	0.206633	0.147489	22198.25	436.7689

Location					Size (MVAr)					Loss (MW)	TACS ($)	ES (ton)
9	12	21	50	61	0.327139	0.260156	0.207273	0.516743	1.209372	0.144004	18436.61	456.182
11	21	50	61	64	0.368775	0.230183	0.313115	1.016253	0.206665	0.144091	20107.53	455.791
11	12	21	61	64	0.174339	0.174395	0.207262	1.00722	0.206662	0.144719	21482.1	452.2192
11	12	21	61	64	0.131328	0.174374	0.207256	0.998138	0.206658	0.144877	21656.68	451.3747
12	21	59	61	64	0.23084	0.20725	0.096208	0.91516	0.206654	0.145115	21841.71	450.0448
12	21	61	64	66	0.178329	0.207244	0.980277	0.206651	0.040218	0.145386	21937.25	448.5722
12	21	59	61	64	0.172218	0.207239	0.069375	0.915007	0.206647	0.145634	22033.01	447.182
12	17	21	61	64	0.126751	0.102031	0.125124	0.960262	0.206644	0.145995	22122.1	445.1829
12	17	21	61	64	0.096865	0.102021	0.125124	0.949396	0.20664	0.146365	22167.48	443.1137
17	21	61	64	68	0.105563	0.125123	0.939385	0.206636	0.058059	0.146826	22198.74	440.5197
17	21	61	64	69	0.101679	0.125122	0.92764	0.206633	0.038249	0.147233	22206.63	438.233

69-bus DSTATCOM allocation with reconfiguration	Location	Size (MVAr)	Loss (MW)	TACS ($)	ES (ton)
Open tie/Sectional switches 14 56 61 69 70	61	1.038301	0.073422	50906.78	857.1781
	61	1.011528	0.073438	51019.87	857.1062
	61	0.984885	0.073486	51120.45	856.8499
	61	0.95837	0.073566	51208.68	856.4113
	61	0.931979	0.073677	51284.7	855.7927
	61	0.90571	0.073819	51348.67	854.9959
	61	0.879558	0.073992	51400.73	854.0231
	61	0.853522	0.074195	51441	852.876
	61	0.827597	0.074428	51469.61	851.5564
	61	0.801781	0.07469	51486.69	850.066
	61	0.776071	0.074983	51492.36	848.4065

Location		Size (MVAr)		Loss (MW)	TACS ($)	ES (ton)
61	64	1.0382	0.341798	0.06739	51646.67	891.8316
61	64	1.01143	0.330005	0.067413	51809.11	891.7211
61	64	0.98479	0.318267	0.067482	51953.59	891.3455
61	64	0.958279	0.306581	0.067597	52080.32	890.708
61	64	0.931891	0.294948	0.067757	52189.52	889.8117
61	64	0.905625	0.283365	0.067961	52281.41	888.6594
61	64	0.879477	0.271832	0.068209	52356.18	887.2541
61	64	0.853443	0.260348	0.0685	52414.02	885.5983
61	64	0.827522	0.248911	0.068835	52455.13	883.6947
61	64	0.801709	0.237521	0.069212	52479.66	881.5457
61	64	0.776003	0.226176	0.069632	52487.81	879.1536

Location			Size (MVAr)			Loss (MW)	TACS ($)	ES (ton)
11	61	64	0.383485	1.037928	0.34175	0.065593	50634.89	902.236
11	61	64	0.334585	1.011192	0.329963	0.065645	51001.35	901.9576
12	61	64	0.249975	0.984612	0.318235	0.065836	51472.11	900.8788
12	61	64	0.21476	0.958124	0.306554	0.066055	51714.41	899.6359
12	61	64	0.179715	0.931762	0.294925	0.06636	51923.11	897.8974
12	61	64	0.14484	0.90552	0.283347	0.06675	52098.63	895.6695
12	61	64	0.11013	0.879397	0.271818	0.067224	52241.39	892.958
61	64	68	0.853394	0.260339	0.067732	0.067842	52363.1	889.4104
27	61	64	0.059049	0.827517	0.205979	0.068646	52454.34	884.7775
61	64	65	0.801707	0.185219	0.060781	0.069099	52484.5	882.1965
61	64	65	0.776001	0.185216	0.047598	0.069539	52493.04	879.6855

Location				Size (MVAr)				Loss (MW)	TACS ($)	ES (ton)
11	50	61	64	0.382752	0.651597	0.952284	0.341679	0.064505	48539.42	908.2621
12	21	61	64	0.285325	0.206778	1.011196	0.227672	0.065034	50984.61	905.4524
12	21	61	64	0.24994	0.182991	0.984585	0.227663	0.065188	51306.16	904.5907
12	21	61	64	0.214729	0.159334	0.958101	0.227653	0.065443	51588.03	903.1454
12	21	61	64	0.179689	0.135806	0.931742	0.227644	0.065798	51830.75	901.1239
12	21	61	64	0.144819	0.112402	0.905505	0.227635	0.066251	52034.83	898.5337
12	22	61	64	0.110113	0.08912	0.879384	0.227462	0.066803	52201.07	895.375
24	61	64	69	0.069373	0.853385	0.221194	0.067656	0.067531	52346.23	891.1981
27	61	64	69	0.059042	0.827487	0.205979	0.040897	0.068225	52432.52	887.217
61	64	65	69	0.801676	0.185238	0.060772	0.01428	0.068944	52479.98	883.0957
61	62	64	65	0.776001	0.023003	0.162211	0.047597	0.069536	52494.22	879.7034

Location					Size (MVAr)					Loss (MW)	TACS ($)	ES (ton)
11	18	50	61	64	0.382675	0.238784	0.651276	0.952284	0.251106	0.063824	48141.33	912.1554
12	21	50	61	64	0.284958	0.20668	0.447553	0.952162	0.227672	0.064053	49633.84	910.9507
11	12	21	61	64	0.131723	0.154085	0.182982	0.98456	0.227663	0.065045	51202.16	905.4187
11	12	21	61	64	0.083331	0.154084	0.159328	0.958085	0.227653	0.065339	51527.29	903.747
12	21	61	64	69	0.139805	0.135806	0.931742	0.227644	0.039878	0.06579	51833.63	901.168
12	21	61	64	65	0.110113	0.072822	0.879384	0.185227	0.058679	0.066784	52207.46	895.4835
12	24	61	64	69	0.035689	0.069371	0.853379	0.221194	0.039878	0.067461	52337.72	891.6036
12	24	61	64	69	0.035689	0.069371	0.853379	0.221194	0.039878	0.067461	52337.72	891.6036
24	61	64	65	68	0.032108	0.827486	0.185221	0.052951	0.040924	0.068166	52431.1	887.5544
26	61	64	65	69	0.020502	0.801695	0.185219	0.044001	0.014255	0.068901	52479.4	883.3385
27	61	62	64	65	0.006035	0.776004	0.022991	0.162217	0.042502	0.069525	52494.29	879.7684